



Classical and quantum out-of-equilibrium dynamics. Formalism and applications.

Camille Aron

► To cite this version:

Camille Aron. Classical and quantum out-of-equilibrium dynamics. Formalism and applications.. Data Analysis, Statistics and Probability [physics.data-an]. Université Pierre et Marie Curie - Paris VI, 2010. English. NNT: . tel-00538099

HAL Id: tel-00538099

<https://theses.hal.science/tel-00538099>

Submitted on 21 Nov 2010

HAL is a multi-disciplinary open access archive for the deposit and dissemination of scientific research documents, whether they are published or not. The documents may come from teaching and research institutions in France or abroad, or from public or private research centers.

L'archive ouverte pluridisciplinaire **HAL**, est destinée au dépôt et à la diffusion de documents scientifiques de niveau recherche, publiés ou non, émanant des établissements d'enseignement et de recherche français ou étrangers, des laboratoires publics ou privés.

**THÈSE DE DOCTORAT DE
L'UNIVERSITÉ PIERRE ET MARIE CURIE**

Spécialité : Physique théorique

École doctorale : « La physique, de la particule au solide »

Réalisée au Laboratoire de Physique Théorique et Hautes Énergies

Présentée par
M. Camille ARON

Pour obtenir le grade de
Docteur de l'Université Pierre et Marie Curie

**Dynamique hors d'équilibre classique et quantique.
Formalisme et applications.**

Soutenue le 20 septembre 2010 devant le jury composé de

M.	Denis	BERNARD	(Président du jury)
M.	Federico	CORBERI	(Examineur)
M ^{me}	Leticia	CUGLIANDOLO	(Directrice de thèse)
M.	Gabriel	KOTLIAR	(Rapporteur)
M.	Marco	PICCO	(Invité)
M.	Frédéric	Van WIJLAND	(Rapporteur)

Abracadabra.

REMERCIEMENTS

LES tous premiers vont bien naturellement à ma directrice de thèse, Leticia Cugliandolo. Au cours de ces trois années de thèse, sa porte m'a toujours été grande ouverte, ce qui m'a permis d'abuser un peu de son indéfectible bonne humeur et de son vaste savoir. J'espère conserver sa confiance et sa sympathie. Je remercie Marco Picco, mon co-directeur de thèse, pour sa disponibilité et ses conseils toujours avisés. Je tiens également à remercier vivement Giulio Biroli avec qui j'ai eu l'occasion de collaborer sur des problèmes passionnants. Je mesure la chance qui fut la mienne d'apprendre à leurs côtés.

Je suis très reconnaissant à Denis Bernard et Federico Corberi d'avoir accepté de faire partie du jury cette thèse, et tout particulièrement à Gabriel Koliar et Frédéric Van Wijland d'avoir accepté d'en être les rapporteurs.

J'ai bénéficié d'un excellent environnement de travail au LPTHE ; non seulement en raison de la qualité scientifique, mais également des qualités humaines de ses membres. Merci à eux tous, et plus particulièrement à Damien Bremont, Benoît Estienne et Alberto Sicilia qui ont égayé mes deux premières années de thèse ainsi qu'à Bernard Diu pour ses visites impromptues et toujours rafraîchissantes.

Enfin, j'ai une pensée particulière pour Monica Guică qui m'a gaiement accompagné ces deux dernières années.

Paris, le 30 juillet 2010.

CONTENTS

1	Introduction	1
1.1	Systems coupled to an environment	3
1.2	Models and methods	9
1.3	Questions	18
2	Symmetries of Langevin Generating Functionals	25
2.1	Langevin equation	28
2.2	The MSRJD path-integral formalism	31
2.3	Equilibrium	38
2.4	Out of equilibrium	51
2.5	Conclusions	59
	Appendices	60
3	Scalings and Super-universality in Coarsening versus Glassy Dynamics	71
3.1	The models	73
3.2	The typical growing length	76
3.3	Fluctuations	85
3.4	Conclusions	88
4	Driven Quantum Coarsening	91
4.1	The model	94
4.2	The dynamics	98
4.3	The influence of the fermionic environment	104
4.4	Results	109
4.5	The current	128
4.6	Conclusions	131
	Appendices	132
5	Conclusions and Outlook	147
6	Synopsis	151
	Bibliography	163

INTRODUCTION

Once upon a time...

UNTIL the second half of the nineteenth century, science studied macroscopic phenomena that were directly perceptible by human senses, even though scientists were often led to enhance the sensory perception with the more objective measurements of instruments. For instance, microscopes allowed biologists to discover cells – the building blocks of life – and their inner structure. In the field of physics, scientists studied mechanics, electricity, optics, acoustics but also thermodynamics and states of matter. All these domains were considered independent in the nineteenth century. In particular, thermodynamicians were far from imagining that their theory would take its roots in mechanics.

Despite its successes, macroscopic physics was condemned to eventually lose its fundamental character to the benefit of microscopic physics. Indeed, the nineteenth century saw the accession at the scientific level of the antique philosophical idea of the atomic hypothesis introduced by Leucippus and his student Democritus in the fifth century B.C. [1]. The quantitative study of chemical reactions revealed some stoichiometric laws that John Dalton and Amedeo Avogadro interpreted very convincingly within the frame of the atomic hypothesis: reactants were aggregates of microscopic components [2, 3]. This hypothesis, which was first considered a convenient way of presenting results – since it was impossible at that time to directly prove the existence of atoms – progressively gained ground during the nineteenth century.

James C. Maxwell, who was at first reluctant to take position in favor of atoms, was the first to introduce probabilistic methods to compute the distribution of particle velocities in a gas in 1860 [4, 5]. In 1872, Ludwig Boltzmann set the building blocks of out-of-equilibrium statistical mechanics by introducing the so-called Boltzmann equation that describes the generic transport properties in a gas by taking into account the dynamics of collisions. In 1877, he was the first to give a probabilistic interpretation of the second principle of thermodynamics with its celebrated formula¹ for the entropy $S = k_B \ln \Omega$ [6]. This resolved the paradox raised by Lord Kelvin (and relayed by Johann J. Loschmidt) that it seemed impossible to deduce irreversible phenomena from microscopic mechanical systems.

In 1902, Josiah W. Gibbs formalized and generalized the previous results of J. C. Maxwell and L. Boltzmann without the use of molecular models in the first modern treaty of statistical physics [7]. Indeed, refusing to enter the debate about the very structure of matter, he reformulated statistical mechanics by introducing the concepts of canonical and grand canonical ensembles. Statistical physics was born and it was ready to be generalized to the study of quantum systems.

In 1905, the same year he unified mechanics and electromagnetism with the theory of special relativity and proposed the quantization of light, Albert Einstein published an article [8] devoted to the observable consequences of statistical physics that he considered as a fundamental theory. Phenomena that occur at our scale are more or less direct consequences of underlying mechanisms involving microscopic constituents and their properties that one is entitled to study to get a fundamental understanding of the whole physical world. A. Einstein was the first, together with Marian von Smoluchovski, to understand that the continual and irregular motion of small particles in water (observed first in 1828 by the botanist Robert Brown with pollen particles, then with inorganic materials [9]) is caused by the thermal agitation of the water molecules. In his 1905 article, he computed the fluctuations of the Brownian particles and showed that they can be tested experimentally. One year later, Jean B. Perrin conducted a series of refined experiments in which he measured the trajectories and velocities of grains of different sizes and masses in solution. By using A. Einstein's theory, he showed, that one could obtain a precise estimate of the Avogadro number by different methods. His experiments put a definitive end to the controversy around the atomic hypothesis [10].

The first theoretical insight into non-equilibrium statistical physics is due to Lars Onsager who, in 1931, worked out the classical thermodynamics of states very close to equilibrium [11, 12]. He established that the crossed effects in a physical system, for instance the coefficient that relates the heat flux to the pressure gradient and the one that relates the particle flux to the temperature gradient, are equal. These relations are now known as the Onsager reciprocal relations. Herbert B. Callen and Theodore A. Welton proved in 1951

1. This expression of the formula was given by Max K. E. L. Planck in 1900.

the so-called *fluctuation-dissipation theorem* which predicts the non-equilibrium behavior of a system – such as the irreversible dissipation of energy into heat – from its reversible fluctuations in thermal equilibrium [13].

The development of far from equilibrium statistical physics had to wait until the second half of the twentieth century. The study of phase ordering dynamics began as soon as a better understanding of the phase transitions was given by the theory of Lev D. Landau [14] and new field theoretical tools were borrowed from high energy physics.

The interest in disordered systems began with Philip W. Anderson who suggested in 1958 the possibility of electron localization inside a semiconductor, provided that the degree of randomness of the impurities or defects of the underlying atomic lattice [15] be sufficiently large. In 1974, together with Samuel F. Edwards, he introduced the so-called Edward-Anderson (EA) model to describe a class of dilute magnetic alloys [16]. This first spin glass model lead to a new phenomenology and new theoretical concepts. In the same paper, they introduced a new order parameter for the study of spin glasses based on the concept of replica. Replicas were later used in 1979 by Giorgio Parisi to solve the statics of the Sherrington-Kirkpatrick (SK) model, introduced in 1975 by David Sherrington and Scott Kirkpatrick [17], which is the mean-field version of the EA model [18]. Its out-of-equilibrium dynamics after a quench in temperature were worked out in 1994 by Leticia F. Cugliandolo and Jorge Kurchan [19]. The techniques and concepts that have been developed in spin glass theory have led to several valuable applications in the other areas such as probability theory [20, 21], computer science, information science, biology and economics [22–24].

A major breakthrough in out-of-equilibrium statistical physics took place over the past twenty years with the discovery of exact fluctuation relations in systems driven far from equilibrium. These so-called *fluctuation theorems* deal with the fluctuations of entropy or related quantities such as irreversible work, heat or matter currents. First proposed and tested using computer simulations by Denis Evans, Eddie G. D. Cohen and Gary Morriss in 1993 [25], much mathematical and computational work has been done in the following years to show that the fluctuation theorems apply to a large variety of situations such as isolated systems or systems in contact with a thermal bath, closed or open systems, classical or quantum systems [26–30].

1.1 Systems coupled to an environment

Systems in nature are never isolated. In order to give an accurate description of their properties or to be able to justify why they can be treated as isolated, one is often led to study the impact of their environment. Both the environment and the system itself are constituents of an energy-conserving global system (so-called universe) and the former is supposed to

have many more degrees of freedom than the latter.

In some simple cases, like when the system and its environment are in equilibrium, a few parameters are needed to characterize the influence of the environment so that one can concentrate again on the system of interest solely. However, in the general case one is constrained to describe the environment and its coupling to the system of interest in detail.

We make the distinction between equilibrium environments and non-equilibrium environments. All the internal variables of the former are in equilibrium. This means in particular that the fluctuation-dissipation theorem is satisfied for all possible correlators of these variables and their corresponding responses. An equilibrium environment is said to be ‘good’ if it stays in equilibrium irrespective of the state of the system it is in contact with. This is typically achieved by environments with a large enough number of degrees of freedom so that their macroscopic properties do not fluctuate.

In the so-called canonical situation, the environment is made of one or several thermostats that are reservoirs of energy. The thermal contacts between the system and the reservoirs allow for the exchange of energy, but particles cannot leave the system. In R. Brown’s experiment of 1828, the pollen particles and the surrounding water molecules that constitute the thermal bath interact through short-ranged and highly non-linear forces such as Lennard-Jones forces. If the environment is composed of several thermostats at the same temperature, they constitute an equilibrium environment. If they have different temperatures, they constitute a non-equilibrium environment which induces a heat flow through the system. Non-equilibrium environments are expected to drive any system to which they are connected out of equilibrium. By extension, we also consider all types of external forces or fields applied directly to the system as non-equilibrium environments.

The canonical set-up can be generalized to the grand canonical situation where the system also exchanges particles with its environment. This describes situations in which a fermionic system is connected to two electronic leads. As soon as they have a different chemical potential, they constitute a non-equilibrium environment and a current establishes through the system.

Finally, we would like to stress the fact that the distinction between the system and what is treated as the environment is not always clear. Sometimes it is even possible to treat one part of the system as an environment of another part. This has been done for example in cosmology with self-interacting quantum fields in which the short-wave length modes serve as thermal baths for longer wave-length modes with slower dynamics [31–35].

Systems with disordered interactions

Disorder breaks spatial homogeneity such as translational symmetry. In a many-body system, disordered interactions can either be found in one-body interactions such as a mag-

netic field or in two(or more)-body interactions between the particles. The first type of disorder is when some of the degrees of freedom of a system are coupled to an external spatially disordered potential. We include the case of the coupling to a disordered field (so-called *random field*). It occurs in most ferromagnets where the underlying crystalline structure shows some defects randomly distributed in the sample that give rise to static random local magnetic fields. In cold atom experiments, a spatially disordered potential trap for the atomic gas can be realized by using a laser speckle. The second type of disorder is when randomness is found in the interactions between the particles of the system (*random bonds*). It occurs for instance just after high temperature initial conditions when the configuration of this system is disordered. In glasses, the Lennard-Jones potential between particles has an attractive and a repulsive part, depending on the inter-particle distance. This creates frustration in the sense that each particle receives from the surrounding particles ‘contradictory’ messages concerning where it should move to. In this example, the disorder is self-induced and co-evolve with the positions of the particles. This is called *annealed* disorder. In the case the time scale on which the competing interactions evolve is much longer than the time of the experiment, they can be considered as constant and the disorder is referred as *quenched*.

Quenched randomness may be weak or strong in the sense that the first type, contrary to the second, does not change the nature of the low-temperature phase. Random fields in a $3d$ ferromagnet belong to the first type as the existence of an ordered state at finite temperature was proved rigorously [36, 37]. In the contrary, random bonds equally distributed between positive and negative values belong to the second category and lead to a highly frustrated and disordered phase at low temperatures. This phase is widely believed to be a glassy phase although it has not been proved analytically.

Glassy systems are systems whose relaxation time becomes extremely long when a control parameter, *e.g.* the temperature, is changed. Experimentally, the slowing down of the dynamics manifests itself in the very fast growth (typically orders of magnitude) of the viscosity with decreasing temperature. A ‘glass transition’ is said to occur when this sudden growth is well localized around a characteristic temperature T_g . Under T_g , the relaxation time grows beyond the experimentally accessible time scales and the system is bound to evolve out of equilibrium. In conventional glasses, this temperature depends on the history of the sample, in particular on the rate at which the temperature has been cooled. Hence the glass transition is not a true thermodynamic transition but rather a dynamic crossover. Disordered interactions is the characteristic ingredient believed to lead to this behavior.

Above T_g , there are two typical phenomenological behaviors of the viscosity as a function of the temperature. In the so-called strong glasses, the viscosity follows an Arrhenius law as it grows as $\exp(A/T)$, where A is some activation energy. The viscosity of the so-called fragile glasses obeys a Vogel-Fulcher law, which is an Arrhenius law with a temperature dependent activation energy $A = BT/(T - T_0)$ where T_0 is a material de-

pendent temperature around which the relaxation diverges even faster than the Arrhenius law [38, 39].

Spin glasses are prototypical systems of glasses with strong quenched disordered interactions. They are simple models of magnetic impurities randomly distributed in a static non-magnetic medium. The Ruderman-Kittel-Kasuya-Yosida (RKKY) interactions between the impurities depend on their relative distances. Since the latter are random, the interactions take random values in sign and strength. In the case of spin glasses, there are many corroborating facts supporting the idea that the glass transition is a true thermodynamic transition (*e.g.* the invariance of T_g with the cooling rate) [40–44].

Quantum spin glasses are spin glasses where quantum fluctuations play a role in addition to thermal fluctuations. These quantum fluctuations act as another disordering field which usually reduces the transition temperature. In the vicinity of a phase transition at nonzero temperature, the critical behavior of a quantum spin glass model is the same as that of the classical model; thus the effect of quantum mechanics merely renormalizes non universal quantities such as the transition temperature [45–47].

Dynamics

Let us consider the most generic situation in which a system is prepared at time t_0 in some initial condition and let us evolve with a given protocol. There are mainly two ways of creating non-equilibrium dynamics.

Equilibrium environment. Quench.

The first one consists in evolving the system with an equilibrium environment that does not correspond to that which is used to prepare the system. For instance, in a *quench* one prepares the system in equilibrium at a very high temperature² and suddenly lowers the temperature of the thermal bath. This very simple protocol is a good starting point to generate and study out-of-equilibrium dynamics. It turns out, as we shall see, that there exist well developed analytical methods to deal with it, from a classical and quantum mechanics standpoint. The system subsequently relaxes on a time scale τ_{relax} to an equilibrium corresponding to the new values of the control parameters. More precisely, this so-called thermalization is said to be reached when the density matrix of the system is given by the Gibbs-Boltzmann distribution. This puts three conditions on the final density matrix: that the final density matrix is constant in time, that it does not depend on the initial microstate of the bath (but rather on macroscopic characteristics such as the temperature) and that it does

2. Notice that it is not always possible to prepare a system in equilibrium at a given temperature. A preparation at very high temperature (compared to all the other energy scales involved) is nevertheless always possible to achieve.

not depend on the initial state of the system. Notice that a general proof for the thermalization of quantum systems is still lacking although the first two conditions above have been shown in [48]. Indeed the main difficulty emerges from the fact that quantum mechanically even when we have complete knowledge of the state of a system, *i.e.*, it is in a pure state and has zero entropy, the state of a subsystem may be mixed and have nonzero entropy. This is different classically where probabilities arise as a purely subjective lack of knowledge, since in principle the knowledge of a whole system implies the knowledge of any subsystem. Both classically and quantum mechanically, the question of knowing whether or not a system thermalizes is not always of practical interest. The relevant question in practice is to know for instance how the typical time of the experiment, τ_{exp} , compares with τ_{relax} . As long as the number of degrees of freedom N stays finite, the system always reaches the equilibrium in a finite time. But in the thermodynamic limit $N \rightarrow \infty$, one has to see how τ_{relax} scales with N . For example, in the $3d$ Ising model which is the simplest model for a $3d$ ferromagnet, the largest relaxation time scales as $\exp(cN^{2/3})$ with the constant $c > 0$ of order one [49].

If τ_{relax} is much shorter than τ_{exp} , once equilibrium is established, the state of the system depends only on the instantaneous values of the state parameters such as temperature or pressure and all equilibrium environments are equivalent no matter the form or the strength of their coupling to the system. The statics of the system can be computed directly in the canonical ensemble with no need to model the environment. If a control parameter (*e.g.* temperature) of the equilibrium environment is changed quasi-statically (*i.e.* on a time scale much larger than τ_{relax}), the system is expected to follow instantaneously the environment and the tools of statistical mechanics can still be used in this time-dependent problem.

If τ_{relax} is much longer than τ_{exp} , the statics are irrelevant since an equilibrium state is never reached, at least within the time of the experiment.

Dynamics through a phase transition. If a quench is performed from a high temperature equilibrium state to another temperature in the high temperature phase, one expects the dynamics to quickly relax towards the new equilibrium state. However, if the quench is performed down to a temperature where the system is expected to show an ordered phase, non-trivial dynamics occur and the new equilibrium state may never be reached.

This is for instance the case of the ferromagnet after a quench through the second order phase transition. The order parameter has to choose between the new two-degenerate minima of the free energy. Because different parts of the system cannot instantaneously communicate with each other, the order parameter takes simultaneously different values in different regions of the sample. The relaxation proceeds by the annihilation of the walls (topological defects) separating the domains of up spins and down spins. In the thermodynamic limit this yields a never-ending competition between domains and the overall magne-

tization remains zero. A growing length scale, $R(t)$, can be easily identified by measuring the typical size of the domains. In the absence of disorder R typically grows as \sqrt{t} .

The picture is slightly different for a quench through a first order phase transition with degenerate free energy minima in the low temperature phase. Domains do not form instantaneously after the quench but there is a temperature-dependent typical nucleation time before the local order parameter chooses a free energy minimum. Therefore the first stage of the dynamics shows some domains forming and expanding freely. It is only when all the sample is populated by domains that competition between them becomes the relevant process.

This out-of-equilibrium phenomena is known in this geometrical context as *phase ordering dynamics*. More generally, the competition between two (or more) low temperature ordered phases is named as *coarsening*.

The two-time observables like two-time correlations or two-time response functions are generally considered in experiments, theories and numerical simulations. Indeed they are the simplest non-trivial quantities that give information on the dynamics of a system [50–52]. In equilibrium, correlation and response are linked through the fluctuation-dissipation theorem which is broken out of equilibrium. Theoretically, they are usually related in a simple way to the Green functions for which an important artillery of computational methods is available. Experimentally or in numerical simulations, two-time correlations are quite easy to measure since they entail taking two snapshots of the system at different times during the evolution. The behavior of the response function was shown to be related to geometric properties of the domain walls such as roughness and topological properties [53, 54]. However its measurement is usually not an easy task since it requires a lot of statistical averaging to get a good signal-to-noise ratio.

In the coarsening regime, the behavior of two-time observables can be decomposed in two steps. For short time differences, the observables probe the local (in space and in time) properties of the sample. They are expected to behave as if equilibrium were achieved. In particular, they should be function of the time-difference only and the fluctuation-dissipation theorem is expected to hold in those short temporal windows. However, for larger time-differences, the non-equilibrium features are expected to show up like the loss of time-translational invariance. The time scale τ_{ag} that separates this two regimes is usually a growing function of the age of the system *i.e.* the time spent after the quench. The older the system is, the longer it will take for two-time observables to relax. This phenomenon is called *aging*.

Effect of disorder. In the presence of weak quenched disorder, dynamics are expected to be slower than in the pure case due to the induced frustration and the pinning of the interfaces. At zero temperature, this can even lead to a complete cessation of growth. For finite

temperatures, thermal fluctuations can release the pins, but in general the typical length $R(t)$ grows slower than in the pure case (typically logarithmically in time) [55–57].

In the presence of strong disorder, such as in spin glasses, the slowing down of the dynamics is even more catastrophic. As the nature of the ground state becomes intrinsically disordered, the identification and the observation of such a growing length scale remains an important question because a diverging length scale at the glassy transition would be a key argument in favor of a true thermodynamic transition scenario.

Non-equilibrium environment. Drive.

The second way to generate non-equilibrium dynamics is to couple the system to a non-equilibrium environment such as those we mentioned earlier. When a constant force, field or drive is applied during the evolution of the system, a steady state may establish after a transient if the system has the capacity to dissipate the energy that is injected. As an example of a classical drive, the rheometer is an instrument used to characterize the rheological properties of fluids such as viscosity. It imposes a constant shear deformation to the fluid, and one monitors the resultant deformation or stress once in a steady state. When it comes to time-dependent non-equilibrium environments, the most important examples are the cyclic protocols in the mechanism of heat engines used to produce or transform energy.

1.2 Models and methods

In the following, we list the particular models we use to study the effect of disorder on coarsening phenomena, the glassy dynamics and the effect of quantum fluctuations. We later briefly present the basic analytical and numerical tools to analyze their dynamics.

Models

Coarsening. The archetypal examples of coarsening phenomena are ferromagnets which can be simply described by the $O(n)$ lattice models. They are made up of n -component vectors of fixed length (called spins) \mathbf{s}_i placed on the nodes of a d -dimensional lattice and interacting through nearest-neighbor ferromagnetic interactions ($J > 0$). Typically, we think of a (hyper-)cubic lattice in d dimensions where each spin has $2d$ nearest neighbors. Their Hamiltonian reads

$$H = - \sum_{\langle i,j \rangle} J \mathbf{s}_i \cdot \mathbf{s}_j , \quad (1.1)$$

with the constraints $\mathbf{s}_i \cdot \mathbf{s}_i = n$. For $n = 3$ it corresponds to the Heisenberg model, for $n = 2$ it is called the XY model whereas for $n = 1$ it reduces to the well known Ising

model ($s_i = \pm 1$). Notice the absence of a kinetic term in the Hamiltonian (1.1). This is justified for processes in which inertia can be neglected or when studying the statics in which kinetic terms typically supply trivial contributions. Therefore there are no intrinsic dynamics and the relevant dynamics will be given by coupling the system to an environment.

At a critical temperature T_c depending on the values of n and d , these models undergo a phase transition from a high-temperature phase where the typical spin configurations are disordered to a low-temperature phase where all the spins tend to align in the same direction.

Although lattice models are quite amenable for numerical simulations, it is often difficult to deal with the discreteness of the lattice analytically. A first possibility is to consider the mean-field (or fully-connected) versions of the models that correspond to the Hamiltonian

$$H = -\frac{1}{N} \sum_{i < j=1}^N J \mathbf{s}_i \cdot \mathbf{s}_j. \quad (1.2)$$

The $1/N$ prefactor is there to ensure that energy scales with N (the total number of spins) in the thermodynamic limit $N \rightarrow \infty$. This approximation is equivalent to taking the $d \rightarrow \infty$ limit and wipes out the effects of small dimensionality. Another possibility is to write an effective field theory *à la* Ginzburg-Landau for the coarse-grained order parameter (*e.g.* the local magnetization). The d -dimensional $O(n)$ non-linear sigma model is a coarse-grained approximation of these $O(n)$ lattice models. The spatial dependence is given by the continuous d -dimensional vector \mathbf{x} and the spins are upgraded to n -dimensional real fields $\phi(\mathbf{x})$. The Hamiltonian reads

$$H = \int d^d \mathbf{x} \left[\frac{J}{2} \nabla \phi(\mathbf{x}) \cdot \nabla \phi(\mathbf{x}) - \frac{g}{2} \phi(\mathbf{x}) \cdot \phi(\mathbf{x}) + \frac{u}{4n} (\phi(\mathbf{x}) \cdot \phi(\mathbf{x}))^2 \right]. \quad (1.3)$$

The first term models the nearest-neighbor interactions. The field components can take any real value. However the interplay between the quadratic and quartic terms (with $u, g > 0$) favors the $\phi(\mathbf{x}) \cdot \phi(\mathbf{x}) = n g/u$ configurations.

Weak disorder. Weak disorder can be introduced in the previous models by adding an interaction with a spatially random magnetic field \mathbf{H} . For the $O(n)$ lattice models this yields the following Hamiltonian:

$$H = - \sum_{\langle i,j \rangle} J \mathbf{s}_i \cdot \mathbf{s}_j - \sum_i \mathbf{H}_i \cdot \mathbf{s}_i. \quad (1.4)$$

We shall focus on the case $d = 3$ and $n = 1$, the so-called random field Ising model (3d RFIM), with 6 nearest neighbors and a bimodal distribution for the random fields ($H_i = \pm H$ with equal probability).

The RFIM is relevant to a large class of materials due to the presence of defects that cause random fields. Dilute anisotropic antiferromagnets in a uniform field are the most

studied systems expected to be described by the RFIM. Several review articles describe its static and dynamic behavior [57] and the experimental measurements in random field samples have been summarized in [58]. Dipolar glasses also show aspects of random field systems [59, 60].

In the case $H = 0$, the RFIM reduces to the pure Ising model with a phase transition from a paramagnetic to a ferromagnetic state occurring at a critical temperature $T_c \simeq 4.515 J$. It is well established that in $d = 3$ (not in $d = 2$) the ordered phase survives for finite H : there is a phase separating line on the (T, H) plane joining $(T_c, H = 0)$ and $(T = 0, H_c)$ with $H_c \simeq 2.215(35) J$ [61, 62]. At $T = 0$ and small magnetic field, it has been rigorously proven that the state is ferromagnetic [36, 37]. The nature of the transition close to zero temperature has been the subject of some debate. Claims of it being first order [63] have now been falsified and a second order phase transition has been proven [64, 65]. The presence of a spin glass phase close to $(T = 0, H_c)$ [66] has been almost invalidated [67] although there is still a possibility it exists [68].

Quenched disorder can also be introduced in the $O(n)$ lattice models by considering some random couplings, J_{ij} , between the spins:

$$H = - \sum_{\langle i,j \rangle} J_{ij} \mathbf{s}_i \cdot \mathbf{s}_j, \quad (1.5)$$

where the J_{ij} 's are independent random variables. The family of models this Hamiltonian encompasses is called *random bond* models. If the couplings are ferromagnetic with a finite probability to be zero, this gives the bond-diluted models (percolation physics). For $n = 1$, the Random Bond Ising Model (RBIM), with ferromagnetic couplings distributed on a small window of width J around $J_0 > J$, is another typical model used to study the domain growth in the presence of weak disorder.

Glasses. The case of strong disorder is realized when the J_{ij} 's are equally distributed between positive (ferromagnetic) and negative (anti-ferromagnetic) values. In this case the models exhibit glassy behavior at low temperatures. For $n = 1$, the corresponding models are often called the Ising spin glasses. The lower-critical dimension of those models is expected to be two and for $d = 2$ the transition occurs at zero temperature. We shall focus on the case $d = 3$, the so-called Edwards-Anderson (3d EA) model, with 6 nearest neighbors and a bimodal distribution for the random couplings ($J_{ij} = \pm J$ with equal probability). The 3d EA is in a sense complementary to the 3d RFIM which has some weak disorder in the local magnetic fields whereas the 3d EA model has a strong disorder localized on the bonds. This model undergoes a static phase transition from a paramagnetic to a spin glass phase at $T_g \simeq 1.14(1) J$ [69]. The nature of its low temperature static phase is not clear yet and, as for the out-of-equilibrium relaxation, two pictures developed around a situation with only two equilibrium states as proposed in the droplet model [70, 71] and a much more

complicated vision emerging from the solution of its mean-field version, the SK model [72] whose Hamiltonian reads

$$H = -\frac{1}{\sqrt{N}} \sum_{i<j=1}^N J_{ij} s_i s_j. \quad (1.6)$$

Notice the $1/\sqrt{N}$ prefactor that is needed to ensure a well defined thermodynamic limit. More generally, the mean-field version of the $O(n)$ lattice model reads

$$H = -\frac{1}{\sqrt{N}} \sum_{i<j=1}^N J_{ij} \mathbf{s}_i \cdot \mathbf{s}_j, \quad (1.7)$$

and is equivalent in the $n \rightarrow \infty$ limit to the soft-spin version of SK model (so-called the $p = 2$ spin glass) where the length constraint on each spin is relaxed and replaced by the global spherical constraint $\frac{1}{N} \sum_{i=1}^N \mathbf{s}_i \cdot \mathbf{s}_i = n$ [73, 74]. The $p = 2$ spin glass model does not have a true spin glass behavior but is more of a ferromagnet. Indeed, we shall see it has a strong connection with the pure $3d$ $O(n)$ ferromagnet model in the limit $n \rightarrow \infty$.

Quantumness. Quantum mechanics determines the behavior of physical systems at atomic and subatomic scales. The search for quantum effects at macroscopic scales started soon after the development of quantum mechanics. A number of quantum manifestations at such scales have been found including quantum tunneling of the phase in Josephson junctions [75] or resonant tunneling of magnetization in spin cluster systems [76]. Quantum fluctuations are expected to play an important role specially in the absence of thermal fluctuations at zero temperature. A way to introduce quantum fluctuations into the $O(n)$ lattice models (or their disordered versions) is to add a non-commuting term to the Hamiltonian. For $n = 1$, one can think of adding a transverse field to the quantum Ising model yielding the following Hamiltonian in $d = 3$:

$$H = -\sum_{\langle i,j \rangle} J \sigma_i^z \sigma_j^z - \sum_i H \sigma_i^x, \quad (1.8)$$

where the σ_i^μ ($\mu = x, y, z$) are the familiar Pauli matrices. This model was proposed to be realized experimentally with $\text{LiHo}_x\text{Y}_{1-x}\text{F}_4$ [77], an insulating magnetic material in which the magnetic ions are in a doublet state due to crystal field splitting. For $n > 1$, quantum fluctuations can be put in by reintroducing a kinetic term to the Hamiltonian, yielding the family of so-called quantum rotor models. For instance the Hamiltonian of the $O(n)$ lattice model is upgraded to

$$H = \frac{1}{n} \sum_{i=1}^N \frac{\Gamma}{2} \mathbf{L}_i^2 - \sum_{\langle i,j \rangle} J \mathbf{s}_i \cdot \mathbf{s}_j. \quad (1.9)$$

The spins \mathbf{s}_i are still n -component vectors (with $\mathbf{s}_i \cdot \mathbf{s}_i = n$) but are now called ‘rotors’ to avoid confusions with real quantum spins described by Pauli matrices. The difference between rotors and quantum spins is that the components of the latter at the same

site do not commute whereas the components of \mathbf{s}_i do. \mathbf{L}_i is the i -th generalized angular momentum operator which involves the momentum operator canonically conjugate to \mathbf{s}_i : $\mathbf{p}_i = -i\hbar\partial/\partial\mathbf{s}_i$. The \mathbf{s}_i 's and the \mathbf{p}_i 's satisfy the usual quantum mechanical commutation relations. $\Gamma > 0$ acts like a moment of inertia and controls the strength of quantum fluctuations; when $\hbar^2\Gamma/J \rightarrow 0$ the model approaches the classical $O(n)$ lattice model. As discussed in [78] models of quantum rotors are non-trivial but still relatively simple and provide coarse-grained descriptions of physical systems such as Bose-Hubbard models and double layer antiferromagnets.

We focus in particular on the mean-field version of the quantum rotor glass the Hamiltonian of which reads

$$H = \frac{1}{n} \sum_{i=1}^N \frac{\Gamma}{2} \mathbf{L}_i^2 - \frac{1}{\sqrt{N}} \sum_{i<j=1}^N J_{ij} \mathbf{s}_i \cdot \mathbf{s}_j . \quad (1.10)$$

The J_{ij} couplings are taken randomly from a Gaussian distribution with zero mean and J^2 variance. We shall see that the connection to the pure $3d$ $O(n \rightarrow \infty)$ ferromagnet holds for the quantum models as well.

Analytical treatment

Classical

Master Equation. The microcanonical postulate (stating the equi-probability of all the accessible microstates in a closed isolated system in macroscopic equilibrium) can be generalized to non-equilibrium situations as the so-called evolution postulate, or Master equation. The Master equation is a first order differential equation describing the time-evolution of an isolated classical system in terms of the probabilities $P_t(s)$ for the system to be in a given microstate s at time t . It can be derived from the first principles of quantum mechanics (basically the Schrödinger equation) under the hypothesis that the quantum phases of wave functions are randomized on a short time scale (quantum chaos) by weak external processes [79]. It reads

$$\frac{dP_t(s)}{dt} = \sum_{r \neq s} [P_t(r)W(r \mapsto s) - P_t(s)W(s \mapsto r)] , \quad (1.11)$$

where $W(r \mapsto s)$ is the probability of transition from the microstate r to the microstate s . These transition rates respect the energy conservation: $W(r \mapsto s) = 0$ if $|E_s - E_r| > \delta E$ where δE is the incertitude on the energy at a macroscopic level. As a consequence of the invariance of the underlying microscopic equations under time-reversal, they are also symmetric: $W(r \mapsto s) = W(s \mapsto r)$. In the canonical set-up, one can write a similar equation for the evolution of the system. The transition rates no longer satisfy the energy

conservation and are no longer symmetric. However, as a consequence of the time-reversal symmetry of the microscopic equations of the equilibrium bath variables, they satisfy the so-called detailed balance condition:

$$W(r \mapsto s) e^{-\beta E_r} = W(s \mapsto r) e^{-\beta E_s} , \quad (1.12)$$

where β is the inverse temperature of the bath and throughout this manuscript we use units in which $k_B = 1$. In order to satisfy the evolution postulate and evolve towards equilibrium, the system must have the so-called mixing property that generalizes the ergodic principle to non-equilibrium situations. For a given set of control parameters, a macroscopic state is characterized by a probability density that is non zero on a manifold of the phase space. During the evolution, the mixing property spreads the non-homogeneous initial distribution on the whole manifold to finally reach the uniform microcanonical distribution. Under this mixing condition, one can show that the probabilities $P_s(t)$ converge to the equilibrium Gibbs-Boltzmann distribution regardless of the initial conditions *i.e.* any macroscopic classical system evolves towards its equilibrium state.

Langevin Equation. It is often difficult to give a precise description of the environment and its interactions with the system. And when it is possible, it is almost always impossible to explicitly integrate out the degrees of freedom of the bath to compute averages in the system of interest. In the Master equation formalism, this difficulty lies in knowing the transition rates $W(r \mapsto s)$. To overcome this difficulty, one is led to find an heuristic way of modeling the environment that should be guided by the symmetries of the system and physical intuition.

In his study of Brownian motion [80], Paul Langevin wrote in 1908 the following equation, that later took his name, for the position q of a Brownian particle of mass m :

$$m\ddot{q} = F(q) - \gamma_0 \dot{q} + \xi(t) . \quad (1.13)$$

$F(q)$ is the systematic interaction force due to the intramolecular and intermolecular interactions. The interaction with the environment is modeled by two heuristic forces. The first is a friction force term that introduces the dissipation and is here proportional to the particle's velocity \dot{x} (Stokes' law). The second is a random force ξ , taken to be a Gaussian process, that models the rapid thermal excitations. If the environment is in equilibrium, the two terms are linked through a fluctuation-dissipation relation that A. Einstein established in his 1905 article on Brownian motion [8].

In many cases of practical interest the Langevin equation is given in the overdamped limit (inertia is neglected) and with a white noise (the environment has a vanishing relaxation time). However, since there are other interesting instances in which the environment exhibits retardation and motivated by the generalization to quantum systems, we keep inertia and introduce color for the noise. Moreover, to be even more generic, we consider the

case in which the noise acts multiplicatively. This situation is expected to occur when the environment is coupled non-linearly to the system.

This heuristic modeling of the interactions with the environment can be transposed at the (even more) mesoscopic level in terms of a coarse-grained order-parameter field $\phi(x, t)$. Once again, the spatio-temporal coarse-graining procedure is rarely tractable but one expects the action of the environment to be similar to the one of the Langevin dynamics. In the so-called model A for non-conserved order-parameter, an overdamped evolution (*i.e.* inertia can be neglected, for instance when the short-time dynamics have been coarse-grained in time) is given by

$$0 = -\frac{\delta\mathcal{F}[\phi]}{\delta\phi(x, t)} - \gamma_0\dot{\phi}(x, t) + \xi(x, t) , \quad (1.14)$$

where \mathcal{F} is the Ginzburg-Landau free-energy functional that one typically constructs using symmetry and simplicity considerations together with physical intuition.

MSRJD formalism. It is possible to give a field theory representation of the stochastic Langevin dynamics by use of the Martin-Siggia-Rose-Janssen-deDominicis (MSRJD) formalism [81–86]. In a nutshell, the generating functional is obtained by first upgrading the physical degrees of freedom of the system and the random noise into fields. The Langevin equation of motion and its initial conditions are turned into a path integral and the action of the corresponding field theory is evaluated on-shell, thanks to the introduction of one extra Lagrange multiplier field for each physical degree of freedom. Since it is Gaussian, the noise field appears quadratically in the action and can thus be integrated out. One is left with a path integral over twice as many fields as number of physical degrees of freedom. The MSRJD formalism is particularly well suited to treating the dynamics of disordered systems following a quench. Indeed, provided that the initial conditions are uncorrelated with disorder (*e.g.* for very high temperature initial conditions), the generating functional evaluated at zero sources is equal to one and can therefore be trivially averaged over the disorder configurations without having to use the Replica Trick [85].

Quantum

Schrödinger equation. Quantum mechanically, the evolution of a system and its environment is given by the Schrödinger equation. This microscopic equation is invariant under time-reversal unless magnetic fields (or spins, or more generally currents) are involved. The evolution for the reduced system, once the degrees of freedom of the bath have been somehow integrated out, is however not unitary. Despite the lack of a general proof, it is widely believed that equilibrium quantum systems in contact with a thermal bath tend to thermalize like in the classical case.

Schwinger-Keldysh formalism. A convenient way to treat the out-of-equilibrium dynamics of a quantum system coupled or not to an environment is the use of the functional Schwinger-Keldysh formalism which can be seen as the quantum generalization of the MSRJD formalism. This was initiated by Julian S. Schwinger in 1961, and has been further developed by Leonid V. Keldysh and many others. For the last 40 years, this technique has been used to attack a number of interesting problems in statistical physics and condensed matter theory such as spin systems [87], superconductivity [88–91], laser [92], tunneling [93, 94], plasma [95], other transport processes [96] and so on. For equilibrium problems, it has also been an alternative to the sometimes cumbersome Matsubara analytical continuation.

For a system initially prepared at time $t_0 = 0$, it involves a closed time-contour \mathcal{C} that goes from zero to plus infinity and then comes back to zero. This two-branch contour and the doubling of the number of degrees of freedom that comes with it take their roots in the time evolution of an operator (let say O) in the Heisenberg picture,

$$\tilde{T} \left\{ e^{-\frac{i}{\hbar} \int_t^0 dt' H_{\text{tot}}(t')} \right\} O(t) T \left\{ e^{-\frac{i}{\hbar} \int_0^t dt' H_{\text{tot}}(t')} \right\},$$

where T and \tilde{T} are respectively the time and anti-time ordering operators. $H_{\text{tot}}(t) = H(t) + H_{\text{int}}(t) + H_{\text{env}}$ is the total Hamiltonian of the system plus the environment. Once the system and the environment have been encoded in this path integral, one has to integrate over the environment variables in order to obtain an effective action for the system. This can be performed in the case the environment is described by a Lagrangian \mathcal{L}_{env} that is quadratic in its variables. The Lagrangian \mathcal{L}_{int} describing the interaction between the system and the environment can be averaged over the environment variables by using perturbation theory in the coupling constant. Like in the classical case, a very simple model of a thermal bath consists in a set of non-interacting harmonic oscillators that are coupled to the system of interest. The interaction with the bath gives rise to non-local terms in the action that play a similar role to the ones of a colored bath in the previous classical picture.

The Schwinger-Keldysh formalism, like its classical analog, is well suited to treating the dynamics of disordered systems after a quench from infinite temperature.

Numerics: Monte Carlo

Equilibrium simulations. It is usually impossible to give an analytical treatment of interacting statistical systems beyond the mean-field or fully-connected approximation that wipes out all the effects of the small dimensionality of the world in which we live. Computer simulations provide a flexible way to tackle such problems. The task of equilibrium statistical mechanics is to compute averages of the type $\sum_s P_{\text{eq}}(s) O(s)$ where s runs over all the configurations and P_{eq} is the equilibrium Gibbs-Boltzmann probability proportional

to $e^{-\beta H(s)}$. The previous sum can never be computed exactly for the number of configurations grows exponentially with the number of degrees of freedom. The idea behind Monte Carlo simulations is to provide numerical estimates of these sums *via* a stochastic trajectory \mathcal{S} in the configuration space. Since the Boltzmann factor $e^{-\beta H(s)}$ vanishes for most of the configurations, Nicholas Metropolis *et al.* introduced the so-called ‘importance sampling’ algorithm [97] in which a configuration s is chosen to be part of the sum with probability $P_{\text{eq}}(s)$. The average then reduces to the arithmetical mean of the type $\sum_{s \in \mathcal{S}} A(s)$. The method Metropolis proposed to obtain this result is based on Markov theory. It generates a sequence of configurations $\mathcal{S} \equiv s_0 \mapsto s_1 \mapsto s_2 \mapsto \dots$ in which each transition has a probability $W(s_i \mapsto s_{i+1})$ to occur. The probability for a configuration s to be selected at the i -th step, $P_i(s)$, converges to the equilibrium distribution $P_{\text{eq}}(s)$ regardless of the initial condition s_0 provided that the detailed balance condition is satisfied: $W(s_i \mapsto s_j)e^{-\beta H(s_i)} = W(s_j \mapsto s_i)e^{-\beta H(s_j)}$. A simple choice for the transition rates W uses the energy variation $\Delta E \equiv H(s_j) - H(s_i)$ by setting $W = 1$ if $\Delta E < 0$ and $W = e^{-\beta \Delta E}$ otherwise. The rapidity of the convergence to the equilibrium distribution and the simplicity to compute ΔE depends on the choice of the transitions between two successive configurations but the final result is independent of that choice. For a system of Ising spins, the simplest transitions consist in flipping one single spin at a time but it is sometimes useful to implement cluster algorithms in which the transitions are collective spin flips. It is only after the Markov chain has converged to equilibrium, that one can start to compute the static averages.

Out of Equilibrium simulations. The Monte Carlo method briefly explained above is *a priori* not suited for out-of-equilibrium dynamics. If one measures observables before equilibrium is achieved, we saw that the choice of the transition rates matters. This is precisely the analogue situation of having the Master equation but not knowing the transition rates since these depend on the details of the environment. If one wants to run a computer simulation to study the out-of-equilibrium dynamics of a system connected to an equilibrium thermal bath without any further information on the environment, the only constraint on the choice of the transitions is that they must satisfy the detailed balance condition.

Fortunately, there are some dynamical properties of the system that are independent of the transition rules, at least within families of these. For example, the exponent z in the Ising model appears to be the same for the Metropolis, the heat-bath or the continuous time algorithms. Such algorithms fall in the same dynamic universality class. Nevertheless, other algorithms like the Wolff cluster one or the simulated tempering do not. In conclusion, when one is interested in the dynamics of a model to get a typical picture of how a system evolves to equilibrium, it is sensible to start by using the simplest dynamics. This is the philosophy we adopt.

1.3 Questions

Equilibrium and time-reversal symmetry

Despite the invariance of the microscopic physics under time reversal³, it is well known from the second principle that the evolution of out-of-equilibrium macroscopic systems is not invariant under this transformation. However, when equilibrium is reached, the symmetry is restored: it is experimentally impossible to determine whether a movie is played forward or backward in time. This time-reversal symmetry, specific to equilibrium, has been addressed many times in the past. It was for instance one of the key ingredients in L. Onsager's work of 1931 [11, 12] to establish the reciprocal relations. Time-reversal is also at the heart of fluctuation theorems that give relations between forward and backward trajectories.

In Chapter 2, we address this question one more time by identifying this symmetry in the context of a field theory description of classical dissipative systems: the MSRJD formalism. For equilibrium situations, we identify the field transformation corresponding to the time-reversal symmetry. It consists in a set of transformations for both the physical fields and the Lagrange multiplier fields involving, as expected, a time-reversal of those fields. This symmetry is presented as a necessary and sufficient condition for equilibrium dynamics. Indeed, at the level of observables, we show that the corresponding Ward-Takahashi identities lead to all the well-known equilibrium properties and relations such as stationarity, fluctuation-dissipation theorem and the Onsager reciprocal relations. This symmetry is a powerful tool to derive, in a rapid and systematic approach, all sorts of fluctuation-dissipation relations.

In equilibrium, the MSRJD formalism can be written in terms of a super-symmetric formulation. It involves the integration over a super-field whose components encode the physical fields, the Lagrange multiplier fields and two extra fermionic fields (introduced to give an integral representation of a functional determinant). This formulation has been introduced and derived for overdamped (no inertia) Langevin equations with an additive white noise environment [98–101]. We generalize this approach to the case with inertia and a multiplicative colored noise. The generating functional is invariant under two continuous super-symmetric field transformations that exchange the bosonic and the fermionic fields. At the level of observables, the corresponding Ward-Takahashi identities lead to some of the already mentioned equilibrium properties like stationarity or fluctuation dissipation theorems. However, they fail to generate relations involving a time-reversal like the Onsager reciprocal relations. We discuss the relations these two super-symmetries have with the previous MSRJD symmetry.

When the system is out of equilibrium, this symmetry of the MSRJD formalism is

3. At least in non-relativistic theories.

broken in a way that leads very naturally to fluctuation relations like the Jarzynski equality or even the underlying fluctuation theorem.

We identify another new symmetry of the MSRJD generating functional, which is valid in but also out of equilibrium. At the level of observables, it generates equations of motion coupling correlations and responses. These Schwinger-Dyson equations provide a nice way to express all sorts of responses in terms of correlation functions without applying any extra field. This has direct applications in computer simulations where the computation of linear responses using weak perturbations (to stay in the linear regime) is not an easy task; besides requiring two simulations (one with and one without the perturbation) it also requires a lot of statistical averaging to get a good signal-to-noise ratio.

Dynamical scaling and universality

Out-of-equilibrium dynamics depend *a priori* on the whole protocol used to prepare and evolve the system. Therefore, finding universal features of the dynamics does not seem easy. However, in many situations the late stage dynamics are believed to be governed by a few properties of the system and environment whereas material details should be irrelevant. The renormalization group (RG) analysis is a powerful tool to detect and describe the universal features of models in equilibrium. In particular, it gives access to scaling relations. Although there were many attempts to include the time evolution in the RG procedure, there is no exact scheme to generalize this approach to dynamical problems away from criticality. The difficulty arises as a result of the absence of a small parameter, analogous to $\epsilon = 4 - d$ for critical phenomena: because of this, one cannot obtain explicit RG relations.

Coarsening. In the field of coarsening phenomena, motivated by experimental observations and simulations, the *dynamical scaling hypothesis* states that there exists, at late times, a single characteristic length scale $R(t)$ such that the domain structure is (in a statistical sense) independent of time when lengths are scaled by $R(t)$ [50]. In terms of observables, this predicts that the time dependence enters only through $R(t)$. For example, the aging contribution⁴ of the two-time correlation function $C(t, t')$ is expected to scale as $C_{\text{ag}}(t, t') = f(R(t)/R(t'))$. In a field theory description, such dynamical scaling can be interpreted as consequences of symmetries of the effective dynamical action that describes the late-stage dynamics.

This scenario has been proven analytically at zero temperature (with Glauber or model A dynamics) in some mean-field models like the $O(n \rightarrow \infty)$ non-linear sigma model [102] and in some very simple one dimensional models like the 1d Ising model [103, 104] or the 1d XY model [105] [both defined in eq. (1.3)]. More recently it has been proven for the

4. As opposed to the thermal contribution that is time-translational invariant.

distribution of domain areas in the $2d$ Ising model [106]. The dynamical scaling hypothesis can be supplemented by the statement that the temperature dependence can be absorbed into the domain scale $R(t)$ such that the scaling functions are independent of the temperature. This is somehow supported by equilibrium renormalization group analysis that predicts the existence of a few fixed points controlling the low temperature phase. This has been tested numerically for instance in the $2d$ Ising model [107] with Metropolis dynamics. Daniel S. Fisher and David A. Huse pushed this idea a bit further, in the presence of weak disorder in which the coarsening picture is expected to hold. They conjectured that once the dynamical scaling hypothesis is used to describe the long times dynamics, so that times and lengths are measured in units of $R(t)$, none of the out-of-equilibrium observables depend on the quenched randomness [70] and their scaling functions are thus identical to those of the pure limit. This is referred as super-universality. Notice that a typical length, L^* , can be associated to disorder by matching the energy barriers it creates and the thermal energy. L^* is by definition temperature and disorder dependent. In this picture, when $R(t) \ll L^*$, the dynamics are the one of the pure system and when $R(t) \gtrsim L^*$, the dynamics are slowed down by activated escape over the barriers. In [108], it was argued in the context of the $1d$ and $2d$ RBIM that the ratio $R(t)/L^*$ should enter the scaling functions independently of the other scalings. For the two-time correlation function, this implies the scaling $C_{\text{ag}}(t, t') = f(R(t)/R(t'), L^*/R(t))$ that violates the super-universality. However, for the late stage dynamics $R(t) \gg L^*$, the ratio $L^*/R(t)$ becomes negligible and the super-universality hypothesis is expected to hold. It has been tested numerically on some selected observables in a few Ising models with weak disorder. It has been shown to hold for the equal-times two-point function of the $3d$ random field Ising model (RFIM) [109] and the $2d$ random bond Ising model (RBIM) [110, 111]. More recently, the distribution of domain areas in this last model [112] and the integrated response [113] has also been shown to be super-universal.

In Chapter 3, we test, by means of numerical simulations, the dynamical scaling and the super-universality hypothesis in the $3d$ RFIM [defined in eq. (1.4)] after a temperature quench in the coarsening phase. We place the emphasis on the spatio-temporal fluctuations by studying the distributions of local coarse-grained observables.

Spin glasses. The droplet picture of the out-of-equilibrium dynamics of spin glasses predicts a single characteristic length scale that is developing in the system after the quench [70, 71, 114, 115]. Its existence is less clear than in the field of coarsening phenomena. Some evidence for a growing length in the $3d$ EA model at low temperatures have been interpreted within the droplet scenario [116–118], but other groups understand this length within the other mean-field picture [119]. The studies of finite dimension structural glasses both from numerical simulations and experimental probes have provided mounting evidence for the existence of a growing length, at least in the super-cooled liquid phase. In the truly glassy regime, the existence of a growing length scale is supported by the fact that correlation

functions show some dynamical scalings which can be naturally explained in that scenario. Dynamics of glasses are believed to be heterogeneous in the sense that different regions of the sample age at different rates [120] and dynamic heterogeneities could be crucial to understand the full temporal evolution. Therefore, considerable attention has been paid to the study of the local fluctuations of two-time observables such as two-time correlations or linear responses. In glasses, the average over disorder makes the spatial correlation functions short ranged. Spatially fluctuating quantities such as locally coarse-grained correlation functions and their probability distribution functions are candidates to detect the growing length.

We study, by means of numerical simulations, the dynamics of the $3d$ EA model [defined in eq. (1.5)] after a temperature quench in the glassy phase. We focus in particular on fluctuating local observables used to describe the heterogeneous dynamics. We show that the super-universality hypothesis does not hold and the comparison with the results of the quenched RFIM sheds a new light on the differences between domain growth versus glassy dynamics from the point of view of out-of-equilibrium scaling relations.

Effect of a drive

The effect of a non-equilibrium environment such as a drive on a macroscopic system close to a quantum phase transition is a by and large unexplored subject. Some works have focused on non-linear transport properties close to an (equilibrium) quantum phase transition [121–123]. Others have studied how the critical properties are affected by non-equilibrium drives [124–126]. However, a global understanding of phase transitions in the control parameter space T, V, Γ , with T the temperature, V the driving strength, and Γ the strength of quantum fluctuations, is still lacking. Furthermore, to the best of our knowledge, the issue of the relaxation toward the quantum non-equilibrium steady state (QNESS) has not been addressed in the past.

In Chapter 4, we address these questions by considering the fully-connected quantum rotor glass defined in eq. (1.10). We prepare the system at very high temperature and then suddenly couple it to two electronic leads [45] at different chemical potentials but at the same temperature T . The voltage drop V creates a current tunneling through the system. In a first part, we study the properties of the non-equilibrium environment composed by the two leads. In particular we show that its effect on the slow modes of the dynamics is the one of a thermal equilibrium bath. Then we study how the dynamical phase transition, which separates the paramagnet and the ordering phase, survives in the presence of the drive by deriving the dynamical phase diagram of the model in the (T, V, Γ, g) parameter space where g is the coupling constant to the environment. In a third part of this chapter, we analytically solve the long-time dynamics in the coarsening phase and we prove that a generalized super-universality hypothesis holds for the long-time behavior of two-time

correlation functions since the scaling functions do not depend on T , the strength of disorder J , Γ nor V . As in the classical $p = 2$ spin glass, the response is found to loose memory in the aging regime, corresponding to an infinite effective temperature. We discuss the connection with real space coarsening by establishing the mapping to the $3d$ $O(n \rightarrow \infty)$ quantum pure ferromagnet. Finally, we compute the current I as a function of V and show that it quickly saturates to a constant value.

In the concluding chapter, we present some lines for future research.

The work presented in this manuscript led to the following publications:

- C. Aron, G. Biroli and L. F. Cugliandolo, “Symmetries of generating functionals of Langevin processes with colored multiplicative noise,” J. Stat. Mech. P11018 (2010), arXiv:1007.5059;
- C. Aron, G. Biroli and L. F. Cugliandolo, “Coarsening of disordered quantum rotors under a bias Voltage,” Phys. Rev. B **82**, 174203 (2010), arXiv:1005.2414;
- C. Aron, G. Biroli and L. F. Cugliandolo, “Driven Quantum Coarsening,” Phys. Rev. Lett. **102**, 050404 (2009), arXiv:0809.0590;
- C. Aron, C. Chamon, L. F. Cugliandolo and M. Picco, “Scaling and Super-Universality in the Coarsening Dynamics of the 3D Random Field Ising Model,” J. Stat. Mech, P05016 (2008), arXiv:0803.0664.

SYMMETRIES OF LANGEVIN GENERATING FUNCTIONALS

Contents

2.1	Langevin equation	28
2.1.1	Additive noise	28
2.1.2	Multiplicative noise	29
2.1.3	Initial conditions	30
2.1.4	Markov limit	30
2.2	The MSRJD path-integral formalism	31
2.2.1	Action in the additive noise case	31
2.2.2	Action in the multiplicative noise case	32
2.2.3	Jacobian	33
2.2.4	Observables	34
2.2.5	Classical Kubo formula	37
2.3	Equilibrium	38
2.3.1	The action	39
2.3.2	Symmetry of the MSRJD generating functional	39
2.3.3	Ward-Takahashi identities	42
2.3.4	Stationarity	42
2.3.5	Equipartition theorem	43
2.3.6	Reciprocity relations	43
2.3.7	Fluctuation-dissipation theorem (FDT)	44

2.3.8	Higher-order FDTs: e.g. 3-time observables	45
2.3.9	Onsager reciprocal relations	46
2.3.10	Supersymmetric formalism	47
2.3.11	Link between \mathcal{T}_{eq} and the supersymmetries	50
2.3.12	Newtonian limit: a phase space approach	50
2.4	Out of equilibrium	51
2.4.1	Non-equilibrium fluctuation relations	52
2.4.2	Generic relations between correlations and linear responses . .	54
2.4.3	Composition of \mathcal{T}_{eom} and \mathcal{T}_{eq}	58
2.5	Conclusions	59
	Appendices	60
2.A	Conventions and notations	60
2.B	Discrete MSRJD for additive noise	61
2.B.1	Discrete Langevin equation	61
2.B.2	Construction of the MSRJD action	61
2.B.3	Jacobian	64
2.C	Discrete MSRJD for multiplicative noise	67

THE stochastic evolution of a classical system coupled to a quite generic environment can be described with the Langevin formalism [80, 127–129] and its generating functional, the Martin-Siggia-Rose-Janssen-deDominicis (MSRJD) path-integral [81–86]. In many cases of practical interest the effect of the environment is captured by an additive white noise and its memory-less friction, Brownian motion being the paradigmatic example [80]. Nevertheless, there are many other interesting instances in which the noise is multiplicative and colored, and the friction effect is consistently described by a memory kernel coupled to a non-linear function of the state variable. Such Langevin equations appear in many different branches of physics (as well as chemistry and other sciences). In magnetism, the motion of the classical magnetic moments of small particles is phenomenologically described by the Landau-Lifshitz-Gilbert equation in which the fluctuations of the magnetic field are coupled multiplicatively to the magnetic moment [130, 131]. Many other examples pertain to soft condensed matter; two of these are confined diffusion, in which the diffusion coefficient of the particle depends on the position via hydrodynamic interactions [132], and the stochastic partial differential equation that rules the time-evolution of the density of an ensemble of N Brownian particles in interaction [133, 134]. In a cosmological framework, they are effective equations of motion for the out of (although close to) equilibrium evolution of self-interacting quantum fields in which the short-wave length modes serve as thermal baths for longer wave-length modes with slower dynamics [32–34, 135, 136]. Such type of fluctuations may yield *a priori* unexpected results such as noise induced phase transitions in systems in which the associated deterministic potential does not exhibit any symmetry breaking [137–140, 140, 141].

In order to better understand these processes it is useful to distinguish cases in which sources of fluctuations and dissipation can be different. On the one hand, the noise and friction term can have an ‘internal’ origin, like in diffusion problems. On the other hand, the stochastic fluctuations can be due to an ‘external’ source [142]. In the former cases one usually assumes that the variables generating the noise and friction are in equilibrium and the terms in the Langevin equation associated to them are linked by a fluctuation-dissipation theorem. In the absence of non-conservative external forces the Boltzmann measure of the system of interest is a steady state of its dynamics. In the latter cases noise and dissipation are not forced to satisfy any equilibrium condition and this translates into the possibility of having any kind of noise and friction terms. For concreteness we shall focus on the first type of problems and only mention a few results concerning the latter.

In treatments of the examples mentioned in the first paragraph, the delicate double limit of vanishing fast variables relaxation time and noise correlation time is often taken. These lead to a first order stochastic differential equation with multiplicative white noise. Its interpretation in the Itô, Stratonovich or other sense requires a very careful analysis of the order of limits, see e.g. [143] and references therein. In the body of this chapter we shall keep both time scales finite and thus avoid the subtleties encountered in the double vanishing limit.

We identify a number of symmetries of the MSRJD generating functional of inertial Langevin processes with multiplicative colored noise. One symmetry is only valid in equilibrium. The corresponding Ward-Takahashi identities between the correlation functions of the field theory lead to various equilibrium relations such as stationarity, fluctuation-dissipation theorems [144–149] or Onsager relations. Away from equilibrium, the symmetry is broken giving rise to various out-of-equilibrium fluctuation relations [25, 27, 150, 29, 151, 152], [153–158], [159–161]. Another symmetry holds for generic out-of-equilibrium set-ups and implies dynamic equations coupling correlations and linear responses. It allows in particular to express the linear response in terms of correlations without applying a perturbing field [162–169], [170–174].

We are aware of the fact that some of the results we derive – especially, in the limit of additive noise – were already known and we do our best to attribute them to the authors of the original papers for review articles. Still, the presentation that we gradually develop allows one to go beyond the simple cases and treat the multiplicative non-Markovian processes with the same level of difficulty. As far as we know, these constitute new results. Moreover, we discuss in greater detail than previously done the transformation of the measure and several Jacobians, and the domain of integration of the fields in the path-integral. The importance of dealing with a colored noise, and to treat the transformation of the fields in the complex plane, is enhanced by our purpose to extend this analysis to quantum dissipative problems.

2.1 Langevin equation

We consider a 0-dimensional field ψ (*e.g.* a particle at position ψ) with mass m driven by a force F and in contact with a thermal bath in equilibrium at inverse temperature β . The initial time, t_0 , is the instant at which the particle is set in contact with the bath and the stochastic dynamics ‘starts’. We call it $t_0 = -T$ and without loss of generality we work within a symmetric time-interval $t \in [-T, T]$. In this chapter, contrary to the rest of the manuscript, T is not a temperature ($T \neq \beta^{-1}$) but a time. The extension to higher dimensional cases is straightforward.

Our conventions are given in [2.A](#).

2.1.1 Additive noise

The Langevin equation with additive noise is given by

$$\text{EQ}([\psi], t) \equiv m\ddot{\psi}(t) - F([\psi], t) + \int_{-T}^T du \, \eta(t, u) \dot{\psi}(u) = \xi(t) , \quad (2.1)$$

with $\dot{\psi}(t) = d\psi(t)/dt$ and $\ddot{\psi}(t) = d^2\psi(t)/dt^2$. The force can be decomposed into conservative and non-conservative parts: $F([\psi], t) = -V'(\psi(t), \lambda(t)) + f^{\text{nc}}([\psi], t)$. V is a local potential the time-dependence of which is controlled externally through a protocol $\lambda(t)$. V' denotes the partial derivative of V with respect to ψ . $f^{\text{nc}}([\psi], t)$ collects all the non-conservative forces that are externally applied. $f^{\text{nc}}([\psi], t)$ is assumed to be causal in the sense that it does not depend on the future states of the system, $\psi(t')$ with $t' > t$. Furthermore, we suppose that $f^{\text{nc}}([\psi], t)$ does not involve second – nor higher – order time-derivatives of the field $\psi(t)$. The last term in the left-hand-side (Lhs) and the right-hand-side (RHS) of the equation model the interaction with the bath. These two heuristic terms can be derived using a model [\[175, 176\]](#) in which the bath consists in a set of non-interacting harmonic oscillators of coordinates q_i that are bilinearly coupled to the state variable of the system of interest ψ . The function η is the retarded friction [$\eta(t, t') = 0$ for $t' > t$] and the noise ξ is a random force taken to be a Gaussian process. This assumption is quite reasonable, for instance, for a Brownian particle with much larger mass than the one of the particles of the bath, its motion being the result of a large number of successive collisions, which is a condition for the central limit theorem to apply. Since we assume the environment to be in equilibrium, $\eta(t, t')$ is a function of $t - t'$ and the bath obeys the fluctuation dissipation theorem of the ‘second kind’ [\[148\]](#):

$$\langle \xi(t) \rangle_{\xi} = 0 , \quad \langle \xi(t) \xi(t') \rangle_{\xi} = \beta^{-1} \mathfrak{N}(t - t') , \quad (2.2)$$

where $\langle \dots \rangle_{\xi}$ denotes the average over the noise history. We introduced the symmetric kernel $\mathfrak{N}(t - t') \equiv \eta(t - t') + \eta(t' - t) = \mathfrak{N}(t' - t)$. If \mathfrak{N} has a finite support, the noise

is said to be colored in reference to optics (it has a non-constant Fourier spectrum). In our context a colored noise refers to a (Gaussian) stochastic process with a memory kernel. One of the simplest examples is the Ornstein-Uhlenbeck process which exhibits an exponential correlation function,

$$\aleph(t - t') = \frac{\eta_0}{\tau_n} e^{-|t-t'|/\tau_n} , \quad (2.3)$$

where τ_n is the correlation time of the noise and $\eta_0 > 0$ is the friction coefficient. The white noise limit, in which the bath has no memory, is achieved by sending τ_n to zero or setting $\eta(t - t') = \eta_0 \delta(t - t')$. The Langevin equation then takes the more familiar form

$$\text{EQ}([\psi], t) \equiv m\ddot{\psi}(t) - F([\psi], t) + \eta_0 \dot{\psi}(t) = \xi(t) , \quad (2.4)$$

with $\langle \xi(t) \xi(t') \rangle_\xi = 2\beta^{-1} \eta_0 \delta(t - t')$.

Notice that colored noises can be generated from underlying white noise processes. For example the Ornstein-Uhlenbeck process given in eq. (2.3) corresponds to the overdamped relaxation of a particle of coordinate ξ in a quadratic potential and in contact with a white noise thermal bath:

$$\eta_0 \dot{\xi}(t) + \frac{\eta_0}{\tau_n} \xi(t) = \zeta(t) ,$$

where ζ is a white noise following $\langle \zeta(t) \zeta(t') \rangle_\zeta = 2\eta_0 \beta^{-1} \delta(t - t')$.

Newtonian dynamics, for which the system is not in contact with a thermal bath, are recovered by simply taking $\eta(t) = \aleph(t) = 0$ at all t . Out of equilibrium environments can be taken into account by relaxing the condition between the noise statistics and the friction kernel $\aleph(t - t') = \eta(t - t') + \eta(t' - t)$.

2.1.2 Multiplicative noise

We generalize our discussion to the multiplicative noise case in which the Gaussian noise ξ is coupled to a state-dependent function $M'(\psi)$. The Langevin equation reads

$$\begin{aligned} \text{EQ}([\psi], t) &\equiv m\ddot{\psi}(t) - F([\psi], t) + M'(\psi(t)) \int du \eta(t - u) M'(\psi(u)) \dot{\psi}(u) \\ &= M'(\psi(t)) \xi(t) . \end{aligned} \quad (2.5)$$

This equation can also be shown by using the oscillator model for the bath and a non-linear coupling of the form $M(\psi) \sum_i c_i q_i$ where c_i are coefficients that depend on the details of the coupling and $M(\psi)$ is a smooth function of the state variable with $M(0) = 0$. By a suitable renormalization of η , one can always achieve $M'(0) = 1$. For reasons that will soon become clear, we need to assume that $M'(\psi) \neq 0 \forall \psi$. These assumptions can be realized with functions of the type $M(\psi) = \psi + L(\psi)$ where L is a smooth and increasing function satisfying $L(0) = L'(0) = 0$. The complicated structure of the friction term takes

its rationale from the fluctuation-dissipation theorem of the second kind that expresses the equilibrium condition of the bath. This equation models situations in which the friction between the system and its bath is state-dependent. ξ has the same statistics as in the additive case, see eq. (2.2). The Langevin equation for the additive noise problem is recovered by taking $M(\psi) = \psi$.

2.1.3 Initial conditions

The Langevin equation is a second order differential equation that needs two initial values, say the field and its derivative at time $-T$. We shall use initial conditions drawn from an initial probability distribution $P_i(\psi(-T), \dot{\psi}(-T))$ and average over them. The initial conditions are not correlated with the thermal noise ξ . In the particular case in which the system is prepared in an equilibrium state, P_i is given by the Boltzmann measure.

2.1.4 Markov limit

Langevin equations are often given in the Markov limit in which they appear to be first order stochastic differential equations. Second and higher order time-derivatives as well as non-local terms such as memory kernels are not allowed. In other words, the effect of inertia is neglected (Smoluchowski limit) and the bath is taken to be white. This is justified in situations in which the two associated time scales are sufficiently small compared to all other time scales involved. Concretely, the resulting equation is derived by using an adiabatic elimination procedure that consists in integrating over the fast variables of the system (the velocities) and of the bath. However, this double limiting procedure requires a careful analysis and leads to the well known Itô–Stratonovich dilemma.

The physics of the resulting equation may depend on how the relaxation time associated to inertia compares with the correlation time of the noise before sending the two of them to zero. In cases in which the latter is much larger than the former, the limiting stochastic equation should be interpreted in the sense of Stratonovich [177, 178]. The RHS of eq. (2.5) is given a meaning by stating that ψ in $M'(\psi(t))$ is evaluated at half the sum of its values before and after the kick. Conversely, when the inertia relaxation time is much larger than the noise correlation time, the limiting equation should be interpreted in the Itô sense [179, 180]. In this scenario, the rule is that $M'(\psi(t))$ is evaluated just before the kick $\xi(t)$. When the noise is additive the two conventions are equivalent (see 2.B.2) for all practical purposes. However, they are not for processes with multiplicative noise [142]. For these it is possible to rewrite the Itô stochastic equation in terms of a Stratonovich stochastic equation by adding an adequate drift term to the deterministic force – and be allowed to use the rules of conventional calculus. The Fokker-Planck equation associated to the Markov process does not depend on the scenario and the Boltzmann distribution is a steady state

independently of the convention used. However, the action of the generating functional acquires extra terms depending on the discretization prescription [132, 181].

In this article, we decide not to cope with the Markov limit and, unless otherwise stated, we always keep the inertia of the system in our equations ($m \neq 0$) and we use a colored noise with a finite relaxation time.

2.2 The MSRJD path-integral formalism

The generating functionals associated to the equations of motion (2.1) and (2.5) are given by the Martin-Siggia-Rose-Janssen-deDominicis (MSRJD) path-integral. In this Section we recall its construction for additive noise [82] and we extend it to multiplicative noise using a continuous time formalism. In App. 2.B we develop a careful construction in the discretized formulation.

2.2.1 Action in the additive noise case

The Langevin equation (2.1) is a second order differential equation with source ξ . The knowledge of the history of the field ξ and the initial conditions $\psi(-T)$ and $\dot{\psi}(-T)$ is sufficient to construct $\psi(t)$. Therefore, the probability $P[\psi]$ of a given ψ history between $-T$ and T is linked to the probability of the noise history $P_n[\xi]$ through

$$P[\psi] \mathcal{D}[\psi] = P_n[\xi] \mathcal{D}[\xi] P_i(\psi(-T), \dot{\psi}(-T)) d\psi(-T) d\dot{\psi}(-T)$$

implying

$$P[\psi] = P_n[\text{EQ}[\psi]] |\mathcal{J}[\psi]| P_i(\psi(-T), \dot{\psi}(-T)) , \quad (2.6)$$

where $\mathcal{J}[\psi]$ is the Jacobian which reads, up to some constant factor,

$$\mathcal{J}[\psi] \equiv \det_{uv} \left[\frac{\delta \xi(u)}{\delta \psi(v)} \right] = \det_{uv} \left[\frac{\delta \text{EQ}[\psi, u]}{\delta \psi(v)} \right] \equiv \mathcal{J}_0[\psi] . \quad (2.7)$$

$\det[\dots]$ stands for the functional determinant. We introduced the notation $\mathcal{J}_0[\psi]$ for future convenience and we shall discuss it in Sec. 2.2.3. After a Hubbard-Stratonovich transformation that introduces the auxiliary real field $\hat{\psi}$, the Gaussian probability for a given noise history to occur reads

$$P_n[\xi] = \mathcal{N}^{-1} \int \mathcal{D}[\hat{\psi}] e^{-\int du i\hat{\psi}(u)\xi(u) + \frac{1}{2} \int \int du dv i\hat{\psi}(u)\beta^{-1}\aleph(u-v)i\hat{\psi}(v)} ,$$

with the boundary conditions $\hat{\psi}(-T) = \hat{\psi}(T) = 0$ and where all the integrals over time run from $-T$ to T . In the following, unless otherwise stated, we shall simply denote them

\int . \mathcal{N} is a infinite constant prefactor that we absorb in a re-definition of the measure $\mathcal{D}[\hat{\psi}]$. Back in eq. (2.6) one has

$$P[\psi] = \int \mathcal{D}[\hat{\psi}] e^{-\int du \, i\hat{\psi}(u) \text{EQ}([\psi], u) + \frac{1}{2} \iint du \, dv \, i\hat{\psi}(u) \beta^{-1} \aleph(u-v) i\hat{\psi}(v) + \ln P_i + \ln |\mathcal{J}_0[\psi]|}$$

and we obtain

$$P[\psi] \mathcal{D}[\psi] = \mathcal{D}[\psi] \int \mathcal{D}[\hat{\psi}] e^{S[\psi, \hat{\psi}]},$$

with the MSRJD action functional

$$\begin{aligned} S[\psi, \hat{\psi}] &\equiv \ln P_i \left(\psi(-T), \dot{\psi}(-T) \right) - \int du \, i\hat{\psi}(u) \text{EQ}([\psi], u) \\ &\quad + \frac{1}{2} \iint du \, dv \, i\hat{\psi}(u) \beta^{-1} \aleph(u-v) i\hat{\psi}(v) + \ln |\mathcal{J}_0[\psi]|. \end{aligned} \quad (2.8)$$

The latter is the sum of a deterministic, a dissipative and a Jacobian term,

$$S[\psi, \hat{\psi}] \equiv S^{\text{det}}[\psi, \hat{\psi}] + S^{\text{diss}}[\psi, \hat{\psi}] + \ln |\mathcal{J}_0[\psi]|,$$

with

$$S^{\text{det}}[\psi, \hat{\psi}] \equiv \ln P_i \left(\psi(-T), \dot{\psi}(-T) \right) - \int du \, i\hat{\psi}(u) \left[m\ddot{\psi}(u) - F([\psi], u) \right], \quad (2.9)$$

$$S^{\text{diss}}[\psi, \hat{\psi}] \equiv \int du \, i\hat{\psi}(u) \int dv \, \eta(u-v) \left[\beta^{-1} i\hat{\psi}(v) - \dot{\psi}(v) \right]. \quad (2.10)$$

S^{det} takes into account inertia and the forces exerted on the field, as well as the measure of the initial condition. S^{diss} has its origin in the coupling to the dissipative bath. In the white noise limit, $\eta(t-t') = \eta_0 \delta(t-t')$, the dissipative action naively simplifies to $S^{\text{diss}}[\psi, \hat{\psi}] = \eta_0 \int du \, i\hat{\psi}(u) \left[\beta^{-1} i\hat{\psi}(u) - \dot{\psi}(u) \right]$ (see Sec. 2.1.4 for additional details on this limit).

Notice that integrating away the auxiliary field $\hat{\psi}$ yields the Onsager-Machlup action functional [11, 12, 182–184]. However, we prefer to work with the action written in terms of ψ and $i\hat{\psi}$ as this is the form that arises as the classical limit of the Schwinger-Keldysh action used to treat interacting out-of-equilibrium quantum systems [176, 185], that we shall analyze along the same lines in [186].

2.2.2 Action in the multiplicative noise case

To shorten expressions, we adopt a notation in which the arguments of the fields and functions appear as subindices, $\psi_u \equiv \psi(u)$, $\eta_{u-v} \equiv \eta(u-v)$, and so on and so forth, and the integrals over time as expressed as $\int_u \equiv \int_{-T}^T du$.

In the case of the Langevin equation (2.5) with multiplicative noise, the relation (2.6) is modified and reads

$$P[\psi] = P_n \left[\frac{\text{EQ}[\psi]}{M'(\psi)} \right] |\mathcal{J}[\psi]| P_i(\psi_{-T}, \dot{\psi}_{-T}),$$

with the Jacobian

$$\mathcal{J}[\psi] = \det_{uv} \left[\frac{\delta \text{EQ}_u[\psi]/M'(\psi_u)}{\delta \psi_v} \right] = \det_{uv} \left[\frac{\delta_{u-v}}{M'(\psi_u)} \right] \mathcal{J}_0[\psi] \quad (2.11)$$

and the generalization of the definition of \mathcal{J}_0 in eq. (2.7) to the multiplicative case:

$$\mathcal{J}_0[\psi] \equiv \det_{uv} \left[\frac{\delta \text{EQ}_u[\psi]}{\delta \psi_v} - \frac{M''(\psi_u)}{M'(\psi_u)} \text{EQ}_u[\psi] \delta_{u-v} \right]. \quad (2.12)$$

The construction of the MSRJD action follows the same steps as in the additive noise case, complemented by a further transformation of the field $i\hat{\psi} \mapsto i\hat{\psi} M'(\psi)$, the Jacobian of which cancels the first determinant factor in the RHS of eq. (2.11). Therefore, the MSRJD action reads

$$\begin{aligned} S[\psi, \hat{\psi}] &\equiv \ln P_i(\psi_{-T}, \dot{\psi}_{-T}) - \int_u i\hat{\psi}_u \text{EQ}_u[\psi] \\ &\quad + \frac{1}{2} \int_u \int_v i\hat{\psi}_u M'(\psi_u) \beta^{-1} \aleph_{u-v} M'(\psi_v) i\hat{\psi}_v + \ln |\mathcal{J}_0[\psi]|, \end{aligned} \quad (2.13)$$

with \mathcal{J}_0 defined in eq. (2.12). The deterministic part of the action is unchanged compared to the additive noise case and the dissipative part is now

$$S^{\text{diss}}[\psi, \hat{\psi}] \equiv \int_u i\hat{\psi}_u \int_v M'(\psi_u) \eta_{u-v} M'(\psi_v) \left[\beta^{-1} i\hat{\psi}_v - \dot{\psi}_v \right]. \quad (2.14)$$

2.2.3 Jacobian

In App. 2.C we prove that even in the multiplicative colored noise case that the Jacobian \mathcal{J}_0 is a field-independent positive constant as long as the Markov limit is not taken. One can therefore safely drop the Jacobian term in the normalization. However, we decide to keep track of this term in our expressions. Furthermore, it will be useful to give an explicit representation of \mathcal{J}_0 in which it is the result of a Gaussian integration over Grassmann conjugate fields c and c^* ,

$$\mathcal{J}_0[\psi] = \int \mathcal{D}[c, c^*] e^{S^{\mathcal{J}}[c, c^*, \psi]}, \quad (2.15)$$

with

$$S^{\mathcal{J}}[c, c^*, \psi] \equiv \int_u \int_v c_u^* \frac{\delta \text{EQ}_u[\psi]}{\delta \psi_v} c_v - \int_u c_u^* \frac{M''(\psi_u)}{M'(\psi_u)} \text{EQ}_u[\psi] c_u, \quad (2.16)$$

and the boundary conditions: $c(-T) = \dot{c}(-T) = c^*(T) = \dot{c}^*(T) = 0$. Plugging in the Langevin equation (2.5), we arrive at

$$S^{\mathcal{J}}[c, c^*, \psi] = \int_u \int_v c_u^* \left[m \partial_u^2 \delta_{u-v} - \frac{\delta F_u[\psi]}{\delta \psi_v} + M'(\psi_u) \partial_u \eta_{u-v} M'(\psi_v) \right] c_v - \int_u c_u^* \frac{M''(\psi_u)}{M'(\psi_u)} [m \partial_u^2 \psi_u - F_u[\psi]] c_u . \quad (2.17)$$

The Grassmann fields c and c^* that enter the integral representation of the determinant are known as Faddeev-Popov ghosts and can be interpreted as spinless fermions. The two-time fermionic Green function defined as

$$\langle c_t^* c_{t'} \rangle_{S^{\mathcal{J}}} \equiv \int \mathcal{D}[c, c^*] c_t^* c_{t'} e^{S^{\mathcal{J}}[c, c^*, \psi]} , \quad (2.18)$$

is related, by use of Wick's theorem, to the inverse operator of $\frac{\delta \text{EQ}_{t'}[\psi]}{\delta \psi_t} - \frac{M''(\psi_t)}{M'(\psi_t)} \text{EQ}[\psi_t] \delta_{t-t'}$. $\langle c_t^* c_{t'} \rangle_{S^{\mathcal{J}}}$ inherits the causality structure of the latter and it vanishes at equal times as long as the Markov limit is not taken (*i.e.* all fermionic tadpole contributions cancel): $\langle c_t^* c_{t'} \rangle_{S^{\mathcal{J}}} = 0$ for $t \geq t'$. The last statement can be easily verified by considering the discretized version of $S^{\mathcal{J}}$ (see App. 2.B.3 and App. 2.C) and by checking that the diagonal terms of the inverse operator vanish in the continuous limit. Notice that $S^{\mathcal{J}}$ only involves combinations of the form $c^* c$, *i.e.* it conserves the fermionic charge and $\langle c_t \rangle_{S^{\mathcal{J}}} = \langle c_t^* \rangle_{S^{\mathcal{J}}} = 0$. This implies furthermore that $S^{\mathcal{J}}[c, c^*, \psi]$ and more generally the MSRJD generating functional (at zero sources) are invariant under the following field transformation

$$\mathcal{T}_{\mathcal{J}}(\alpha) \equiv \begin{cases} c_t & \mapsto \alpha c_t , \\ c_t^* & \mapsto \alpha^{-1} c_t^* , \end{cases} \quad \forall \alpha \in \mathbb{C}^* . \quad (2.19)$$

The Jacobian of the transformation is trivially equal to one and the measure $\mathcal{D}[c, c^*]$ is left unchanged. One has $\mathcal{T}_{\mathcal{J}}(\alpha) \mathcal{T}_{\mathcal{J}}(\beta) = \mathcal{T}_{\mathcal{J}}(\alpha\beta)$.

The total MSRJD action given in eq. (2.13) can be written equivalently as a functional of $\psi, \hat{\psi}, c$ and c^* provided that the path-integral measure is extended to the newly introduced fermionic fields:

$$S[\psi, \hat{\psi}, c, c^*] \equiv S^{\text{det}}[\psi, \hat{\psi}] + S^{\text{diss}}[\psi, \hat{\psi}] + S^{\mathcal{J}}[c, c^*, \psi] . \quad (2.20)$$

2.2.4 Observables

Measure.

We denote $\langle \dots \rangle$ the average over the thermal noise and the initial conditions. Within the MSRJD formalism, the average is evaluated with respect to the action functional $S[\psi, \hat{\psi}]$ or

$S[\psi, \hat{\psi}, c, c^*]$ and we use the notation $\langle \dots \rangle_S$:

$$\langle \dots \rangle_S \equiv \int \mathcal{D}[\psi, \hat{\psi}] \dots e^{S[\psi, \hat{\psi}]} \quad (2.21)$$

$$= \int \mathcal{D}[\psi, \hat{\psi}, c, c^*] \dots e^{S[\psi, \hat{\psi}, c, c^*]} \text{ equivalently.} \quad (2.22)$$

Local observable.

The value of a generic local observable A at time t is a function of the field and its time-derivatives evaluated at time t , *i.e.* a functional of the field ψ around t , $A([\psi], t)$. Unless otherwise specified we assume it does not depend explicitly on time and denote it $A[\psi(t)]$. Its mean is value

$$\langle A[\psi(t)] \rangle = \langle A[\psi(t)] \rangle_S. \quad (2.23)$$

Time-reversal.

Since it will be used in the rest of this work, we introduce the time-reversed field $\bar{\psi}$ by $\bar{\psi}(t) \equiv \psi(-t)$ for all t . The time-reversed observable is defined as

$$A_r([\psi], t) \equiv A([\bar{\psi}], -t). \quad (2.24)$$

It has the effect of changing the sign of all odd time-derivatives in the expression of local observables, *e.g.* if $A[\psi(t)] = \partial_t \psi(t)$ then $A_r[\psi(t)] = -\partial_t \psi(t)$. As an example for non-local observables, the time-reversed Langevin equation (2.1) reads

$$\text{EQ}_r([\psi], t) = m\ddot{\psi}(t) - F_r([\psi], t) - \int_{-T}^T du \, \eta(u-t) \dot{\psi}(u). \quad (2.25)$$

Notice the change of sign in front of the friction term that is no longer dissipative in this new equation.

Generating functional

Formally, the generating functional reads

$$Z[J, \hat{J}] \equiv \langle e^{\int du \, J(u)\psi(u) + \hat{J}(u)i\hat{\psi}(u)} \rangle_S, \quad (2.26)$$

where J and \hat{J} are the sources for ψ and $\hat{\psi}$ respectively and $Z[0, 0]$ is normalized to unity by construction.

Two-time correlation.

We define the two-time self correlation function as

$$C(t, t') \equiv \langle \psi(t) \psi(t') \rangle = \langle \psi(t) \psi(t') \rangle_S . \quad (2.27)$$

In terms of the generating functional it is expressed as

$$C(t, t') = \frac{\delta^2 Z[J, \hat{J}]}{\delta J(t) \delta J(t')} \bigg|_{J=\hat{J}=0} . \quad (2.28)$$

Given two local observables A and B , we similarly introduce the two-time generic correlation as

$$C_{\{AB\}}(t, t') \equiv \langle A[\psi(t)] B[\psi(t')] \rangle_S , \quad (2.29)$$

The curly brackets are here to stress the symmetry that underlies this definition: $C_{\{AB\}}(t, t') = C_{\{BA\}}(t', t)$.

Linear response.

If we slightly modify the potential according to $V(\psi) \mapsto V(\psi) - f_\psi \psi$, the self linear response at time t to an infinitesimal perturbation linearly coupled to the field at a previous time t' is defined as

$$R(t, t') \equiv \frac{\delta \langle \psi(t) \rangle}{\delta f_\psi(t')} \bigg|_{f_\psi=0} = \frac{\delta \langle \psi(t) \rangle_{S[f_\psi]}}{\delta f_\psi(t')} \bigg|_{f_\psi=0} . \quad (2.30)$$

It is clear from causality that if t' is later than t , $\langle \psi(t) \rangle_{S[f_\psi]}$ cannot depend on the perturbation $f_\psi(t')$ so $R(t, t') = 0$ for $t' > t$. At equal times, the linear response $R(t, t)$ also vanishes as long as inertia is not neglected ($m \neq 0$)¹. More generally, the linear response of A at time t to an infinitesimal perturbation linearly applied to B at time $t' < t$ is

$$R_{AB}(t, t') \equiv \frac{\delta \langle A[\psi(t)] \rangle}{\delta f_B(t')} \bigg|_{f_B=0} = \frac{\delta \langle A[\psi(t)] \rangle_{S[f_B]}}{\delta f_B(t')} \bigg|_{f_B=0} , \quad (2.31)$$

with $V(\psi) \mapsto V(\psi) - f_B B[\psi]$.

1. In the double limit of a white noise and $m \rightarrow 0$, the equal-time response can slightly violate the causality principle depending on the order in which the limits are taken. In the Itô scenario it vanishes whereas in the Stratonovich one it has a finite value.

2.2.5 Classical Kubo formula

By computing explicitly the functional derivative $\delta/\delta f_\psi$ in the path integral generating functional, we get

$$\begin{aligned} \left. \frac{\delta \langle \dots \rangle_{S[f_\psi]}}{\delta f_\psi(t)} \right|_{f_\psi=0} &= \left\langle \dots \frac{\delta S[\psi, \hat{\psi}, c, c^*; f_\psi]}{\delta f_\psi(t)} \right\rangle_S \Big|_{f_\psi=0} \\ &= \langle \dots i\hat{\psi}(t) \rangle_S + \left\langle \dots \frac{M''(\psi(t))}{M'(\psi(t))} c^*(t)c(t) \right\rangle_S . \end{aligned}$$

The first term in the RHS comes from the functional derivative of S^{det} . The second term comes from the Jacobian term expressed with the fermionic ghosts, $S^{\mathcal{J}}$, and vanishes identically (see the discussion on the equal-time fermionic Green function in Sec. 2.2.3). One has

$$\langle i\hat{\psi}(t) \rangle_S = \left. \frac{\delta \langle 1 \rangle_{S[f_\psi]}}{\delta f_\psi(t)} \right|_{f_\psi=0} = 0 , \quad (2.32)$$

$$\langle i\hat{\psi}(t)i\hat{\psi}(t') \rangle_S = \left. \frac{\delta^2 \langle 1 \rangle_{S[f_\psi]}}{\delta f_\psi(t) \delta f_\psi(t')} \right|_{f_\psi=0} = 0 . \quad (2.33)$$

From the definition of the linear response, eq. (2.30), we get the ‘classical Kubo formula’ [148]

$$R(t, t') = \langle \psi(t)i\hat{\psi}(t') \rangle_S . \quad (2.34)$$

The linear response is here written within the MSRJD formalism as a correlation computed with an unperturbed action. The causality of the response is not explicit, nevertheless following the lines of [132] one can check it is built-in². Because of this expression, the auxiliary field $\hat{\psi}$ is often called the response field. Observe that we have not specified the nature of the initial probability distribution P_i nor the driving forces; eq. (2.34) holds even out of equilibrium. In terms of the generating functional it is expressed as

$$R(t, t') = \left. \frac{\delta^2 Z[J, \hat{J}]}{\delta J(t) \delta \hat{J}(t')} \right|_{J=\hat{J}=0} . \quad (2.35)$$

Similarly, by plugging eq. (2.23) into eq. (2.31), we obtain the classical Kubo formula

2. In general, a multi-time correlator involving $i\hat{\psi}(t_1)$ vanishes if t_1 is the largest time involved.

for generic observables:

$$\begin{aligned}
R_{AB}(t, t') &= \left\langle A[\psi(t)] \frac{\delta S[\psi, \hat{\psi}, c, c^*; f_B]}{\delta f_B(t')} \right\rangle_{f_B=0} \Big|_S \\
&= \left\langle A[\psi(t)] \int du \, i\hat{\psi}(u) \frac{\delta B[\psi(t')]}{\delta \psi(u)} \right\rangle_S \\
&= \left\langle A[\psi(t)] \sum_{n=0}^{\infty} \partial_{t'}^n i\hat{\psi}(t') \frac{\partial B[\psi(t')]}{\partial \partial_{t'}^n \psi(t')} \right\rangle_S .
\end{aligned} \tag{2.36}$$

This formula is valid in and out of equilibrium and allows us to write the response functions associated to generic observables (*e.g.* functions of the position, velocity, acceleration, kinetic energy, etc.) as correlators of ψ , $\hat{\psi}$ and their time derivatives. For example if B is just a function of the field (and not of its time-derivatives), only the $n = 0$ -term subsists in the above sum, yielding

$$R_{AB}(t, t') = \left\langle A[\psi(t)] i\hat{\psi}(t') \frac{\partial B[\psi(t')]}{\partial \psi(t')} \right\rangle_S . \tag{2.37}$$

As another example, if one is interested in the response of the acceleration $A[\psi(t)] = \partial_t^2 \psi(t)$ to a perturbation of the kinetic energy $B[\psi(t)] = \frac{1}{2}m(\partial_t \psi(t))^2$ one should compute

$$R_{AB}(t, t') = m \langle \partial_t^2 \psi(t) \partial_{t'} i\hat{\psi}(t') \partial_{t'} \psi(t') \rangle_S . \tag{2.38}$$

Furthermore, it is straightforward to see that within the MSRJD formalism we can extend all the previous definitions and formulæ to A being a local functional of the auxiliary field: $A[\hat{\psi}(t)]$. For example, if $A[\hat{\psi}(t)] = i\hat{\psi}(t)$ and $B[\psi(t)] = \psi(t)$, we obtain the mixed response

$$R_{i\hat{\psi}\psi}(t, t') = \langle i\hat{\psi}(t) i\hat{\psi}(t') \rangle_S = 0 , \tag{2.39}$$

where we used eq. (2.33).

2.3 Equilibrium

In this Section we focus on situations in which the system is in equilibrium. We identify a field transformation that leaves the MSRJD generating functional (evaluated at zero sources) invariant. The corresponding Ward-Takahashi identities between the expectation values of different observables imply a number of model independent equilibrium properties including stationarity, Onsager relations and the fluctuation-dissipation theorem (FDT). These proofs are straightforward in the generating functional formalism, demonstrating its advantage with respect to the Fokker-Planck formalism or master equation ones, when the

environment acts multiplicatively and has a non-vanishing correlation time. We shall report soon [186] on the extension to the quantum case where the Keldysh action also exhibits a non-trivial symmetry for equilibrium dynamics. Similarly to the classical case, this symmetry leads to the quantum FDT.

2.3.1 The action

Equilibrium dynamics are guaranteed provided that, apart from its interactions with the bath, the system is prepared and driven with the same time-independent and conservative forces ($F = -V'$). In such situations, the initial state is taken from the Boltzmann probability distribution

$$\ln P_i(\psi_{-T}, \dot{\psi}_{-T}) = -\beta \mathcal{H}[\psi_{-T}] - \ln \mathcal{Z} ,$$

where $\mathcal{H}[\psi_t] \equiv \frac{1}{2}m\dot{\psi}_t^2 + V(\psi_t)$ is the internal energy of the system, and \mathcal{Z} is the partition function. The Langevin evolution of the system in contact with the bath can be put in the form

$$-\int_u \frac{\delta \mathcal{L}[\psi_u]}{\delta \psi_t} + M'(\psi_t) \int_u \eta_{t-u} M'(\psi_u) \dot{\psi}_u = M'(\psi_t) \xi_t , \quad (2.40)$$

with $\mathcal{L}[\psi_u] \equiv \frac{1}{2}m\dot{\psi}_u^2 - V(\psi_u)$ being the Lagrangian of the system. In this equilibrium set-up, the deterministic part of the MSRJD action functional reads

$$\begin{aligned} S^{\text{det}}[\psi, \hat{\psi}] &= -\beta \mathcal{H}[\psi_{-T}] - \ln \mathcal{Z} + \int_u \int_v \hat{\psi}_u \frac{\delta \mathcal{L}[\psi_v]}{\delta \psi_u} \\ &= -\beta \left(\frac{1}{2}m\dot{\psi}_{-T}^2 + V(\psi_{-T}) \right) - \ln \mathcal{Z} - \int_u \hat{\psi}_u \left[m\ddot{\psi}_u + V'(\psi_u) \right] . \end{aligned} \quad (2.41)$$

The dissipative part of the MSRJD action functional remains the same, see eq. (2.14). As discussed in Sec. 2.2.3, the Jacobian \mathcal{J}_0 enters the action through the constant term $\ln \mathcal{J}_0$ or it can be expressed in terms of a Gaussian integral over the ghosts fields c and c^* . In that case, its contribution to the action reads

$$\begin{aligned} S^{\mathcal{J}}[c, c^*, \psi] &= \int_u \int_v c_u^* \left[m\partial_u^2 \delta_{u-v} + M'(\psi_u) \partial_u \eta_{u-v} M'(\psi_v) \right] c_v \\ &\quad - \int_u c_u^* \left[-V''(\psi_u) + \frac{M''(\psi_u)}{M'(\psi_u)} \partial_u^2 \psi_u + \frac{M''(\psi_u)}{M'(\psi_u)} V'(\psi_u) \right] c_u . \end{aligned} \quad (2.42)$$

2.3.2 Symmetry of the MSRJD generating functional

We shall prove that $\int \mathcal{D}[\psi, \hat{\psi}, c, c^*] e^{S[\psi, \hat{\psi}, c, c^*]}$ is invariant under the field transformation:

$$\mathcal{T}_{\text{eq}} \equiv \begin{cases} \psi_u & \mapsto \psi_{-u} , \\ \hat{\psi}_u & \mapsto \hat{\psi}_{-u} + \beta \partial_u \psi_{-u} , \end{cases} \quad \begin{cases} c_u & \mapsto c_{-u}^* , \\ c_u^* & \mapsto -c_{-u} . \end{cases} \quad (2.43)$$

This transformation is involutory, $\mathcal{T}_{\text{eq}}\mathcal{T}_{\text{eq}} = 1$, when applied to the fields ψ or $i\hat{\psi}$ and the composite field c^*c . It does not involve the kernel η and includes a time-reversal. It is interesting to notice that the invariance is achieved independently by the deterministic (S^{det}), the dissipative (S^{diss}) and the Jacobian ($S^{\mathcal{J}}$) contributions to the action. This means that it is still valid in the Newtonian limit ($\eta = 0$).

In terms of the generating functional, the symmetry reads

$$Z[J, \hat{J}] = Z[\bar{J} + \beta\partial\bar{\hat{J}}, \bar{\hat{J}}], \quad (2.44)$$

where $\bar{J}(u) \equiv J(-u)$ and $\bar{\hat{J}}(u) \equiv \hat{J}(-u)$.

The detailed proof that we develop here consists of two parts: we first show that the Jacobian of the transformation is unity, then that the integration domain of the transformed fields is unchanged. Afterwards we show that the action functional $S[\psi, \hat{\psi}, c, c^*]$ is invariant under \mathcal{T}_{eq} .

Invariance of the measure.

The transformation \mathcal{T}_{eq} acts separately on the fields ψ and $i\hat{\psi}$ on the one hand, and the fields c and c^* on the other. The Jacobian \mathcal{J}_{eq} thus factorizes into a bosonic part and a fermionic part. The bosonic part is the determinant of a triangular matrix:

$$\mathcal{J}_{\text{eq}}^{\text{b}} \equiv \det \left[\frac{\delta(\psi, \hat{\psi})}{\delta(\mathcal{T}_{\text{eq}}\psi, \mathcal{T}_{\text{eq}}\hat{\psi})} \right] = \det_{uv}^{-1} \begin{bmatrix} \frac{\delta\psi_{-u}}{\psi_v} & 0 \\ \frac{\delta\hat{\psi}_{-u}}{\psi_v} & \frac{\delta\hat{\psi}_{-u}}{\hat{\psi}_v} \end{bmatrix} = (\det_{uv}^{-1} [\delta_{u+v}])^2 = 1$$

and it is thus identical to one [187]. It is easy to verify that the fermionic part $\mathcal{J}_{\text{eq}}^{\text{f}} = 1$ as well.

Invariance of the integration domain.

Before and after the transformation, the functional integration on the field ψ is performed for values of ψ_t on the real axis. However, the new domain of integration for the field $\hat{\psi}$ is complex. For a given time t , $\hat{\psi}_t$ is now integrated over the complex line with a constant imaginary part $-i\beta\partial_t\psi_t$. One can return to an integration over the real axis by closing the contour at both infinities. Indeed the integrand, e^S , goes to zero sufficiently fast at $\psi_t \rightarrow \pm\infty$ for neglecting the vertical ends of the contour thanks to the term $\beta^{-1}\eta_0(i\hat{\psi}_t)^2$ in the action. Furthermore the new field is also integrated with the boundary conditions $\hat{\psi}(-T) = \hat{\psi}(T) = 0$.

The transformation \mathcal{T}_{eq} leaves the measure $\mathcal{D}[c, c^*]$ unchanged together with the set of boundary conditions $c(-T) = \dot{c}(-T) = c^*(T) = \dot{c}^*(T) = 0$.

Invariance of the action functional.

The MSRJD action functional $S[\psi, \hat{\psi}, c, c^*] = S^{\text{det}}[\psi, \hat{\psi}] + S^{\text{diss}}[\psi, \hat{\psi}] + S^{\mathcal{J}}(c, c^*, \psi)$ is invariant term by term. The deterministic contribution given in eq. (2.41) satisfies

$$\begin{aligned} S^{\text{det}}[\mathcal{T}_{\text{eq}}\psi, \mathcal{T}_{\text{eq}}\hat{\psi}] &= \ln P_1(\psi_T, \dot{\psi}_T) - \int_u \left[i\hat{\psi}_{-u} + \beta \partial_u \psi_{-u} \right] \left[m \partial_u^2 \psi_{-u} + V'(\psi_{-u}) \right] \\ &= \ln P_1(\psi_T, \dot{\psi}_T) - \int_u i\hat{\psi}_u \left[m \ddot{\psi}_u + V'(\psi_u) \right] + \beta \int_u \dot{\psi}_u \left[m \ddot{\psi}_u + V'(\psi_u) \right] \\ &= \ln P_1(\psi_T, \dot{\psi}_T) - \int_u i\hat{\psi}_u \left[m \ddot{\psi}_u + V'(\psi_u) \right] + \beta \int_u \partial_u \mathcal{H}[\psi_u] \\ &= S^{\text{det}}[\psi, \hat{\psi}] , \end{aligned}$$

where we used the initial equilibrium measure $\ln P_1(\psi, \dot{\psi}) = -\beta \mathcal{H}[\psi] - \ln \mathcal{Z}$. In the first line we just applied the transformation, in the second line we made the substitution $u \mapsto -u$, in the third line we wrote the last integrand as a total derivative the integral of which cancels the first term and creates a new initial measure.

Secondly, we show that the dissipative contribution $S^{\text{diss}}[\psi, \hat{\psi}]$, defined in eq. (2.10), is also invariant under \mathcal{T}_{eq} . We have

$$\begin{aligned} S^{\text{diss}}[\mathcal{T}_{\text{eq}}\psi, \mathcal{T}_{\text{eq}}\hat{\psi}] &= \int_u \left[i\hat{\psi}_{-u} + \beta \partial_u \psi_{-u} \right] \int_v \beta^{-1} M'(\psi_{-u}) \eta_{u-v} M'(\psi_{-v}) i\hat{\psi}_{-v} \\ &= \int_u \left[i\hat{\psi}_u - \beta \dot{\psi}_u \right] \int_v M'(\psi_u) \eta_{v-u} M'(\psi_v) \beta^{-1} i\hat{\psi}_v \\ &= S^{\text{diss}}[\psi, \hat{\psi}] . \end{aligned}$$

In the first line we just applied the transformation, in the second line we made the substitution $u \mapsto -u$ and in the last step we exchanged u and v .

Finally, we show that the Jacobian term in the action is invariant once it is expressed in terms of a Gaussian integral over conjugate Grassmann fields (c and c^*). We start from eq. (2.42)

$$\begin{aligned} S^{\mathcal{J}}(\mathcal{T}_{\text{eq}}c, \mathcal{T}_{\text{eq}}c^*, \mathcal{T}_{\text{eq}}\psi) &= - \int_u \int_v c_{-u} \left[m \partial_u^2 \delta_{u-v} + M'(\psi_{-u}) \partial_u \eta_{u-v} M'(\psi_{-v}) \right] c_{-v}^* \\ &\quad + \int_u c_{-u} \left[-V''(\psi_{-u}) + \frac{M''(\psi_{-u})}{M'(\psi_{-u})} \partial_u^2 \psi_{-u} + \frac{M''(\psi_{-u})}{M'(\psi_{-u})} V'(\psi_{-u}) \right] c_{-u}^* \\ &= \int_u \int_v c_u^* \left[m \partial_u^2 \delta_{v-u} - M'(\psi_u) \partial_u \eta_{v-u} M'(\psi_v) \right] c_u \\ &\quad - \int_u c_u^* \left[-V''(\psi_u) + \frac{M''(\psi_u)}{M'(\psi_u)} \partial_u^2 \psi_u + \frac{M''(\psi_u)}{M'(\psi_u)} V'(\psi_u) \right] c_u \\ &= S^{\mathcal{J}}(c, c^*, \psi) . \end{aligned}$$

In the first line we just applied the transformation, in the second line we exchanged the anti-commuting Grassmann variables and made the substitutions $u \mapsto -u$ and $v \mapsto -v$, in the last step we used $\partial_v \eta_{v-u} = -\partial_v \eta_{u-v}$ and exchanged u and v .

2.3.3 Ward-Takahashi identities

We just proved that equilibrium dynamics manifest themselves as a symmetry of the MSRJD action and more generally at the level of the generating functional. This symmetry has direct consequences at the level of correlation functions. If A is a generic functional of ψ and $\hat{\psi}$ we get the following Ward-Takahashi identity

$$\langle A[\psi, \hat{\psi}] \dots \rangle_S = \langle A[\mathcal{T}_{\text{eq}}\psi, \mathcal{T}_{\text{eq}}\hat{\psi}] \dots \rangle_S . \quad (2.45)$$

The use of this identity leads to all the possible equilibrium relations between observables as we shall now describe in the following.

2.3.4 Stationarity

In equilibrium, one expects noise-averaged observables to be independent of the time t_0 at which the system was prepared (in our case $t_0 = -T$). One-time dependent noise-averaged observables are expected to be constant, $\langle A[\psi_t] \rangle = \text{ct}$, and two-time correlations to be time-translational invariant: $\langle A[\psi_t] B[\psi_{t'}] \rangle = f_{t-t'}$. Similarly, one argues that multi-time correlations can only depend upon all possible independent time-differences between the times involved. These statements have been proven for additive white noise processes using the Fokker-Planck [188] or SUSY formalisms [99–101]. The use of the transformation \mathcal{T}_{eq} allows one to show these properties very easily for generic Langevin processes.

One-time observables. Taking $A = 1$ and letting B be a generic local observable, the equal-time linear response vanishes, $R_{AB}(t, t) = 0$. Using the classical Kubo formula (2.36) we obtain

$$R_{AB}(t, t) = \left\langle \sum_{n=0}^{\infty} \partial_t^n \hat{\psi}_t \frac{\partial B[\psi_t]}{\partial \partial_t^n \psi_t} \right\rangle_S = 0 .$$

Applying the transformation \mathcal{T}_{eq} , we find

$$R_{AB}(t, t) = \left\langle \sum_{n=0}^{\infty} \partial_t^n \hat{\psi}_{-t} \frac{\partial B_r[\psi_{-t}]}{\partial \partial_t^n \psi_{-t}} \right\rangle_S + \beta \left\langle \sum_{n=0}^{\infty} \partial_t^{n+1} \psi_{-t} \frac{\partial B_r[\psi_{-t}]}{\partial \partial_t^n \psi_{-t}} \right\rangle_S .$$

The LHS and the first term in the RHS vanish identically at all times. One is left with the second term in the RHS that simply reads $\langle \partial_t B_r[\psi_{-t}] \rangle = \partial_t \langle B_r[\psi_{-t}] \rangle = 0$, proving that all one-time local observables are constant in time.

Two-time observables. Because we just showed that $\langle A[\psi(t)] \rangle$ is constant in equilibrium, the response $R_{AB}(t, t')$, see its formal definition in eq. (2.31), can only be a function of the time-difference between the observation time and the time at which the perturbation is applied. Therefore can it be written in the form $R_{AB}(t, t') = f(t - t')\theta(t - t')$. We shall see in Sec. 2.3.7 that the fluctuation-dissipation theorem relates, in equilibrium, the linear response $R_{AB}(t, t')$ to the two-time correlation $C_{\{AB\}}(t, t')$ implying that this last quantity is also time-translational invariant.

Similarly, $(n + 1)$ -time correlators can be proven to be functions of n independent time-differences because they are related, in equilibrium, to responses of n -time correlators that are time-translational invariant.

2.3.5 Equipartition theorem

Let us consider the local observables $A[\psi(t)] = \partial_t \psi(t)$ and $B[\psi(t)] = \psi(t)$. In that case $R_{AB}(t, t') = \langle \partial_t \psi_t \hat{\psi}_{t'} \rangle_S = \partial_t \langle \psi_t \hat{\psi}_{t'} \rangle_S$ and we recognize $\partial_t R(t, t')$. Using the field transformation \mathcal{T}_{eq} , we get

$$\begin{aligned} \partial_t R(t, t') &= \partial_t \langle \psi_{-t} \hat{\psi}_{-t'} \rangle_S + \beta \langle \partial_t \psi_{-t} \partial_{t'} \psi_{-t'} \rangle_S \\ &= \partial_t \langle \psi_{-t} \hat{\psi}_{-t'} \rangle_S + \beta \langle \partial_t \psi_t \partial_{t'} \psi_{t'} \rangle_S \end{aligned}$$

If $t > t'$, the first term in the RHS vanishes by causality. Considering moreover the limit $t' \rightarrow t^-$ the LHS is $1/m$ as we shall show in Sec. 2.4.2. Finally, we get the equipartition theorem

$$\beta m \langle (\partial_t \psi_t)^2 \rangle = 1 . \quad (2.46)$$

2.3.6 Reciprocity relations

If we use \mathcal{T}_{eq} in the expression (2.29) of generic two-time correlation functions, we get

$$\langle A[\psi_t] B[\psi_{t'}] \rangle_S = \langle A_r[\psi_{-t}] B_r[\psi_{-t'}] \rangle_S ,$$

reading

$$C_{\{AB\}}(t, t') = C_{\{A_r B_r\}}(-t, -t') . \quad (2.47)$$

In the cases in which A and B have a definite parity under time-reversal we obtain

$$\begin{aligned} C_{\{AB\}}(\tau) &= C_{\{AB\}}(|\tau|) \text{ if } A \text{ and } B \text{ have the same parity,} \\ C_{\{AB\}}(\tau) &= -C_{\{AB\}}(-\tau) \text{ otherwise.} \end{aligned}$$

2.3.7 Fluctuation-dissipation theorem (FDT)

Self FDT.

Applying the transformation to the expression (2.34) of the self response $R(t, t')$ we find

$$\langle \psi_t \hat{\psi}_{t'} \rangle_S = \langle \mathcal{T}_{\text{eq}} \psi_t \mathcal{T}_{\text{eq}} \hat{\psi}_{t'} \rangle_S = \langle \psi_{-t} \hat{\psi}_{-t'} \rangle_S + \beta \langle \psi_{-t} \partial_{t'} \psi_{-t'} \rangle_S ,$$

and we read

$$R(t, t') = R(-t, -t') + \beta \partial_{t'} C(-t, -t')$$

that, using the equilibrium time-translational invariance, becomes

$$R(\tau) - R(-\tau) = -\beta \partial_\tau C(-\tau) ,$$

where we set $\tau \equiv t - t'$. Since $C(\tau)$ is symmetric in τ by definition, this expression can be recast, once multiplied by $\Theta(\tau)$, as

$$R(\tau) = -\Theta(\tau) \beta \partial_\tau C(\tau) . \quad (2.48)$$

Equation (2.48) is the well-known fluctuation-dissipation theorem. It allows one to predict the slightly out-of-equilibrium behavior of a system – such as the irreversible dissipation of energy into heat – from its reversible fluctuations in equilibrium.

Generic two-time FDTs.

We generalize the previous FDT relation to the case of generic local observables A and B . Applying the transformation \mathcal{T}_{eq} to expression (2.36) of the linear response $R_{AB}(t, t')$

$$\begin{aligned} \langle A[\psi_t] \sum_{n=0}^{\infty} \partial_{t'}^n \hat{\psi}_{t'} \frac{\partial B[\psi_{t'}]}{\partial \partial_{t'}^n \psi_{t'}} \rangle_S &= \langle A_r[\psi_{-t}] \sum_{n=0}^{\infty} \partial_{t'}^n \hat{\psi}_{-t'} \frac{\partial B_r[\psi_{-t'}]}{\partial \partial_{t'}^n \psi_{t'}} \rangle_S \\ &\quad + \beta \langle A_r[\psi_{-t}] \sum_{n=0}^{\infty} \partial_{t'}^{n+1} \psi_{-t'} \frac{\partial B_r[\psi_{-t'}]}{\partial \partial_{t'}^n \psi_{t'}} \rangle_S \\ &= \langle A_r[\psi_{-t}] \sum_{n=0}^{\infty} \partial_{t'}^n \hat{\psi}_{-t'} \frac{\partial B_r[\psi_{-t'}]}{\partial \partial_{t'}^n \psi_{t'}} \rangle_S + \beta \partial_{t'} \langle A_r[\psi_{-t}] B_r[\psi_{-t'}] \rangle_S . \end{aligned}$$

Applying once again the transformation to the last term in the RHS yields

$$\langle A[\psi_t] \sum_{n=0}^{\infty} \partial_{t'}^n \hat{\psi}_{t'} \frac{\partial B[\psi_{t'}]}{\partial \partial_{t'}^n \psi_{t'}} \rangle_S = \langle A_r[\psi_{-t}] \sum_{n=0}^{\infty} \partial_{t'}^n \hat{\psi}_{-t'} \frac{\partial B_r[\psi_{-t'}]}{\partial \partial_{t'}^n \psi_{t'}} \rangle_S + \beta \partial_{t'} \langle A[\psi_t] B[\psi_{t'}] \rangle_S$$

which reads

$$R_{AB}(\tau) - R_{A_r B_r}(-\tau) = -\beta \partial_\tau C_{\{AB\}}(\tau) . \quad (2.49)$$

By multiplying both sides by $\Theta(\tau)$ we obtain the FDT for any local A and B

$$R_{AB}(\tau) = -\Theta(\tau) \beta \partial_\tau C_{\{AB\}}(\tau) . \quad (2.50)$$

2.3.8 Higher-order FDTs: e.g. 3-time observables

We give a derivation, *via* the symmetry of the MSRJD formalism, of relations shown and discussed in, *e.g.* [188], within the Fokker-Planck formalism for stochastic processes with white noise.

Response of a two-time correlation.

We first look at the response of a two-time correlator to a linear perturbation applied at time t_1

$$R(t_3, t_2; t_1) \equiv \left. \frac{\delta \langle \psi_{t_3} \psi_{t_2} \rangle}{\delta f_{\psi_{t_1}}} \right|_{f_\psi=0} . \quad (2.51)$$

In the MSRJD formalism, it can be expressed as the 3-time correlator

$$R(t_3, t_2; t_1) = \langle \psi_{t_3} \psi_{t_2} i \hat{\psi}_{t_1} \rangle_S . \quad (2.52)$$

Causality ensures that the response vanishes if the perturbation is posterior to the observation times: $R(t_3, t_2; t_1) = 0$ if $t_1 > \max(t_2, t_3)$. We assume without loss of generality that $t_2 < t_3$. Under equilibrium conditions, the response transforms under \mathcal{T}_{eq} as

$$R(t_3, t_2; t_1) = \langle \psi_{-t_3} \psi_{-t_2} i \hat{\psi}_{-t_1} \rangle_S + \beta \partial_{t_1} \langle \psi_{-t_3} \psi_{-t_2} \psi_{-t_1} \rangle_S .$$

Multiplying both sides by $\Theta(t_3 - t_1)$ and transforming once again the last term in the RHS, we get

$$R(t_3, t_2; t_1) = \begin{cases} \beta \partial_{t_1} \langle \psi_{t_3} \psi_{t_2} \psi_{t_1} \rangle_S & \text{if } t_1 < t_2 < t_3 , \\ R(-t_3, -t_2; -t_1) + \beta \partial_{t_1} \langle \psi_{t_3} \psi_{t_2} \psi_{t_1} \rangle_S & \text{if } t_2 < t_1 < t_3 , \\ 0 & \text{if } t_2 < t_3 < t_1 . \end{cases} \quad (2.53)$$

Second order response.

Let us now look at the response to a perturbation at time t_1 of the linear response $R(t_3, t_2)$:

$$R(t_3; t_2, t_1) \equiv \left. \frac{\delta^2 \langle \psi_{t_3} \rangle}{\delta f_{\psi_{t_1}} \delta f_{\psi_{t_2}}} \right|_{f_{\psi}=0} . \quad (2.54)$$

In the MSRJD formalism, it can be expressed as the 3-time correlator

$$R(t_3; t_2, t_1) = \langle \psi_{t_3} i\hat{\psi}_{t_2} i\hat{\psi}_{t_1} \rangle_S . \quad (2.55)$$

It is clear from causality that the response vanishes if the observation time is before the two perturbations: $R(t_3; t_2, t_1) = 0$ if $t_3 < \min(t_1, t_2)$. The response transforms under \mathcal{T}_{eq} as

$$\begin{aligned} R(t_3; t_2, t_1) &= R(-t_3; -t_2, -t_1) + \beta \partial_{t_1} R(-t_3, -t_1; -t_2) \\ &+ \beta \partial_{t_2} R(-t_3, -t_2; -t_1) + \beta^2 \partial_{t_1} \partial_{t_2} \langle \psi_{-t_3} \psi_{-t_2} \psi_{-t_1} \rangle_S . \end{aligned}$$

Let us assume without loss of generality that $t_1 < t_2$. Using causality arguments and applying once more the \mathcal{T}_{eq} transformation to the remaining terms we obtain

$$R(t_3; t_2, t_1) = \begin{cases} 0 & \text{if } t_3 < t_1 < t_2 , \\ R(-t_3; -t_2, -t_1) + \beta \partial_{t_1} R(t_3, t_1; t_2) & \text{if } t_1 < t_3 < t_2 , \\ \beta \partial_{t_1} R(t_3, t_1; t_2) & \text{if } t_1 < t_2 < t_3 . \end{cases} \quad (2.56)$$

2.3.9 Onsager reciprocal relations

Rewriting twice eq. (2.49) as

$$\begin{aligned} R_{AB}(\tau) - R_{A_r B_r}(-\tau) &= -\beta \partial_\tau C_{\{AB\}}(\tau) , \\ R_{BA}(-\tau) - R_{B_r A_r}(\tau) &= \beta \partial_\tau C_{\{BA\}}(-\tau) = \beta \partial_\tau C_{\{AB\}}(\tau) , \end{aligned}$$

and summing up these two equations with $\tau > 0$ we get

$$R_{AB}(\tau) = R_{B_r A_r}(\tau) .$$

These equilibrium relations, known as the Onsager reciprocal relations, express the fact that the linear response of an observable A to a perturbation coupled to another observable B can be deduced by the response of B_r to a perturbation coupled to A_r .

2.3.10 Supersymmetric formalism

Generating functional.

The generating functional of stochastic equations with conservative forces admits a supersymmetric formulation. This has been derived and discussed for additive noise in a number of publications [189, 98–101]. We extend it here to multiplicative non-Markov Langevin processes (see [190] for a study of the massless and white noise limits). To this end, let us introduce θ and θ^* , two anticommuting Grassmann coordinates, and the superfield

$$\Psi(t, \theta, \theta^*) \equiv \psi(t) + c^*(t) \theta + \theta^* c(t) + \theta^* \theta \left(i\hat{\psi}(t) + c^*(t) c(t) \frac{M''(\psi(t))}{M'(\psi(t))} \right).$$

The MSRJD action S [see eq. (2.20)] has a compact representation in terms of this superfield:

$$S = S_{\text{susy}}^{\text{det}} + S_{\text{susy}}^{\text{diss}}, \quad (2.57)$$

with

$$\begin{aligned} S_{\text{susy}}^{\text{det}}[\Psi] &\equiv -\beta \int d\theta d\theta^* \theta^* \theta \mathcal{H}[\Psi(-T, \theta, \theta^*)] - \ln \mathcal{Z} + \int d\Upsilon \mathcal{L}[\Psi(\Upsilon)], \\ S_{\text{susy}}^{\text{diss}}[\Psi] &\equiv \frac{1}{2} \iint d\Upsilon' d\Upsilon M(\Psi(\Upsilon')) \mathbf{D}^{(2)}(\Upsilon', \Upsilon) M(\Psi(\Upsilon)), \end{aligned}$$

$\mathcal{H}[\Psi] \equiv \frac{1}{2} m \dot{\Psi}^2 + V(\Psi)$ and $\mathcal{L}[\Psi] \equiv \frac{1}{2} m \dot{\Psi}^2 - V(\Psi)$. We used the notation $\Upsilon \equiv (t, \theta, \theta^*)$ and $d\Upsilon \equiv dt d\theta d\theta^*$. The ‘dissipative’ differential operator is defined as

$$\mathbf{D}^{(2)}(\Upsilon', \Upsilon) \equiv \eta(t' - t) \delta(\theta^{*'} - \theta^*) \delta(\theta' - \theta) \left(2\beta^{-1} \frac{\partial^2}{\partial \theta \partial \theta^*} + \overrightarrow{\text{sig}}_{\theta} \frac{\partial}{\partial t} \right),$$

where $\overrightarrow{\text{sig}}_{\theta}$ is a short notation for $2\theta \frac{\partial}{\partial \theta} - 1$. It is equal to 1 if there is a θ factor in the right and to -1 otherwise. $\mathbf{D}^{(2)}$ can be written as

$$\mathbf{D}^{(2)}(\Upsilon', \Upsilon) = \eta(t' - t) \delta(\theta^{*'} - \theta^*) \delta(\theta' - \theta) (\bar{\mathbf{D}} \mathbf{D} - \mathbf{D} \bar{\mathbf{D}}),$$

with the (covariant³) derivatives acting on the superspace:

$$\bar{\mathbf{D}} \equiv \frac{\partial}{\partial \theta}, \quad \mathbf{D} \equiv \beta^{-1} \frac{\partial}{\partial \theta^*} - \theta \frac{\partial}{\partial t}, \quad (2.58)$$

that obey⁴ $\{\bar{\mathbf{D}}, \mathbf{D}\} = -\frac{\partial}{\partial t}$ and $\{\mathbf{D}, \mathbf{D}\} = \{\bar{\mathbf{D}}, \bar{\mathbf{D}}\} = 0$. In the white noise limit the dissipative part of the action simplifies to

$$S_{\text{susy}}^{\text{diss}}[\Psi] = \frac{1}{2} \int d\Upsilon M(\Psi(\Upsilon)) \mathbf{D}^{(2)}(\Upsilon) M(\Psi(\Upsilon)),$$

3. Covariant in the sense that the derivative of a supersymmetric expression is still supersymmetric.

4. Therefore the $\dot{\Psi}^2$ term in $\mathcal{L}[\Psi]$ can be written in terms of covariant derivatives as $(\{\bar{\mathbf{D}}, \mathbf{D}\} \Psi)^2$.

with the ‘dissipative’ differential operator

$$\mathbf{D}^{(2)}(\Upsilon) \equiv \eta_0 \left(2\beta^{-1} \frac{\partial^2}{\partial \theta \partial \theta^*} + \vec{\text{sig}}_\theta \frac{\partial}{\partial t} \right) = \eta_0 (\bar{\mathbf{D}}\mathbf{D} - \mathbf{D}\bar{\mathbf{D}}) .$$

Notice that this formulation is only suitable situations in which the applied forces are conservative. The Jacobian term $S^{\mathcal{J}}$ contributes to both the deterministic ($S_{\text{susy}}^{\text{det}}$) and the dissipative part ($S_{\text{susy}}^{\text{diss}}$) of the action.

Symmetries.

In terms of the superfield, the transformation $\mathcal{T}_{\mathcal{J}}(\alpha)$ defined in eq. (2.19) acts as

$$\mathcal{T}_{\mathcal{J}}(\alpha) \equiv \Psi(t, \theta, \theta^*) \mapsto \Psi(t, \alpha^{-1}\theta, \alpha\theta^*) \quad \forall \alpha \in \mathbb{C}^* , \quad (2.59)$$

and leaves the action $S[\Psi]$, see eq. (2.57), invariant. The transformation \mathcal{T}_{eq} given in eq. (2.43) acts as

$$\mathcal{T}_{\text{eq}} \equiv \Psi(t, \theta, \theta^*) \mapsto \Psi(-t - \beta\theta^*\theta, -\theta^*, \theta) , \quad (2.60)$$

and leaves the action $S[\Psi]$, see eq. (2.57), invariant.

The action $S[\Psi]$ given in (2.57) has an additional supersymmetry generated by

$$\mathbf{Q} \equiv \frac{\partial}{\partial \theta^*} , \quad \bar{\mathbf{Q}} \equiv \beta^{-1} \frac{\partial}{\partial \theta} + \theta^* \frac{\partial}{\partial t} ,$$

that obey $\{\bar{\mathbf{Q}}, \mathbf{Q}\} = \frac{\partial}{\partial t}$ and $\{\mathbf{Q}, \mathbf{Q}\} = \{\bar{\mathbf{Q}}, \bar{\mathbf{Q}}\} = \{\mathbf{D}, \mathbf{Q}\} = \{\mathbf{D}, \bar{\mathbf{Q}}\} = \{\bar{\mathbf{D}}, \mathbf{Q}\} = \{\bar{\mathbf{D}}, \bar{\mathbf{Q}}\} = 0$. Both operators \mathbf{Q} and $\bar{\mathbf{Q}}$ are thus nilpotent and $\{\bar{\mathbf{Q}}, \mathbf{Q}\}$ is the generator of the Lie sub-group. They act on the superfield as

$$e^{\epsilon^* \mathbf{Q}} \Psi = \Psi + \epsilon^* \mathbf{Q} \Psi , \quad e^{\epsilon \bar{\mathbf{Q}}} \Psi = \Psi + \epsilon \bar{\mathbf{Q}} \Psi ,$$

where ϵ and ϵ^* are two extra independent⁵ Grassmann constants and

$$\mathbf{Q} \Psi = c + \theta \left(i\hat{\psi} + c^* c \frac{M''(\psi)}{M'(\psi)} \right) , \quad (2.61)$$

$$\bar{\mathbf{Q}} \Psi = -\beta^{-1} c^* - \theta^* \left(\beta^{-1} i\hat{\psi} - \partial_t \psi + \beta^{-1} c^* c \frac{M''(\psi)}{M'(\psi)} \right) - \theta^* \theta \partial_t c^* . \quad (2.62)$$

Expressed in terms of superfield transformations, $S[\Psi]$ is invariant under both

$$\Psi(t, \theta, \theta^*) \mapsto \Psi(t, \theta, \theta^* + \epsilon^*) , \quad (2.63)$$

5. ϵ and ϵ^* are independent in particular of the coordinates θ and θ^* .

and

$$\Psi(t, \theta, \theta^*) \mapsto \Psi(t + \epsilon\theta^*, \theta + \beta^{-1}\epsilon, \theta^*) . \quad (2.64)$$

Here again, the invariance of the action is achieved independently by the deterministic (S^{det}) and the dissipative (S^{diss}) contributions. We would like to stress the fact that the presence of the boundary term accounting for the initial equilibrium measure of the field ψ as well as the boundary conditions for the fields $i\hat{\psi}$, c and c^* are necessary to obtain a full invariance of the action.

BRS symmetry.

The symmetry generated by \mathbf{Q} is the BRS symmetry that generically arises when a system has dynamical constraints (here we impose the system to obey the Langevin equation of motion). Applying the corresponding superfield transformation in $\langle \Psi(t, \theta, \theta^*) \rangle_S$ gives

$$\langle \Psi(t, \theta, \theta^*) \rangle_S = \langle \Psi(t, \theta, \theta^*) + \epsilon^* \mathbf{Q} \Psi(t, \theta, \theta^*) \rangle_S ,$$

and therefore $\langle \mathbf{Q} \Psi(t, \theta, \theta^*) \rangle_S = 0$. This leads to

$$\langle c_t \rangle_S = 0 , \quad \langle i\hat{\psi}_t + c_t^* c_t \frac{M''(\psi_t)}{M'(\psi_t)} \rangle_S = 0 . \quad (2.65)$$

Applying the transformation inside the two-point correlator $\langle \Psi(t, \theta, \theta^*) \Psi(t', \theta', \theta^{*'}) \rangle_S$, we get $\langle \mathbf{Q} \Psi(t, \theta, \theta^*) \Psi(t', \theta', \theta^{*'}) \rangle_S + (t, \theta, \theta^*) \leftrightarrow (t', \theta', \theta^{*'}) = 0$. This leads in particular to identify the two-time fermionic correlator as being the (bosonic) linear response:

$$R(t, t') \equiv \langle \psi_t \left[i\hat{\psi}_{t'} + c_{t'}^* c_{t'} \frac{M'(\psi_{t'})}{M''(\psi_{t'})} \right] \rangle_S = \langle c_{t'}^* c_t \rangle_S . \quad (2.66)$$

Corroborating the discussion in Sec. 2.2.3, this tells us in particular that $\langle c_t^* c_{t'} \rangle_S$ (and more generally the fermionic Green function $\langle c_t^* c_{t'} \rangle_{S\mathcal{J}}$) vanishes for $t > t'$ and also for $t = t'$ provided that the Markov limit is not taken. Using this result, the second relation in (2.65) now yields $\langle i\hat{\psi}_t \rangle_S = 0$.

FDT.

The use of the symmetry generated by $\bar{\mathbf{Q}}$ on $\langle \Psi(t, \theta, \theta^*) \rangle_S$ gives,

$$\langle c_t^* \rangle_S = 0 , \quad \langle i\hat{\psi}_t - \beta \partial_t \psi_t \rangle_S = 0 . \quad (2.67)$$

By use of $\langle i\hat{\psi}_t \rangle_S = 0$ (which was a consequence of the BRS symmetry), the second relation becomes $\partial_t \langle \psi_t \rangle_S = 0$. This expresses the stationarity and can be easily generalized to more complicated one-time observables, $A(\psi)$, by use of the supersymmetry in $\langle A(\Psi) \rangle_S$.

The use of the symmetry generated by $\bar{\mathbf{Q}}$ on a two-point correlator of the superfield reads

$$\langle \Psi(t, \theta, \theta^*) \Psi(t', \theta', \theta'^*) \rangle_S = \langle \Psi(t + \epsilon \theta^*, \theta + \beta \epsilon, \theta^*) \Psi(t' + \epsilon \theta'^*, \theta' + \beta \epsilon, \theta'^*) \rangle_S ,$$

giving, amongst other relations,

$$\langle \psi_t \left[i \hat{\psi}_{t'} - \beta \partial_{t'} \psi_{t'} + c_t^* c_t \frac{M''(\psi_t)}{M'(\psi_t)} \right] - c_t^* c_{t'} \rangle_S = 0 . \quad (2.68)$$

As discussed in Sec. 2.3.10, $\langle c_t^* c_{t'} \rangle_{S\mathcal{J}}$ vanishes for $t \geq t'$. Therefore, the term in $c_t^* c_t$ disappears from eq. (2.68) and the FDT is obtained by multiplying both sides of the equation by $\Theta(t - t')$

$$R(t, t') = \beta \partial_{t'} C(t, t') \Theta(t - t') .$$

2.3.11 Link between \mathcal{T}_{eq} and the supersymmetries

It is interesting to remark that both supersymmetries (the one generated by \mathbf{Q} and the one generated by $\bar{\mathbf{Q}}$) are needed to derive equilibrium relations such as stationarity or the FDT. All the Ward-Takahashi identities generated by the combined use of these supersymmetries can be generated by \mathcal{T}_{eq} but the inverse is not true. The supersymmetries do not yield relations in which a time-reversal appears explicitly such as the Onsager reciprocal relations.

It is clear from its expression in terms of the superfield, eq. (2.60), that the equilibrium transformation \mathcal{T}_{eq} cannot be written using the generator of a continuous supersymmetry. However, the transformation \mathcal{T}_{eq} can be formally written in terms of the supersymmetry generators as

$$\mathcal{T}_{\text{eq}} \equiv \Psi \mapsto \Pi \Xi e^{\tilde{\mathbf{Q}}} \Psi , \quad (2.69)$$

where Π is the time-reversal operator ($t \mapsto -t$), Ξ exchanges the extra Grassmann coordinates ($\theta \mapsto -\theta^*$ and $\theta^* \mapsto \theta$) and the generator $\tilde{\mathbf{Q}}$ is defined in terms of \mathbf{Q} and $\bar{\mathbf{Q}}$ as

$$\tilde{\mathbf{Q}} \equiv -\beta \theta^* \theta \{ \bar{\mathbf{Q}}, \mathbf{Q} \} = -\beta \theta^* \theta \frac{\partial}{\partial t} . \quad (2.70)$$

2.3.12 Newtonian limit: a phase space approach

For a system described by the time-independent Hamiltonian $\mathcal{H}(x, p)$, where x is the coordinate and p the conjugate momentum, the dynamics are given by the two Hamilton's equations:

$$\begin{aligned} \text{EQX}[x(t), p(t)] &\equiv \dot{x} - \partial_p \mathcal{H}(x, p) = 0 , \\ \text{EQP}[x(t), p(t)] &\equiv \dot{p} + \partial_x \mathcal{H}(x, p) = 0 . \end{aligned} \quad (2.71)$$

For a given set of initial conditions x_i and p_i , they have only one set of solutions $x_{\text{sol}}(t)$ and $p_{\text{sol}}(t)$. One can construct a path integral as

$$\begin{aligned} \langle A[x, p] \rangle &\propto \int \mathcal{D}[x, p] A[x, p] \delta[x - x_{\text{sol}}] \delta[p - p_{\text{sol}}] e^{-\beta \mathcal{H}(x(-T), p(-T))} \\ &\propto \int \mathcal{D}[x, p, \hat{x}, \hat{p}] A[x, p] |\mathcal{J}^x \mathcal{J}^p| e^{S[x, p, \hat{x}, \hat{p}]}, \end{aligned} \quad (2.72)$$

with the boundary conditions $\hat{x}(-T) = \hat{p}(-T) = \hat{x}(T) = \hat{p}(T) = 0$. We averaged over equilibrium initial conditions and introduced the action functional

$$\begin{aligned} S[x, p, \hat{x}, \hat{p}] &\equiv -\beta \mathcal{H}(x(-T), p(-T)) \\ &\quad - \int_u i \hat{x}_u [\dot{p}_u + \partial_{x_u} \mathcal{H}(x_u, p_u)] + i \hat{p}_u [\dot{x}_u - \partial_{p_u} \mathcal{H}(x_u, p_u)]. \end{aligned}$$

Let us now assume that $\mathcal{H}(x, p) = g(p) + f(x)$. It follows that the Jacobians $\mathcal{J}^x \equiv \det_{uv} \left[\frac{\delta \text{EQX}[x(u), p(u)]}{\delta x(v)} \right]$ and $\mathcal{J}^p \equiv \det_{uv} \left[\frac{\delta \text{EQP}[x(u), p(u)]}{\delta p(v)} \right]$ are field independent constants that can be dropped in the normalization. The generating functional at zero sources is invariant under the transformation

$$\mathcal{T}'_{\text{eq}} \equiv \begin{cases} x_u \mapsto x_{-u}, & p_u \mapsto -p_{-u}, \\ i \hat{x}_u \mapsto i \hat{x}_{-u} + \beta \partial_u x_{-u}, & i \hat{p}_u \mapsto -i \hat{p}_{-u} + \beta \partial_u p_{-u}, \end{cases} \quad (2.73)$$

as long as the Hamiltonian is time-reversal invariant, *i.e.* $\mathcal{H}(x, p) = \mathcal{H}_r(x, p) = \mathcal{H}(x, -p)$.

2.4 Out of equilibrium

We now turn to more generic situations in which the system does no longer evolve in equilibrium. This means that it can now be prepared with an arbitrary distribution and it can evolve with time-dependent and non-conservative forces f^{nc} .

We first show that the way in which the symmetry \mathcal{T}_{eq} is broken gives a number of so-called transient⁶ fluctuations relations [25, 27, 150, 29, 151, 152], [153–158], [159–161]. Although fluctuation theorems in cases with additive colored noise were studied in several publications [154–157], we are not aware of similar studies in cases with multiplicative noise.

We then exhibit another symmetry of the MSRJD generating functional, valid in and out of equilibrium. This new symmetry implies out-of-equilibrium relations between correlations and responses and generalizes the formulæ in [162–169] obtained for additive white noise. Finally, we come back to the equilibrium case to combine the two symmetries and deduce other equilibrium relations.

6. As opposed to *steady-state* fluctuation relations the validity of which is only asymptotic, in the limit of long averaging times.

2.4.1 Non-equilibrium fluctuation relations

Work fluctuation theorems.

Let us assume that the system is initially prepared in thermal equilibrium with respect to the potential $V(\psi, \lambda_{-T})$ ⁷. The expression for the deterministic part of the MSRJD action functional [see eq. (2.9)] is

$$S^{\text{det}}[\psi, \hat{\psi}; \lambda, f^{\text{nc}}] = -\beta \mathcal{H}([\psi_{-T}], \lambda_{-T}) - \ln \mathcal{Z}(\lambda_{-T}) \\ - \int_u \dot{\psi}_u \left[m \ddot{\psi}_u + V'(\psi_u, \lambda_u) - f_u^{\text{nc}}[\psi] \right],$$

where $\mathcal{H}([\psi_t], \lambda_t) \equiv \frac{1}{2} m \dot{\psi}_t^2 + V(\psi_t, \lambda_t)$. The external work done on the system along a given trajectory between times $-T$ and T is the sum of the work induced by the non-conservative forces and the one performed through the external protocol λ :

$$W[\psi; \lambda, f^{\text{nc}}] \equiv \int_u \dot{\psi}_u f_u^{\text{nc}}[\psi] + \int_u \partial_u \lambda_u \partial_\lambda V(\psi_u, \lambda_u). \quad (2.74)$$

The transformation \mathcal{T}_{eq} does not leave S^{det} invariant but yields

$$S^{\text{det}}[\psi, \hat{\psi}; \lambda, f^{\text{nc}}] \mapsto S^{\text{det}}[\psi, \hat{\psi}; \bar{\lambda}, f_r^{\text{nc}}] + \beta \Delta \mathcal{F}_r - \beta W[\psi; \bar{\lambda}, f_r^{\text{nc}}], \quad (2.75)$$

or equivalently

$$S^{\text{det}}[\psi, \hat{\psi}; \lambda, f^{\text{nc}}] + \beta \Delta \mathcal{F} - \beta W[\psi; \lambda, f^{\text{nc}}] \mapsto S^{\text{det}}[\psi, \hat{\psi}; \bar{\lambda}, f_r^{\text{nc}}]. \quad (2.76)$$

$S^{\text{det}}[\psi, \hat{\psi}; \bar{\lambda}, f_r^{\text{nc}}]$ corresponds to the MSRJD action of the system that is prepared (in equilibrium) and evolves under the time-reversed protocol $\bar{\lambda}(u) \equiv \lambda(-u)$ and external forces $f_r^{\text{nc}}([\psi], u) \equiv f^{\text{nc}}([\bar{\psi}], -u)$. $\Delta \mathcal{F}_r$ is the change in free energy associated to this time-reversed protocol: $\beta \Delta \mathcal{F}_r = -\ln \mathcal{Z}(\bar{\lambda}(T)) + \ln \mathcal{Z}(\bar{\lambda}(-T)) = -\beta \Delta \mathcal{F}$ between the initial and the final ‘virtual’ equilibrium states. The dissipative part of the action, S^{diss} , is still invariant under \mathcal{T}_{eq} . This means that, contrary to the external forces F , the interaction with the bath is time-reversal invariant: the friction is still dissipative after the transformation. This immediately yields

$$e^{\beta \Delta \mathcal{F}} \langle A[\psi, \hat{\psi}] e^{-\beta W[\psi; \lambda, f^{\text{nc}}]} \rangle_{S[\lambda, f^{\text{nc}}]} = \langle A[\mathcal{T}_{\text{eq}} \psi, \mathcal{T}_{\text{eq}} \hat{\psi}] \rangle_{S[\bar{\lambda}, f_r^{\text{nc}}]} \quad (2.77)$$

for any functional A of ψ and $\hat{\psi}$. In particular for a local functional of the field, $A[\psi(t)]$, it leads to the relation [152]

$$e^{\beta \Delta \mathcal{F}} \langle A[\psi(t)] e^{-\beta W[\psi; \lambda, f^{\text{nc}}]} \rangle_{S[\lambda, f^{\text{nc}}]} = \langle A_r[\psi(-t)] \rangle_{S[\bar{\lambda}, f_r^{\text{nc}}]}, \quad (2.78)$$

7. This is in fact a restriction on the initial velocities, $\dot{\psi}_{-T}$, that are to be taken from the Boltzmann distribution with temperature β^{-1} , independently of the positions ψ_{-T} . The distribution of these latter can be tailored at will through the λ dependence of V .

or also

$$\begin{aligned} e^{\beta\Delta\mathcal{F}} \langle A[\psi(t)]B[\psi(t')]e^{-\beta W[\psi;\lambda,f^{\text{nc}}]} \rangle_{S[\lambda,f^{\text{nc}}]} \\ = \langle A_{\text{r}}[\psi(-t)]B_{\text{r}}[\psi(-t')] \rangle_{S[\bar{\lambda},f_{\text{r}}^{\text{nc}}]}. \end{aligned} \quad (2.79)$$

Setting $A[\psi, \hat{\psi}] = 1$, we obtain the Jarzynski equality [191, 150]

$$e^{\beta\Delta\mathcal{F}} \langle e^{-\beta W[\psi;\lambda,f^{\text{nc}}]} \rangle_{S[\lambda,f^{\text{nc}}]} = 1. \quad (2.80)$$

Setting $A[\psi, \hat{\psi}] = \delta(W - W[\psi; \lambda, f^{\text{nc}}])$ we deduce the Crooks fluctuation theorem [27, 29, 192]

$$P(W) = P_{\text{r}}(-W) e^{\beta(W-\Delta\mathcal{F})}, \quad (2.81)$$

where $P(W)$ is the probability for the external work done between $-T$ and T to be W given the protocol $\lambda(t)$ and the non-conservative force $f^{\text{nc}}([\psi], t)$. $P_{\text{r}}(W)$ is the same probability, given the time-reversed protocol $\bar{\lambda}$ and time-reversed force f_{r}^{nc} . The previous Jarzynski equality is the integral version of this theorem.

Fluctuation theorem.

Let us now relax the condition that the system is prepared in thermal equilibrium and allow for any initial distribution P_{i} . We recall the corresponding deterministic part of the MSRJD action functional given in Sec. 2.2, eq. (2.9)

$$\begin{aligned} S^{\text{det}}[\psi, \hat{\psi}] &\equiv \ln P_{\text{i}}(\psi(-T), \dot{\psi}(-T)) \\ &\quad - \int du \, i\hat{\psi}(u) \left[m\ddot{\psi}(u) + V'(\psi(u), \lambda(u)) - f^{\text{nc}}([\psi], u) \right]. \end{aligned}$$

The transformation \mathcal{T}_{eq} does not leave S^{det} invariant but one has

$$S^{\text{det}}[\psi, \hat{\psi}; \lambda, f^{\text{nc}}] - \mathcal{S} \mapsto S^{\text{det}}[\psi, \hat{\psi}; \bar{\lambda}, f_{\text{r}}^{\text{nc}}],$$

with the stochastic entropy $\mathcal{S} \equiv - \left[\ln P_{\text{i}}(\psi(T), -\dot{\psi}(T)) - \ln P_{\text{i}}(\psi(-T), \dot{\psi}(-T)) \right] - \beta\mathcal{Q}$. The first term is the Shannon entropy whereas the second term is the exchange entropy defined through the heat transfer $\mathcal{Q} \equiv \Delta\mathcal{H} - W[\psi; \lambda, f^{\text{nc}}]$. $\Delta\mathcal{H} \equiv \mathcal{H}([\psi(T)], \lambda(T)) - \mathcal{H}([\psi(-T)], \lambda(-T))$ is the change of internal energy. The dissipative part of the action, S^{diss} , is still invariant under \mathcal{T}_{eq} . This immediately yields

$$\langle A[\psi, \hat{\psi}]e^{-\mathcal{S}} \rangle_{S[\lambda,f^{\text{nc}}]} = \langle A[\mathcal{T}_{\text{eq}}\psi, \mathcal{T}_{\text{eq}}\hat{\psi}] \rangle_{S[\bar{\lambda},f_{\text{r}}^{\text{nc}}]} \quad (2.82)$$

for any functional A of ψ and $\hat{\psi}$. Setting $A[\psi, \hat{\psi}] = 1$, we obtain the integral fluctuation theorem (sometimes referred as the Kawasaki identity [193, 194])

$$1 = \langle e^{-\mathcal{S}} \rangle_{S[\psi,\hat{\psi};\lambda,f^{\text{nc}}]}. \quad (2.83)$$

which using the Jensen inequality gives $\langle \mathcal{S} \rangle_{S[\psi, \hat{\psi}; \lambda, f^{\text{nc}}]} \geq 0$, expressing the second law of thermodynamics. Setting $A[\psi, \hat{\psi}] = \delta(\zeta - \mathcal{S})$ we obtain the fluctuation theorem [27, 29, 192]

$$P(\zeta) = P_r(-\zeta) e^{\zeta}, \quad (2.84)$$

where $P(\zeta)$ is the probability for the entropy created between $-T$ and T to be ζ given the protocol $\lambda(t)$ and the non-conservative force $f^{\text{nc}}([\psi], t)$. $P_r(\zeta)$ is the same probability, given the time-reversed protocol $\bar{\lambda}$ and time-reversed force f_r^{nc} .

Similar results can be obtained for isolated systems by switching off the interaction with the bath, *i.e.* by taking $\eta = 0$. It is also straightforward to obtain extended relations when the bath is taken to be out of equilibrium, for example by using $\aleph(t-t') \neq \eta(t-t') + \eta(t'-t)$, and the contribution of the change in the dissipative action is taken into account. This kind of fluctuation relation may be specially important in quantum systems.

2.4.2 Generic relations between correlations and linear responses

A number of generic relations between linear responses and the averages of other observables have been derived for different types of stochastic dynamics: Langevin with additive white noise [162], Ising variables with Glauber updates [163], or the heat-bath algorithm [164–167], and even molecular dynamics of hard spheres or Lennard-Jones particle systems [168]. Especially interesting are those in which the relation is established with functions of correlations computed with the unperturbed dynamics [162, 165] as explained in [169]. The main aim of the studies in [163–169] was to give the most efficient computational method to obtain the linear response in the theoretical limit of no applied field. Another set of recent articles discusses very similar with the goal of giving a thermodynamic interpretation to the various terms contributing the linear response [170–173].

In the concrete case of Langevin processes this kind of relations can be very simply derived by multiplying the equation by the field or the noise and averaging over the noise in the way done in [162]. We derive here the same relations within the MSRJD formalism, using a symmetry property that is more likely to admit an extension to systems with quantum fluctuations.

A symmetry of the MSRJD generating functional valid also out of equilibrium.

We consider the most generic out-of-equilibrium situation. We allow for any initial preparation (P_i) and any evolution of the system (F). $\int \mathcal{D}[\psi, \hat{\psi}] e^{S[\psi, \hat{\psi}]}$ is invariant under

the involutory field transformation \mathcal{T}_{eom} , given by

$$\mathcal{T}_{\text{eom}} \equiv \begin{cases} \psi_u & \mapsto \psi_u, \\ i\hat{\psi}_u & \mapsto -i\hat{\psi}_u + \frac{2\beta}{M'(\psi_u)} \int_v \aleph_{u-v}^{-1} \frac{\text{EQ}_v[\psi]}{M'(\psi_v)}, \end{cases} \quad (2.85)$$

The meaning of the subscript referring to ‘equation of motion’ will become clear in the following. For additive noise [$M'(\psi) = 1$] the transformation becomes

$$i\hat{\psi}_u \mapsto -i\hat{\psi}_u + 2\beta \int_v \aleph_{u-v}^{-1} \left[m\ddot{\psi}_v - F_v[\psi] + \int_w \eta_{v-w} \dot{\psi}_w \right],$$

and in the additive white noise limit simplifies to

$$i\hat{\psi}_u \mapsto -i\hat{\psi}_u + \beta\eta_0^{-1} \left[m\ddot{\psi}_u - F_u[\psi] + \eta_0 \dot{\psi}_u \right]. \quad (2.86)$$

The proof is similar to the one of the previous equilibrium symmetry (see Sec. 2.3.2). The Jacobian of this transformation is unity since its associated matrix is block triangular with ones on the diagonal. The integration domain of ψ is unchanged while the one of $\hat{\psi}$ can be chosen to be the real axis by a simple complex analysis argument. In the following lines we show that the action S evaluated in the transformed fields remains identical to the action evaluated in the original fields. We give the proof in the case of an additive noise but the generalization to a multiplicative noise is straightforward. We start from the expression (2.8) and evaluate

$$\begin{aligned} S[\mathcal{T}_{\text{eom}}\psi, \mathcal{T}_{\text{eom}}\hat{\psi}] &= \ln P_1(\psi_{-T}, \dot{\psi}_{-T}) + \int_u \left[i\hat{\psi}_u - 2\beta \int_v \aleph_{u-v}^{-1} \text{EQ}_v[\psi] \right] \\ &\quad \times \left[\text{EQ}_u[\psi] - \frac{1}{2} \int_w \beta^{-1} \aleph_{u-w} \left(-i\hat{\psi}_w + 2\beta \int_z \aleph_{w-z}^{-1} \text{EQ}_z[\psi] \right) \right] \\ &= \ln P_1(\psi_{-T}, \dot{\psi}_{-T}) + \int_u \left[i\hat{\psi}_u - 2\beta \int_v \aleph_{u-v}^{-1} \text{EQ}_v[\psi] \right] \left[\frac{1}{2} \int_w \beta^{-1} \aleph_{u-w} i\hat{\psi}_w \right] \\ &= S[\psi, \hat{\psi}]. \end{aligned}$$

Contrary to the equilibrium transformation \mathcal{T}_{eq} , it does not include a time-reversal and is not defined in the Newtonian limit ($\eta = 0$).

Supersymmetric version.

In Sec. 2.3.10, in the equilibrium case, we encoded the fields ψ , $i\hat{\psi}$, c and c^* in a unique superfield Ψ . In this fashion, the transformation \mathcal{T}_{eom} given in eq. (2.85) acts as

$$\Psi(t, \theta, \theta^*) \mapsto \Psi \left(t + \theta^* \theta \frac{2\beta \int_u \aleph_{t-u}^{-1} M'(\Psi(u, \theta, \theta^*)) \text{EQ}_u[\Psi]}{\partial_t M(\Psi(t, \theta, \theta^*))}, \theta, \theta^* \right), \quad (2.87)$$

and leaves the equilibrium action $S[\Psi]$, see eq. (2.57), invariant.

Out of equilibrium relations.

We first derive some relations in the additive case [$M'(\psi) = 1$] and then we generalize the results to the case of a multiplicative noise.

Additive noise. Using \mathcal{T} in the expression (2.34) of the self response $R(t, t')$ we find

$$\langle \psi_t \hat{\psi}_{t'} \rangle_S = \langle \mathcal{T}_{\text{eom}} \psi_t \mathcal{T}_{\text{eom}} \hat{\psi}_{t'} \rangle_S = -\langle \psi_t \hat{\psi}_{t'} \rangle_S + 2\beta \int_v \aleph_{t'-v}^{-1} \langle \psi_t \text{EQ}_v[\psi] \rangle_S ,$$

giving an explicit formula for computing the linear response without perturbing field:

$$\begin{aligned} R(t, t') &= \beta \int dv \aleph^{-1}(t' - v) \\ &\times \left[m\partial_v^2 C(t, v) + \int du \eta(v - u) \partial_u C(t, u) - \langle \psi(t) F([\psi], v) \rangle \right]. \end{aligned} \quad (2.88)$$

Once multiplied by $\aleph_{t''-t'}$ and integrated over t' yields

$$\begin{aligned} m\partial_t^2 C(t, t') &+ \int du \eta(t' - u) \partial_u C(t, u) \\ &- \langle \psi(t) F([\psi], t') \rangle = \beta^{-1} \int du \aleph(t' - u) R(t, u) , \end{aligned} \quad (2.89)$$

with no assumption on the initial $P_1(\psi_{-T}, \dot{\psi}_{-T})$.

If one now uses \mathcal{T} in $\langle \text{EQ}_t[\psi] \hat{\psi}_{t'} \rangle_S$, one obtains

$$\begin{aligned} \langle \text{EQ}_t[\psi] \hat{\psi}_{t'} \rangle_S &= \langle \text{EQ}_t[\mathcal{T}_{\text{eom}} \psi] \mathcal{T}_{\text{eom}} \hat{\psi}_{t'} \rangle_S \\ &= -\langle \text{EQ}_t[\psi] \hat{\psi}_{t'} \rangle_S + 2\beta \int_u \aleph_{t'-u}^{-1} \langle \text{EQ}_t \text{EQ}_u \rangle_S . \end{aligned}$$

Since $\langle \text{EQ}_t[\psi] \text{EQ}_u[\psi] \rangle_S = \beta^{-1} \aleph_{t-u}$, this simplifies in

$$\langle \text{EQ}_t[\psi] \hat{\psi}_{t'} \rangle_S = \delta_{t-t'} ,$$

that yields

$$m\partial_t^2 R(t, t') + \int dv \eta(t - v) \partial_v R(v, t') - \langle \hat{\psi}(t') F([\psi], t) \rangle_S = \delta(t - t') \quad (2.90)$$

with no assumption on the initial P_1 . One can trade the last term in the LHS of eq. (2.90) for $\beta \int_u \aleph_{t'-u}^{-1} \langle \xi(u) F_t[\psi] \rangle_\xi$ by use of Novikov's theorem.

Notice that despite the fact that the transformation \mathcal{T}_{eom} is not defined in the Newtonian limit ($\eta = 0$), both eqs. (2.89) and (2.90) are well defined in this limit. Therefore, in order to compute out-of-equilibrium relations in a isolated system, one can add a fictitious

equilibrium bath interacting with the system, use \mathcal{T}_{eom} to compute the out-of-equilibrium relations and then finally send η to 0.

Integrating both eqs. (2.89) and (2.90) around $t = t'$ we find the equal-time conditions

$$m \partial_{t'} C(t, t')|_{t'=t} = 0, \quad m \partial_t R(t, t')|_{t' \rightarrow t-} = 1, \quad m \partial_t R(t, t')|_{t' \rightarrow t+} = 0. \quad (2.91)$$

The last two conditions above imply that the first derivative of the response function is discontinuous at equal times⁸.

The use of this symmetry is an easy way to get a generalization of eq. (2.88) for a generic response R_{AB} . Indeed, applying this transformation to expression (2.36) of the linear response we obtain

$$\begin{aligned} R_{AB}(t, t') = & \beta \int du \mathbb{N}^{-1}(t' - u) \sum_{n=0}^{\infty} \left\{ m \partial_u^{n+2} \langle A[\psi(t)] \psi(u) \frac{\partial B[\psi(t')]}{\partial \partial_{t'}^n \psi(t')} \rangle_S \right. \\ & - \partial_u^n \langle A[\psi(t)] F([\psi], u) \frac{\partial B[\psi(t')]}{\partial \partial_{t'}^n \psi(t')} \rangle_S \\ & \left. + \int dv \eta(u - v) \partial_v^{n+1} \langle A[\psi(t)] \psi(v) \frac{\partial B[\psi(t')]}{\partial \partial_{t'}^n \psi(t')} \rangle_S \right\}. \quad (2.92) \end{aligned}$$

This formula gives the linear response as an explicit function of multiple-time correlators of the field ψ . For example, if B is a function of the field only (and not of its time-derivatives), just the $n = 0$ -term subsists in the above sum:

$$\begin{aligned} R_{AB}(t, t') = & \beta \int du \mathbb{N}^{-1}(t' - u) \left\{ m \partial_u^2 \langle A[\psi(t)] \psi(u) \frac{\partial B[\psi(t')]}{\partial \psi(t')} \rangle_S \right. \\ & - \langle A[\psi(t)] F([\psi], u) \frac{\partial B[\psi(t')]}{\partial \psi(t')} \rangle_S \\ & \left. + \int dv \eta(u - v) \partial_v \langle A[\psi(t)] \psi(v) \frac{\partial B[\psi(t')]}{\partial \psi(t')} \rangle_S \right\}. \quad (2.93) \end{aligned}$$

As another example if one is interested in the self-response of the velocity, $A[\psi(t)] = B[\psi(t)] = \partial_t \psi(t)$, one obtains

$$\begin{aligned} R_{AB}(t, t') = & \beta \int du \mathbb{N}^{-1}(t' - u) \left\{ m \partial_t \partial_u^3 C(t, u) - \partial_t \partial_u \langle \psi(t) F([\psi], u) \rangle_S \right. \\ & \left. + \int dv \eta(u - v) \partial_v^2 C(t, v) \right\}. \quad (2.94) \end{aligned}$$

8. It is clear from the expressions given in (2.91) that the overdamped $m \rightarrow 0$ limit allows for a sudden discontinuity of the response function as well as a finite slope of the correlation function at equal times.

Multiplicative noise. Similar results can be obtained in the case of a multiplicative noise. Applying the transformation in the correlator $\int_u \aleph_{t'-u} \langle \psi_t M'(\psi_{t'}) M'(\psi_u) i\hat{\psi}_u \rangle_S$ we get

$$\langle \psi_t \text{EQ}_{t'}[\psi] \rangle_S = \beta^{-1} \int_u \aleph_{t'-u} \langle \psi_t M'(\psi_{t'}) M'(\psi_u) i\hat{\psi}_u \rangle_S ,$$

yielding

$$\begin{aligned} m\partial_{t'}^2 C(t, t') &+ \int_u \eta_{t'-u} \langle \psi_t M'(\psi_{t'}) M'(\psi_u) \partial_u \psi_u \rangle_S \\ &- \langle \psi_t F_{t'}[\psi] \rangle_S = \beta^{-1} \int_u \aleph_{t'-u} \langle \psi_t M'(\psi_{t'}) M'(\psi_u) i\hat{\psi}_u \rangle_S . \end{aligned} \quad (2.95)$$

Applying now the transformation in the correlator $\langle \text{EQ}_t[\psi] i\hat{\psi}_{t'} \rangle_S$, one obtains

$$\langle \text{EQ}_t[\psi] i\hat{\psi}_{t'} \rangle_S = \delta_{t-t'} + \beta^{-1} \int_u \aleph_{t-u} \langle M'(\psi_t) M'(\psi_u) i\hat{\psi}_u i\hat{\psi}_{t'} \rangle_S , \quad (2.96)$$

yielding

$$\begin{aligned} m\partial_t^2 R(t, t') &+ \int_u \eta_{t-u} \langle M'(\psi_{t'}) M'(\psi_u) \partial_u \psi_u i\hat{\psi}_{t'} \rangle_S \\ &- \langle F_t[\psi] i\hat{\psi}_{t'} \rangle_S = \delta_{t-t'} \beta^{-1} \int_u \aleph_{t-u} \langle \psi_t M'(\psi_{t'}) M'(\psi_u) i\hat{\psi}_u \rangle_S . \end{aligned} \quad (2.97)$$

One can check from eqs. (2.95) and (2.97) that the equal-time conditions given in eqs. (2.91) are still valid in the multiplicative case.

2.4.3 Composition of \mathcal{T}_{eom} and \mathcal{T}_{eq}

For an equilibrium situation, the MSRJD action functional is fully invariant under the composition of \mathcal{T}_{eom} and \mathcal{T}_{eq} ,

$$\mathcal{T}_{\text{eq}} \circ \mathcal{T}_{\text{eom}} = \begin{cases} \psi_u & \mapsto \psi_{-u} , \\ i\hat{\psi}_u & \mapsto -i\hat{\psi}_{-u} - \beta \partial_u \psi_{-u} + \frac{2\beta}{M'(\psi_{-u})} \int_v \aleph_{u-v}^{-1} \frac{\text{EQ}_v[\bar{\psi}]}{M'(\psi_{-v})} , \end{cases} \quad (2.98)$$

that simply reads in the white noise limit

$$\mathcal{T}_{\text{eq}} \circ \mathcal{T}_{\text{eom}} = \begin{cases} \psi_u & \mapsto \psi_{-u} , \\ i\hat{\psi}_u & \mapsto -i\hat{\psi}_{-u} + \frac{\beta}{\eta_0 M'(\psi_{-u})^2} [m\partial_u^2 \psi_{-u} + V'(\psi_{-u})] . \end{cases} \quad (2.99)$$

For simplicity we only show the implication of this symmetry in this limit and in the additive noise case:

$$R(t, t') = -R(-t, -t') + \frac{\beta}{\eta_0} [m\partial_t^2 C(-t, -t') + \langle \psi(-t) V'(\psi(-t')) \rangle_S] .$$

Using equilibrium properties, *i.e.* time-translational invariance of all observables and time-reversal symmetry of two-time correlation functions of the field ψ (shown in Sec. 2.3.2), and causality of the response, we get

$$R(\tau) = \Theta(\tau) \frac{\beta}{\eta_0} [m \partial_\tau^2 C(\tau) + \Lambda(\tau)] , \quad (2.100)$$

with $\tau \equiv t - t'$ and $\Lambda(\tau) \equiv \langle \psi(t) V'(\psi(t')) \rangle_S$ which is eq. (2.89) after cancellation of the LHS with the last term in the rhs when FDT between R and C holds [also eq. (2.90) after a similar simplification]. Here again, one can easily obtain a generalization of this last relation for a generic response R_{AB} by plugging the transformation into the expression (2.36) of the linear response.

2.5 Conclusions

In this chapter we recalled the path-integral approach to classical stochastic dynamics with generic multiplicative colored noise. The action has three terms: a deterministic (Newtonian dynamics) contribution, a dissipative part and a Jacobian. We identified a number of symmetries of the generating functional when the sources are set to zero. The invariance of the action is achieved by the three terms independently.

One of these symmetries applies only when equilibrium dynamics are assumed. Equilibrium dynamics are ensured whenever the system is prepared with equilibrium initial conditions at temperature β^{-1} (a statistical mixture given by the Gibbs-Boltzmann measure), evolves with the corresponding time-independent conservative forces, and is in contact with an equilibrium bath at the same temperature β^{-1} . The invariance also holds in the limit in which the contact with the bath is suppressed, *i.e.* under deterministic (Newtonian) dynamics, but the initial condition is still taken from the Gibbs-Boltzmann measure. This symmetry yields all possible model-independent fluctuation-dissipation theorems as well as stationarity and Onsager reciprocal relations. When the field-transformation is applied to driven problems, the symmetry no longer holds, but it gives rise to different kinds of fluctuation theorems.

We identified another more general symmetry that applies to equilibrium and out-of-equilibrium set-ups. It holds for any kind of initial conditions – they can be any statistical mixture or even deterministic, and the evolution can be dictated by time-dependent and/or non-conservative forces as long as the system is coupled to an equilibrium bath. The symmetry implies exact dynamic equations that couple generic correlations and linear responses. These equations are model-dependent in the sense that they depend explicitly on the applied forces. They are the starting point to derive Schwinger-Dyson-type approximations and close them on two-time observables. Although the symmetry is ill-defined in

the Newtonian limit, the dynamic relations it yields can nevertheless be evaluated in the Newtonian case.

Finally, we gave a supersymmetric expression of the path-integral for problems with multiplicative colored noise and conservative forces. We expressed all the previous symmetries in terms of superfield transformations and we discussed the relationship between supersymmetry and other symmetries.

Appendices

2.A Conventions and notations

Θ is the Heaviside step function. When dealing with Markov Langevin equations, the choice of the value of the Heaviside step function $\Theta(t)$ at $t = 0$ is imposed by the choice of the Itô [$\Theta(0) = 0$] or the Stratonovich convention [$\Theta(0) = 1/2$]. However, away from the Markov case, *i.e.* as long as both inertia and the color of the bath are not neglected simultaneously, the choice of $\Theta(0)$ is unconstrained and the physics should not depend on it. We recall the identities

$$\int_{-\infty}^{\infty} \frac{dx}{2\pi} e^{ixy} = \delta(y) \quad \text{and} \quad \int_{-\infty}^y dx \delta(x) = \Theta(y), \quad (2.101)$$

where δ is the Dirac delta function.

Field theory notations. Let ψ be a real field. The integration over this field is denoted $\int \mathcal{D}[\psi]$. If A is a functional of the field, we denote it $A[\psi]$. If it also depends on one or several external parameters, such as the time t and a protocol λ , we denote it $A([\psi], \lambda, t)$. Whenever A is a local functional of the field at time t (*i.e.* a function of $\psi(t)$ and its first time-derivatives), we use the short-hand notation $A[\psi(t)]$. The time-reversed field constructed from ψ is denoted $\bar{\psi}$: $\bar{\psi}(t) \equiv \psi(-t)$. The time-reversed functional constructed from $A([\psi], \lambda, t)$ is called A_r : $A_r([\psi], \lambda, t) \equiv A([\bar{\psi}], \lambda, -t)$. Applied on local observables of ψ , it has the effect of changing the sign of all odd time-derivatives in the expression of A .

To shorten expressions, we adopt a notation in which the arguments of the fields appear as subindices, $\psi_t \equiv \psi(t)$, $\eta_{t-t'} \equiv \eta(t - t')$, and so on and so forth, and the integrals over time as expressed as $\int_t \equiv \int dt$.

Grassmann numbers. Let θ_1 and θ_2 be two anticommuting Grassmann numbers and θ_1^* and θ_2^* their respective Grassmann conjugates. We adopt the following convention for the complex conjugate of a product of Grassmann numbers: $(\theta_1 \theta_2)^* = \theta_2^* \theta_1^*$.

2.B Discrete MSRJD for additive noise

In this appendix we discuss the MSRJD action for processes with additive colored noise.

2.B.1 Discrete Langevin equation

The Langevin equation is a stochastic differential equation and one can give a rigorous meaning to it by specifying a particular discretization scheme.

Let us divide the time interval $[-T, T]$ into $N + 1$ infinitesimal slices of width $\epsilon \equiv 2T/(N + 1)$. The discretized times are $t_k = -T + k\epsilon$ with $k = 0, \dots, N + 1$. The discretized version of $\psi(t)$ is $\psi_k \equiv \psi(t_k)$. The continuum limit is achieved by sending N to infinity and keeping $(N + 1)\epsilon = 2T$ constant. Given some initial conditions ψ_i and $\dot{\psi}_i$, we set $\psi_1 = \psi_i$ and $\psi_0 = \psi_i - \epsilon\dot{\psi}_i$ meaning that the first two times (t_0 and t_1) are reserved for the integration over the initial conditions whereas the N following ones correspond to the stochastic dynamics given by the discretized Langevin equation:

$$\begin{aligned} \text{EQ}_{k-1} &\equiv m \frac{\psi_{k+1} - 2\psi_k + \psi_{k-1}}{\epsilon^2} - F_k(\psi_k, \psi_{k-1}, \dots) + \epsilon \sum_{l=1}^k \eta_{kl} \frac{\psi_l - \psi_{l-1}}{\epsilon} \\ &= \xi_k, \end{aligned} \quad (2.102)$$

defined for $k = 1, \dots, N$. The force F_k typically depends on the state ψ_k but can have a memory kernel (*i.e.* it can depend on previous states ψ_{k-1} , ψ_{k-2} , etc.). The notation η_{kl} stands for $\eta_{kl} \equiv \epsilon^{-1} \int_0^\epsilon du \eta(t_k - t_l + u)$. The ξ_k are independent Gaussian random variables with variance $\langle \xi_k \xi_l \rangle = \beta^{-1} \aleph_{kl}$ where $\aleph_{kl} \equiv \eta_{kl} + \eta_{lk}$. Inspecting the equation above, we notice that the value of ψ_k depends on the realization of the previous noise realization ξ_{k-1} and there is no need to specify ξ_0 and ξ_{N+1} .

In the white noise limit, one has $\eta_{kl} = \epsilon^{-1} \eta_0 \delta_{kl}$, $\langle \xi_k \xi_l \rangle = 2\eta_0 \beta^{-1} \epsilon^{-1} \delta_{kl}$ where δ is the Kronecker delta, and

$$\text{EQ}_{k-1} \equiv m \frac{\psi_{k+1} - 2\psi_k + \psi_{k-1}}{\epsilon^2} - F_k(\psi_k, \psi_{k-1}, \dots) + \eta_0 \frac{\psi_k - \psi_{k-1}}{\epsilon} = \xi_k.$$

2.B.2 Construction of the MSRJD action

The probability density P for a complete field history $(\psi_0, \psi_1, \dots, \psi_{N+1})$ is set by the relation

$$\begin{aligned} P(\psi_0, \psi_1, \dots, \psi_{N+1}) d\psi_0 d\psi_1 \dots d\psi_{N+1} \\ = P_i(\psi_i, \dot{\psi}_i) d\psi_i d\dot{\psi}_i P_n(\xi_1, \xi_2, \dots, \xi_N) d\xi_1 d\xi_2 \dots d\xi_N. \end{aligned}$$

P_i is the initial probability distribution of the field. The probability for a given noise history to occur between times t_1 and t_N is given by

$$P_n(\xi_1, \dots, \xi_N) = \mathcal{M}_N^{-1} e^{-\frac{1}{2} \sum_{k,l=1}^N \xi_k \beta \aleph_{kl}^{-1} \xi_l} \quad (2.103)$$

where \aleph_{kl}^{-1} is the inverse matrix of \aleph_{kl} (and not the discretized version of the inverse operator of \aleph) and the normalization is given by $\mathcal{M}_N^2 \equiv \frac{(2\pi)^N}{\det_{kl}(\beta \aleph_{kl}^{-1})}$ where $\det(\dots)$ stands for the matrix determinant. From eq. (2.103), one derives

$$P(\psi_0, \psi_1, \dots, \psi_{N+1}) = |\mathcal{J}_N| P_i(\psi_1, \frac{\psi_1 - \psi_0}{\epsilon}) P_n(\text{EQ}_0, \dots, \text{EQ}_{N-1}) , \quad (2.104)$$

with the Jacobian

$$\mathcal{J}_N \equiv \det \left(\frac{\partial (\psi_1, \psi_i, \xi_1, \dots, \xi_N)}{\partial (\psi_0, \psi_1, \dots, \psi_{N+1})} \right) = \det \left(\frac{\partial (\psi_1, \psi_i, \text{EQ}_0, \dots, \text{EQ}_{N-1})}{\partial (\psi_0, \psi_1, \dots, \psi_{N+1})} \right) ,$$

that will be discussed in App. 2.B.3. The expression (2.103) for the noise history probability reads, after a Hubbard-Stratonovich transformation that introduces the auxiliary variables $\hat{\psi}_k$ ($k = 1, \dots, N$),

$$\begin{aligned} \mathcal{N}_N P_n(\xi_1, \dots, \xi_N) &= \int d\hat{\psi}_1 \dots d\hat{\psi}_N e^{-\epsilon \sum_k i\hat{\psi}_k \xi_k + \frac{1}{2} \beta^{-1} \epsilon^2 \sum_{kl} i\hat{\psi}_k \aleph_{kl} i\hat{\psi}_l} \\ &= \int d\hat{\psi}_0 \dots d\hat{\psi}_{N+1} \delta(\hat{\psi}_0) \delta(\hat{\psi}_{N+1}) e^{-\epsilon \sum_k i\hat{\psi}_k \text{EQ}_{k-1} + \frac{1}{2} \beta^{-1} \epsilon^2 \sum_{kl} i\hat{\psi}_k \aleph_{kl} i\hat{\psi}_l} , \end{aligned} \quad (2.105)$$

with $\mathcal{N}_N \equiv (2\pi/\epsilon)^N$. In the last step, we replaced ξ_k by EQ_{k-1} and we allowed for summations over $k = 0$ and $k = N + 1$ as well as integrations over $\hat{\psi}_0$ and $\hat{\psi}_{N+1}$ at the cost of introducing delta functions. The Hubbard-Stratonovich transformation allows for some freedom in the choice of the sign in front of $i\hat{\psi}_k$ in the exponent (indeed P_n is real so $P_n = P_n^*$). Together with eq. (2.104) this gives

$$\begin{aligned} \mathcal{N}_N P(\psi_0, \psi_1, \dots, \psi_{N+1}) &= |\mathcal{J}_N| \int d\hat{\psi}_0 \dots d\hat{\psi}_{N+1} \delta(\hat{\psi}_0) \delta(\hat{\psi}_{N+1}) \\ &\quad \times e^{-\sum_k i\hat{\psi}_k \text{EQ}_{k-1} + \frac{1}{2} \beta^{-1} \epsilon^2 \sum_{kl} i\hat{\psi}_k \aleph_{kl} i\hat{\psi}_l + \ln P_i\left(\psi_1, \frac{\psi_1 - \psi_0}{\epsilon}\right)} \end{aligned}$$

that in the continuum limit becomes

$$\mathcal{N} P[\psi] = |\mathcal{J}[\psi]| e^{\ln P_i} \int \mathcal{D}[\hat{\psi}] e^{-\int du i\hat{\psi}(u) \text{EQ}([\psi], u) + \frac{1}{2} \int \int du dv i\hat{\psi}(u) \beta^{-1} \aleph(u-v) i\hat{\psi}(v)} ,$$

with the boundary conditions $\hat{\psi}(-T) = \hat{\psi}(T) = 0$ and where all the integrals over time run from $-T$ to T . In the following, unless otherwise stated, we shall simply denote them by \int . The infinite prefactor $\mathcal{N} \equiv \lim_{N \rightarrow \infty} (2\pi/\epsilon)^N$ can be absorbed in the definition of the measure:

$$\mathcal{D}[\psi, \hat{\psi}] = \lim_{N \rightarrow \infty} \left(\frac{\epsilon}{2\pi} \right)^N \prod_{k=0}^{N+1} d\psi_k d\hat{\psi}_k . \quad (2.106)$$

Markov case. In the Markov limit, the Langevin equation is a first order differential equation, therefore only the first time t_0 should be reserved for integrating over the initial conditions. Moreover, one has to specify the discretization:

$$\text{EQ}_{k-1} \equiv \eta_0 \frac{\psi_k - \psi_{k-1}}{\epsilon} - F_k(\tilde{\psi}_k) = \xi_k, \quad (2.107)$$

where $\tilde{\psi}_k \equiv a\psi_k + (1-a)\psi_{k-1}$ with $a \in [0, 1]$. $a = 0$ corresponds to the Itô interpretation whereas $a = 1/2$ corresponds to the Stratonovich one (see the discussion in Sec. 2.1.4). Following the steps in App. 2.B.2, we upgrade eq. (2.107) to the following a -dependent action⁹:

$$S_N(a) = \epsilon \sum_k \left(\beta^{-1} \eta_0 (\dot{\psi}_k)^2 - i\dot{\psi}_k \left[\eta_0 \frac{\psi_k - \psi_{k-1}}{\epsilon} - F_k(\tilde{\psi}_k) \right] - \frac{a}{\eta_0} F'_k(\tilde{\psi}_k) \right). \quad (2.108)$$

The last term in the RHS comes from the Jacobian:

$$\mathcal{J}_N = \prod_k \frac{\partial \text{EQ}_{k-1}}{\partial \psi_k} = \prod_k \left(\frac{\eta_0}{\epsilon} - a F'_k(\tilde{\psi}_k) \right) = \left(\frac{\eta_0}{\epsilon} \right)^N e^{-\epsilon \sum_k \frac{a}{\eta_0} F'_k(\tilde{\psi}_k)}.$$

In the Itô discretization scheme ($a = 0$) this Jacobian term disappears from the action. Although $S_N(a)$ seems to be a -dependent, we now prove that all discretization schemes yield the same physics by showing that the difference $S_N(a) - S_N(0)$ is negligible. The Taylor expansion of $F_k(\tilde{\psi}_k)$ around ψ_{k-1} , $F_k(\psi_{k-1}) + a(\psi_k - \psi_{k-1}) F'(\psi_{k-1}) + O(\epsilon)$ [since $\psi_k - \psi_{k-1} = O(\sqrt{\epsilon})$], yields

$$S_N(a) - S_N(0) = a\epsilon \sum_k F'(\psi_{k-1}) \left[i\dot{\psi}_k (\psi_k - \psi_{k-1}) - \frac{1}{\eta_0} \right] + O(\epsilon^2). \quad (2.109)$$

Although the first term within the square brackets looks smaller than the second one, they are actually both $O(1)$ since $i\dot{\psi}_k = O(1/\sqrt{\epsilon})$. Thus, each term in the sum in the RHS is $O(\epsilon)$. We now compute the average of $S_N(a) - S_N(0)$ with respect to $S_N(0)$ by neglecting in the latter the term $i\dot{\psi}_k F_k(\psi_{k-1})$ which is of order $\sqrt{\epsilon}$ whereas the others are of order 1. Since $\langle i\dot{\psi}_k (\psi_k - \psi_{k-1}) \rangle_{S_N(0)} = 1/\eta_0$, it is easy to show that $\langle S_N(a) - S_N(0) \rangle_{S_N(0)} = 0$ and therefore all the $S_N(a)$ actions are equivalent to the simpler Itô one.

9. We omit the initial measure which is not relevant in this discussion.

2.B.3 Jacobian

Discrete evaluation of the Jacobian.

In this Section we take the continuum limit of the Jacobian defined in eq. (2.105). In the additive noise case, we start from

$$\begin{aligned}
 \mathcal{J}_N &= \det \left(\frac{\partial (\psi_i, \dot{\psi}_i, \text{EQ}_0, \dots, \text{EQ}_{N-1})}{\partial (\psi_0, \psi_1, \dots, \psi_{N+1})} \right) \\
 &= \det \begin{pmatrix} 0 & 1 & 0 & \dots & 0 \\ -1/\epsilon & 1/\epsilon & 0 & \dots & 0 \\ \frac{\partial \text{EQ}_0}{\partial \psi_0} & \frac{\partial \text{EQ}_0}{\partial \psi_1} & \frac{\partial \text{EQ}_0}{\partial \psi_2} & 0 & \dots \\ \frac{\partial \text{EQ}_1}{\partial \psi_0} & \frac{\partial \text{EQ}_1}{\partial \psi_1} & \frac{\partial \text{EQ}_1}{\partial \psi_2} & \frac{\partial \text{EQ}_1}{\partial \psi_3} & 0 \\ \dots & \dots & \dots & \dots & 0 \\ \frac{\partial \text{EQ}_{N-1}}{\partial \psi_0} & \dots & \dots & \dots & \frac{\partial \text{EQ}_{N-1}}{\partial \psi_{N+1}} \end{pmatrix} \\
 &= \frac{1}{\epsilon} \det \begin{pmatrix} \frac{\partial \text{EQ}_0}{\partial \psi_2} & 0 & \dots & 0 \\ \frac{\partial \text{EQ}_1}{\partial \psi_2} & \frac{\partial \text{EQ}_1}{\partial \psi_3} & 0 & \dots \\ \dots & \dots & 0 & \dots \\ \frac{\partial \text{EQ}_{N-1}}{\partial \psi_2} & \dots & \dots & \frac{\partial \text{EQ}_{N-1}}{\partial \psi_{N+1}} \end{pmatrix}. \tag{2.110}
 \end{aligned}$$

Causality manifests itself in the lower triangular structure of the last matrix. One can evaluate the last determinant by plugging eq. (2.102). It yields

$$\mathcal{J}_N = \frac{1}{\epsilon} \prod_{k=1}^N \frac{\partial \text{EQ}_{k-1}}{\partial \psi_{k+1}} = \frac{1}{\epsilon} \left(\frac{m}{\epsilon^2} \right)^N.$$

The Jacobian $\mathcal{J} \equiv \lim_{N \rightarrow \infty} \mathcal{J}_N$ is therefore a field-independent positive constant that can be absorbed in a redefinition of the measure:

$$\mathcal{D}[\psi, \hat{\psi}] \equiv \lim_{N \rightarrow \infty} \frac{1}{\epsilon} \left(\frac{m}{2\pi\epsilon} \right)^N \prod_{k=0}^{N+1} d\psi_k d\hat{\psi}_k. \tag{2.111}$$

We show that this result also holds for multiplicative noise in App. 2.C.

Continuous evaluation of the Jacobian.

One might also wish to check this result in the continuous notations. A very similar approach can be found in [157]. In the continuous notations, $\lim_{N \rightarrow \infty} \mathcal{J}_N$ reads up to some constant factor

$$\mathcal{J}[\psi] = \det_{uv} \left[\frac{\delta \text{EQ}([\psi], u)}{\delta \psi(v)} \right].$$

where $\det[\dots]$ stands for the functional determinant. Defining F'_{uv} as $\delta F_u[\psi]/\delta\psi_v$, the Jacobian reads

$$\begin{aligned}
\mathcal{J}[\psi] &= \det_{uv} \left[m\partial_u^2 \delta_{u-v} + \int_w \eta_{u-w} \partial_w \delta_{w-v} - F'_{uv}[\psi] \right] \\
&= \det_{uv} \left[m\partial_u^2 \delta_{u-v} + \int_w \eta_{u-w} \partial_w \delta_{w-v} \right] \det_{uv} \left[\delta_{u-v} - \int_w G_{u-w} F'_{wv}[\psi] \right] \\
&= \det_{uv} \left[m\partial_u^2 \delta_{u-v} + \int_w \eta_{u-w} \partial_w \delta_{w-v} \right] \exp \text{Tr}_{uv} \ln [\delta_{u-v} - M_{uv}] \\
&= \det_{uv} \left[m\partial_u^2 \delta_{u-v} + \int_w \eta_{u-w} \partial_w \delta_{w-v} \right] \exp - \sum_{n=1}^{\infty} \frac{1}{n} \int_u \left\{ \underbrace{M \circ M \circ \dots \circ M}_{n \text{ times}} \right\}_{uu} \quad (2.112)
\end{aligned}$$

where we used the notations $M_{uv} \equiv \{G \circ F'\}_{uv} \equiv \int_w G_{u-w} F'_{wv}[\psi]$. G is the retarded Green function solution to

$$m\partial_u^2 G(u-v) + \int dw \eta(u-w) \partial_w G(w-v) = \delta(u-v). \quad (2.113)$$

Since both G_{u-v} and F'_{uv} are causal, it is easy to see that the $n \geq 2$ terms do not contribute to the sum in eq. (2.112). If the force $F([\psi], t)$ does not have any local term (involving the value of ψ or $\dot{\psi}$ at time t) the $n = 1$ term is also zero. Otherwise the $n = 1$ term can still be proven to be zero provided that $G(t=0) = 0$. This will be true, as we shall show in the next paragraph, unless the white noise limit is taken together with the Smoluchowski limit ($m = 0$). Away from this Markov limit we establish

$$\mathcal{J}[\psi] = \det_{uv} \left[m\partial_u^2 \delta(u-v) + \int_w \eta_{u-w} \partial_w \delta_{w-v} \right],$$

meaning that the Jacobian is a constant that does not depend on the field ψ .

We now give a proof that $G(t=0) = 0$. Taking the Fourier transform of eq. (2.113),

$$G(t=0) = \int_{-\infty}^{\infty} \frac{d\omega}{2\pi} G(\omega) = - \int_{-\infty}^{\infty} \frac{d\omega}{2\pi} \frac{1}{m\omega^2 + i\omega\eta(\omega)}. \quad (2.114)$$

$G(\omega)$ and $\eta(\omega)$ are the Fourier transforms of the retarded Green function and friction. They are both analytic in the upper half plane (UHP) thanks to their causality structure. The convergence of the integrals around $|\omega| \rightarrow \infty$ in eq. (2.114) is ensured by either the presence of inertia or the colored noise. For a white noise [$\eta(\omega) = \eta_0$], it is clear that the mass term renders the integrals in eq. (2.114) well defined. In the $m = 0$ limit the convergence is still guaranteed as long as the white noise limit is not taken simultaneously. Indeed, because $\eta(\omega)$ is analytic in the UHP, it is hence either divergent on the boundaries of the UHP or constant everywhere [$\eta(\omega) = \eta_0$]. In the first case, which corresponds to a generic colored

noise, this renders the integrals in eq. (2.114) well defined. In the second case, corresponding to a white noise limit, they are ill-defined and require a more careful treatment¹⁰. When the integrals in eq. (2.114) are well defined on the boundaries, the absence of poles (or branch cuts) in the UHP of $G(\omega)$ gives, after a little deformation of the integration contour in eq. (2.114) above the $\omega = 0$ pole, the result $G(t = 0) = 0$.

Representation in terms of a fermionic field integral.

The determinant can be represented as a Gaussian integration over Grassmannian conjugate fields c and c^* . This formulation is a key ingredient to the supersymmetric representation of the MSRJD path integral. Let us first recall the discretized expression of the Jacobian obtained in eq. (2.110):

$$\mathcal{J}_N = \frac{1}{\epsilon} \det_{kl} \left(\frac{\partial \text{EQ}_{k-1}}{\partial \psi_{l+1}} \right),$$

where k and l run from 1 to N . Introducing ghosts, it can be put in the form

$$\begin{aligned} \mathcal{J}_N &= \frac{1}{\epsilon} \frac{1}{\epsilon^N} \int dc_2 dc_0^* \dots dc_{N+1} dc_{N-1}^* e^{\epsilon^2 \sum_{k=0}^{N-1} \sum_{l=2}^{N+1} c_k^* \frac{1}{\epsilon} \frac{\partial \text{EQ}_k}{\partial \psi_l} c_l} \\ &= \frac{1}{\epsilon} \frac{1}{\epsilon^N} \int dc_0 dc_0^* \dots dc_{N+1} dc_{N+1}^* c_{N+1}^* c_N^* c_1 c_0 e^{\epsilon^2 \sum_{k=0}^{N+1} \sum_{l=0}^{N+1} c_k^* \frac{1}{\epsilon} \frac{\partial \text{EQ}_k}{\partial \psi_l} c_l}, \end{aligned}$$

where in the last step, we allowed integration over c_0, c_1, c_N^* and c_{N+1}^* at the cost of introducing delta functions (remember that for a Grassmann number c , the delta function is achieved by c itself). In the continuum limit, absorbing the prefactor into a redefinition of the measure,

$$\mathcal{D}[\psi, \hat{\psi}] = \lim_{N \rightarrow \infty} \frac{1}{(2\pi)^N} \frac{1}{\epsilon} \prod_{k=0}^{N+1} d\psi_k d\hat{\psi}_k \quad \text{and} \quad \mathcal{D}[c, c^*] = \lim_{N \rightarrow \infty} \prod_{k=0}^{N+1} dc_k dc_k^*, \quad (2.115)$$

this yields

$$\mathcal{J}[\psi] = \int \mathcal{D}[c, c^*] e^{S^{\mathcal{J}}[c, c^*, \psi]}$$

10. In the white noise limit, $G(t) = \eta_0^{-1} [1 - e^{-\eta_0 t/m}] \Theta(t)$ is a continuous function that vanishes at $t = 0$. If we take $m \rightarrow 0$ in the previous expression, we still have $G(0) = 0$ and $G(t) = \Theta(t)/\eta_0$ for $t \gg m/\eta_0$. By choosing $\Theta(0) = 0$, these two results can be collected in $G(t) = \Theta(t)/\eta_0$ for all t . The Jacobian is still a constant. This limiting procedure where inertia has been sent to zero after the white noise limit was taken, is the so-called Itô convention. However if m is set to 0 from the beginning, in the so-called Stratonovich convention with $\Theta(0) = 1/2$, then $G(t) = \Theta(t)/\eta_0$ for all t and $G(0) = 1/(2\eta_0)$. This can lead to a so-called Jacobian extra-term in the action. If $F([\psi], t)$ is a function of $\psi(t)$ only (ultra-local functional), it reads $-1/(2\eta_0) \int_u F'_u(\psi_u)$. It is invariant under time-reversal of the field $\psi_u \mapsto \psi_{-u}$ as long as F' is itself time-reversal invariant.

with

$$S^{\mathcal{J}}[c, c^*, \psi] \equiv \int_u \int_v c_u^* \frac{\delta \text{EQ}_u[\psi]}{\delta \psi_v} c_v ,$$

and the extra boundary conditions: $c(-T) = \dot{c}(-T) = c^*(T) = \dot{c}^*(T) = 0$. Plugging the Langevin equation (2.1), we have

$$\frac{\delta \text{EQ}_u[\psi]}{\delta \psi_v} = m \partial_u^2 \delta_{u-v} - \frac{\delta F_u[\psi]}{\delta \psi_v} + \int_w \eta_{w-v} \partial_w \delta_{w-v} .$$

The kinetic term in $S^{\mathcal{J}}[c, c^*, \psi]$ can be recast

$$\int_u \int_v c_u^* \partial_u^2 \delta_{u-v} c_v = \int_u c_u^* \partial_u^2 c_u + \Theta_0 [\dot{c}^* c - c^* \dot{c}]_{-T}^T + \Theta_0 \delta_0 [c^* c]_{-T}^T .$$

The last two terms in the RHS vanish by use of the boundary conditions ($c_{-T} = \dot{c}_{-T} = c_T^* = \dot{c}_T^* = 0$). The retarded friction can be recast

$$\int_u \int_v c_u^* \partial_u \eta_{u-v} c_v - \Theta_0 \int_u c_u^* [\eta_{u+T} c_{-T} - \eta_{u-T} c_T] ,$$

where the second term vanishes identically for two reasons: the boundary condition ($c_{-T} = 0$) kills the first part and the causality of the friction kernel ($\eta_u = 0 \forall u < 0$) suppresses the second one. If there is a Dirac contribution to η centered at $u = 0$ such as in the white noise case, the other boundary condition ($c_{-T}^* = 0$) cancels the second part. Finally, we have

$$S^{\mathcal{J}}[c, c^*, \psi] = \int_u c_u^* \partial_u^2 c_u + \int_u \int_v c_u^* \left[\partial_u \eta_{u-v} - \frac{\delta F_u[\psi]}{\delta \psi_v} \right] c_v . \quad (2.116)$$

2.C Discrete MSRJD for multiplicative noise

The discretized Langevin equation reads:

$$\begin{aligned} \text{EQ}_{k-1} &\equiv m \frac{\psi_{k+1} - 2\psi_k + \psi_{k-1}}{\epsilon^2} - F_k(\tilde{\psi}_k, \tilde{\psi}_{k-1}, \dots) \\ &\quad + M'(\tilde{\psi}_k) \epsilon \sum_{l=1}^k \eta_{kl} M'(\tilde{\psi}_l) \frac{\psi_l - \psi_{l-1}}{\epsilon} = M'(\tilde{\psi}_k) \xi_k . \end{aligned}$$

with $\tilde{\psi}_k \equiv a\psi_k + (1-a)\psi_{k-1}$ and $k = 1, \dots, N$. In the Markov limit ($m = 0$ and $\eta_{kl} = \epsilon^{-1} \eta_0 \delta_{kl}$) the results depend on a (see the discussion in Sec. 2.1.4). In the additive noise case, the choices $a = 0$ and $a = 1/2$ correspond to the Itô and Stratonovich conventions, respectively. However, we decide to stay out of the Markov limit: the results are then independent of a and we choose to work with $a = 1$. The probability for a field history is

$$P(\psi_0, \psi_1, \dots, \psi_{N+1}) = |\mathcal{J}_N| P_i(\psi_1, \frac{\psi_1 - \psi_0}{\epsilon}) P_n(\widetilde{\text{EQ}}_0, \dots, \widetilde{\text{EQ}}_{N-1}) , \quad (2.117)$$

where we introduced the shorthand notation $\widetilde{\text{EQ}}_k \equiv \text{EQ}_k/M'(\psi_{k+1})$. The Jacobian is

$$\mathcal{J}_N \equiv \det \left(\frac{\partial (\psi_i, \dot{\psi}_i, \xi_1, \dots, \xi_N)}{\partial (\psi_0, \psi_1, \dots, \psi_{N+1})} \right) = \det \left(\frac{\partial (\psi_i, \dot{\psi}_i, \widetilde{\text{EQ}}_0, \dots, \widetilde{\text{EQ}}_{N-1})}{\partial (\psi_0, \psi_1, \dots, \psi_{N+1})} \right). \quad (2.118)$$

P_n is still given by expression (2.105) and $P_n(\widetilde{\text{EQ}}_0, \dots, \widetilde{\text{EQ}}_{N-1})$ reads, after the substitution $\hat{\psi}_k \mapsto \hat{\psi}_k M'(\psi_k)$,

$$\mathcal{N}_N^{-1} \int d\hat{\psi}_0 \dots d\hat{\psi}_{N+1} \delta(\hat{\psi}_0) \delta(\hat{\psi}_{N+1}) |\hat{\mathcal{J}}_N| e^{-\epsilon \sum_k i\hat{\psi}_k \text{EQ}_{k-1} + \frac{1}{2} \beta^{-1} \epsilon^2 \sum_{kl} i\hat{\psi}_k M'(\psi_k) \aleph_{kl} M'(\psi_l) i\hat{\psi}_l},$$

where $\hat{\mathcal{J}}_N \equiv \det_{kl} (\delta_{kl} M'(\psi_k))$ is the Jacobian of the previous substitution. The probability for a given history is therefore

$$P(\psi_0, \psi_1, \dots, \psi_{N+1}) = \mathcal{N}_N^{-1} \int d\hat{\psi}_0 \dots d\hat{\psi}_{N+1} |\mathcal{J}_N \hat{\mathcal{J}}_N| \times e^{-\sum_k i\hat{\psi}_k \text{EQ}_{k-1} + \frac{1}{2} \beta^{-1} \sum_{kl} i\hat{\psi}_k M'(\psi_k) \aleph_{kl} M'(\psi_l) i\hat{\psi}_l + \ln P_1\left(\psi_1, \frac{\psi_1 - \psi_0}{\epsilon}\right)}.$$

The Jacobian \mathcal{J}_N defined in eq. (2.118) reads

$$\begin{aligned} \mathcal{J}_N &= \frac{1}{\epsilon} \det_{kl} \left(\frac{1}{M'(\psi_k)} \frac{\partial \text{EQ}_{k-1}}{\partial \psi_{l+1}} - \frac{M''(\psi_k)}{M'(\psi_k)^2} \text{EQ}_{k-1} \delta_{kl+1} \right) \\ &= \frac{1}{\epsilon} \hat{\mathcal{J}}_N^{-1} \det_{kl} \left(\frac{\partial \text{EQ}_{k-1}}{\partial \psi_{l+1}} - \frac{M''(\psi_k)}{M'(\psi_k)} \text{EQ}_{k-1} \delta_{kl+1} \right) \end{aligned} \quad (2.119)$$

where k and l run from 1 to N . Causality is responsible for the triangular structure of the matrix involved in the last expression. The second term within the square brackets yields matrix elements below the main diagonal and these do not contribute to the Jacobian. Therefore, we find

$$\mathcal{J}_N \hat{\mathcal{J}}_N = \frac{1}{\epsilon} \prod_{k=1}^N \frac{\partial \text{EQ}_{k-1}}{\partial \psi_{k+1}} = \frac{1}{\epsilon} \left(\frac{m}{\epsilon^2} \right)^N.$$

that is the same field-independent positive constant as in the additive noise case that can be dropped in the measure, see eq. (2.111).

A fermionic functional representation of the Jacobian can be obtained by introducing ghosts, expression (2.119) can be put in the form

$$\mathcal{J}_N \hat{\mathcal{J}}_N = \frac{1}{\epsilon} \frac{1}{\epsilon^N} \int dc_0 dc_0^* \dots dc_{N+1} dc_{N+1}^* c_{N+1}^* c_N^* c_1 c_0 e^{S_N^{\mathcal{J}}},$$

with

$$S_N^{\mathcal{J}} \equiv \epsilon^2 \sum_{k=0}^{N+1} \sum_{l=0}^{N+1} c_k^* \frac{1}{\epsilon} \frac{\partial \text{EQ}_k}{\partial \psi_l} c_l - \epsilon \sum_{k=0}^{N+1} c_k^* \frac{M''(\psi_{k+1})}{M'(\psi_{k+1})} \text{EQ}_k c_{k+1}.$$

In the continuum limit it becomes

$$S^{\mathcal{J}} \equiv \lim_{N \rightarrow \infty} S_N^{\mathcal{J}} = \int_u \int_v c_u^* \frac{\delta \mathbf{E} \mathbf{Q}_u[\psi]}{\delta \psi_v} c_v - \int_u c_u^* \frac{M''(\psi_u)}{M'(\psi_u)} \mathbf{E} \mathbf{Q}_u[\psi] c_u ,$$

with the boundary conditions $c(-T) = \dot{c}(-T) = 0$ and $c^*(T) = \dot{c}^*(T) = 0$ and the measure of the corresponding path integral is given in (2.115).

SCALINGS AND SUPER-UNIVERSALITY IN COARSENING VERSUS GLASSY DYNAMICS

Contents

3.1	The models	73
3.1.1	The Random Field Ising Model	73
3.1.2	The Edwards-Anderson spin glass	74
3.1.3	Methods	74
3.2	The typical growing length	76
3.2.1	The RFIM	76
3.2.2	3d EA	83
3.2.3	Colloidal glasses	84
3.2.4	Summary	85
3.3	Fluctuations	85
3.4	Conclusions	88

THE physics of domain growth is well understood [50, 195]. Just after the initial thermal quench into the ordered phase, the spins in a ferromagnetic system tend to order and form domains of the equilibrium states. In clean systems the ordering dynamics is governed by the symmetry and conservation properties of the order parameter. When impurities are present the dynamics are naturally slowed down by domain-wall pinning [55–57]. The *dynamic scaling hypothesis* states that the time-dependence in any macroscopic observable enters only through a growing length scale, $R(t)$, either the instantaneous *averaged* or *typ-*

ical domain radius. However, a complete description of the phenomenon is lacking. In the clean cases the scaling functions are not known analytically and no fully satisfactory approximation scheme to estimate them is known [50]. In presence of disorder the limitations are more severe in the sense that the growth laws are derived by assuming that the relaxation is driven by activation over free-energy barriers and the properties of the latter are estimated with energy balancing arguments applied to single interfaces that are hard to put to the test. Even in the relatively simple random bond Ising model (RBIM) the time dependence of the growth law remains a subject of controversy [196–199].

The dynamics of generic glassy systems is less well understood but presents some similar aspects to those mentioned above. The droplet model of finite-dimensional spin glasses is based on the assumption that in the low-temperature phase these systems also undergo domain growth of two competing equilibrium states [70]. In the mean-field limit spin glasses have, though, a very different kind of dynamics [19, 200] that cannot be associated to a simple growth of two types of domains. Numerical studies of the 3d Edwards-Anderson (EA) model [201, 116–118, 202–206] have not been conclusive in deciding for one or the other type of evolution and, in a sense, show aspects of both. A one-time dependent ‘coherence’-length, $R(t)$, has been extracted from the distance and time dependence of the *equal-time* overlap between two replicas evolving independently with the same quenched disordered interactions [203, 204, 206]. A power-law $R(t) \sim t^{1/z(T)}$ with the dynamic exponent $z(t) = z(T_c)T_c/T$ fits the available data for the 3d EA and $z(T_c) = 6.86(16)$ with Gaussian [206] and $z(T_c) = 6.54(20)$ with bimodal [203, 204] couplings. Still, it was claimed in [206] that the overlap decays to zero as a power law at long distances and long times such that $r/R(t)$ is fixed, implying that there are more than two types of growing domains in the low temperature phase.

A two-time dependent length, $\xi(t, t')$, can be extracted from the analysis of the spatial decay of the correlation between two spins in the same system at distance r and different times t and t' after preparation [207, 208]. The latter method is somehow more powerful than the former one in the sense that it can be easily applied to glassy problems without quenched disorder. If there is only one characteristic length scale in the dynamics $R(t)$ should be recovered as a limit of $\xi(t, t')$ but this fact has not been demonstrated.

The mechanism leading to the slow relaxation of structural glasses is also not understood. Still, molecular dynamic studies of Lennard-Jones mixtures [209] and the analysis of confocal microscopy data in colloidal suspensions [210] show that two-time observables have similar time dependence as in the 3d EA model. Two-time correlations scale using ratios of one-time growing functions that, however, cannot be associated to a domain radius yet. A two-time correlation length ξ with characteristics similar to the one in the 3d EA can also be defined and measured.

The understanding of dynamic fluctuations in out-of-equilibrium relaxing systems ap-

appears as a clear challenge [211]. In systems with quenched randomness different sample regions feel a different environment and one expects to see their effect manifest in different ways working at fixed randomness. In structural or polymer glasses there are no quenched interactions instead, but still one expects to see important fluctuations in their dynamic behavior both in metastable equilibrium and in the glassy low temperature regime. The question of whether the fluctuations in generic glassy systems resemble those in coarsening systems has only been studied in a few solvable cases such as the model of ferromagnetic coarsening in the large n limit [212] and the Ising chain [213, 214].

We study ferromagnetic ordering in the $3d$ RFIM following a quench from infinite temperature and we compare it to the dynamics of the $3d$ EA spin glass. Our aim is to signal which aspects of their out-of-equilibrium evolution differ and which are similar by focusing on freely relaxing observables – no external perturbation is applied to measure linear responses. We test the scaling and super-universality hypothesis in the RFIM and we explicitly show that the latter does not apply to the EA model. We analyze the spatio-temporal fluctuations in the coarsening problem and we compare them to the ones found in spin glasses [205, 207, 208], the $O(n)$ ferromagnetic coarsening in the large n limit [212], and other glassy systems [210, 215, 216].

The organization of the chapter is the following. In Sec. 3.1 we define the models and we describe the numerical procedure. Section 3.2 is devoted to the study of the growing length scale, R , the scaling and super-universality hypothesis, and the two-time growing length, ξ . In Sec. 3.3 we focus on the local fluctuations of two time observables. We study two-time coarse-grained correlations and we analyze their statistical properties as time evolves. Finally, in Sec. 3.4 we present our conclusions.

3.1 The models

Two varieties of quenched disorder are encountered in spin models: randomness in the strength of an externally applied magnetic field (*random field*) and randomness in the strength of the bonds (*random bond*). The RFIM and the EA spin glass are two archetypal examples of these which were introduced in Sec. 1.2. In this Section we briefly recall their definitions and some of their main properties.

3.1.1 The Random Field Ising Model

The $3d$ Random Field Ising model (RFIM) is defined by the Hamiltonian [217]

$$H = -J \sum_{\langle i,j \rangle} s_i s_j - \sum_i H_i s_i. \quad (3.1)$$

The first term encodes short range ferromagnetic ($J > 0$) interactions between nearest neighbor Ising spins, $s_i = \pm 1$, placed on the nodes of a cubic lattice with linear size L . H_i represents a local random magnetic field on site i . We adopt a bimodal distribution for these independent identically distributed random variables ($H_i = \pm H$ with equal probability). H quantifies the strength of the quenched disorder. Hereafter in this Chapter, we set $J = 1$.

In the case $H = 0$, the RFIM reduces to the clean Ising model with a phase transition from a paramagnetic to a ferromagnetic state occurring at $T_c \simeq 4.515$. In $d = 3$, the ordered phase survives for finite H : there is a phase separating line on the (T, H) plane joining $(T_c, H = 0)$ and $(T = 0, H_c)$ with $H_c \simeq 2.215(35)$ [61, 62].

3.1.2 The Edwards-Anderson spin glass

The 3d Edwards-Anderson (EA) spin glass is defined by

$$H = - \sum_{\langle i, j \rangle} J_{ij} s_i s_j. \quad (3.2)$$

The interaction strengths J_{ij} act on nearest neighbors on a cubic three-dimensional lattice and are independent identically distributed random variables. We adopt a bimodal distribution, $J_{ij} = \pm J$ with equal probability. Hereafter in this Chapter, we set $J = 1$. This model undergoes a static phase transition from a paramagnetic to a spin glass phase at $T_g \simeq 1.14(1)$ [69]. The nature of the low temperature static phase is not clear yet and, as for the out-of-equilibrium relaxation, two pictures developed around a situation with only two equilibrium states as proposed in the droplet model and a much more complicated vision emerging from the solution of the Sherrington-Kirkpatrick model, its mean-field version [72].

3.1.3 Methods

We study the relaxation dynamics with non-conserved order parameter in the ($d = 3$) ferromagnetic phase of the RFIM at relatively low temperature and small applied field after a quench from very high temperature.

It is difficult to give an accurate analytical treatment for the dynamics of the 3d RFIM. A continuous coarse-grained version of the model can be given with the $n = 1$ non-linear sigma model [defined in eq. (1.3)] (*i.e.* a ϕ^4 theory) with an extra random field. One can write down a Langevin equation for the dynamics of this model. The simplest choice for the environment is a thermal bath with a non-correlated noise in time (white noise) and space: $\langle \xi(x, t) \xi(x, t') \rangle_\xi = 2\beta^{-1} \gamma_0 \delta(x - x') \delta(t - t')$. In the MSRJD formalism, the action reads

after integration over the noise

$$\begin{aligned}
S[\phi, \hat{\phi}] = & - \iint dx du \, i\hat{\phi}(x, u) \left[\gamma_0 \partial_u \phi(x, u) + J \Delta \phi(x, u) \right. \\
& \left. + g\phi(x, u) - u\phi^3(x, u) + h(x) \right] \\
& + \beta^{-1} \gamma_0 \iint dx du \, \left(i\hat{\phi}(x, u) \right)^2 .
\end{aligned} \tag{3.3}$$

We omitted the initial measure since the system is supposed to be prepared at infinite temperature ($\beta = 0$). The field $h(x)$ is spatially random and taken from a Gaussian distribution with $\langle h(x) \rangle_h = 0$ and $\langle h(x)h(x') \rangle_h = H^2 \delta(x - x')$. Therefore, after integration over the random field, one gets [218]

$$\begin{aligned}
S[\phi, \hat{\phi}] = & - \iint dx du \, i\hat{\phi}(x, u) \left[\gamma_0 \partial_u \phi(x, u) + J \Delta \phi(x, u) + g\phi(x, u) - u\phi^3(x, u) \right] \\
& + \beta^{-1} \gamma_0 \iint dx du \, \left(i\hat{\phi}(x, u) \right)^2 + \frac{1}{2} H^2 \iiint dx du dv \, i\hat{\phi}(x, u) i\hat{\phi}(x, v) .
\end{aligned}$$

Due to the interaction term $u\hat{\phi}\phi^3$, the action is not quadratic, and one has to use perturbation theory in powers of u in order to be able to compute anything.

Instead of working with approximate expressions, and since the RFIM is particularly well suited to using numerical simulations (lattice model with short-range interactions and a discrete set of configurations), we follow the dynamics by means of Monte Carlo simulations. The instantaneous quench from infinite temperature at the initial time, $t = 0$, is realized by choosing a random initial condition: $s_i(t = 0) = \pm 1$ with probability one half. The order parameter is not conserved during the evolution. For the dynamics, we use the continuous time Monte Carlo (MC) procedure [219–221]. This algorithm, which is nothing else but a re-organization of the standard Metropolis transition rules, is rejection free. This makes it spectacularly faster than standard Metropolis algorithm which would have a rejection rate close to 1 in the ferromagnetic phase of the RFIM. Times are expressed in usual Monte Carlo steps (MCs): 1 MCs corresponds to $N = L^d$ spin updates with the standard Metropolis algorithm. The way to translate from the continuous time MC to standard MC units, in which we present our results, is explained in [219–221].

Interesting times are not too short – to avoid a short transient regime – and not too long – to avoid reaching equilibration (in ferromagnetic coarsening a non-zero magnetization density indicates that the coarsening regime is finished and other more refined methods are used in the spin glass case¹). We delay equilibration by taking large systems since the equilibration time rapidly grows with the size of the lattice. A reasonable numerical

1. A way to check whether a spin glass model gets close to equilibration is to follow the evolution of spin replicas with the same quenched randomness and testing when the overlap distribution develops a non-trivial structure. Some papers explaining and using this technique are [222, 223, 200].

time-window is $[10^3, 10^7]$ MCs. We show results obtained using lattices with $L = 250$ ($N = 1.5 \times 10^7$ spins) in the RFIM and $L = 100$ ($N = 10^6$ spins) in the spin glass. We checked that finite size effects are not important in any of these cases for averaged quantities.

3.2 The typical growing length

In this Section we study the typical growing length (a geometric object) in the RFIM and the EA model. We establish scaling and super-universality relations for three types of correlations functions (statistical objects). Two of them involve either two space points and one time, or one space point and two times, and are the usual observables studied in coarsening phenomena. The third one is commonly used in the study of glassy systems where two-point correlations are not sufficient to characterize the dynamics of the systems [205, 207–210] and allows for the definition of a two-time dependent length that we can compare to the one obtained in the $3d$ EA model and glassy particle systems.

3.2.1 The RFIM

During the ferromagnetic coarsening regime, there are as many positive as negative spins in such a way that the magnetization density stays zero in the thermodynamic limit and weakly fluctuates around zero for finite size systems. Everywhere in the sample, there is a local competition between growing domains. Eventually, after an equilibration time τ_{eq} (that diverges with the system size), one of the two phases conquers the whole system scale.

In the coarsening regime (times shorter than τ_{eq}) dynamic scaling [50] applies and the growth of order is characterized by a *typical domain radius*, $R(t; T, H)$, that increases in time and depends on the control parameters, T and H , and the dimension of space, d^2 . While in the absence of impurities it is clearly established that, for non-conserved order parameter dynamics, the domain length R grows as $R \sim t^{1/2}$ independently of d [50] with a prefactor that monotonically decreases upon increasing temperature [107], the functional form of R is less clear in random cases. Scaling arguments based on the energetics of single interfaces [55–57, 224–228] predict a crossover from the clean case result at short time scales when it is easy to inflate, to a logarithmic growth,

$$R(t; H, T) = \frac{T}{H^2} \ln(t/\tau(T, H)) . \quad (3.4)$$

The fact that the prefactor grows with T (as opposed to what happens for clean curvature driven dynamics [107]) is due to the activated character of the dynamics. Several proposals

2. Note that some coarsening problems have a distribution of domain radii with long-tails, see [106] and [107].

for the characteristic time τ exist: $\tau \sim (T/H^2)^2$ [224, 225, 195] and $\tau \sim \tau_0 e^{A(T)/H^2}$ with $A(T)$ a weakly temperature dependent function [109]. To ease the notation in what follows we do not write explicitly the T and H dependence of R .

From the point of view of the renormalization group (RG), all points within the ferromagnetic region of the (T, H) phase diagram flow to the stable, zero-temperature, zero-disorder sink. Hence, randomness and temperature should be irrelevant in equilibrium at $T < T_c$. The super-universality hypothesis states that for non-equilibrium ordering dynamics, once lengths are scaled with the typical length R , quenched random fields are irrelevant and all scaling functions are the ones of the clean $3d$ Ising system at $T = 0$ with non-conserved order parameter [70]. It has been tested numerically on some selected observables in a few Ising models with weak disorder. It has been shown to hold for the equal-times two-point function of the $3d$ random field Ising model (RFIM) [109] and the $2d$ random bond Ising model (RBIM) with disordered ferromagnetic interactions [110, 111]. More recently, the distribution of domain areas in this last model [112] and the integrated response [113] has also been shown to be super-universal.

In the context of the $1d$ and $2d$ Random Bond Ising Model (RBIM) with disordered ferromagnetic couplings, it was argued based on numerical simulations, that a disorder typical length L^* should enter the scaling functions *via* the ratio $R(t)/L^*$ independently of the other scalings [108]. For the $1d$ case, the two-time correlation function was measured after a quench in the critical region (just above $T_c = 0$) and the data were shown to obey the following scaling: $C(t, t') = f(R(t)/R(t'), L^*/R(t))$ which violates super-universality. For the $d = 2$ case, other simulations deep in the ferromagnetic phase also showed a super-universality violation for the two-time correlation. However, super-universality was showed to be restored for spatio-temporal correlations $C(r; t, t')$ as soon as r is sufficiently large (a few lattice spacings) [113]. This could be interpreted by a scaling of the form $C(r; t, t') = g(R(t)/R(t'), L^*/R(t), L^*/r)$ which would saturate to $g(R(t)/R(t'), L^*/R(t), 0)$ as soon as $r \gg L^*$ and therefore restore the super-universality property. For the $d = 2$ case, notice that even in equilibrium at the critical point, where the irrelevance of disorder was shown rigorously [229–232], numerical simulations are rather inconclusive since one needs very large lattices to observe the convergence of the RG flow to the zero-disorder fixed point [233].

The equal-time spatial correlation.

A careful analysis of the field and time dependence of the growing length scale together with tests of the scaling hypothesis applied to the equal-time correlation

$$C_2(r; t) \equiv \langle s_i(t) s_j(t) \rangle_{|\vec{r}_i - \vec{r}_j| = r}, \quad (3.5)$$

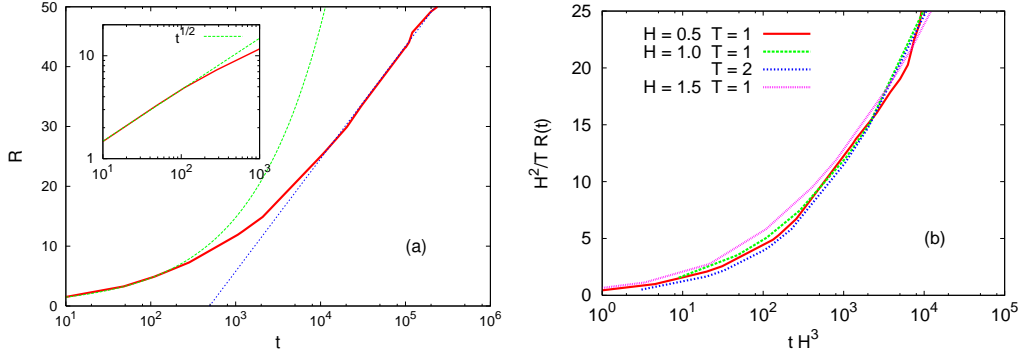


Figure 3.1: (a) With line-points (red), the growing length $R(t)$ at $T = 1$ and $H = 1$. The green curve is the power law \sqrt{t} that describes well the data at short times, right after the temperature quench. The blue line is a logarithmic law apt to describe the behavior at longer time scales. In the inset: the same data in a log-log scale to highlight the quality of the \sqrt{t} behavior at short times. (b) Study of the dependence of R on the parameters T and H for two values of T and three random field strengths H given in the key.

where the average runs over all spins in the sample, appeared in [109, 234]. In the coarsening regime, at distances $a \ll r \ll L$ with a the lattice spacing and $r/R(t)$ finite, $C_2(r; t)$ is expected to depend on r and time t only through the ratio r/R ,

$$C_2(r; t) \simeq m_{\text{eq}}^2 f_2(r/R(t)) , \quad (3.6)$$

with m_{eq} the equilibrium magnetization density (that decreases with increasing T and/or H), $\lim_{x \rightarrow 0} f_2(x) = 1$ and $\lim_{x \rightarrow \infty} f_2(x) = 0$. Since the spatial decay is approximately exponential, $C_2(r; t) \propto e^{-r/R(t)}$ for not too long r , we use this functional form to extract R from the data fit at each set of parameters (T, H, t) . Figure 3.1 (a) shows that the growing length R has two regimes: shortly after the quench R grows as $t^{1/2}$ like in the clean case and it later crosses over to a logarithmic growth. This is consistent with previous numerical studies in $2d$ [110, 235] and $3d$ systems [109, 234]. In Fig. 3.1 (b) we test the dependence on T and H by plotting $\frac{H^2}{T} R$ versus t/τ for $T = 1, 2$ and $H = 0.5, 1, 1.5$. We found the best collapse using $\tau \sim H^{-3}$ but the precision of our data is not high enough to distinguish between this and the τ s proposed in [224, 225] and [109]. Our numerical results tend to confirm the T/H^2 dependence of R even in the early stages of the growth.

Since the work of [109], it is now clear that f_2 in Eq. (3.6) is independent of H , and very similar to the one of the clean system. In Fig. 3.2 we also find that the scaling functions f_2 at different T fall on top of one another. Thus f_2 is independent of H and T .

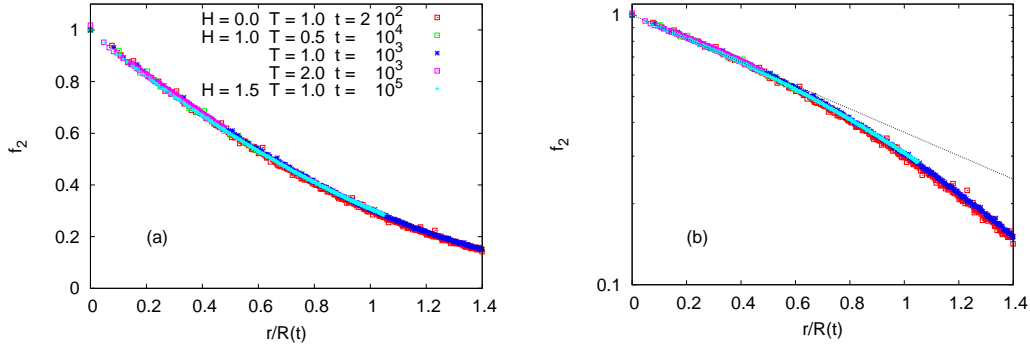


Figure 3.2: (a) The scaling function $f_2(r/R)$ for $T = 0.5, 1, 2$ and $H = 1, 1.5$. (b) The same data in a linear-log scale showing that f_2 is close to an exponential at short r/R .

The two-time self-correlation.

It is commonly defined as

$$C(t, t') \equiv \frac{1}{N} \sum_{i=1}^N \langle s_i(t) s_i(t') \rangle, \quad (3.7)$$

and quantifies how two spin configurations of the same system, one taken at t' (waiting-time) and the other one at $t \geq t'$, are close to each other. The angular brackets here indicate an average over different realizations of the thermal noise. In the large N limit, this quantity is self-averaging with respect to noise and disorder induced fluctuations. This two-time function has been used as a clock for the out-of-equilibrium dynamics of glassy systems [19, 200] and we shall use this property again, in the study of the two-time growing length and fluctuations.

The behavior of C is well understood for coarsening systems. As long as the domain walls have not significantly moved between t' and $t(> t')$ (that defines what we shall call later short time delay), the self-correlation is given by the fluctuations of spins that are in thermal equilibrium inside the domains. As any other equilibrium two-time function, the self-correlation depends then only on $t - t'$. Later, for longer time delays, the displacement of domain walls cannot be neglected any more and C loses its time-translational invariance. The self-correlation can be written as a sum of two terms representing the thermal and aging regimes:

$$C(t, t') = C_{\text{th}}(t - t') + C_{\text{ag}}(t, t') \quad (3.8)$$

with the limit conditions

$$\begin{aligned} C_{\text{th}}(0) &= 1 - q_{\text{EA}}, & \lim_{t' \rightarrow t^-} C_{\text{ag}}(t, t') &= q_{\text{EA}}, \\ \lim_{t \gg t'} C_{\text{th}}(t - t') &= 0, & \lim_{t \gg t'} C_{\text{ag}}(t, t') &= 0. \end{aligned}$$

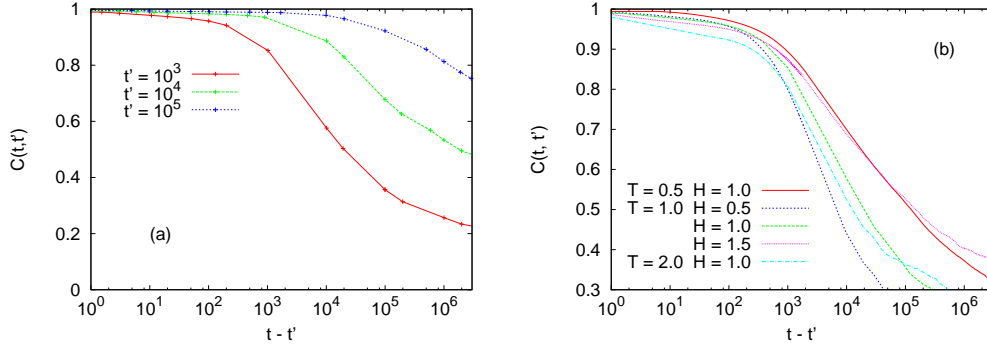


Figure 3.3: The global correlation C vs $t - t'$. (a) $T = 1$ and $H = 1$ and different t' given in the key. (b) $t' = 10^3$ at various pairs of (T, H) given in the key.

q_{EA} is a measure of the order parameter and in a ferromagnetic phase it simply equals m_{eq}^2 , the magnetization squared.

In Fig. 3.3 (a) we show the decay of the two-time correlation C as a function of the time delay $t - t'$ for $t' = 10^3, 10^4, 10^5$ at $T = 1$ and $H = 1$. On each of these curves, one can distinguish the two dynamic regimes. The longer the waiting-time t' the later the aging regime appears. In Fig. 3.3 (b) we show the decay of the two-time correlation as a function of time-delay for $t' = 10^3$ and five pairs of parameters (T, H) given in the key. It is clear that the full relaxation depends strongly on the external parameters: raising the temperature or reducing the random field strength speeds up the decay. For these values of T and H , q_{EA} does not change much but the decay in the aging regime does.

Dynamic scaling implies that in the aging regime

$$C_{\text{ag}}(t, t') = q_{\text{EA}} f\left(\frac{R(t)}{R(t')}\right), \quad (3.9)$$

with R the typical length extracted from C_2 , $f(1) = 1$ and $f(\infty) = 0$. For our choice of parameters (T, H) , q_{EA} is close to unity so we can easily compute f from the measured C by using $f = C_{\text{ag}}/q_{\text{EA}} \simeq C/q_{\text{EA}}$. Super-universality states that f does not depend on T and H . In Fig. 3.4 we show that both hypotheses apply to this quantity. In panel (a) we use a linear-linear scale while in panel (b) we present the same data in a double logarithmic scale. Although the scaling function f looks like a power law it is not. One expects that its tail [$R(t) \gg R(t')$] becomes a power-law with an exponent λ . The actual function f is not known. Most of the analytic efforts in domain growth studies are devoted to develop approximation schemes to derive f , f_2 and other scaling functions but none of them is fully successful [50].

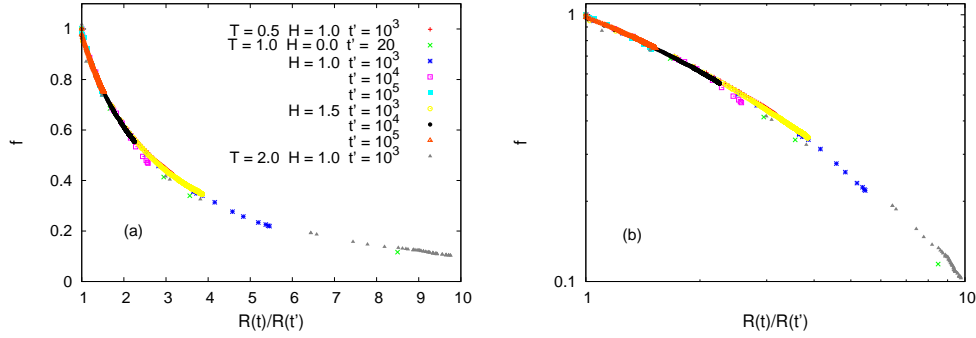


Figure 3.4: Test of the scaling and super-universality hypothesis. (a) $f = C_{ag}/q_{EA}$ vs. $R(t)/R(t')$ at various pairs of (T, H) and t' given in the key. (b) The same data in log-log scale.

The four point-correlation function.

In order to successfully identify a growing correlation length in glassy systems including the 3d EA spin glass, one defines the two-time two-site correlation function [205, 207–210, 236]

$$C_4(r; t, t') \equiv \langle s_i(t) s_i(t') s_j(t) s_j(t') \rangle_{|\vec{r}_i - \vec{r}_j| = r}. \quad (3.10)$$

We extract ξ from its approximate spatial exponential decay: $C_4(r; t, t') - C^2(t, t') \propto e^{-r/\xi(t, t')}$ at relatively *short* r/ξ . (Other methods, such as defining the connected four spin-correlation and extracting ξ from its volume integral yield similar qualitative results though slightly different quantitatively.) Results of this analysis are shown in Fig. 3.5 (a) where we plot $\xi(t, t')$ as a function of t for different t' at $T = 1$ and $H = 1$. We identify a short $t - t'$ regime that is independent of t' (thermal regime), whereas for long $t - t'$, time-translational invariance is broken (aging regime). In Fig. 3.5 (b) we plot $\xi(t, t')$ versus $1 - C(t, t')$ for the three same values of t' , using t as a parameter. The dependence on $1 - C$ and t' is monotonic and very similar to the one obtained in the 3d EA model [205] (see Fig. 3.8). The thermal regime is almost invisible here since it is contained between $C = 1$ and $C = q_{EA}$, with $q_{EA} \simeq 1$ for this set of parameters. We then propose

$$\xi(t, t') = R(t') g(C). \quad (3.11)$$

The limit $g(C = 1) = 0$ is found by taking $t = t'$, that corresponds to $C = 1$ [extending the scaling form (3.11) to include the thermal regime]. In this case $C_4(r; t, t) = 1$. If one uses $C_4(r; t, t) = \tilde{C}_4(r/\xi, C(t, t) = 1)$, see Sec. 3.2.1, then $\xi(t, t)$ must vanish to obtain C_4 independent from r , and this imposes $g(1) = 0$. In the other extreme, when $t \gg t'$ and $C = 0$ one expects $g(0) = 1$. The reason is the following. $\lim_{t \gg t'} C_4(r; t, t') = C_2(r, t) C_2(r, t')$, for the temporal decoupling of C_4 can be done in the $t \gg t'$ limit. Recalling that $C_2(r, t) \propto f_2(r/R(t))$ with $\lim_{x \rightarrow 0} f_2(x) = 1$, the only spatial contribution to $\lim_{t \gg t'} C_4(r; t, t')$

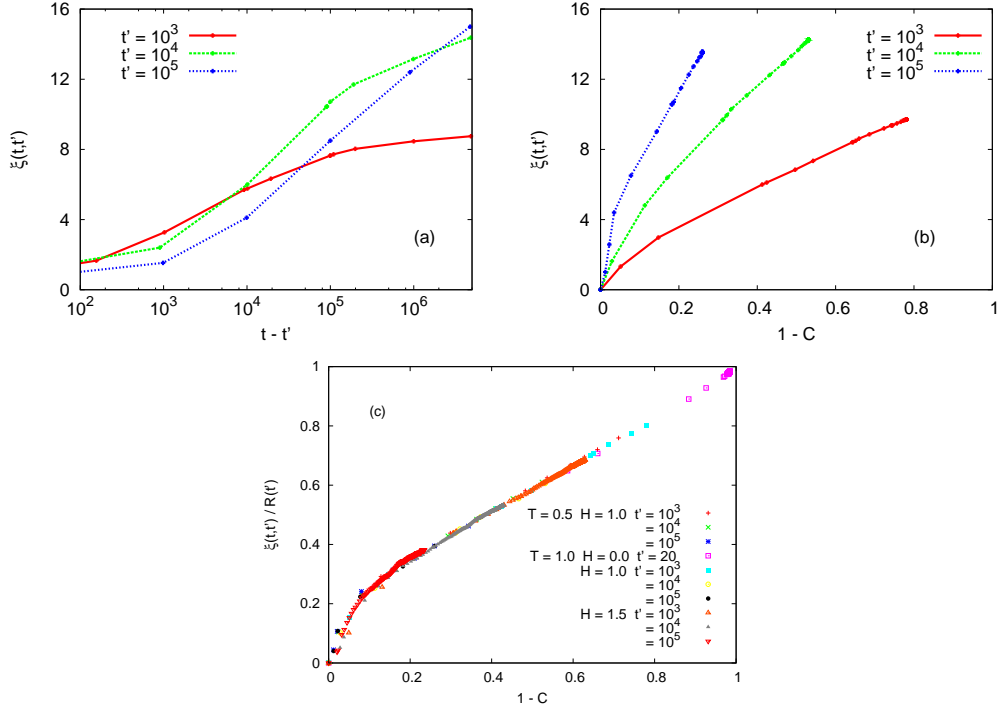


Figure 3.5: The two-time correlation length, ξ , in the RFIM. (a) ξ as a function of time-delay, $t - t'$ for several values of t' given in the key at $T = 1$ and $H = 1$. (b) ξ as a function of the global correlation in a parametric plot at $T = 1$ and $H = 1$. (c) Scaling $\xi(t, t') = R(t') g(C)$ at two temperatures and two values of the random field using three waiting-times t' for each set of parameters. The clean case $H = 0, T = 1$ is also included with a very short t' to avoid equilibration.

comes from the term $C_2(r, t') \propto f_2(r/R(t'))$. Using $\lim_{t \gg t'} \xi(t, t') = R(t')g(0)$ and further assuming that the functional forms of $C_4(x)$ and $f_2(x)$ are, to a first approximation, the same we deduce $g(0) = 1$.

Figure 3.5 (c), where we plot $\xi(t, t')/R(t')$ versus $1 - C(t, t')$ for different t' , illustrates the validity of the scaling hypothesis (3.11). We see that, as expected, $g(C = 1) = 0$ and it seems plausible that $\lim_{C \rightarrow 0} g(C) = 1$. The scaling function g is found to satisfy super-universality, *i.e.* it is independent of H and T .

C_4 and super-universality.

Using the monotonicity properties of C as a function of $t - t'$ and t' , and of ξ as a function of t' and $1 - C$ we can safely exchange the dependence of C_4 on the two times by a dependence on ξ and C . In other words, $C_4(r, \xi, C)$ where, again for simplicity, we did not write explicitly the dependence on T and H . Now, a reasonable scaling assumption is

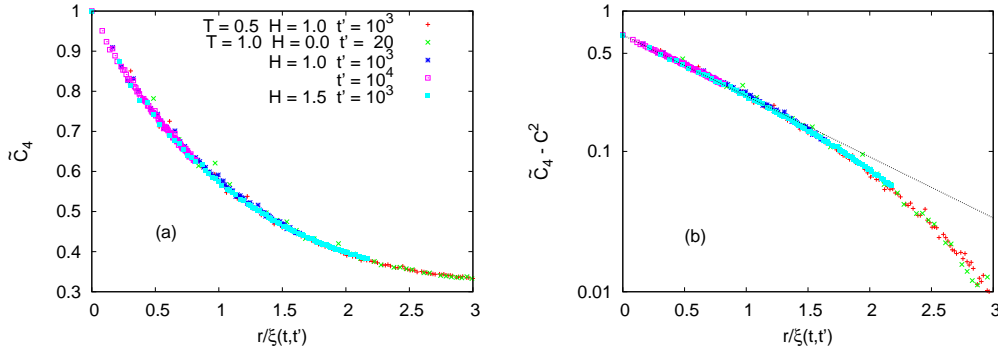


Figure 3.6: (a) Test of scaling, $\tilde{C}_4(r/\xi, C)$, and the super-universality of \tilde{C}_4 for the parameters T and H given in the key. Times t and t' are chosen in such a way that $C(t, t') = 0.57$ in all cases. (b) The same data in linear-log scale showing that $\tilde{C}_4 - C^2$ is very close to an exponential at short r/ξ .

that one can measure r in units of ξ such that

$$C_4(r, t, t') = \tilde{C}_4(r/\xi(t, t'), C(t, t')) . \quad (3.12)$$

In Fig. 3.6 we put this scaling form to the test and we examine the possible super-universality of \tilde{C}_4 . We use different values of the parameters t, t', T, H such that $C = 0.57$ in all cases. Both scaling and super-universality relations are well satisfied. Note that the scaling relation in Eq. (3.12) can also be transformed into

$$C_4(r; t, t') = C_4(r/R(t'), R(t)/R(t')) \quad (3.13)$$

by using Eq. (3.9). This last scaling form was also found for the $O(N)$ ferromagnetic model in the large N limit although the scaling function does not have a simple exponential relaxation [212].

3.2.2 3d EA

A detailed analysis of the relaxation properties of similar correlations in the 3d EA model appeared in [205]. The spatial one-time correlation, $C_2(r, t)$, vanishes identically in this model due to the quenched random interactions. It seems pretty clear from numerical studies CITE that the scenario given in eq. (3.8) for the two-time correlation function in coarsening phenomena is valid for the case of the 3d EA model. In Fig. 3.7 (a) we give the typical behavior of the two-time correlation function $C(t, t')$ at a given temperature, for different waiting-times. Moreover, the aging part is found to scale as $C_{\text{ag}}(t, t') = q_{\text{EA}} f(t/t')$ (so-called *simple aging*) as illustrated in Fig. 3.7 (b) (see also [202]). If there is a dynamical growing length scale in the system, the dynamical scaling hypothesis states that it should therefore grow as $R \sim t^{1/z(T)}$. The question as to whether the scaling function f is super-universal is not well posed since the T -dependent power $1/z(T)$ can be absorbed in f .

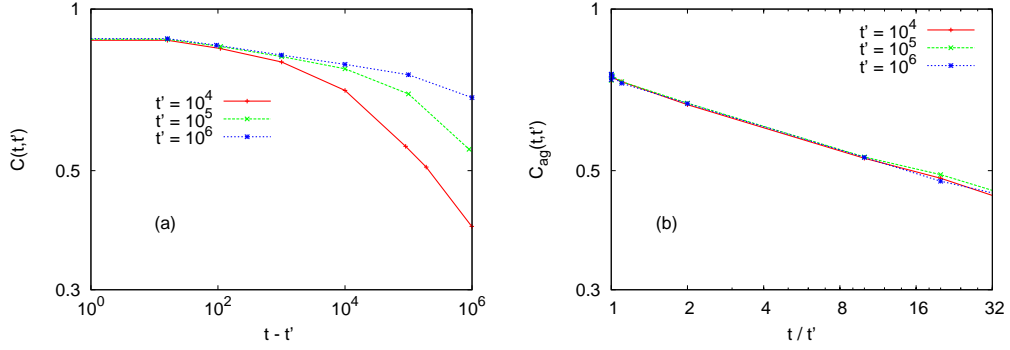


Figure 3.7: (a) 3d EA: the global two-time correlation $C(t, t')$ at $T/T_g = 0.6$ is plotted vs $t - t'$ in logarithmic scale for different t' given in the key. (b) Test of the simple aging scaling, the scaling function $f = C_{ag}/q_{EA}$ is plotted vs t/t' for the same values of t and t' .

The four-point correlation allows for the definition of a two-time growing length scale ξ that behaves qualitatively as in Eq. (3.11). In Fig. 3.8 we present $\xi(t, t')$ for the 3d EA. Its behavior is very similar to the one of the RFIM exposed previously, but we would like to stress the fact that this quantity reaches much lower values in the 3d EA case (around 2a) than in the RFIM (around 15a). Figure 3.8 (c) demonstrates that the super-universality property does not hold in the 3d EA model. We used $R(t) \propto t^{0.03}$ for both temperatures and the resulting $g(C)$ curves are significantly different. It is important to remark that no T -dependent power-law in R would make the two curves collapse. Turning back to the scaling of the two-time correlation and fixing the power law, $C \propto f[(t/t')^{0.03}]$ one finds $f(x) \sim x^{-4.5}$ (at $T/T_g \sim 0.6$) a much faster decaying power than in the RFIM. Note that previous estimates of the dynamic exponent using the one-time replica overlap [203, 204] yield $1/z(T = 0.3T_g) \approx 0.045$ a slightly larger value; the reason for the discrepancy could be traced to the lack of accuracy in the determination of ξ and then R .

3.2.3 Colloidal glasses

The structure factor of colloidal suspensions and Lennard-Jones mixtures are obviously very different from the one of a sample undergoing ferromagnetic ordering. Still, two-time self-correlations satisfy scaling with $R(t) \propto t^{1/z}$ although a clear interpretation of R is not available.

Castillo and Parsaeian studied ξ in a Lennard-Jones mixture of particles undergoing a glassy arrest. One notices that, at short time delays ($t - t' \sim 10$ molecular dynamic units), ξ is monotonic with respect to $t - t'$ and t' in this system, while one needs to reach much longer time delays (and indeed go beyond the simulation window) in the 3d EA and RFIM cases [cfr. Figs. 3.5 (a) and 3.8 (a) to the first panel in Fig. 2 in [209]]. A form such as (3.11) describes ξ in this case too with $R(t) \sim t^{1/z}$ and $1/z \sim 0.1$.

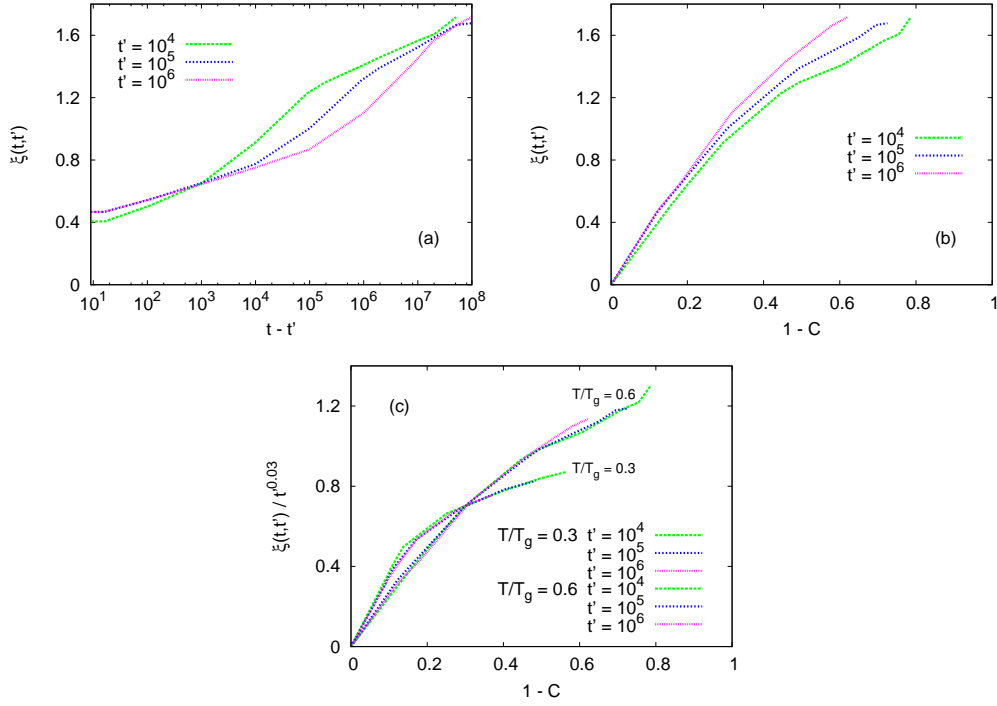


Figure 3.8: Study of the two-time correlation length in the 3d EA model. (a) ξ as a function of time-delay $t - t'$ for several t' 's given in the key at $T/T_g = 0.6$. (b) Evolution of ξ with the global correlation in a parametric plot at $T/T_g = 0.6$. (c) Test of the scaling hypothesis $\xi(t, t') = R(t') g(C)$ with $R(t) \propto t^{0.03}$ at $T/T_g = 0.3$ and $T/T_g = 0.6$.

The two-time correlation length of colloidal suspensions was analyzed in [210] using a mapping to a spin problem. The data for ξ remains, though, quite noisy and although a similar trend in time emerges the precise functional form is hard to extract.

3.2.4 Summary

In short, the macroscopic correlations in all these systems admit the same dynamic scaling analysis although there is no clear interpretation of R as a domain size in the case of the 3d EA and colloidal suspensions.

3.3 Fluctuations

An approach apt to describe problems with and without quenched randomness focuses on thermally induced fluctuations [211]. The local dynamics can then be examined by studying two-time spin-spin functions which, instead of being spatially averaged over the

whole bulk, are only averaged over a coarse-graining cell with volume $V_r = (2l)^3$ centered at some site r [207, 208]:

$$C_r(t, t') \equiv \frac{1}{V_r} \sum_{\vec{r}_i \in V_r} s_i(t) s_i(t') . \quad (3.14)$$

One can then characterize the fluctuations by studying their probability distribution function (pdf) $\rho(C_r; t, t', l, L, T, H)$ with mean value $C(t, t')$.

In general, the variation of $\rho(C_r)$ with the size of the coarse-graining boxes is as follows. For $l < R$ the pdf is peaked around q_{EA} and has a fat tail towards small values of C_r including negative ones. Indeed, well in the coarsening regime, most of the small coarse-grained cells fall inside domains and one then expects to find mostly a thermal equilibrium distribution – apart from the tail. For larger values of l such as $l \simeq R$, a second peak close to C appears and the one at q_{EA} progressively diminishes in height. For still larger values of l , the peak at q_{EA} disappears and a single peak centered at C (the mean value of the distribution) takes all the pdf weight.

At fixed temperature and field, the pdf $\rho(C_r; t, t', l, L)$ in the RFIM depends on four parameters, two times t and t' and two lengths l and L . In the *aging* regime the dependence on t and t' can be replaced by a dependence on $C(t, t')$ and $\xi(t, t')$, the former being the global correlation and the latter the two-time dependent correlation length. Indeed, $C(t, t')$ is a monotonic function on the two times [*cfr.* Fig. 3.3 (a)] and ξ is a growing function of t [*cfr.* Fig. 3.1), thus allowing for the inversion $(t, t') \rightarrow (C, \xi)$. Note that we do not need to enter the aging, coarsening regime to propose this form. One can now make the natural scaling assumption that the pdfs depend on ξ , the coarse-graining length l , and the system linear size L through the ratios l/ξ and l/L . In the end, the pdfs characterizing the heterogeneous aging of the system read

$$\rho(C_r; C(t, t'), l/\xi(t, t'), l/L) . \quad (3.15)$$

We numerically test this proposal by assuming that the thermodynamic limit applies and the last scaling ratio vanishes identically. Figure 3.9 (a) shows the pdfs at two pairs of times t and t' such that the global correlation $C(t, t')$ is the same, and $l = 9$. It is clear that the two distributions are different. In panel (b) we further choose l so that $l/\xi \simeq 0.7$ is also fixed. The two distributions now collapse as expected from the scaling hypothesis Eq. (3.15). Note that another peak at $C = -1$ exists, though with a lower weight. Figure 3.10 (a) and (b) show the scaling for $l/\xi \simeq 1.4$ and $l/\xi \simeq 2.9$, respectively. While the collapse is still good in the case of panel (a), it is not satisfactory in panel (b). Indeed, this plot suffers from the fact that the thermodynamic limit is far from being reached ($l/L \sim 0.15$ is not so small).

In Fig. 3.10 (a) we used several values of T and H and we found that all pdfs collapse on the same master curve. We conclude that as long as coarse-graining lengths are not too

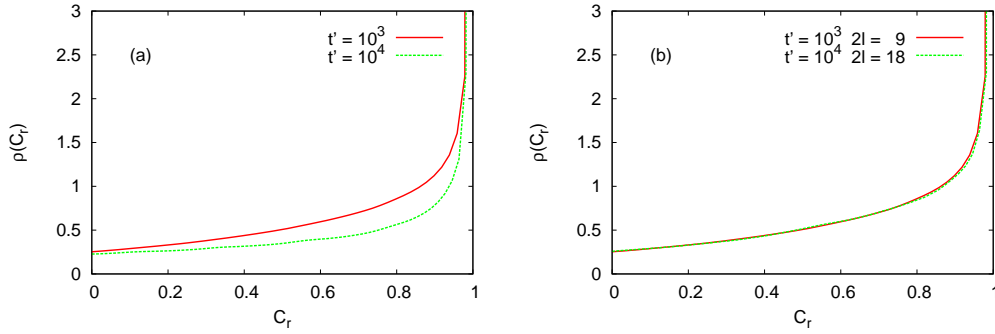


Figure 3.9: Pdf of local two-time functions C_r in the RFIM at $T = 1$ and $H = 1$. The waiting-times t' are given in the key and time t is chosen such that $C(t, t') = 0.6$. (a) C_r is coarse-grained on boxes of linear size $l = 9$. (b) C_r is coarse-grained on boxes with variable length l so as to keep $l/\xi(t, t') \simeq 0.7$ constant. The collapse is much improved with respect to panel (a).

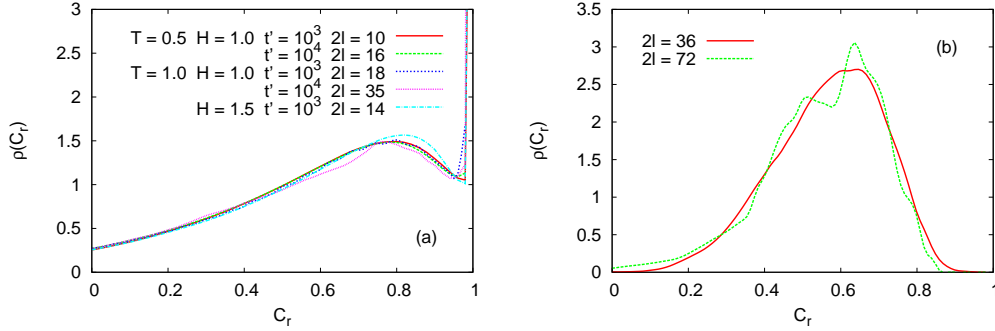


Figure 3.10: Test of the scaling and super-scaling hypothesis. The two pairs of t and t' are the same as in Fig. 3.9 and $C = 0.6$ as well. (a) $l/\xi \simeq 1.4$. (b) $l/\xi \simeq 2.9$.

close to the system size, the pdf of local correlation satisfy the scaling(3.15) with a scaling function that is super-universal.

Let us now compare the forms of the pdfs in the RFIM and $3d$ EA model. In the RFIM the peak at q_{EA} is visible until $l/\xi \simeq 2$. Given that in this model ξ is quickly rather large (ξ reaches $15a$ in the simulation time-window) one has a relatively large interval of l for which the peak at q_{EA} can be easily seen. Instead, in the $3d$ EA the two-time correlation length grows very slowly and reaches only $\xi \sim 2a$ in similar times, meaning that the peak at q_{EA} is hardly visible as soon as one coarse-grains the two-time observables [205].

Figure 3.11 demonstrates that the pdf of local correlations is not super-universal with respect to T in the $3d$ EA model, and compares the functional form at two temperatures, $T/T_g = 0.3$ and $T/T_g = 0.6$, with the one in the RFIM. The global correlation, C , and the ratio of coarse-graining to correlation lengths, l/ξ , are the same in all curves. Although

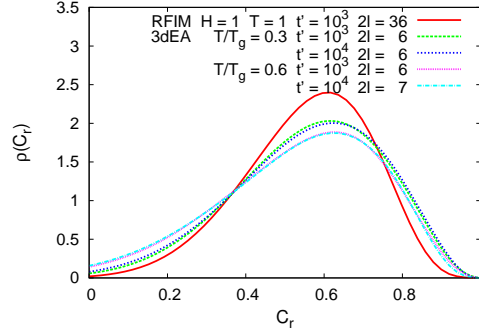


Figure 3.11: Pdf of local correlations in the 3d EA model at $T/T_g = 0.3$ and $T/T_g = 0.6$, for two waiting-times t' such that $C = 0.6$ and $l/\xi = 2.9$. The solid line (red) displays the super-universal pdf in the RFIM.

qualitatively similar, the pdf in the RFIM and 3d EA models are different, with the RFIM one being more centered around the global value.

The study of Lennard-Jones mixtures in [216] used a constant coarse-graining length and the pdfs of local correlations at constant C showed a slow drift that should be cured by taking into account the variation of ξ . In colloidal suspensions the scaling form (3.15) is well satisfied [210]. In the context of coarsening phenomena these pdfs are to be compared to the ones calculated for the $O(n)$ model in its large n limit [212].

3.4 Conclusions

We performed an extensive analysis of the dynamics of the RFIM in its coarsening regime. We showed that the equal-time correlation functions, global two-time correlation functions, and the four point correlation functions obey scaling and super-universality relations in the aging regime. The scaling relations, by means of the typical growing length, $R \propto \ln t/\tau$, reveal a non-trivial time-invariance for these statistical objects. Super-universality encodes the irrelevance of quenched randomness and temperature on the scaling functions and it is demonstrated by the fact that they are the same as for the clean Ising case.

In the 3d EA, similar scaling forms were found for global two-time correlations and four-point correlations [205]. The function $R(t)$ could be associated to a domain radius though a clear-cut confirmation of this is lacking. On the contrary, the results of recent large scale simulations have been interpreted as evidence for an SK-like dynamic scenario [206]. The one-time function playing the role of the domain radius is a very weak power law, $t^{0.03}$ at $T/T_g \sim 0.3 - 0.6$, and, in consequence, the two-time correlation length reaches much shorter values than in the RFIM in equivalent simulation times. Super-universality (with respect to temperature) does not apply in this case.

A similar scenario applies to the Lennard-Jones mixtures [216] and colloidal suspensions [210]. The two-time correlation length remains also very short in accessible numerical and experimental times.

In all these systems the analysis of local fluctuations of two-time functions leads to scaling of their probability distribution functions. In the RFIM these also verify super-scaling with respect to T and H . In the 3d EA they do not. The intriguing possibility of a kind of super-scaling in colloidal suspensions (with respect to concentration) has been signaled in [210] and deserves a more careful study.

We conclude that all these systems, with *a priori* very different microscopic dynamic processes admit a similar dynamic scaling description of their macroscopic and mesoscopic out-of-equilibrium evolution.

DRIVEN QUANTUM COARSENING

Contents

4.1	The model	94
4.1.1	System of disordered quantum rotors	94
4.1.2	Reservoirs of electrons	94
4.1.3	Coupling between the system and the reservoirs	97
4.2	The dynamics	98
4.2.1	Quench setup	98
4.2.2	Schwinger-Keldysh formalism	99
4.2.3	Macroscopic observables	100
4.3	The influence of the fermionic environment	104
4.3.1	Self-energy	104
4.3.2	Some limits	105
4.4	Results	109
4.4.1	Average over disorder	110
4.4.2	Schwinger-Dyson equations	111
4.4.3	Quantum non-equilibrium steady state (QNESS) phase	111
4.4.4	Critical manifold	112
4.4.5	Coarsening phase	118
4.5	The current	128
4.6	Conclusions	131
	Appendices	132
4.A	Conventions	132

4.A.1	Fourier transform	132
4.A.2	Heisenberg representation	132
4.A.3	Time-ordering operator	133
4.A.4	Green's functions	133
4.B	Fermionic reservoir	134
4.B.1	Keldysh rotation	134
4.B.2	Symmetry properties under $t \leftrightarrow t'$	135
4.B.3	Free fermions	135
4.C	Fluctuation-Dissipation Theorem	136
4.D	Computing the self-energy	138
4.D.1	Derivation within the Schwinger-Keldysh formalism	138
4.D.2	FDT check	140
4.E	Dynamics	142
4.E.1	Quadratic effective action	142
4.E.2	Saddle-point evaluation	143
4.E.3	Schwinger-Dyson equations	144

DYNAMIC issues in isolated quantum many body systems are the focus of active research. Some of the problems that are currently being studied theoretically are: the time evolution of the entropy of entanglement in spin systems [237], the nature of non-equilibrium steady states in small quantum systems driven out of equilibrium [238, 239] due to their relevance for nano-devices, quantum annealing techniques [240, 241], and the density of defects left over after a gradual change in a parameter [242]. The influence of an environment on the dynamics of quantum systems was also dealt with in a number of cases such as the spin-boson model [75], disordered spin chains coupled to bosonic baths [243, 244], or an electronic ring coupled to leads and further driven by a time-dependent field [245–247].

Once the interest is set upon macroscopic systems, the question as to whether these undergo phase transitions naturally arises. The theory of equilibrium classical and quantum phase transitions is well developed. *Non-equilibrium* phase transitions in which quantum fluctuations can be neglected are also quite well understood. These are realized when a system is forced in a non-equilibrium steady state (by a shear rate, an external current flowing through it, etc.) [248–251] or when it just fails to relax (*e.g.* after a quench) and displays aging phenomena [252, 52]. In contrast, the effect of a drive on a *macroscopic* system close to a quantum phase transition is a rather unexplored subject. Some works have focused on non-linear transport properties close to an (equilibrium) quantum phase transition [121–123]. Others have studied how the critical properties are affected by non-equilibrium drives [124–126]. However, a global understanding of phase transitions in the control parameter space T, V, Γ , with T the temperature, V the driving strength, and Γ the strength of quantum fluctuations, is still lacking. Furthermore, to the best of our knowledge, the issue

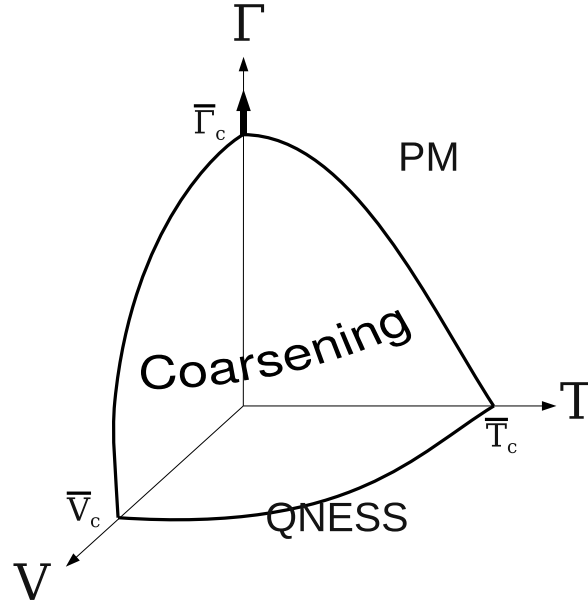


Figure 4.1: Non-equilibrium phase diagram of the fully connected driven quantum rotor model with an infinite number of components.

of the *relaxation* toward the quantum non-equilibrium steady state (QNESS) has not been addressed in the past.

In this chapter we study a class of analytically tractable models, systems of n -component N quantum rotors that encompass an infinite range spin glass and its three dimensional pure counterpart modeling coarsening phenomena. As discussed in [78] models of quantum rotors are non-trivial but still relatively simple and provide coarse-grained descriptions of physical systems such as Bose-Hubbard models and double layer antiferromagnets. The system is coupled to two different external electron reservoirs that lead to a current flowing through it and driving it out of equilibrium. (For a two dimensional model the current flows perpendicular to it, see the sketch in Fig. 1 of [124].) In the simplest setting [124] each rotor is coupled to independent reservoirs; more realistic couplings are discussed in [126]. Using the Schwinger-Keldysh formalism [176, 253, 254] we obtain the complete out of equilibrium dynamics of these models in the large nN limit. We show that at sufficiently low T, V, Γ , see Fig. 1, the system never reaches a QNESS and coarsens with remarkable universal properties. We study the critical properties of the phase transitions, in particular in the vicinity of the (drive-induced) quantum out-of-equilibrium critical point \bar{V}_c at $\Gamma = 0$, $T = 0$ and the “usual” quantum critical point $\bar{\Gamma}_c$ at $V = 0$, $T = 0$. We analyze in detail the relaxation in the coarsening regime and uncover the scaling properties of correlation functions and linear response. We derive a general formula for the current flowing through

the system under such a voltage drop and we analyze its dependence on the dynamics of the system. Some of these results were announced recently in [255].

4.1 The model

4.1.1 System of disordered quantum rotors

The model we focus on is a quantum disordered system made of N n -component rotors interacting via random infinite-range couplings [45, 256].

The quantum rotors should not be confused with true quantum Heisenberg spins present in any isotropic antiferromagnet; the different components of the rotor variables all commute with each other, unlike the quantum spins.

We consider a fully-connected (mean-field) model where there is no underlying geometry: each rotor is equivalently coupled to all the others. The Hamiltonian is given by

$$H = \frac{\Gamma}{2n} \sum_{i=1}^N \mathbf{L}_i^2 - \frac{n}{\sqrt{N}} \sum_{i,j < i} J_{ij} \mathbf{s}_i \cdot \mathbf{s}_j . \quad (4.1)$$

s_i^μ ($\mu = 1 \dots n$) are the n components of the i -th rotor. The coordinates s_i^μ constitute a complete set of commuting observables. The scalar product $\mathbf{s}_i \cdot \mathbf{s}_j$ is given by $\sum_{\mu=1}^n s_i^\mu s_j^\mu$. In order to better apprehend the large n limit, we slightly changed the writing of the Hamiltonian compared to the one given in eq. (1.10) by rescaling $\mathbf{s}_i \mapsto \sqrt{n} \mathbf{s}_i$. The length of rotors is now fixed to unity, $\mathbf{s}_i \cdot \mathbf{s}_i = 1 \forall i = 1 \dots N$, at the price of an extra n factor in front of the potential term. The strengths J_{ij} 's are taken from a Gaussian distribution with zero mean and variance J^2 . J controls the strength of disorder. \mathbf{L}_i is the i -th generalized angular momentum operator which $n(n-1)/2$ components are given by

$$L_i^{\mu\nu} = -i\hbar \left(s_i^\mu \frac{\partial}{\partial s_i^\nu} - s_i^\nu \frac{\partial}{\partial s_i^\mu} \right) \quad \text{for } 1 \leq \mu < \nu \leq n , \quad (4.2)$$

$\mathbf{L}_i^2 = \sum_{\mu < \nu} (L_i^{\mu\nu})^2$ [78, 45, 256]. Γ acts like a moment of inertia and controls the strength of quantum fluctuations; when $\hbar^2 \Gamma / J \rightarrow 0$ the model approaches the classical Heisenberg fully-connected spin glass. In the large n limit it is equivalent to the quantum fully-connected $p = 2$ spin glass [257, 258]. The classical mapping to ferromagnetic coarsening in the $3d$ $O(n)$ model with $n \rightarrow \infty$ [52] holds, as we shall show in Sec. 4.4.5, for the quantum model as well.

4.1.2 Reservoirs of electrons

The system is coupled to two, ‘left’ (L) and ‘right’ (R), reservoirs of electrons. These independent reservoirs are both in equilibrium at inverse temperature β_L and β_R . The situa-

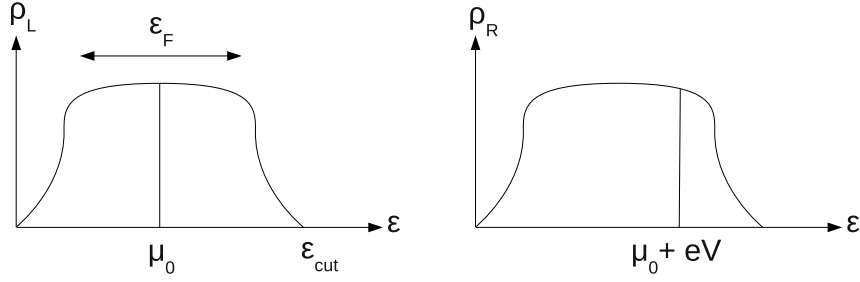


Figure 4.2: Density of states (DOS) of type A reservoirs. μ_0 and $\mu_0 + eV$ are the left and right Fermi levels, respectively. The left reservoir is half-filled.

tion $\beta_L \neq \beta_R$ would create a heat flow from one reservoir to the other. We are interested in the simpler case in which $\beta_L = \beta_R \equiv \beta \equiv T^{-1}$. An electric current is forced by imposing different chemical potentials, $\mu_L = \mu_0$ and $\mu_R = \mu_0 + eV$ (where $-e$ is the electric charge of one electron). eV is the strength of the drive. As $eV/J \rightarrow 0$, the effect of the reservoirs on the system approaches the one of an equilibrium bath at temperature T . The details of the reservoir Hamiltonians H_L and H_R are not important since only the electronic Green's functions matter in the small rotor-environment coupling we concentrate on. We consider the simple case in which left and right fermionic reservoirs have the same density of states (DOS) $\rho_L = \rho_R = \rho$. Moreover, we focus on simple cases in which the shape of the DOS is controlled by only one typical energy scale ϵ_F . In the rest of this chapter, we often consider the limit in which ϵ_F is much larger than all the other energy scales involved. In this limit the results become independent of the detailed functional form of the DOS. We also give some results for finite ϵ_F using the specific DOS that we introduce below.

DOS with a finite bandwidth

We first consider regular DOS which have a finite typical width (finite bandwidth) controlled by ϵ_F and μ_0 is set around the maximum of the distribution. In the limit where ϵ_F is very large, they can be seen as almost flat distributions. We call ϵ_{cut} the finite energy cut-off beyond which the DOS vanishes, $\rho(|\epsilon| > \epsilon_{\text{cut}}) = 0$. Since the DOS we consider have a single energy scale ϵ_F , ϵ_{cut} should scale with ϵ_F . Notice that a finite ϵ_{cut} constrains the voltage not to exceed $eV_{\text{max}} = \epsilon_{\text{cut}} - \mu_0$ since the right reservoir is then completely filled and therefore it cannot accept more fermions.

We call reservoir of type A a half-filled¹ reservoir the DOS of which has a finite bandwidth controlled by ϵ_F and is symmetric and derivable in the vicinity of its maximum (see Fig. 4.2). The simplest example of a type A reservoir is given by the semi-circular DOS

1. Half-filled means that half the total number of available states are occupied: $\int_{-\infty}^{\mu_0} d\epsilon \rho(\epsilon) = \frac{1}{2}$ at $T = 0$.

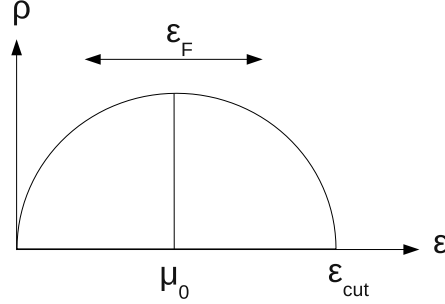


Figure 4.3: An example of type A reservoir: the semi-circle density of states (half-filled).

(see Fig. 4.3),

$$\rho_A(\epsilon) \equiv \frac{2}{\pi \epsilon_F} \sqrt{1 - \left(\frac{\epsilon - \epsilon_F}{\epsilon_F} \right)^2}, \quad (4.3)$$

that is symmetric and centered around ϵ_F . Here $\epsilon_{\text{cut}} = 2\epsilon_F$. We choose $\mu_0 = \epsilon_F$ so that the reservoirs are half-filled at zero drive ($eV = 0$). In this case, at $T = 0$, the voltage applied between both reservoirs cannot exceed $eV_{\text{max}} = \epsilon_{\text{cut}} - \mu_0 = \epsilon_F$.

Type B reservoirs have finite bandwidth but no energy cut-off: $\epsilon_{\text{cut}} = eV_{\text{max}} \rightarrow \infty$. A realization of these reservoirs is given by the following DOS [see Fig. 4.4(a)]

$$\rho_B(\epsilon) \equiv \frac{\alpha}{\epsilon_F} \sqrt{\frac{\epsilon}{\epsilon_F}} e^{-\frac{1}{2} \left(\frac{\epsilon}{\epsilon_F} \right)^2}, \quad (4.4)$$

where $\alpha \approx 0.97$ is a numerical constant fixed by normalization. The maximum of this distribution is located at $\epsilon_F/\sqrt{2}$. This reservoir is half-filled for $\mu_0 \approx 0.95 \epsilon_F$. This distribution resembles the semi-circular one in the sense that they both start with a square root behavior, have a maximum, and a bandwidth of order ϵ_F . In contrast, the DOS in eq. (4.4) is different from zero at all finite ϵ and one can exploit this feature to apply strong voltages.

DOS at low energy

In the previous examples (ρ_A and ρ_B), we focused on values of μ_0 corresponding to high energy states where the DOS is regular. We are also interested in studying cases where μ_0 is centered around low energy states. To analyze these cases, we focus on a DOS which reads [see Fig. 4.4(b)]:

$$\rho_{C3d}(\epsilon) \equiv \frac{3}{4\sqrt{2}\epsilon_F} \sqrt{\frac{\epsilon}{\epsilon_F}}. \quad (4.5)$$

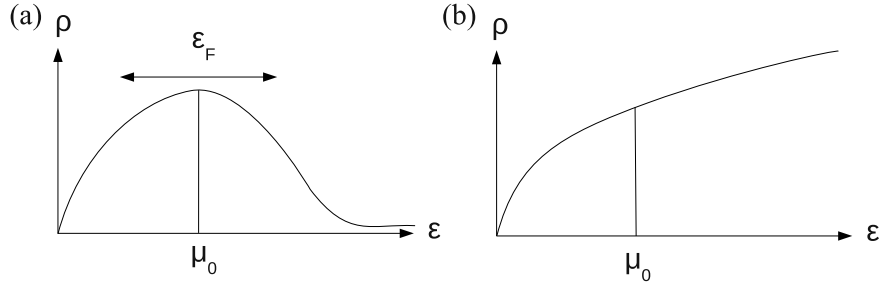


Figure 4.4: Two examples of type B reservoirs. (a) The distribution ρ_B vanishes asymptotically. (b) The square root distribution diverges asymptotically.

This square root behavior is actually the one of the $3d$ free fermions reservoir. In this case ϵ_F is of the order of the hopping term for the free fermions. Since we shall only focus on the low energy states of the reservoir, we can neglect the non trivial high energy structure of the reservoir and take the DOS equal to zero for $\epsilon > 2\epsilon_F$.

For the $2d$ free fermions, the density of states is given by

$$\rho_{C2d}(\epsilon) \equiv \frac{1}{2\epsilon_F}, \quad (4.6)$$

whereas for the $1d$ free fermions, the density of states is given by

$$\rho_{C1d}(\epsilon) \equiv \frac{1}{2\sqrt{2}\epsilon_F} \sqrt{\frac{\epsilon_F}{\epsilon}} \quad (4.7)$$

and, as for ρ_{C3d} , we take these two densities of states to be equal to zero for $\epsilon > 2\epsilon_F$.

4.1.3 Coupling between the system and the reservoirs

An electron hop from the $L(R)$ reservoir to the $R(L)$ reservoir is linearly coupled to each rotor component:

$$H_{\text{int}} = -\frac{\sqrt{n}}{N_s} \sum_{i=1}^N \sum_{\mu=1}^n \sum_{k,k'=1}^{N_s} \sum_{l,l'=1}^M V_{kk'} s_i^\mu [\psi_{Likl}^\dagger \sigma_{ll'}^\mu \psi_{Rik'l'} + L \leftrightarrow R], \quad (4.8)$$

where ψ_{Likl}^\dagger is the l -th component of an M -component spinor operator that creates an additional fermion with energy $\hbar\omega_k$ in the L reservoir associated to the i -th rotor. k labels the electron energy inside the reservoirs, N_s is the total number of states in each reservoir. σ^μ are the generalized Pauli matrices for $SU(M)$ of dimension $M \times M$ with $M^2 - 1 = n$. They are chosen to be normalized such that $\text{Tr} \sigma^\mu \sigma^\nu = \delta_{\mu\nu}$. $V_{kk'}$ are the rotor-environment coupling parameters chosen to be constant: $V_{kk'} = \hbar\omega_c$. H_{int} is $O(n)$ and $O(N)$ invariant.

4.2 The dynamics

4.2.1 Quench setup

The system is initially prepared (at times $t < 0$) in such a way that its initial configuration (at time $t = 0$) is neither correlated with disorder (J_{ij} 's) nor with the reservoirs. This can be realized, for instance, by coupling the system to an equilibrium bath at temperature $T_0 \gg J, \Gamma$ so that any correlation in the system is suppressed. At time $t = 0$ the quench is performed by suddenly coupling the system to the L and R reservoirs. These are supposed to be “good reservoirs” in the sense that their properties are not affected by the state of the system.

This setup generates non-equilibrium dynamics at times $t > 0$ for multiple reasons. First of all, the rapid quenching procedure puts the system in a non-equilibrium initial condition with respect to its new environment. Moreover, the latter is not an equilibrium bath but a bias drive the role of which is to constantly destabilize the system. Finally, as a consequence of its disordered interactions, the system of rotors experiences intrinsic difficulties to reach equilibrium. Indeed, even if it were embedded within an equilibrium environment it would show a glassy phase [258–260] in some parts of the phase diagram.

Since system and reservoirs are decoupled at times $t < 0$, the initial density matrix of the whole system is given by

$$\varrho(t=0)_{\text{tot}} = \varrho(t=0) \bigotimes_{i=1}^N \varrho_{Li} \bigotimes_{i=1}^N \varrho_{Ri} . \quad (4.9)$$

$\varrho_{Li/Ri}$ corresponds to the equilibrium density matrix of the L/R reservoir associated with the i -th rotor. The system of rotors being prepared at very high temperature, its initial density matrix is the identity in the rotors space:

$$\varrho(t=0) \propto I . \quad (4.10)$$

All these density matrices are normalized to be of unit trace. The $t > 0$ evolution of the whole system plus environment is encoded in

$$\varrho_{\text{tot}}(t) = U(t, 0) \varrho_{\text{tot}}(0) [U(t, 0)]^\dagger , \quad (4.11)$$

where the unitary evolution operator is given by $U(t, 0) \equiv \mathcal{T} e^{-\frac{i}{\hbar} \int_0^t dt' H_{\text{tot}}(t')}$ with $H_{\text{tot}} = H + H_L + H_R + H_{\text{int}}$ and \mathcal{T} the time-ordering operator (see App. 4.A). We analyze the non-equilibrium dynamics using the Schwinger-Keldysh formalism (see [253, 254] for a modern review) that we briefly introduce in the following lines.

4.2.2 Schwinger-Keldysh formalism

The Suzuki-Trotter decomposition of the two unitary evolution operators that appear in

$$\mathcal{Z} \equiv \lim_{\tau \rightarrow \infty} \text{Tr} U(\tau, 0) \varrho_{\text{tot}}(0) [U(\tau, 0)]^\dagger = 1, \quad (4.12)$$

yields a path-integral involving two sets of fields with support on two different branches. The first ones are time-integrated on a forward branch from $t = 0$ to $+\infty$. In the following, these fields carry a $+$ superscript. The other ones are time-integrated on a backward branch from $+\infty$ to 0 and carry a $-$ superscript. These two branches constitute the Keldysh contour \mathcal{C} , see Fig. 4.5. The identity (4.12) can now be expressed as a path integral,

$$\mathcal{Z} = \int_{\mathcal{C}} \mathcal{D}[s^\pm, \psi^\pm, \bar{\psi}^\pm] e^{\frac{i}{\hbar} S_{\text{tot}}} \langle s^+(0), \bar{\psi}^+(0) | \varrho_{\text{tot}}(0) | s^-(0), \psi^-(0) \rangle, \quad (4.13)$$

where we collected all the $s_i^{\mu a}$ fields into the notation s^a , and all the fermionic fields $\psi_{\alpha i}^a$ and their Grassmannian conjugates into ψ^a and $\bar{\psi}^a$ (with $a = \pm$).

$\langle s^+(0), \bar{\psi}^+(0) | \varrho_{\text{tot}}(0) | s^-(0), \psi^-(0) \rangle$ is the matrix element of the density matrix which has support at time $t = 0$ only. The action S_{tot} is a functional of all these fields:

$$S_{\text{tot}} = \sum_{a=\pm} a \int_0^\infty dt \mathcal{L}([s^a, \psi^a, \bar{\psi}^a]; t). \quad (4.14)$$

The Lagrangian is given by $\mathcal{L}_{\text{tot}} = \mathcal{L} + \mathcal{L}_{\text{int}} + \mathcal{L}_L + \mathcal{L}_R$ with

$$\mathcal{L}([s^a]; t) = \frac{n}{2\Gamma} \sum_i \dot{s}_i^a(t)^2 + \frac{n}{\sqrt{N}} \sum_{i,j < i} J_{ij} \mathbf{n}_i^a(t) \cdot \mathbf{n}_j^a(t), \quad (4.15)$$

$$\mathcal{L}_{\text{int}}([s^a, \psi^a, \bar{\psi}^a]; t) = \sqrt{n} \frac{\hbar \omega_c}{N_s} \sum_{i\mu k k' l l'} s_i^{\mu a}(t) [\bar{\psi}_{L i k l}^a(t) \sigma_{ll'}^\mu \psi_{R i k' l'}^a(t) + L \leftrightarrow R]. \quad (4.16)$$

\mathcal{L}_L and \mathcal{L}_R are the Lagrangians of the free fermions in the L and R reservoirs. The index ‘c’ at the bottom of the integral sign in eq. (4.13) is here to remind us that the integration is performed over fields satisfying the constraint that each rotor has a fixed unit length: $\mathbf{s}_i^a(t)^2 = 1 \ \forall \ a, i, t$. The path-integral formalism gives a nice way to restore an unconstrained integration over all fields \mathbf{s}_i^a by the introduction of Lagrange multipliers z_i^a :

$$\int_{\mathcal{C}} \mathcal{D}[s^a] = \int \mathcal{D}[s^a] \prod_{i,t} \delta(1 - \mathbf{s}_i^a(t)^2) \quad (4.17)$$

$$= \int \mathcal{D}[s^a, z^a] \exp \left(\frac{i}{\hbar} \int_0^\infty dt a \frac{n}{2} \sum_i z_i^a(t) (1 - \mathbf{s}_i^a(t)^2) \right). \quad (4.18)$$

where we used the integral representation of the delta function (see App. 4.A) and collected the new auxiliary real fields z_i^a into the notation z^a . In terms of a Lagrangian, this gives rise to the new term

$$\mathcal{L}_{\text{LM}}([s^a, z^a]; t) = \frac{n}{2} \sum_i z_i^a(t) [1 - \mathbf{s}_i^a(t)^2]. \quad (4.19)$$

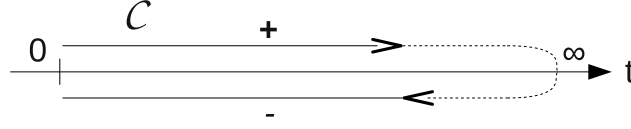


Figure 4.5: The Keldysh contour \mathcal{C} goes from 0 to $+\infty$ and then back to 0. The Keldysh action involves forward fields (that live on the $+$ -branch of \mathcal{C}) that are time-integrated from 0 to $+\infty$ and backward fields (that live on the $-$ -branch of \mathcal{C}) and are time-integrated from $+\infty$ to 0.

4.2.3 Macroscopic observables

We are interested in the macroscopic dynamics of the rotors after an infinitely rapid quench and we wish to give an answer to the following questions (among others). Does the system reach a steady state? Does a steady state current establish? What are the long-time dynamics? We first obtain an effective generating functional for the rotors by expanding the system-drive interaction up to second order in the coupling, integrating away the fermionic degrees of freedom, and averaging over the disorder distribution.

Introducing the external real fields $h_{i\mu}^a(t)$ that we collect in the notation $\mathbf{h}^a(t)$ ($a = \pm$), the generating functional $\mathcal{Z}[\mathbf{h}^\pm]$ reads

$$\mathcal{Z}[\mathbf{h}^\pm] \equiv \int \mathcal{D}[\mathbf{s}^\pm, z^\pm, \boldsymbol{\psi}^\pm, \bar{\boldsymbol{\psi}}^\pm] e^{\frac{i}{\hbar} S_{\text{tot}}[\mathbf{s}^\pm, z^\pm, \boldsymbol{\psi}^\pm, \bar{\boldsymbol{\psi}}^\pm, \mathbf{h}^\pm]} \times \langle \mathbf{s}^+(0), \bar{\boldsymbol{\psi}}^+(0) | \varrho_{\text{tot}}(0) | \mathbf{s}^-(0), \boldsymbol{\psi}^-(0) \rangle, \quad (4.20)$$

where we introduced the source term

$$S_{\text{tot}} \mapsto S_{\text{tot}} + \frac{\hbar}{i} \sum_{a=\pm} \int dt \sum_i \sum_\mu s_i^{\mu a}(t) h_i^{\mu a}(t). \quad (4.21)$$

The generating functional obeys the normalization property $\mathcal{Z}[\mathbf{h}^\pm = \mathbf{0}] = \mathcal{Z} = 1$ which is a fundamental feature of the Keldysh formalism in this setup (see eq. (4.12) and Sec. 4.4.1). One has

$$\langle s_i^{\mu a}(t) \rangle = \frac{1}{\mathcal{Z}} \left. \frac{\delta \mathcal{Z}[\mathbf{h}^\pm]}{\delta h_i^{\mu a}(t)} \right|_{\mathbf{h}^\pm = \mathbf{0}}, \quad (4.22)$$

where we introduced the notation

$$\langle \dots \rangle \equiv \int \mathcal{D}[\mathbf{s}^\pm, z^\pm, \boldsymbol{\psi}^\pm, \bar{\boldsymbol{\psi}}^\pm] \dots e^{\frac{i}{\hbar} S_{\text{tot}}} \langle \mathbf{s}^+(0), \bar{\boldsymbol{\psi}}^+(0) | \varrho_{\text{tot}}(0) | \mathbf{s}^-(0), \boldsymbol{\psi}^-(0) \rangle. \quad (4.23)$$

Notice that one can distinguish this bracket notation from the quantum statistical average that we denote similarly by the occurrence of Keldysh indices inside the brackets. However, they coincide in the case of one time observables, *e.g.*

$$\langle s_i^\mu(t) \rangle = \langle s_i^{\mu a}(t) \rangle, \quad (4.24)$$

with $a = +$ or $-$ equivalently if the observable is time-reversal invariant.

Keldysh Green's functions

We introduce the two-time Green's functions $G_{ij\mu\nu}^{ab}(t, t')$, defined on the Keldysh contour ($a, b = \pm$), as

$$\langle s_i^{\mu a}(t) s_j^{\nu b}(t') \rangle = \frac{1}{\mathcal{Z}} \frac{\delta^2 \mathcal{Z}[\mathbf{h}^\pm]}{\delta h_i^{\mu a}(t) \delta h_j^{\nu b}(t')} \Big|_{\mathbf{h}^\pm = \mathbf{0}} \equiv i\hbar G_{ij\mu\nu}^{ab}(t, t') . \quad (4.25)$$

$s_i^{\mu a}$ being real fields, one has the following time-reversal property

$$G_{ij\mu\nu}^{ab}(t, t') = G_{ji\nu\mu}^{ba}(t', t) . \quad (4.26)$$

In the operator formalism, the Keldysh Green's functions read

$$i\hbar G_{ij\mu\nu}^{ab}(t, t') = \text{Tr} \left[\mathbb{T}_{\mathcal{C}} s_{iH}^\mu(t, a) s_{jH}^\nu(t', b) \varrho_{\text{tot}}(0) \right] , \quad (4.27)$$

where $s_{iH}^\mu(t, a)$ denotes the Heisenberg representation of the operator s_i^μ at time t and on the a -branch of the Keldysh contour. $\mathbb{T}_{\mathcal{C}}$ is the time-ordering operator acting with respect to the relative position of (t, a) and (t', b) on the Keldysh contour \mathcal{C} (see App. 4.A).

We define the macroscopic Keldysh Green's functions by summing over the N rotors and each of their n components

$$G^{ab}(t, t') \equiv \frac{1}{N} \sum_{i=1}^N \sum_{\mu=1}^n G_{ii\mu\mu}^{ab}(t, t') . \quad (4.28)$$

From the identity (4.27), one establishes two relations between the four Green's functions

$$\begin{aligned} G^{++}(t, t') &= G^{-+}(t, t') \Theta(t - t') + G^{+-}(t, t') \Theta(t' - t) , \\ G^{--}(t, t') &= G^{+-}(t, t') \Theta(t - t') + G^{-+}(t, t') \Theta(t' - t) , \end{aligned} \quad (4.29)$$

leading to

$$\begin{aligned} G^{++} + G^{--} &= G^{+-} + G^{-+} , \\ G^{++}(t, t') - G^{--}(t, t') &= \text{sign}(t - t') [G^{-+}(t, t') - G^{+-}(t, t')] . \end{aligned} \quad (4.30)$$

Self correlation

We define the macroscopic two-time correlation as

$$C(t, t') \equiv \frac{1}{N} \sum_{i=1}^N \frac{1}{2} \langle \mathbf{s}_i^+(t) \cdot \mathbf{s}_i^-(t') + \mathbf{s}_i^-(t) \cdot \mathbf{s}_i^+(t') \rangle \quad (4.31)$$

$$= \frac{i\hbar}{2} [G^{+-}(t, t') + G^{-+}(t, t')] = \frac{i\hbar}{2} [G^{--}(t, t') + G^{++}(t, t')] . \quad (4.32)$$

It is symmetric in its time arguments $C(t, t') = C(t', t)$. Given the constraint $\mathbf{s}(t) \cdot \mathbf{s}(t) = 1$, it is one at equal times: $C(t, t) = 1$. The two-time correlation function is the simplest non-trivial quantity giving information on the dynamics of a system. In particular, a loss of its time translational invariance is a signature of aging.

Self linear response

The response at time t of the observable s_i^μ to an infinitesimal perturbation performed at a previous time t' on an observable f_i^μ linearly coupled to s_i^μ is defined as

$$R_i^\mu(t, t') \equiv \left. \frac{\delta \langle s_i^\mu(t) \rangle}{\delta f_i^\mu(t')} \right|_{f_i^\mu=0}, \quad (4.33)$$

with the modified Hamiltonian

$$H \mapsto H - f_i^\mu s_i^\mu. \quad (4.34)$$

Causality ensures that the response vanishes if $t < t'$. We define the macroscopic linear response as

$$R(t, t') = \frac{1}{N} \sum_{i=1}^N \sum_{\mu=1}^n R_i^\mu(t, t'). \quad (4.35)$$

The functional derivative with respect to $f_i^\mu(t')$ in eq. (4.33) can be written in terms of the source fields $h_i^{\mu\pm}(t')$ since f_i^μ appears to play a similar role in the action functional:

$$\frac{\delta}{\delta f_i^\mu(t')} \longleftrightarrow \frac{i}{\hbar} \left(\frac{\delta}{\delta h_i^{\mu+}(t')} - \frac{\delta}{\delta h_i^{\mu-}(t')} \right). \quad (4.36)$$

Therefore we obtain a Kubo relation, stating that the response can be expressed in terms of two-time Green's functions:

$$\begin{aligned} R(t, t') &= \frac{1}{N} \sum_{i=1}^N \sum_{\mu=1}^n \frac{i}{\hbar} \frac{1}{\mathcal{Z}} \left(\left. \frac{\delta^2 \mathcal{Z}[\mathbf{h}^\pm]}{\delta h_i^{\mu a}(t) \delta h_i^{\mu+}(t')} \right|_{\mathbf{h}^\pm=0} - \left. \frac{\delta^2 \mathcal{Z}[\mathbf{h}^\pm]}{\delta h_i^{\mu a}(t) \delta h_i^{\mu-}(t')} \right|_{\mathbf{h}^\pm=0} \right) \\ &= G^{a-}(t, t') - G^{a+}(t, t') \text{ with } a = + \text{ or } - \text{ equivalently} \\ &= \frac{1}{2} [G^{--}(t, t') + G^{+-}(t, t') - G^{++}(t, t') - G^{-+}(t, t')] \\ &= [G^{+-}(t, t') - G^{-+}(t, t')] \Theta(t - t'), \end{aligned} \quad (4.37)$$

where we made use of the relations (4.29).

Finally the four Keldysh Green's functions $G^{ab}(t, t')$ can be re-expressed in terms of a couple of physical observables (namely correlation and response):

$$i\hbar G^{ab}(t, t') = C(t, t') - \frac{i\hbar}{2} [aR(t', t) + bR(t, t')]. \quad (4.38)$$

Keldysh rotation

The Keldysh rotation of the fields is a change of basis that simplifies the expressions of the physical observables such as the correlation C and the response R in terms of Green's functions. One introduces new fields as

$$\begin{cases} 2 \mathbf{s}_i^{(1)} & \equiv \mathbf{s}_i^+ + \mathbf{s}_i^- , \\ \hbar \mathbf{s}_i^{(2)} & \equiv \mathbf{s}_i^+ - \mathbf{s}_i^- , \end{cases} \quad (4.39)$$

and the inversion relation

$$\mathbf{s}_i^a = \mathbf{s}_i^{(1)} + a \frac{\hbar}{2} \mathbf{s}_i^{(2)} . \quad (4.40)$$

We define the Green's functions of these new fields as $i\hbar G^{rs}(t, t') \equiv 1/N \sum_{i=1}^N \langle \mathbf{s}_i^r(t) \cdot \mathbf{s}_i^s(t') \rangle$ with $r, s = (1), (2)$. We have

$$\begin{aligned} i\hbar G^{(11)}(t, t') &= C(t, t') , & i\hbar G^{(12)}(t, t') &= -iR(t, t') , \\ i\hbar G^{(21)}(t, t') &= -iR(t', t) , & i\hbar G^{(22)}(t, t') &= 0 . \end{aligned} \quad (4.41)$$

The fact that $G^{(22)}$ vanishes identically is very general and can be tracked back to be a consequence of causality. The unit length constraint imposed on the rotor coordinates, $\mathbf{s}_i^a(t) \cdot \mathbf{s}_i^a(t) = 1$, becomes an orthogonality constraint between the fields in the new basis, $\mathbf{s}_i^{(1)}(t) \cdot \mathbf{s}_i^{(2)}(t) = 0$, and a relation between their norms: $\mathbf{s}_i^{(1)}(t)^2 + \frac{\hbar^2}{4} \mathbf{s}_i^{(2)}(t)^2 = 1$.

After the Keldysh rotation, the connection with the classical MSRJD generating functional presented in Chapter 2 is straightforward [253, 254, 259, 260]. Indeed, comparing the relations (4.41) with eqs. (2.27) and (2.34) reveals a very strong resemblance between the fields $\mathbf{s}_i^{(1)}$ and ψ on the one hand, and between $i\mathbf{s}_i^{(2)}$ and $\hat{\psi}$ on the other hand. We shall come back to this connection in Sec. 4.4.5.

Bosonic FDT

When the system of rotors is in equilibrium at a given temperature β^{-1} , the fluctuation-dissipation theorem holds (in its bosonic version) giving an extra relation between the Green's functions. In Fourier space (see App. 4.A for our Fourier conventions) it reads

$$C(\omega) = \hbar \coth(\beta\hbar\omega/2) \operatorname{Im} R(\omega) . \quad (4.42)$$

For completeness, we derive this theorem in App. 4.D.2.

4.3 The influence of the fermionic environment

4.3.1 Self-energy

We treat the interactions with the environment in perturbation theory up to second order in the coupling. After the fermionic degrees of freedom are integrated out, the resulting effective action for the rotors acquires an extra term encoding the effects of the reservoirs. The detailed computation, given in App. 4.D.1, yields

$$S_{\text{eff}} = S + S_{\text{LM}} + S_{\text{int}}^{(2)}, \quad (4.43)$$

with

$$\frac{i}{\hbar} S_{\text{int}}^{(2)}[\mathbf{s}^{(1)}, \mathbf{s}^{(2)}] = \frac{1}{2} n \sum_{rs=(1),(2)} \iint_0^\infty dt dt' \Sigma_{\text{env}}^{rs}(t, t') \sum_{i=1}^N \mathbf{s}_i^r(t) \cdot \mathbf{s}_i^s(t'), \quad (4.44)$$

and the four self-energy components

$$\Sigma_{\text{env}}^{(22)} = 2(\hbar\omega_c)^2 \text{Re} \left[G_L^K G_R^{K*} - \hbar^2/4 \left(G_L^A G_R^{A*} + G_L^R G_R^{R*} \right) \right] \equiv -\Sigma_{\text{env}}^K, \quad (4.45)$$

$$\Sigma_{\text{env}}^{(21)} = -2i(\hbar\omega_c)^2 \text{Re} \left[G_L^R G_R^{K*} + G_L^K G_R^{R*} \right] \equiv i\Sigma_{\text{env}}^R, \quad (4.46)$$

$$\Sigma_{\text{env}}^{(12)} = 2i(\hbar\omega_c)^2 \text{Re} \left[G_L^A G_R^{K*} + G_L^K G_R^{A*} \right] \equiv -i\Sigma_{\text{env}}^A, \quad (4.47)$$

$$\Sigma_{\text{env}}^{(11)} = 0. \quad (4.48)$$

The fact that $\Sigma_{\text{env}}^{(11)}$ vanishes identically is a consequence of causality. Similarly to what we have done in Sec. 4.2.3 we renamed $\Sigma_{\text{env}}^{(22)}$, $\Sigma_{\text{env}}^{(21)}$ and $\Sigma_{\text{env}}^{(12)}$ into Σ_{env}^K , Σ_{env}^R and Σ_{env}^A . These real functions are usually referred to as the Keldysh, retarded and advanced components of the self-energy. G_α^K , G_α^R and G_α^A are the Keldysh, retarded and advanced Green's functions of the free electrons in the α -reservoir respectively (see App. 4.B.1). Using their properties under time reversal (see App. 4.B.2), we establish

$$\Sigma_{\text{env}}^K(\tau) = \Sigma_{\text{env}}^K(-\tau), \quad \Sigma_{\text{env}}^R(\tau) = -\Sigma_{\text{env}}^A(-\tau). \quad (4.49)$$

These relations reduce the number of independent self-energy components to two (namely Σ_{env}^K and Σ_{env}^R). By plugging the expressions of the fermionic Green's functions given in App. 4.B.1, we obtain

$$\begin{aligned} \Sigma_{\text{env}}^K(\tau) &= -\frac{1}{2}(\hbar\omega_c)^2 \langle \left[\tanh\left(\beta \frac{\epsilon_L - \mu_L}{2}\right) \tanh\left(\beta \frac{\epsilon_R - \mu_R}{2}\right) - 1 \right] \cos\left(\frac{\epsilon_L - \epsilon_R}{\hbar} \tau\right) \rangle_L \rangle_R, \\ \Sigma_{\text{env}}^R(\tau) &= \frac{1}{\hbar}(\hbar\omega_c)^2 \langle \left[\tanh\left(\beta \frac{\epsilon_L - \mu_L}{2}\right) - \tanh\left(\beta \frac{\epsilon_R - \mu_R}{2}\right) \right] \sin\left(\frac{\epsilon_L - \epsilon_R}{\hbar} \tau\right) \rangle_L \rangle_R \Theta(\tau). \end{aligned}$$

The notation $\langle \langle \dots \rangle_L \rangle_R$ stands for $\int d\epsilon_L d\epsilon_R \rho_L(\epsilon_L) \rho_R(\epsilon_R) \dots$. The Fourier transforms read

$$\Sigma_{\text{env}}^K(\omega) = -\frac{1}{2}\pi\hbar(\hbar\omega_c)^2 \langle \langle \left[\tanh\left(\beta\frac{\epsilon_L - \mu_L}{2}\right) \tanh\left(\beta\frac{\epsilon_R - \mu_R}{2}\right) - 1 \right] \times [\delta(\hbar\omega - \epsilon_{LR}) + \delta(\hbar\omega + \epsilon_{LR})] \rangle_L \rangle_R, \quad (4.50)$$

$$\begin{aligned} \text{Re } \Sigma_{\text{env}}^R(\omega) &= -(\hbar\omega_c)^2 \langle \langle \left[\tanh\left(\beta\frac{\epsilon_L - \mu_L}{2}\right) - \tanh\left(\beta\frac{\epsilon_R - \mu_R}{2}\right) \right] \text{pv} \frac{\epsilon_{LR}}{(\hbar\omega)^2 - \epsilon_{LR}^2} \rangle_L \rangle_R, \\ \text{Im } \Sigma_{\text{env}}^R(\omega) &= \frac{1}{2}\pi\hbar(\hbar\omega_c)^2 \langle \langle \left[\tanh\left(\beta\frac{\epsilon_L - \mu_L}{2}\right) - \tanh\left(\beta\frac{\epsilon_R - \mu_R}{2}\right) \right] \times [\delta(\hbar\omega - \epsilon_{LR}) - \delta(\hbar\omega + \epsilon_{LR})] \rangle_L \rangle_R, \end{aligned} \quad (4.51)$$

where $\epsilon_{LR} \equiv \epsilon_L - \epsilon_R$. Since $\Sigma_{\text{env}}^K(\tau)$ is a real and even function of τ , $\Sigma_{\text{env}}^K(\omega)$ is also a real and even function of ω . $\Sigma_{\text{env}}^R(\tau)$ being real, $\Sigma_{\text{env}}^R(\omega)$ is Hermitian: $\Sigma_{\text{env}}^R(\omega) = \Sigma_{\text{env}}^R(-\omega)^*$.

4.3.2 Some limits

Expressions (4.50) and (4.51) of the Keldysh and retarded self-energies are somehow cumbersome. We simplify them here in some physical limits. These expressions are heavily used in the rest of this work.

Zero drive

The L and R reservoirs constitute an equilibrium bath for the rotors as soon as they share the same temperature and the strength of the drive is set to zero ($\mu_L = \mu_R$, $eV = 0$). In this case, the fluctuation-dissipation theorem applies to the environment variables, and gives an extra relation between the environment self-energy components. It reads

$$\Sigma_{\text{env}}^K(\omega) = \hbar \coth\left(\beta\frac{\hbar\omega}{2}\right) \text{Im } \Sigma_{\text{env}}^R(\omega). \quad (4.52)$$

Ultimately the number of independent self-energy components reduces to one. We checked in App. 4.D.2 that the expressions (4.50) and (4.51) comply with the FDT in the equilibrium case.

Low frequency

Let us consider the low frequency limit ($\omega \rightarrow 0$), or long time-difference in real time, of the self-energy components of a generic non-equilibrium environment ($eV \neq 0$ *a priori*). Parity considerations on Σ_{env}^K and Σ_{env}^R show that $\Sigma_{\text{env}}^K(\omega)$ approaches $\Sigma_{\text{env}}^K(\omega = 0)$ which depends on T , eV and ϵ_F whereas $\text{Im } \Sigma_{\text{env}}^R(\omega) \propto \omega$. The low frequency limit, which can

also be seen as the classical limit ($\hbar\omega \ll T$) of the quantum fluctuation-dissipation theorem in eq. (4.52) gives a way to express the temperature of an equilibrium bath as

$$T = \lim_{\omega \rightarrow 0} \frac{1}{2} \frac{\Sigma_{\text{env}}^K(\omega)}{\partial_{\omega} \text{Im} \Sigma_{\text{env}}^R(\omega)} . \quad (4.53)$$

By analogy with the equilibrium case, we introduce for non-equilibrium situations

$$T^* \equiv \lim_{\omega \rightarrow 0} \frac{1}{2} \frac{\Sigma_{\text{env}}^K(\omega)}{\partial_{\omega} \text{Im} \Sigma_{\text{env}}^R(\omega)} . \quad (4.54)$$

We expect that the effect of the reservoirs on the long time-difference dynamics of the rotors is the one of an equilibrium bath at temperature T^* .

ϵ_F much larger than all other energy scales

The reservoirs act as an *Ohmic* bath in the limit in which ϵ_F is much larger than the temperature, the drive and $\hbar\omega$ ($eV, T, \hbar\omega \ll \epsilon_F$). Equation (4.51) with $\Delta\epsilon \equiv \epsilon_L - \epsilon_R$ reads

$$\begin{aligned} \text{Im} \Sigma_{\text{env}}^R(\omega) &= \frac{1}{2} \pi (\hbar\omega_c)^2 \int d\epsilon' \int d\Delta\epsilon \rho(\epsilon') \rho(\epsilon' - \Delta\epsilon) [\delta(\hbar\omega - \Delta\epsilon) - \delta(\hbar\omega + \Delta\epsilon)] \\ &\quad \times \left[\tanh\left(\beta \frac{\epsilon' - \mu_0}{2}\right) - \tanh\left(\beta \frac{\hbar(\epsilon' - \Delta\epsilon) - \mu_0 - eV}{2}\right) \right] . \end{aligned} \quad (4.55)$$

In the limit $\hbar\omega \ll \epsilon_F$, we use $\rho(\epsilon' \pm \hbar\omega) \simeq \rho(\epsilon')$ and we derive

$$\begin{aligned} \text{Im} \Sigma_{\text{env}}^R(\omega) &\simeq \frac{1}{2} \pi (\hbar\omega_c)^2 \int d\epsilon' \rho^2(\epsilon') \\ &\quad \times \left[\tanh\left(\beta \frac{\epsilon' + \hbar\omega - \mu_0 - eV}{2}\right) - \tanh\left(\beta \frac{\epsilon' - \hbar\omega - \mu_0 - eV}{2}\right) \right] . \end{aligned} \quad (4.56)$$

The factor within the square brackets in the integrand is peaked at $\epsilon' = \mu_0 + eV$. Hence we can approximate $\rho^2(\epsilon') \simeq \rho^2(\mu_0)$ and then compute the remaining integral exactly to obtain an Ohmic (in the sense that it is proportional to ω) behavior for the imaginary part of the retarded self-energy:

$$\text{Im} \Sigma_{\text{env}}^R(\omega) \simeq 2\pi \hbar (\hbar\omega_c)^2 \rho^2(\mu_0) \omega . \quad (4.57)$$

Interesting enough, this expression is independent of T and V . Similar calculations give

$$\Sigma_{\text{env}}^K(\omega) \simeq 2\pi \hbar (\hbar\omega_c)^2 \rho^2(\mu_0) \frac{eV \sinh(\beta eV) - \hbar\omega \sinh(\beta \hbar\omega)}{\cosh(\beta eV) - \cosh(\beta \hbar\omega)} . \quad (4.58)$$

In order to determine T^* , we investigate the low frequency limit of $\Sigma_{\text{env}}^K(\omega)$ given in eq. (4.58).

Zero drive. For $eV \ll T \ll \epsilon_F$, eq. (4.58) yields

$$\Sigma_{\text{env}}^K(\omega) \simeq 2\pi\hbar^2(\hbar\omega_c)^2\rho^2(\mu_0) \omega \coth(\beta\hbar\omega/2) . \quad (4.59)$$

Equations (4.57) and (4.59) are linked through FDT. In the low frequency limit ($\hbar\omega, eV \ll T \ll \epsilon_F$) it reads

$$\Sigma_{\text{env}}^K(\omega) \simeq 4\pi\hbar(\hbar\omega_c)^2\rho^2(\mu_0) T , \quad (4.60)$$

yielding $T^* = T$ as expected in this equilibrium situation.

Finite drive. As soon as the drive is not negligible compared to temperature, in the low frequency regime ($\hbar\omega \ll T \ll \epsilon_F$ and $eV \ll \epsilon_F$)

$$\Sigma_{\text{env}}^K(\omega) \simeq 2\pi\hbar(\hbar\omega_c)^2\rho^2(\mu_0) eV \coth(\beta eV/2) , \quad (4.61)$$

yielding

$$T^* = \frac{eV}{2} \coth(\beta eV/2) . \quad (4.62)$$

An “FDT like” relation is verified in these limits

$$\Sigma_{\text{env}}^K(\omega) = \hbar \coth(\hbar\omega/2T^*) \text{Im} \Sigma_{\text{env}}^R(\omega) . \quad (4.63)$$

A similar interpretation of the effect of a two-leads environment in these limits on the dynamics of a single localized spin was given in [261] and [262].

Furthermore, in the low temperature limit ($\hbar\omega \ll T \ll eV \ll \epsilon_F$)

$$\Sigma_{\text{env}}^K(\omega) \simeq 2\pi\hbar(\hbar\omega_c)^2\rho^2(\mu_0) |eV| , \quad (4.64)$$

yielding $T^* \equiv |eV|/2$.

Finally in the zero temperature limit ($0 = T \ll \hbar\omega, eV \ll \epsilon_F$)

$$\Sigma_{\text{env}}^K(\omega) = 2\pi\hbar(\hbar\omega_c)^2\rho^2(\mu_0) \begin{cases} |eV| & \text{if } |\hbar\omega| \leq |eV| , \\ |\hbar\omega| & \text{if } |\hbar\omega| > |eV| . \end{cases} \quad (4.65)$$

In the low frequency regime, we recover expression (4.64). In the zero temperature and zero drive limit ($0 = T = eV \ll \hbar\omega \ll \epsilon_F$) the Keldysh component of the environment self-energy reads $\Sigma_{\text{env}}^K(\omega) = 2\pi\hbar(\hbar\omega_c)^2\rho^2(\mu_0) |\hbar\omega|$ that goes linearly to zero in the $\hbar\omega \rightarrow 0$ limit.

Zero temperature

In the $T = 0$ limit, we obtain for finite values of the other parameters ($eV, \hbar\omega, \epsilon_F$)

$$\Sigma_{\text{env}}^K(\omega) = \pi \hbar (\hbar\omega_c)^2 \left[\text{sign}(eV + \hbar\omega) \int_{\mu_0}^{\mu_0 + eV + \hbar\omega} d\epsilon \rho(\epsilon) \rho(\epsilon - \hbar\omega) \right. \\ \left. + \text{sign}(eV - \hbar\omega) \int_{\mu_0}^{\mu_0 + eV - \hbar\omega} d\epsilon \rho(\epsilon) \rho(\epsilon + \hbar\omega) \right] \quad (4.66)$$

$$\text{Im } \Sigma_{\text{env}}^R(\omega) = \pi (\hbar\omega_c)^2 \left[\int_{\mu_0}^{\mu_0 + eV + \hbar\omega} d\epsilon \rho(\epsilon) \rho(\epsilon - \hbar\omega) \right. \\ \left. - \int_{\mu_0}^{\mu_0 + eV - \hbar\omega} d\epsilon \rho(\epsilon) \rho(\epsilon + \hbar\omega) \right]. \quad (4.67)$$

In the low frequency limit ($0 = T \ll \hbar\omega \ll eV, \epsilon_F$) they yield

$$\Sigma_{\text{env}}^K(\omega) \simeq 2\pi \hbar (\hbar\omega_c)^2 \text{sign}(eV) \int_{\mu_0}^{\mu_0 + eV} d\epsilon \rho^2(\epsilon), \quad (4.68)$$

$$\text{Im } \Sigma_{\text{env}}^R(\omega) \simeq \pi \hbar (\hbar\omega_c)^2 [\rho^2(\mu_0) + \rho^2(\mu_0 + eV)] \omega, \quad (4.69)$$

so that

$$T^*(T = 0) = \text{sign}(eV) \frac{\int_{\mu_0}^{\mu_0 + eV} d\epsilon \rho^2(\epsilon)}{\rho^2(\mu_0) + \rho^2(\mu_0 + eV)}. \quad (4.70)$$

Some specific reservoirs

For the half-filled semi-circular DOS (type A), at zero drive and zero temperature, we establish the following analytical results at finite ϵ_F :

$$\Sigma_{\text{env}}^K(\tau) = 2 \left(\frac{\hbar\omega_c}{\epsilon_F} \right)^2 \frac{J_1^2(\tau\epsilon_F/\hbar) - S_1^2(\tau\epsilon_F/\hbar)}{(\tau/\hbar)^2}, \quad (4.71)$$

$$\Sigma_{\text{env}}^R(\tau) = \frac{8}{\hbar} \left(\frac{\hbar\omega_c}{\epsilon_F} \right)^2 \frac{J_1(\tau\epsilon_F/\hbar) S_1(\tau\epsilon_F/\hbar)}{(\tau/\hbar)^2} \Theta(\tau), \quad (4.72)$$

with $\Sigma_{\text{env}}^R(\tau = 0) = 0$, $\Sigma_{\text{env}}^K(\tau = 0) = \frac{1}{2}(\hbar\omega_c)^2$. J_1 and S_1 are the Bessel and the Struve functions of first kind and first order, respectively. From eqs. (4.71) and (4.72), we see that the temporal extent of both Σ_{env}^R and Σ_{env}^K is of order \hbar/ϵ_F . In the limit in which ϵ_F is much larger than any other energy scale, a numerical analysis shows that this property holds for finite values of the temperature and the drive as well. As a way of summary, in Fig. 4.6 (a) we plot Σ_{env}^K as a function of $\tau\epsilon_F$ for $\epsilon_F = 10J, 100J$ and at ($T = J, V = 0$) and ($T = 0, V = J$). In the case in which ϵ_F is finite, one can compute T^* for the half-filled semi-circular DOS at zero temperature:

$$T^*(T = 0) = \frac{|eV|}{2} \frac{1 - 1/3 (eV/\epsilon_F)^2}{1 - 1/2 (eV/\epsilon_F)^2} \text{ for } |eV| < eV_{\text{max}} = \epsilon_F. \quad (4.73)$$

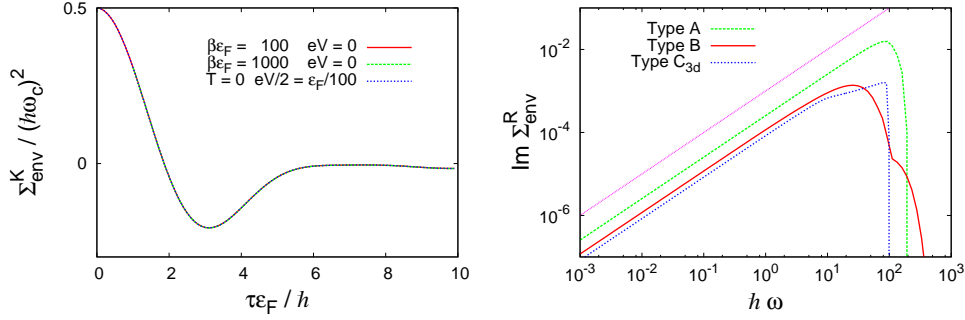


Figure 4.6: (a) Σ_{env}^K (for the half-filled semi-circle DOS) as a function of $\tau\epsilon_F$ in the regime where ϵ_F is much larger than any other energy scale: for $\beta\epsilon_F = 100$ and $\beta\epsilon_F = 1000$ at $eV = 0$ and also for $eV/2 = \epsilon_F/100$ at $T = 0$. The three curves are indistinguishable. This shows that Σ_{env}^K is indeed a function of $\tau\epsilon_F$ in this regime and shows furthermore that $eV/2$ plays the same role as T . (b) $\text{Im } \Sigma_{\text{env}}^R(\omega)$ is represented in a double logarithmic scale for the three following DOS with $\beta\epsilon_F = \epsilon_F/eV = 100$: the half-filled semi-circle $\rho_A(\epsilon)$, the half-filled type B with $\rho_B(\epsilon)$ and the 3d free electrons DOS $\rho_{C3d}(\epsilon)$. The straight line above all is a guide to the eye for a pure Ohmic ($\propto \omega$) behavior. The rapid decay above $\hbar\omega \sim \epsilon_F$ is a signature of the energy cut-off, $\epsilon_{\text{cut}} \propto \epsilon_F$, of the DOS.

In Fig. 4.6 (b) we give a numerical integration of $\text{Im } \Sigma_{\text{env}}^R(\omega)$ for the three types of reservoirs we introduced in Sec. 4.1.2 and in the case in which ϵ_F is the largest energy scale. This shows that the self-energy is indeed the one of an Ohmic bath. The fact that their Ohmic behavior is approximately valid until $\hbar\omega = \epsilon_F$ supports the property that the temporal extent of the self-energies (in real time) is of the order of \hbar/ϵ_F .

4.4 Results

In this Section we present our results. We first complete the calculation of disorder averaged generating function and, from it, we derive Schwinger-Dyson equations for the two-time correlation and linear response valid for all values of the parameters. We next derive the dynamical phase diagram as a function of the temperature of the reservoirs (T), the strength of quantum fluctuations (Γ), the voltage (eV) and the coupling to the leads for which we introduce the new dimensionless parameter $g \equiv \hbar\omega_c/\epsilon_F$. We distinguish two phases separated by a second order phase transition. For high values of the temperature and/or strong drive and/or strong quantum fluctuations, we find a non-equilibrium steady state that approaches the usual paramagnet when $eV \rightarrow 0$. Whereas for low temperatures and/or low drive and/or quantum fluctuations we find a coarsening phase.

4.4.1 Average over disorder

At this stage, after tracing out all fermionic degrees of freedom, the effective action of our system is quadratic in the fields and reads

$$\begin{aligned}
\frac{i}{\hbar} S_{\text{eff}} = & n \sum_{i=1}^N \int dt \left\{ \frac{i}{\Gamma} \dot{\mathbf{s}}_i^{(1)}(t) \cdot \dot{\mathbf{s}}_i^{(2)}(t) \right. \\
& + \frac{i}{\sqrt{N}} \sum_{j < i}^N J_{ij} \left[\mathbf{s}_i^{(1)}(t) \cdot \mathbf{s}_j^{(2)}(t) + \mathbf{s}_i^{(2)}(t) \cdot \mathbf{s}_j^{(1)}(t) \right] \\
& - \frac{1}{2} \int dt' \Sigma_{\text{env}}^K(t-t') \mathbf{s}_i^{(2)}(t) \cdot \mathbf{s}_i^{(2)}(t') + i \int dt' \Sigma_{\text{env}}^R(t-t') \mathbf{s}_i^{(2)}(t) \cdot \mathbf{s}_i^{(1)}(t') \\
& \left. + \frac{i}{2\hbar} \sum_{a=\pm} a z_i^a(t) \left[1 - \frac{1}{2} \left(\mathbf{s}_i^{(1)}(t) \right)^2 - a\hbar \mathbf{s}_i^{(1)}(t) \cdot \mathbf{s}_i^{(2)}(t) - \frac{\hbar^2}{4} \left(\mathbf{s}_i^{(2)}(t) \right)^2 \right] \right\}. \tag{4.74}
\end{aligned}$$

Given that the initial condition for the rotors is taken to be uncorrelated with the disorder configuration (the J_{ij} 's), neither the initial density matrix $\varrho(0)$ nor the generating functional without sources ($\mathcal{Z}[\mathbf{h}^\pm = 0] = 1$) depend upon disorder. This property allows us to write dynamic equations by averaging over disorder the generating functional itself hence without resorting to the use of replicas [259, 260]. As in other quantum systems with quenched disorder [258–260, 263–265, 46, 47, 266–270], we are therefore interested in

$$\overline{\mathcal{Z}[\mathbf{h}^\pm]}^J \equiv \int \left(\prod_{i,j < i} dJ_{ij} P(J_{ij}) \right) \mathcal{Z}[\mathbf{h}^\pm], \tag{4.75}$$

where $P(J_{ij})$ is the Gaussian density distribution for the rotor couplings with zero mean and variance J^2 . The disorder average over a random Gaussian potential can be readily done and the effective action of the system is quartic in the fields and reads

$$\begin{aligned}
\frac{i}{\hbar} S_{\text{eff}} = & n \sum_{i=1}^N \int dt \left\{ \frac{i}{\Gamma} \dot{\mathbf{s}}_i^{(1)}(t) \cdot \dot{\mathbf{s}}_i^{(2)}(t) \right. \\
& - \frac{J^2 n}{2N} \int dt' \sum_j \left[\mathbf{s}_i^{(1)}(t) \cdot \mathbf{s}_j^{(2)}(t) \right] \left[\mathbf{s}_i^{(1)}(t') \cdot \mathbf{s}_j^{(2)}(t') + \mathbf{s}_i^{(2)}(t') \cdot \mathbf{s}_j^{(1)}(t') \right] \\
& - \frac{1}{2} \int dt' \Sigma_{\text{env}}^K(t-t') \mathbf{s}_i^{(2)}(t) \cdot \mathbf{s}_i^{(2)}(t') + i \int dt' \Sigma_{\text{env}}^R(t-t') \mathbf{s}_i^{(2)}(t) \cdot \mathbf{s}_i^{(1)}(t') \\
& \left. + \frac{i}{2\hbar} \sum_{a=\pm} a z_i^a(t) \left[1 - \frac{1}{2} \left(\mathbf{s}_i^{(1)}(t) \right)^2 - a\hbar \mathbf{s}_i^{(1)}(t) \cdot \mathbf{s}_i^{(2)}(t) - \frac{\hbar^2}{4} \left(\mathbf{s}_i^{(2)}(t) \right)^2 \right] \right\}. \tag{4.76}
\end{aligned}$$

4.4.2 Schwinger-Dyson equations

In the large n limit, we show that the Lagrange multipliers are homogeneous,

$$z_i^+(t) = z_i^-(t) \equiv z(t) \quad \forall i, t. \quad (4.77)$$

See App. 4.E for a detailed computation. Moreover, introducing

$$\Sigma^K \equiv J^2 C + \Sigma_{\text{env}}^K, \quad \Sigma^R \equiv J^2 R + \Sigma_{\text{env}}^R, \quad (4.78)$$

we obtain the Schwinger-Dyson equations which fully determine the dynamics of the system:

$$\left[\frac{1}{\Gamma} \frac{\partial^2}{\partial t^2} + z(t) \right] C(t, t') = \int_0^{t'} dt'' \Sigma^K(t, t'') R(t', t'') + \int_0^t dt'' \Sigma^R(t, t'') C(t'', t'), \quad (4.79)$$

$$\left[\frac{1}{\Gamma} \frac{\partial^2}{\partial t^2} + z(t) \right] R(t, t') = \delta(t - t') + \int_{t'}^t dt'' \Sigma^R(t, t'') R(t'', t'), \quad (4.80)$$

$$z(t) = \int_0^t dt'' \Sigma^K(t, t'') R(t, t'') + \Sigma^R(t, t'') C(t, t'') - \frac{1}{\Gamma} \frac{\partial^2 C}{\partial t^2}(t, t' \rightarrow t^-). \quad (4.81)$$

We remark that the expression for the response is decoupled from the self correlation apart from a residual coupling through the Lagrange multiplier. This is actually a consequence of two features of the model: the disordered potential is quadratic in the rotors and the coupling to the reservoirs is linear in the rotors. The “initial” conditions are given by

$$C(t, t) = 1, \quad R(t, t) = 0 \quad \forall t. \quad (4.82)$$

Moreover, integrating eqs. (4.79) and (4.80) over an infinitesimal interval around $t' = t$, one sees that the first derivative of the correlation is continuous at equal times

$$\lim_{t' \rightarrow t^-} \partial_t C(t, t') = \lim_{t' \rightarrow t^+} \partial_t C(t, t') = 0, \quad (4.83)$$

whereas the one of the response function is discontinuous

$$\lim_{t' \rightarrow t^-} \partial_t R(t, t') = \Gamma, \quad \lim_{t' \rightarrow t^+} \partial_t R(t, t') = 0. \quad (4.84)$$

The structure of these equations is the same as the one in other out-of-equilibrium problems studied in [258–260, 263–265, 46, 47, 266–271].

4.4.3 Quantum non-equilibrium steady state (QNESS) phase

One expects that if the system is quenched into the high temperature phase, after a short transient it should relax toward a quantum non-equilibrium steady state (QNESS). The

system of rotors cannot be in equilibrium since, for $V \neq 0$, an electronic current is passing through it. Nevertheless the dynamics are still stationary (time translationally invariant). This implies that $C(t, t')$ and $R(t, t')$ are only functions of $t - t'$. Guided by a numerical analysis (see Sec. 4.4.5), we make the assumption (that we later check to be consistent) that the quantity $z(t)$ is a one-time observable that converges toward a finite value z^∞ . In this situation, one can Fourier transform the Schwinger-Dyson equations (4.79) and (4.80) with respect to $t - t'$ to find

$$R(\omega) = \frac{1}{-\Gamma^{-1}\omega^2 + z^\infty - \Sigma^R(\omega)}, \quad (4.85)$$

$$C(\omega) = \Sigma^K(\omega) |R(\omega)|^2, \quad (4.86)$$

$$C(\omega) = \frac{\Sigma_{\text{env}}^K(\omega)}{\text{Im } \Sigma_{\text{env}}^R(\omega)} \text{Im } R(\omega), \quad (4.87)$$

Using the fact that $\lim_{\omega \rightarrow \infty} R(\omega)$ has to vanish, eq. (4.85) implies

$$R(\omega) = \frac{1}{2J^2} \left(-\Gamma^{-1}\omega^2 + z^\infty - \Sigma_{\text{env}}^R(\omega) + \sqrt{(-\Gamma^{-1}\omega^2 + z^\infty - \Sigma_{\text{env}}^R(\omega))^2 - 4J^2} \right). \quad (4.88)$$

We note that in the cases in which the DOS of the reservoirs have an energy cut-off ϵ_{cut} ,

$$C(\omega) = \text{Im } R(\omega) = \Sigma_{\text{env}}^K(\omega) = \text{Im } \Sigma_{\text{env}}^R(\omega) = 0 \text{ for } \hbar\omega > \epsilon_{\text{cut}}. \quad (4.89)$$

4.4.4 Critical manifold

Equation for criticality

Approaching the putative critical manifold from the disordered phase, see Fig. 4.1, where after a short transient the system should be time translationally invariant, we look for a singularity in the Fourier transformed Schwinger-Dyson equations that would be the signature of the loss of time translational invariance and ultimately of a phase transition toward an out-of-equilibrium behavior. Anticipating a second order phase transition scenario where the onset of criticality is characterized by long-wavelength instabilities, we inspect these equations at $\omega = 0$.

The constraint that rotors have a unit length $C(t, t) = 1$ implies

$$\int_0^\infty \frac{d\omega}{2\pi} C(\omega) = \frac{1}{2}, \quad (4.90)$$

and replacing $C(\omega)$ with its expression in eq. (4.87):

$$\int_0^\infty \frac{d\omega}{2\pi} \frac{\Sigma_{\text{env}}^K(\omega)}{\text{Im } \Sigma_{\text{env}}^R(\omega)} \text{Im } R(\omega) = \frac{1}{2}. \quad (4.91)$$

Equation (4.88) at $\omega = 0$ reads

$$R(\omega = 0) = \frac{1}{2J^2} \left(z^\infty - \Sigma_{\text{env}}^R(\omega = 0) + \sqrt{(z^\infty - \Sigma_{\text{env}}^R(\omega = 0))^2 - 4J^2} \right). \quad (4.92)$$

$R(\omega = 0) = \int_0^\infty d\tau R(\tau)$ has to be real since $R(\tau)$ is real². However, it is clear from eq. (4.92) that $z^\infty = z_c^\infty \equiv 2J + \Sigma_{\text{env}}^R(\omega = 0)$ is a singular point (a minus sign would be incoherent with the approach in Sec. 4.4.5). This is the signature of the phase transition we were looking for. At criticality,

$$R(\omega = 0)|_{z^\infty = z_c^\infty} = 1/J. \quad (4.93)$$

Concomitantly, the value of $C(\omega = 0)$ blows up. Inserting z_c^∞ in eq. (4.91), we obtain the equation for the critical manifold,

$$\int_0^\infty \frac{d\omega}{2\pi} \frac{\Sigma_{\text{env}}^K(\omega)}{\text{Im} \Sigma_{\text{env}}^R(\omega)} \text{Im} R(\omega)|_{z_c^\infty} = \frac{1}{2}. \quad (4.94)$$

The parameters are the strength of quantum fluctuations Γ , the temperature T , the voltage applied between the two reservoirs V . We recall that J is the typical interaction between two rotors. The energy variation scale of the reservoirs is characterized by ϵ_F and $\hbar\omega_c$ quantifies the coupling strength of the rotors to their environment through the dimensionless small parameter $g \equiv \hbar\omega_c/\epsilon_F$.

In the rest of this section, we use eq. (4.94) to uncover the phase diagram of Fig. 4.1. The critical surface is parametrized in the T, Γ, V space by T_c, Γ_c, V_c (g is kept constant). We introduce the critical points $\bar{T}_c \equiv T_c(\Gamma = V = 0)$, $\bar{V}_c \equiv V_c(T = \Gamma = 0)$, $\bar{\Gamma}_c \equiv \Gamma_c(T = V = 0)$. Anticipating the coming results, we introduce the dimensionless reduced parameters $\theta \equiv T/J$, $v \equiv eV/2J$, $\gamma \equiv (4\hbar/3\pi)^2 \Gamma/J$. In the plane $V = 0$, where the reservoirs act like an equilibrium bath, we recover the results in [258]. In the classical limit $V = \Gamma = 0$, we recover the ones in [272, 273].

In the limit in which ϵ_F is much larger than any other energy scale, using eqs. (4.57) and (4.58), the equation for the critical surface reads

$$\int_0^\infty \frac{d\omega}{2\pi} \frac{1}{\omega} \frac{eV \sinh(\beta eV) - \hbar\omega \sinh(\beta\hbar\omega)}{\cosh(\beta eV) - \cosh(\beta\hbar\omega)} \text{Im} R(\omega)|_{z_c^\infty} = \frac{1}{2}. \quad (4.95)$$

Critical points on the $\Gamma = 0$ plane

Taking the $\Gamma \rightarrow 0$ limit of expression (4.88) one has

$$\text{Im} R(\omega')|_{z_c^\infty} = \begin{cases} \frac{1}{J} \sqrt{1 - (1 - \omega'^2)^2} & \text{for } \omega' \in [0, \sqrt{2}] , \\ 0 & \text{for } \omega' \geq \sqrt{2} , \end{cases} \quad (4.96)$$

2. $\Sigma_{\text{env}}^R(\omega = 0)$ is real for the same reason.

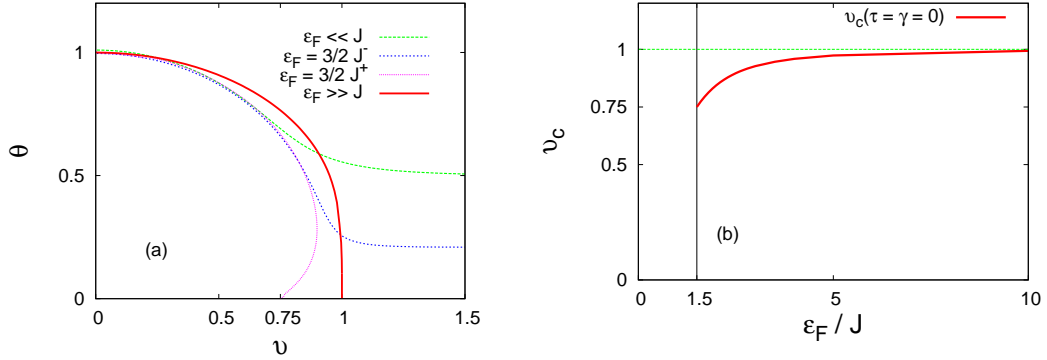


Figure 4.7: Study of the behavior of the $\gamma = 0$ critical line with the ratio ϵ_F/J for the half-filled semi-circle DOS. (a) The $\gamma = 0$ critical line $\theta_c(\nu)$ is given for four different values of the ratio ϵ_F/J . The analytical expression of the $\epsilon_F/J \rightarrow \infty$ curve is given in eq. (4.99). For $\epsilon_F/J < 3/2$ the critical point $\bar{\nu}_c$ is rejected to infinity. (b) $\bar{\nu}_c \equiv \nu_c(\theta = \gamma = 0)$ is plotted against ϵ_F/J . All these $\gamma = 0$ results are independent of the value g .

where we introduced $\omega' \equiv \omega/\sqrt{2J\Gamma}$. The expression of $\text{Im } R(\omega)$ does not involve the reservoirs: the time scale of the rotors (controlled by Γ) totally decouples from the one of the reservoirs in such a way that the rotors only couple with the zero mode (the slowest) of the reservoirs. Using eq. (4.94), we write the equation of the critical manifold in the $\Gamma = 0$ plane

$$\lim_{\Gamma \rightarrow 0} \sqrt{\frac{2\Gamma}{J}} \int_0^{\sqrt{2}} \frac{d\omega'}{2\pi} \sqrt{1 - (1 - \omega'^2)^2} \frac{\Sigma_{\text{env}}^K(\sqrt{2J\Gamma}\omega')}{\text{Im } \Sigma_{\text{env}}^R(\sqrt{2J\Gamma}\omega')} = \frac{1}{2}. \quad (4.97)$$

Using the definition (4.54) of $T^*(T, eV)$ introduced in Sec. 4.3.2, this simply reads

$$T^*(T_c, eV_c) = J. \quad (4.98)$$

At $eV = 0$, the reservoirs constitute an equilibrium bath and the ratio $\Sigma_{\text{env}}^K/\text{Im } \Sigma_{\text{env}}^R$ is given by the FDT and we find a temperature-induced classical critical point $\bar{T}_c \equiv T_c(\Gamma = V = 0) = J$. In terms of the reduced temperature this reads $\bar{\theta}_c = 1$. In the next two paragraphs we look at how this critical point is affected by a finite drive ($eV \neq 0$).

Infinite ϵ_F . We first consider the limit $\epsilon_F \rightarrow \infty$, using the explicit expression (4.62) for T^* one finds:

$$T_c(eV) = \frac{eV}{2} \left/ \text{arccoth} \left(\frac{2J}{eV} \right) \right. . \quad (4.99)$$

From this equation we find a drive-induced critical point at $e\bar{V}_c/2 = J$. In terms of the reduced voltage this reads $\bar{\nu}_c = 1$. The departure from the classical critical temperature on

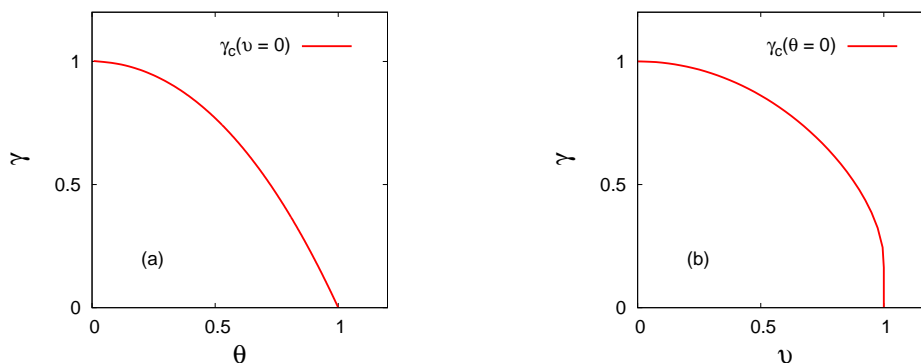


Figure 4.8: Phase diagram in terms of the reduced parameters analytically determined in the limit $g \rightarrow 0$. (a) Critical line for $V = 0$. (b) Critical line for $T = 0$ in the limit $\epsilon_F \rightarrow \infty$.

the $\gamma = 0$ plane is quadratic: $\theta_c \simeq 1 - 1/3 v^2$ for $v \ll 1$. Instead, on the zero-drive plane, $v = 0$, the critical line leaves $\bar{\theta}_c$ linearly: $\theta_c \simeq 1 - 3\pi^2/16 \gamma$ for $\gamma \ll 1$. More details on the critical line $\gamma_c(t)$ at $v = 0$ are given in [45, 256]. Close to \bar{v}_c on the $\theta = 0$ and $\gamma = 0$ planes the departure of the critical lines $\gamma_c(v)$ and $\theta_c(v)$, respectively, are non-analytical and thus very steep [see Figs. 4.7 (a) and 4.8 (b)].

Finite ϵ_F . Let us now investigate the $T = 0$ critical point \bar{V}_c for finite values of ϵ_F . For our simple DOS depending on a unique parameter ϵ_F , \bar{v}_c is controlled by ϵ_F/J . Plugging the expression (4.70) for $T^*(T = 0)$ into the expression (4.98) we obtain

$$\text{sign}(e\bar{V}_c) \frac{1}{J} \frac{\int_{\mu_0}^{\mu_0 + e\bar{V}_c} d\epsilon' \rho^2(\epsilon')}{\rho^2(\mu_0) + \rho^2(\mu_0 + e\bar{V}_c)} = 1. \quad (4.100)$$

The existence and the value of the solution \bar{V}_c depend on the details of the DOS $\rho(\epsilon)$. If the DOS has an energy cut-off ϵ_{cut} , the existence of a solution is guaranteed if the cut-off is larger than the solution $\epsilon_{\text{cut}}^{\text{min}}$ of

$$\int_{\mu_0}^{\epsilon_{\text{cut}}^{\text{min}}} d\epsilon \rho^2(\epsilon) = J\rho^2(\mu_0). \quad (4.101)$$

For the type A half-filled semi-circle distribution ($\mu_0 = \epsilon_F$, $\epsilon_{\text{cut}} = 2\epsilon_F$), it turns out that eq. (4.100) admits a finite solution as soon as $\epsilon_F/J \geq 3/2$. For $\epsilon_F/J = 3/2$, one finds $e\bar{V}_c = 3/2 J$ ($\bar{v}_c = 3/4$). For $\epsilon_F/J > 3/2$, the finite solution \bar{v}_c goes to one as one increases the ratio ϵ_F/J . For $\epsilon_F/J < 3/2$ the critical point is rejected to infinity and the critical line in the $\Gamma = 0$ plane converges to the asymptotic value $\theta_c(v \gg 1) = 1/2$ as $\epsilon_F/J \rightarrow 0$. See Fig. 4.7.

For the distribution B, if $\mu_0 \neq 0$, the scenario is the same as for the semi-circle distribution there is a finite value of the ratio ϵ_F/J under which, the critical point \bar{v}_c is rejected

to infinity, and above which, \bar{v}_c has a finite value that goes to 1 in the limit $\epsilon_F \rightarrow \infty$. If $\mu_0 = 0$ then \bar{v}_c remains finite.

For the distribution of type C, eq. (4.100) always admits a finite solution \bar{v}_c independent of ϵ_F . For the distribution $C3d$, $\bar{v}_c = 1$ regardless of μ_0 , ϵ_F and J . For the distribution $C2d$, we also get $\bar{v}_c = 1$. For the distribution $C1d$, one can show that as long as $\mu_0 > 0$, there is a finite \bar{v}_c , function only of $u \equiv J/\mu_0$: $\bar{v}_c = [\exp(u + L(ue^{-u})) - 1]/2u$, where $L(x)$ is the only solution of the equation $Le^L = x$ that is analytic in 0. For $\mu_0(\epsilon_F \rightarrow \infty) \rightarrow \infty$, we recover $\bar{v}_c = 1$.

Quantum critical point

Weak coupling limit. We first consider the limit of the weak coupling to the reservoirs $g \rightarrow 0$ after the long-time limit such that the asymptotic regime has been established. It is actually in this $g \rightarrow 0$ limit that the self-energy was computed (we expanded the total action up to second order in g) in Sec. 4.3. $g \equiv \hbar\omega_c/\epsilon_F$ can be sent to zero by sending the coupling parameters to zero, but for our simple DOS, it can also be realized by sending ϵ_F to infinity.

In equilibrium ($V = 0$) at $T = 0$, the FDT gives

$$\frac{\Sigma_{\text{env}}^K(\omega)}{\text{Im } \Sigma_{\text{env}}^R(\omega)} = \hbar \text{ for } 0 < \hbar\omega < \epsilon_{\text{cut}}. \quad (4.102)$$

By turning off the coupling to the reservoirs ($g \rightarrow 0$) in eq. (4.92) one has

$$\text{Im } R(\omega')|_{z_c^\infty} = \begin{cases} \frac{1}{J} \sqrt{1 - (1 - \omega'^2)^2} & \text{for } \omega' \in [0, \sqrt{2}] , \\ 0 & \text{for } \omega' \geq \sqrt{2} , \end{cases} \quad (4.103)$$

where we introduced $\omega' \equiv \omega/\sqrt{2J\Gamma}$. Plugging eqs. (4.102) and (4.103) in the equation for the critical manifold (4.94) gives the quantum critical point

$$\hbar^2 \bar{\Gamma}_c \equiv \left(\frac{3\pi}{4}\right)^2 J \text{ if } \epsilon_{\text{cut}} > \frac{3\pi}{2} J \text{ and no solution otherwise.} \quad (4.104)$$

For type A reservoirs in the $\epsilon_F \rightarrow \infty$ limit, one can prove that the critical surface is parabolic close to the quantum critical point $\bar{\gamma}_c$ i.e. $\gamma_c \simeq 1 - 16/3\pi^2 \theta^2$ at $\theta \ll 1$ and $v = 0$, and $\gamma_c \simeq 1 - 16/3\pi^2 v^2$ for $v \ll 1$ and $\theta = 0$.

Finite coupling. When the coupling to the electronic reservoirs g is finite this quantum critical point (actually the whole critical surface) moves upward when increasing the coupling constant (see Fig. 4.9). The coarsening phase is thus stabilized when increasing the coupling to the reservoirs. In the $\epsilon_F \rightarrow \infty$ limit, one has for $g \ll 1$

$$\bar{\gamma}_c \simeq 1 + 2 \left(\frac{3\pi}{4}\right)^2 (\hbar\omega_c)^2 \rho^2(\mu_0). \quad (4.105)$$

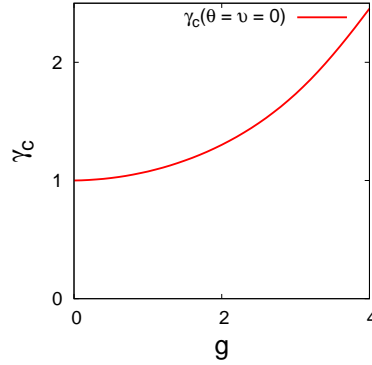


Figure 4.9: Numerical study of the evolution of the critical point $\bar{\gamma}_c \equiv \gamma_c(\theta = 0, v = 0)$ with the coupling parameter g (here for $\epsilon_F/J = 10$).

$\Gamma_c(V=0) \sim \bar{T}_c - T$	$T_c(\Gamma=0) \sim \text{NA}$	$V_c(T=0) \sim (\bar{\Gamma}_c - \Gamma)^{1/2}$
$\Gamma_c(T=0) \sim \text{NA}$	$T_c(V=0) \sim (\bar{\Gamma}_c - \Gamma)^{1/2}$	$V_c(\Gamma=0) \sim (\bar{T}_c - T)^{1/2}$

Table 4.1: Behavior of the critical manifold close to the critical points for $g \rightarrow 0$ and $\epsilon_F \rightarrow \infty$. Close to the critical point $\bar{V}_c = V_c(T = \Gamma = 0)$ the critical lines are non-analytical (NA).

In the case of the type A half-filled semi-circle distribution this reads $\bar{\gamma}_c \simeq 1 + 9/2 g^2$. This is similar to what was found for other quantum spin models embedded in an Ohmic harmonic oscillator bath and is due to a spin-localization-like effect [258, 263, 264]. This similitude is not surprising since we showed in Sec. 4.3.2, eq. (4.57), that the mixed electronic reservoirs behave like an Ohmic bath in the $\epsilon_F \rightarrow \infty$ limit.

Summary of the phase diagram

Let us summarize the key features of the critical manifold in the case of a DOS with $\epsilon_F \rightarrow \infty$. When the coupling to the reservoir g is set to zero, the values of three critical points $(\bar{T}_c, \bar{\Gamma}_c, e\bar{V}_c)$ are only controlled by J that measures the disorder strength. Figure 4.1 gathers all the $g \rightarrow 0$ results in the T, Γ, V space. The increase of either the thermal or quantum fluctuations, by raising Γ or the temperature T , respectively, leads to the destabilization of the coarsening phase. The same occurs for an increase of the bias voltage V . The summary of the behavior of the critical manifold close to the critical points $\bar{T}_c, \bar{\Gamma}_c$ and \bar{V}_c is given in Table 4.1. Furthermore, an increase of the rotors-reservoirs coupling g pulls the quantum critical point $\bar{\Gamma}_c$ upward (as indicated in Fig. 4.1 by a vertical arrow) enlarging the low temperature phase.

4.4.5 Coarsening phase

We study the dynamics in the low T , weak Γ , weak V region of the phase diagram by solving the Schwinger-Keldysh equations in two ways: with an exact numerical approach and using analytic approximation in the long-time dynamics. We prove that in this region of the phase diagram there is coarsening and that the aging dynamics that occur are universal and equivalent to the ones of the classical (and undriven) limit of our model (*a.k.a.* the $p = 2$ spherical model with quenched disorder).

Numerical solution

Our numerical analysis consists in solving the Schwinger-Dyson equations (4.79), (4.80) and (4.81) after a quench into the low temperature, weak quantumness, weak drive phase. Thanks to their causal structure, the equations on C , R and z can be integrated step by step in time, with a Runge-Kutta method. Apart from arbitrarily small numerical errors, this approach is exact.

We concentrate on reservoirs at temperature T that have a type A semi-circle DOS (both L and R reservoirs). L reservoirs are kept half-filled while a voltage V is applied between L and R reservoirs. ϵ_F is chosen to be the largest energy scale. Typically, we consider the following values for the parameters: $T \sim \Gamma \sim eV \sim 0.1J$ and $\epsilon_F \sim 10J$.

The analysis shows (analytical arguments are given in Sec. 4.4.5) that the dynamics after the quench below the critical surface do not reach a QNESS. There is a separation of two-time scales typical of aging phenomena [52]. The data in Figs. 4.10-4.12 were obtained using the algorithm briefly described.

Mapping to Langevin dynamics

The goal of this subsection is to map our quantum field theory description of the rotors dynamics, which involves the two fields $s^{(1)}$ and $s^{(2)}$ (see Sec. 4.2.3), to an equivalent description in terms of Langevin dynamics. In the long-time limit of the coarsening dynamics, we establish that the equation of motion for the field $s^{(1)}$ is actually a Langevin equation driven by a colored noise ξ the statistical characteristics of which are controlled by the self-energies of the fermion reservoirs.

Let us take a step back and rewrite the effective action as it was before averaging over disorder. Making the assumption (we later check its consistency) that the Lagrange multi-

pliers satisfy $z_i^+(t) = z_i^-(t) = z_i(t) \forall i, t$, the effective action reads

$$\begin{aligned} \frac{i}{\hbar} S_{\text{eff}}[\mathbf{s}^{(1)}, \mathbf{s}^{(2)}, z] = n \sum_{i=1}^N \int dt \left\{ \frac{i}{\Gamma} \dot{\mathbf{s}}_i^{(1)}(t) \cdot \dot{\mathbf{s}}_i^{(2)}(t) + i \sum_{j=1}^N \mathcal{J}_{ij} \mathbf{s}_i^{(1)}(t) \cdot \mathbf{s}_j^{(2)}(t) \right. \\ \left. - \frac{1}{2} \int dt' \Sigma_{\text{env}}^K(t-t') \mathbf{s}_i^{(2)}(t) \cdot \mathbf{s}_i^{(2)}(t') + i \int dt' \Sigma_{\text{env}}^R(t-t') \mathbf{s}_i^{(2)}(t) \cdot \mathbf{s}_i^{(1)}(t') \right. \\ \left. - i z_i(t) \mathbf{s}_i^{(1)}(t) \cdot \mathbf{s}_i^{(2)}(t) \right\} \end{aligned}$$

where introduced the real and symmetric matrix \mathcal{J} defined by $\mathcal{J}_{ij} \equiv J_{ji}/\sqrt{N}$ if $j < i$, $\mathcal{J}_{ij} \equiv \mathcal{J}_{ji}$ if $j > i$. Like the other components of this matrix, we set \mathcal{J}_{ii} to be taken from a Gaussian distribution with zero mean and variance J^2/N [we saw that the constraint $\mathbf{s}_i(t)^2 = 1$ yields $\mathbf{s}_i^{(1)}(t) \cdot \mathbf{s}_i^{(2)}(t) = 0$]. The total effective action adopts the quadratic form

$$\frac{i}{\hbar} S_{\text{eff}} = -n \sum_{i=1}^N \int dt \left\{ i \mathbf{s}_i^{(2)}(t) \cdot \mathbf{E}\mathbf{Q}_i(t) + \frac{1}{2} \int dt' \mathbf{s}_i^{(2)}(t) \cdot \Sigma_{\text{env}}^K(t-t') \mathbf{s}_i^{(2)}(t') \right\},$$

where we introduced the notation

$$\mathbf{E}\mathbf{Q}_i(t) \equiv \sum_{j=1}^N \int dt' \left\{ \left[\left(\frac{1}{\Gamma} \partial_t^2 + z_i(t) \right) \delta_{ij} - \mathcal{J}_{ij} \right] \delta(t-t') - \Sigma_{\text{env}}^R(t-t') \delta_{ij} \right\} \mathbf{s}_j^{(1)}(t'). \quad (4.106)$$

By comparing this action with the action of the MSRJD formalism [see for example eq. (2.8)], the quantity $\mathbf{E}\mathbf{Q}_i$ can be interpreted as a Gaussian random process and can therefore be written as a set of coupled Langevin equations

$$\mathbf{E}\mathbf{Q}_i(t) = \boldsymbol{\xi}_i(t), \quad (4.107)$$

with $\boldsymbol{\xi}_i(t)$ a Gaussian random noise with statistics $\langle \boldsymbol{\xi}_i(t) \cdot \boldsymbol{\xi}_j(t') \rangle_{\xi} = \delta_{ij} \Sigma_{\text{env}}^K(t-t')$. This mapping is possible since the action of the rotor system, once the constraint on each rotor has been imposed through $z_i(t)$ and $z_i(t)$ is treated independently, is quadratic. In more general models the mapping is not exact, see *e.g.* the discussion in [274–277].

Under the further assumption $z_i(t) = z(t)$, justified in the large N limit, the stochastic equations (4.106) are rendered independent – apart from a residual coupling through the Lagrange multiplier – by a rotation onto the basis that diagonalizes the interaction matrix \mathcal{J} . Indeed, J being real and symmetric, it has N real eigenvalues σ with corresponding eigenvectors $\boldsymbol{\sigma}$ that constitute a complete and orthonormal basis of the space of rotor sites: $\boldsymbol{\sigma} \bullet \boldsymbol{\sigma}' = \delta_{\sigma\sigma'}$ where \bullet is the usual scalar product in this space. Let us collect all the rotors in the vector $\mathbf{s} \equiv \{\mathbf{s}_i^{(1)}\}_{i \in [1, N]}$ and introduce its projections on the eigenvectors: $\mathbf{s}_{\sigma} \equiv \mathbf{s} \bullet \boldsymbol{\sigma}$. If we project eq. (4.106) onto $\boldsymbol{\sigma}$, we are left with N uncoupled Langevin equations reading

$$\left(\frac{1}{\Gamma} \partial_t^2 - \sigma + z(t) \right) \mathbf{s}_{\sigma}(t) - \int dt' \Sigma_{\text{env}}^R(t-t') \mathbf{s}_{\sigma}(t') = \boldsymbol{\xi}_{\sigma}(t), \quad (4.108)$$

with

$$\langle \xi_\sigma(t) \rangle_\xi = 0, \quad \langle \xi_\sigma(t) \cdot \xi_{\sigma'}(t') \rangle_\xi = \delta_{\sigma\sigma'} \Sigma_{\text{env}}^K(t - t'). \quad (4.109)$$

There are *classical* Langevin equation for the fields \mathbf{s}_σ . The noise statistics is controlled by Σ_{env}^K and is peculiar because of the quantum origin of the environment: it has memory (colored), and depends on T, eV, \hbar . Σ_{env}^R appears like a friction kernel. Because Σ_{env}^K and Σ_{env}^R do not satisfy a classical fluctuation-dissipation relation, it is a non-equilibrium environment even in the $eV = 0$ case.

Two-time self correlation. Within the effective Langevin formalism, the two-time self correlation function defined in eq. (4.31) reads

$$C(t, t') = \overline{\langle \mathbf{s}_\sigma(t) \cdot \mathbf{s}_\sigma(t') \rangle}^J, \quad (4.110)$$

where the average over disorder is realized by

$$\overline{\cdots}^J \equiv \int d\sigma \rho_J(\sigma) \cdots, \quad (4.111)$$

and $\rho_J(\sigma)$ is the probability density of the eigenvalues of the interaction matrix \mathcal{J} . For our case of an infinite ($N \rightarrow \infty$) and symmetric random matrix with Gaussian elements of variance J^2/N it is given by the Wigner semi-circle distribution:

$$\rho_J(\sigma) \equiv \frac{1}{\pi J} \sqrt{1 - \left(\frac{\sigma}{2J}\right)^2} \quad \text{for} \quad \sigma \in [-2J; +2J], \quad (4.112)$$

and zero elsewhere.

Following the analysis in [272, 273], the correlation function (4.110) is expected to show a separation of time scales (at least in some parts of the phase diagram). This is usual in coarsening phenomena and corresponds to a stationary regime at short time-difference and an aging one at long time-difference with respect to a waiting-time dependent characteristic time. The stationary part of the correlation approaches a plateau at the Edwards-Anderson order parameter, $q_{\text{EA}} \equiv \overline{\langle \mathbf{s}_\sigma \rangle_\xi^2}^J$, that measures the of frozen rotor fluctuations on time scales much smaller than this characteristic time. The value of q_{EA} depends on all parameters (T, eV, Γ, g). It is non-vanishing in the spontaneously symmetry-broken phase and continuously goes to 0 on the critical surface. In certain cases it can be computed exactly.

It is reasonable to expect that the long-time aging dynamics is determined by the low frequency (or long time) form of the Langevin equations only. The simplification arising in this asymptotic limit are discussed below.

Long-time dynamics

In the low-frequency, long time-difference limit, $\hbar\omega \ll T$, the Keldysh self-energy can be approximated by a constant [see, *e.g.*, eq. (4.61) in Sec. 4.3.2 for its exact expression in the $\epsilon_F \rightarrow \infty$ limit]

$$\Sigma_{\text{env}}^K(\tau) \simeq \delta(\tau) \Sigma_{\text{env}}^K(\omega = 0) \geq 0. \quad (4.113)$$

Similarly, we keep the leading contributions in the derivative expansion of Σ_{env}^R :

$$\Sigma_{\text{env}}^R(\tau) \simeq \Sigma_{\text{env}}^R(\omega = 0) \delta(\tau) + \eta_0 \delta(\tau) \partial_\tau, \quad (4.114)$$

with $\eta_0 \equiv \partial_\omega \text{Im} \Sigma_{\text{env}}^R(\omega = 0) > 0$. The Langevin equations read in this limit

$$\frac{1}{\Gamma} \partial_t^2 \mathbf{s}_\sigma(t) + \eta_0 \partial_t \mathbf{s}_\sigma(t) = (\sigma - z(t) + \Sigma_{\text{env}}^R(\omega = 0)) \mathbf{s}_\sigma(t) + \boldsymbol{\xi}_\sigma(t), \quad (4.115)$$

where η_0 plays the role of a friction coefficient and $\boldsymbol{\xi}_\sigma(t)$ has white noise statistics:

$$\langle \boldsymbol{\xi}_\sigma(t) \cdot \boldsymbol{\xi}_{\sigma'}(t') \rangle_\xi = \delta_{\sigma\sigma'} \delta(t - t') \Sigma_{\text{env}}^K(\omega = 0). \quad (4.116)$$

In the Langevin formalism, the kernel of an equilibrium white bath is given by the Einstein relation (known as the FDT of the second kind): $\langle \xi(t) \xi(t') \rangle_\xi = 2\eta_0 T \delta(t - t')$. Thus, the temperature T of the bath can be seen as the ratio of the diffusion coefficient of a particle embedded in that bath with the friction coefficient η_0 of the bath on the particle. For our reservoirs, in the low-frequency long time-difference limit, one can associate this ratio to an equivalent temperature T^*

$$T^* \equiv \lim_{\omega \rightarrow 0} \frac{1}{2} \frac{\Sigma_{\text{env}}^K(\omega)}{\partial_\omega \text{Im} \Sigma_{\text{env}}^R(\omega)}, \quad (4.117)$$

the properties of which were discussed in Sec. 4.3.2. Thus, we confirm here that T^* acts like a temperature in the sense that the effect of the (out-of-equilibrium) reservoirs on the long-time dynamics is the one of an *equilibrium* dissipative (Ohmic) bath at a temperature T^* . This has been reported in different works and is at the root of the derivation of the stochastic Gilbert equation for a spin under bias [261].

We expect that as far as the long time dynamical behavior is concerned, the inertial term in eq. (4.115) can also be dropped, thus leading to the equations:

$$\partial_t \mathbf{s}_\sigma(t) = \lambda_\sigma(t) \mathbf{s}_\sigma(t) + \frac{1}{\eta_0} \boldsymbol{\xi}_\sigma(t), \quad (4.118)$$

where we introduced the shorthand notation $\lambda_\sigma(t) \equiv [\sigma - \Delta z(t)] / \eta_0$ and $\Delta z(t) \equiv z(t) - \Sigma_{\text{env}}^R(\omega = 0)$.

This particular Langevin equation has been analyzed intensively in the study of the classical spherical Sherrington-Kirkpatrick model (or spherical $p = 2$ spin glass model)

and the results in [272, 273] apply to our problem with $T \mapsto T^*$. The solution to eq. (4.118) for a given disorder realization and noise history is

$$\mathbf{s}_\sigma(t) = \mathbf{s}_\sigma(0) \exp \left(\int_0^t d\tau \lambda_\sigma(\tau) \right) + \frac{1}{\eta_0} \int_0^t d\tau \boldsymbol{\xi}_\sigma(\tau) \exp \left(\int_\tau^t d\tau' \lambda_\sigma(\tau') \right). \quad (4.119)$$

Copying results in [272, 273], the aging part of the correlation (in the limit $t' \gg t \rightarrow \infty$) shows a simple aging scaling behavior

$$C(t, t') \simeq 2\sqrt{2} q_{\text{EA}} \frac{(t/t')^{3/4}}{(1 + t/t')^{3/2}} = C(t/t'). \quad (4.120)$$

The solution to eqs. (4.118) leads to $q_{\text{EA}} = 1 - T^*(eV, T)/J$. However, this result is obtained by taking the limit of relatively close times – with respect to t' – whereas, as we stressed, eq. (4.118) is valid for the long time t' and long time-difference $t - t'$ properties only. As a consequence, we expect the scaling result, eq. (4.120), to hold at long times with the value of the Edwards-Anderson parameter not necessarily given by $1 - T^*(eV, T)/J$. Its computation requires a full solution of the equations of motion.

We now focus on the aging dynamics in different parts of the phase diagram and argue that the Langevin dynamics (4.115) indeed provide a correct description of the dynamical evolution.

Dynamics in the $eV = 0$ plane. In this case, the Edwards-Anderson order parameter q_{EA} measures the static order parameter. Static calculations yield the following equation [256]

$$1 = \int d\sigma \rho_J(\sigma) \frac{\sqrt{\Gamma}}{2\sqrt{z^\infty - \sigma}} \coth \left(\frac{\sqrt{\Gamma}\sqrt{z^\infty - \sigma}}{2T} \right), \quad (4.121)$$

that gives in principle the value of $z^\infty(T, eV)$ for any temperature and strength of the quantum fluctuations. It is large for $T, eV \gg J$ and decreases with both T and eV . However, because of the square roots in the above equation, it cannot go below the critical value fixed by the upper edge σ^* of the distribution of eigenvalues ρ_J . In the case of the Wigner semi-circle distribution [see eq. (4.112)], this corresponds to $z_c^\infty = \sigma^* = 2J$ and the critical line is given by

$$1 = \int d\sigma \rho_J(\sigma) \frac{\sqrt{\Gamma_c}}{2\sqrt{2J - \sigma}} \coth \frac{1}{2T_c} \sqrt{\Gamma_c} \sqrt{2J - \sigma}. \quad (4.122)$$

Under the critical line, there is some sort of Bose-Einstein condensation. Indeed, in order for the constraint $\sum_i \langle \mathbf{s}_i^2 \rangle = \sum_\sigma \langle \mathbf{s}_\sigma^2 \rangle = N$ to be satisfied, the weight of the edge eigenvalue $\sigma^* = 2J$ has to become macroscopic and q_{EA} is a measure of the fraction of ‘frozen’ rotors in the condensate. In the classical limit eq. (4.121) simplifies considerably yielding $1 = \int d\sigma \rho_J(\sigma) \frac{T}{z^\infty - \sigma}$ and one identifies $q_{\text{EA}} = \frac{1}{N} \langle \mathbf{s}_{\sigma^*} \rangle = 1 - T/T_c$.

The dynamic calculations based on the use of the quantum FDT to relate the correlation to the linear response in the stationary regime detailed in [258], or the replica equilibrium computation in [263, 264], can be easily extended to deal with a generic electronic bath in equilibrium. One confirms that $q_{\text{EA}} = 1$ at $T = \Gamma = eV = 0$ and continuously approaches 0 on the critical line $\Gamma_c(T)$ for all values of g . The precise variation of q_{EA} within the coarsening phase depends on the bath kernels. In the $\epsilon_F \rightarrow \infty$ limit, the results in [258] apply also to our problem. The solution of the Schwinger-Dyson equations in the aging regime confirms that the scaling result, eq. (4.120), holds.

Dynamics in the $\Gamma = 0$ plane. Another interesting case is the effective overdamped Langevin limit obtained for $\Gamma \rightarrow 0$ and (eV, T) in the coarsening phase. In this case dropping the inertial term in eq. (4.115) is exact and not an approximation.

Here the result $q_{\text{EA}} = 1 - T^*(eV, T)/J$ can be shown to hold. The Edwards Anderson parameter approaches one for $T = V = \Gamma = 0$ and goes continuously to zero on the critical line, as in a second order phase transition. Consistently with the analysis of the critical surface derived from the QNESS phase (see Sec. 4.4.4), one finds $T^*(T_c, eV_c) = J$. Numerical integration of the integro-differential equations of motion confirms that the scaling result, eq. (4.120), holds in the aging regime.

Despite the fact that dropping the inertial term is exact, the equations (4.118) are still not exact at all times. In particular, the initial conditions for this approximated equation of motion should be given by the state of the system a short while after the quench, when the long-timescale description starts to be valid. Apparently, this delay seems to be not sufficient to significantly correlate the rotors with the interaction matrix \mathcal{J} and, to any practical purpose $s_\sigma(0)$ can still be considered “random”, at least as far as the Edwards-Anderson parameter is concerned.

Dynamics in the $T = 0$ plane. The zero-temperature plane is more difficult to deal with analytically. One is not entitled to use FDT since the system is driven by eV nor dropping the second time-derivative is exact. Furthermore, this is the case where the simplification leading to eq. (4.118) are more dangerous because of the power law tails appearing at $T = 0$ in correlation and response functions.

In order to check that the scaling result, eq. (4.120), holds we numerically integrate the full set of Schwinger-Dyson equations.

In Fig. 4.10 (a) we show the decay of the two-time correlation function. For short time differences $t - t'$ with respect to the waiting time t' , there is a stationary regime depending on all control parameters in which the correlation approaches a plateau asymptotically in the time-difference. The plateau value is q_{EA} and measures the fraction of frozen rotor fluctuations on time scales much smaller than t' . Afterwards, there is an aging regime in

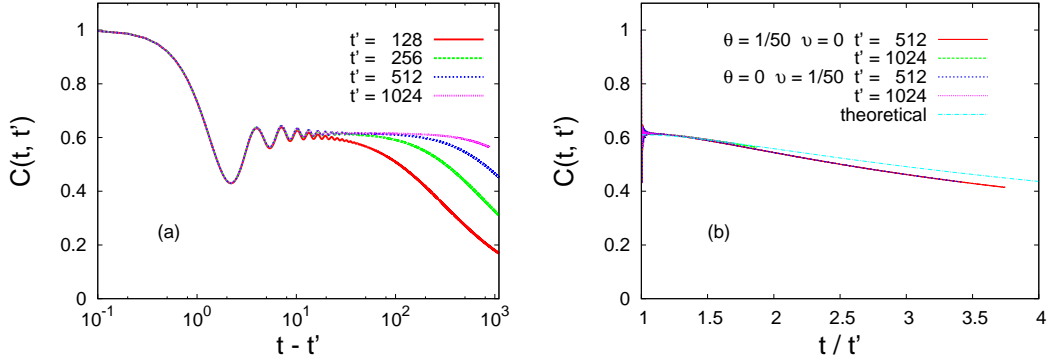


Figure 4.10: Dynamics in the driven coarsening regime: numerical solution to Schwinger-Dyson eqs. (4.79) and (4.80) where the reservoirs have a half-filled semi-circle DOS with $\epsilon_F = 10J$. (a) The self correlation $C(t, t')$ after a quench to $\theta = 0.02, v = 0.02, \gamma = 0.2, g = 1$ (in reduced quantities) shows first a stationary regime for short $t - t'$, then a slow aging regime where the time translational invariance is lost. (b) The self correlation C is plotted versus t/t' for two waiting times after two quenches into the coarsening region: $\theta = 0.02, v = 0, \gamma = 0.2$ and $\theta = 0, v = 0.02, \gamma = 0.2$. There is a double collapse of the curves. The collapse for the different t' proves the simple aging scaling $C(t'/t)$ and the collapse for the two different quenches shows that $T^* \simeq eV/2$ plays the role of a temperature. The theoretical curve is the solution eq. (4.120) with $q_{EA} \approx 0.6$.

which C depends on the two times explicitly. In Fig. 4.10 (b), we plot C against t/t' to prove that the simple aging scaling predicted analytically with eq. (4.120) holds at these long times. Moreover, we show that the dynamics after a quench to $\theta = 0.02, v = 0$ are the same that the ones after a quench to $\theta = 0, v = 0.02$, illustrating the fact that $T^* \simeq eV/2$ acts here like a temperature.

Super-universality. It is remarkable that in the large nN limit, the long-time dynamics of our model are exactly the ones of the classical fully connected $p = 2$ spherical spin glass. The latter being a classical model in contact with an equilibrium bath ($\Gamma = 0, eV = 0$), the former being its quantum version in contact with a non-equilibrium environment ($\Gamma \neq 0, eV \neq 0$). The fact that the scaling functions are *super-universal*, in the sense that they do not depend on the external parameters T, eV, Γ once q_{EA} is extracted as a factor, can be understood as follows. First the fact that the non-equilibrium environment of our model give rise to the same long-time dynamics than an equilibrium environment can be seen as a consequence of the Ohmic behavior of the reservoirs self-energy kernels at small frequencies (see Sec. 4.3.2). Secondly, the fact that our quantum model shows a classical behavior at late times can be understood as a consequence of decoherence due to the dissipative (and Ohmic) bath. Furthermore, the effect of the temperature T on the long-time dynamics being irrelevant (in a RG sense) in the classical limit, one can expect the same to hold in the quantum case with respect to all parameters.

We found quite naturally that the long-time dynamics correspond to a Bose-Einstein-like condensation process of the N n -dimensional ‘vectors’ \mathbf{s}_σ on the direction of the edge eigenvector. The relaxation is controlled by the decay of $\rho_J(\sigma)$ close to its edge σ^* . For Gaussian i.i.d. couplings .

We now prove the strong connection with the dynamics of the pure $3d$ $O(n \rightarrow \infty)$ models. For the $3d$ $O(n \rightarrow \infty)$ non-linear sigma model [defined in eq. (1.3) and after rescaling $\mathbf{s}_i \mapsto \sqrt{n} \mathbf{s}_i$], the equations of motion are rendered independent in Fourier space and read

$$\left(\frac{1}{\Gamma} \partial_t^2 - Jk^2 - g \sum_q |\mathbf{s}_q(t)|^2 - 1 \right) \mathbf{s}_k(t) - \int dt' \Sigma_{\text{env}}^R(t-t') \mathbf{s}_k(t') = \boldsymbol{\xi}_k(t) \quad (4.123)$$

$E = -k^2$ are the Laplacian eigenvalues the distribution of which is given by $\rho_\Delta(E) = \rho_k(k) \left| \frac{dk}{dE} \right|$ where $\rho_k(k) dk \sim d^d \mathbf{k} \sim k^{d-1} dk$. This yields $\rho_\Delta(E) \sim (-E)^{d/2-1}$ which coincides for $d = 3$ with the edge of the distribution of eigenvalues of the \mathcal{J}_{ij} matrix, $\rho_J(\sigma) \stackrel{\sigma \approx \sigma^*}{\sim} (2J - \sigma)^{1/2}$. For this reason all models with a square root singularity of the distribution of “masses” σ , such as the ferromagnetic rotor model in $d = 3$ and the completely connected spin glass rotor model, are characterized by the same long-time dynamics.

This result has an interesting consequence. In the case of (large n) quantum $3d$ coarsening the classical-quantum mapping extends to space-time correlations and proves the existence of a growing coherence length $R(t) \propto t^{1/2}$ over which the rotors are oriented in the same direction. This real-space interpretation of aging unveils the connection with coarsening that was announced all along this manuscript.

Linear response

It has already been noticed in Sec. 4.4.2 that the response function was somehow peculiar since its equation of motion is decoupled from the one of the self correlation. Having argued that the long-time dynamics are governed by their classical counterparts, the linear response should also scale as in the classical limit. Therefore, the quantum fluctuation-dissipation relation between integrated linear response, $\chi(t, t') \equiv \int_{t'}^t dt'' R(t, t'')$ and self correlation $C(t, t')$ approaches the classical one, $\chi \sim ct + (q_{\text{EA}} - C)/T_{\text{eff}}$, with an *infinite* effective temperature [278], $T_{\text{eff}} \rightarrow \infty$, as shown in Fig. 4.11. The relations between integrated responses and correlation functions in other quantum problems that also approach classical-like form in the aging regime were shown in [259, 260, 265, 46, 47, 266–270].

The Lagrange multiplier

One should check the validity of a key assumption that was used to derive the phase diagram: the convergence of $z(t)$ to an asymptotic value on the critical manifold. We first

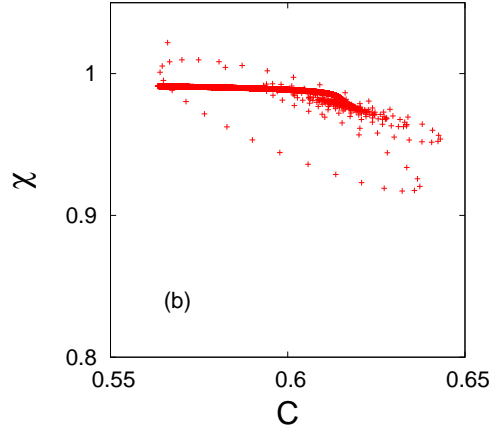


Figure 4.11: The integrated linear response, $\chi(t, t') = \int_{t'}^t d\tau R(t, \tau)$ against $C(t, t')$, for $t' = 1024$ and using t as a parameter. The curved part corresponds to the stationary and oscillatory regime with $(t - t')/t' \rightarrow 0$ while the straight line is for times in the monotonic aging decay of C .

derive analytically the asymptotic behavior (within our long-time approximation) of $z(t)$ in the $\Gamma = 0$ coarsening phase showing that this is indeed the case. Then we give numerical evidence that $z(t)$ converges in the whole phase space.

The condition $C(t, t) = \int d\sigma \rho_J(\sigma) \langle \mathbf{s}_\sigma(t) \cdot \mathbf{s}_\sigma(t) \rangle_\xi = 1$ reads after taking its time derivative and assuming furthermore that $\mathbf{s}_\sigma(0)$ is uncorrelated with σ ($\mathbf{s}_\sigma(0) = \mathbf{s}_0, \forall \sigma$), that is valid for random initial conditions (coming from infinite temperature for instance)

$$\begin{aligned} 0 &= \int d\sigma \rho_J(\sigma) \langle \partial_t \mathbf{s}_\sigma(t) \cdot \mathbf{s}_\sigma(t) \rangle_\xi \\ &= \int d\sigma \rho_J(\sigma) \left\{ \mathbf{s}_0^2 \lambda_\sigma(t) e^{2 \int_0^t d\tau \lambda_\sigma(\tau)} + \frac{T^*}{\eta_0} \left[1 + 2 \lambda_\sigma(t) \int_0^t d\tau' e^{2 \int_{\tau'}^t d\tau'' \lambda_\sigma(\tau'')} \right] \right\}. \end{aligned} \quad (4.124)$$

Taking the derivative with respect to \mathbf{s}_0^2 yields

$$0 = \int d\sigma \rho_J(\sigma) \lambda_\sigma(t) e^{2 \int_0^t d\tau \lambda_\sigma(\tau)}, \quad (4.125)$$

that can be recast into

$$\Delta z(t) = \frac{\eta_0}{2} \partial_t \ln \int d\sigma \rho_J(\sigma) e^{2\sigma t / \eta_0}. \quad (4.126)$$

Asymptotic behavior of $z(t)$. By plugging in ρ_J the Wigner semi-circle distribution given in eq. (4.112), we get

$$\Delta z(t) = \frac{\eta_0}{2} \partial_t \ln \frac{\eta_0}{2J} \frac{1}{t} I_1 \left(\frac{4J}{\eta_0} t \right), \quad (4.127)$$

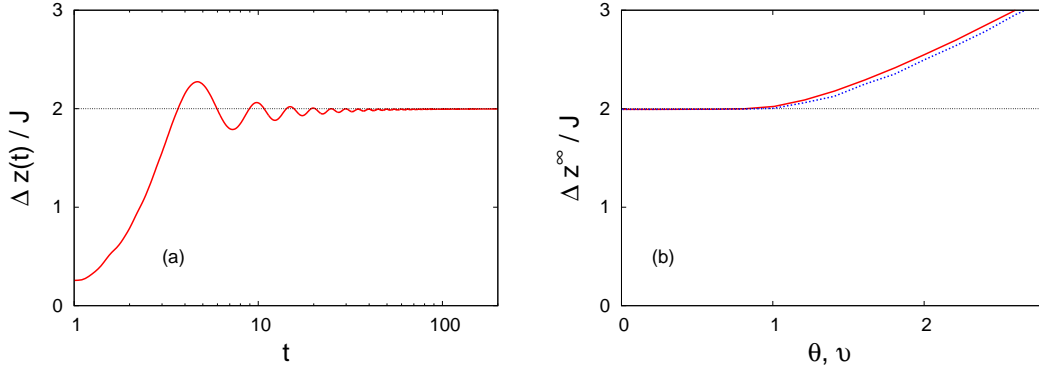


Figure 4.12: (a) $\Delta z(t) \equiv z(t) - \Sigma_{\text{env}}^R(\omega = 0)$ quickly converges toward $2J$, the largest eigenvalue of the \mathcal{J}_{ij} matrix (here $\Gamma = eV = T = 0.1J$, $g = 1$ and $\epsilon_F = 10J$). (b) Dependence of z^∞ with T (plain curve) and eV (dashed curve).

where I_1 is the modified Bessel function of the first kind and first order. we obtain, the pre-asymptotic behavior for $t \gg \eta_0/J$

$$z(t) \simeq 2J + \Sigma_{\text{env}}^R(\omega = 0) - \eta_0 \frac{3}{4t}. \quad (4.128)$$

We just showed that inside the coarsening phase, the Lagrange multiplier $z(t)$ reaches an asymptotic value which is actually the critical value, $z_c^\infty = 2J + \Sigma_{\text{env}}^R(\omega = 0)$, calculated in Sec. 4.4.3 from the QNESS phase TTI equations without neglecting any term. The coherence between those two results somehow justifies the approximations made previously. In the $\epsilon_F \rightarrow \infty$ limit (reservoirs acting like an Ohmic bath) $\Sigma_R(\omega = 0)$ vanishes and we recover the same mechanism as in the classical case [272, 273].

These analytical results are supported by the numerical analysis. Computed after the quench, the Lagrange multiplier $z(t)$ quickly converges to an asymptotic value z^∞ . As an example, we plot in Fig. 4.12 (a) the behavior of $z(t)$ after a quench into the QNESS phase. The oscillations and the zero initial slope are signatures of the second and higher order derivatives in eq. (4.108). These terms were dropped in the analytical study of the long-time limit, see eq. (4.118), but the numerical integration does not neglect them. We give in Fig. 4.12 (b) the dependence of z^∞ with T and eV . It is quite clear that z^∞ is constant (and equal to z_c^∞) inside the critical surface and increases with T , Γ and eV as soon as entering the QNESS phase. This justifies the assumptions made in Sec. 4.4.3.

To summarize the results, in the whole phase diagram $z(t)$ always rapidly reaches an asymptotic value z^∞ . Inside the QNESS phase, z^∞ is a growing function of the parameters T, Γ, V whereas on the critical surface and inside the coarsening region, it is fixed to z_c^∞ .

Link between $z(t)$ and the potential energy density One is interested in computing the energy density $\epsilon(t)$ of the effective Brownian particle. It is given by

$$\epsilon(t) = -\frac{1}{2} \sum_{i,j=1}^N \overline{J_{ij} \mathbf{s}_i(t) \mathbf{s}_j(t)}^J = -\frac{1}{2} \int d\sigma \rho_J(\sigma) \sigma \mathbf{s}_\sigma^2(t) . \quad (4.129)$$

Using the solution (4.119) for $\mathbf{s}_\sigma(t)$ at $T^* = 0$, one has

$$2\epsilon(t) = -\mathbf{s}_0^2 e^{-\frac{2}{\eta_0} \int_0^t d\tau \Delta z(\tau)} \int d\sigma \sigma \rho(\sigma) e^{2\sigma t/\eta_0} . \quad (4.130)$$

By use of eq. (4.126), we obtain

$$2\epsilon(t) = -\frac{\eta_0}{2} \partial_t \ln \int d\sigma \rho(\sigma) e^{2\sigma t/\eta_0} . \quad (4.131)$$

We recognize eq. (4.127) in the Rhs of this last expression, giving finally

$$\epsilon(t) = -\frac{1}{2} \Delta z(t) . \quad (4.132)$$

This result is valid for any disorder density $\rho(\sigma)$. For a non-zero T^* , similar calculations give, see [272, 273],

$$\epsilon(t) = \frac{1}{2} [T^* - \Delta z(t)] . \quad (4.133)$$

4.5 The current

The physics of electric currents through mesoscopic quantum impurities in out-of-equilibrium settings has attracted a lot of attention in the recent years. The Kondo impurity is the canonical example of a strongly correlated system that has both been tackled experimentally [279–281] and theoretically by non-perturbative methods [282–285]. It is, to our knowledge, the first time that some fermionic reservoirs are coupled to a macroscopic disordered quantum system. In the previous sections we analyzed the effects of the voltage drop on the system dynamics. In this Section we study the properties of the current that establishes between the two reservoirs. In particular we are interested in the possible influence of the rotors on the current. Is the current, that is rather easy to measure experimentally, able to give information about the dynamics of the rotors ?

We recall the expression of the interaction Hamiltonian given in eq. (4.8):

$$H_{\text{int}} = -\sqrt{n} \frac{\hbar \omega_c}{N_s} \sum_{i=1}^N \sum_{\mu=1}^n \sum_{k,k'=1}^{N_s} \sum_{l,l'=1}^M s_i^\mu [\psi_{L i k l}^\dagger \sigma_{l l'}^\mu \psi_{R i k' l'} + L \leftrightarrow R] . \quad (4.134)$$

From the point of view of the electric current, our model consists in two reservoirs coupled through time-dependent tunneling constants $s_i^\mu(t)$. It is different from the usual quantum impurity problems in the fact that the electrons cannot stay on the rotor system but only hop directly from one reservoir to the other. Furthermore, the quantum character of the system is not expected to play any significant role since its level spacings are smaller than any other energy scale in the large nN limit. The computation of the current will therefore lead to Landauer formula [286, 287] *a priori* dependent on the rotors states.

The electric current carried by the fermions flowing from the right to the left reservoirs is

$$I_{R \rightarrow L}(t) = -e \left\langle \frac{dN_L}{dt} \right\rangle = -\frac{ie}{\hbar} \langle [H_{\text{tot}}, N_L] \rangle = -\frac{ie}{\hbar} \langle [H_{\text{int}}, N_L] \rangle, \quad (4.135)$$

where $-e$ is the electric charge of a fermion and $N_L \equiv \sum_{ikl} \psi_{Likl}^\dagger \psi_{Likl}$ is the number operator of the left reservoirs. H_{int} is the part of the total Hamiltonian H_{tot} that couples the system and the reservoirs, see eq. (4.8). After straightforward algebra, we obtain

$$I_{R \rightarrow L}(t) = -\frac{ie}{\hbar} \langle \sqrt{n} \frac{\hbar\omega_c}{N_s} \sum_{i\mu kk' ll} \sigma_{ll'}^\mu s_i^\mu \left[\psi_{Likl}^\dagger \psi_{Rjk'l'} - L \leftrightarrow R \right] \rangle. \quad (4.136)$$

In the Keldysh field theory formalism, this corresponds to the quantity

$$I_{R \rightarrow L}(t) = \frac{1}{2} (I_{R \rightarrow L}^+(t) + I_{R \rightarrow L}^-(t)), \quad (4.137)$$

with

$$I_{R \rightarrow L}^a(t) \equiv -\frac{ie}{\hbar} \langle \sqrt{n} \frac{\hbar\omega_c}{N_s} \sum_{i\mu kk' ll} \sigma_{ll'}^\mu s_i^{\mu a}(t) [\bar{\psi}_{Likl}^a(t) \psi_{Rjk'l'}^a(t) - L \leftrightarrow R] \rangle. \quad (4.138)$$

Expanding the action up to first order in the coupling constant g , we obtain an average over the rotors and the free fermions that are now uncoupled, that we note $\langle \dots \rangle_{\text{int}}$

$$\begin{aligned} I_{R \rightarrow L}(t) &= \frac{1}{2} \langle (I_{L \rightarrow R}^+(t) + I_{L \rightarrow R}^-(t)) \frac{i}{\hbar} S_{\text{int}} \rangle_{\text{int}} \\ &= \frac{e}{2\hbar^2} n \left(\frac{\hbar\omega_c}{N_s} \right)^2 \sum_{ab} \sum_{i\mu kk' ll' j\nu qq' mm'} \sum_b \int dt' \sigma_{ll'}^\mu \sigma_{mm'}^\nu \langle s_i^{\mu a}(t) s_j^{\nu b}(t') \rangle \\ &\quad \times [\bar{\psi}_{Likl}^a(t) \psi_{Rjk'l'}^a(t) - L \leftrightarrow R] [\bar{\psi}_{Ljqm}^b(t') \psi_{Rjq'm'}^b(t') + L \leftrightarrow R] \rangle_{\text{int}}. \end{aligned} \quad (4.139)$$

Averaging over the free fermions, we obtain

$$I_{R \rightarrow L}(t) = \frac{e}{2\hbar^2} n N (\hbar\omega_c)^2 \sum_{ab=\pm} b \int dt' i\hbar G^{ab}(t, t') [\bar{\psi}_{Likl}^a(t, t') i\hbar G_R^{ba}(t', t) - L \leftrightarrow R].$$

G^{ab} are the macroscopic Keldysh Green's functions for the rotors and $G_{L/R}^{ab}$ are the Green's functions of the free fermions in the L/R -reservoirs. This reads, after Keldysh rotations,

$$I_{R \rightarrow L}(t) = -\frac{e}{\hbar} n N \int_0^t d\tau C(t, t - \tau) \Pi_{\text{env}}^R(\tau) + R(t, t - \tau) \Pi_{\text{env}}^K(\tau), \quad (4.140)$$

with

$$\begin{aligned}\Pi_{\text{env}}^K &\equiv -2(\hbar\omega_c)^2 \text{Im} \left[G_L^K G_R^{K*} - \frac{\hbar^2}{4} (G_L^R G_R^{R*} + G_L^A G_R^{A*}) \right], \\ \Pi_{\text{env}}^R &\equiv -2(\hbar\omega_c)^2 \text{Im} \left[G_L^R G_R^{K*} + G_L^K G_R^{R*} \right].\end{aligned}\quad (4.141)$$

The expression for the current given in eq. (4.140) is quite generic. It is valid as soon as the system and the fermionic leads are coupled with an interaction H_{int} . The details of the system and the leads enter in the formula through their respective Green's functions. The formula was obtained after a first order expansion in the coupling constant g . The second order term like all the even order terms are zero by use of Wick's theorem. The third and higher odd order terms would have involved higher order correlation functions of the system. Plugging the expressions of the fermionic Green's functions G_α^K , G_α^R , G_α^A ($\alpha = L, R$) that are given in App. 4.B.1, we get

$$\begin{aligned}\Pi_{\text{env}}^K(\tau) &= \frac{1}{2}(\hbar\omega_c)^2 \langle \langle \left[\tanh\left(\beta \frac{\epsilon_L - \mu_L}{2}\right) \tanh\left(\beta \frac{\epsilon_R - \mu_R}{2}\right) - 1 \right] \sin\left(\frac{\epsilon_L - \epsilon_R}{\hbar} \tau\right) \rangle_L \rangle_R, \\ \Pi_{\text{env}}^R(\tau) &= \frac{1}{\hbar}(\hbar\omega_c)^2 \langle \langle \left[\tanh\left(\beta \frac{\epsilon_L - \mu_L}{2}\right) - \tanh\left(\beta \frac{\epsilon_R - \mu_R}{2}\right) \right] \cos\left(\frac{\epsilon_L - \epsilon_R}{\hbar} \tau\right) \rangle_L \rangle_R \Theta(\tau),\end{aligned}$$

where the notation $\langle \langle \dots \rangle_L \rangle_R$ stands for $\int \int d\epsilon d\epsilon' \rho_L(\epsilon) \rho_R(\epsilon') \dots$. One can check that the current vanishes when the bias voltage ($eV \equiv \mu_R - \mu_L$) is set to zero.

Linear conductance. We develop the current formula (4.140) to the first order in eV and compute the linear conductance

$$\begin{aligned}I_{R \rightarrow L}(t) &= -\frac{e}{\hbar} n N eV \\ &\times \int_0^t d\tau \mathcal{C}(t, t - \tau) \Big|_{eV=0} \frac{d\Pi_{\text{env}}^R(\tau)}{deV} \Big|_{eV=0} + R(t, t - \tau) \Big|_{eV=0} \frac{d\Pi_{\text{env}}^K(\tau)}{deV} \Big|_{eV=0}.\end{aligned}\quad (4.142)$$

One can derive for a flat half-filled DOS, $\rho(\epsilon) \propto \Theta(\epsilon_F - |\epsilon - \epsilon_F|)$, in the limit $\epsilon_F \rightarrow \infty$ (in that limit we expect the results to depend very little on the precise shape of the DOS)

$$\frac{d\Pi_{\text{env}}^R(\tau)}{deV} \Big|_{eV=0} = -\pi g^2 \delta(\tau), \quad (4.143)$$

$$\frac{d\Pi_{\text{env}}^K(\tau)}{deV} \Big|_{eV=0} = -\hbar g^2 \frac{1}{2\tau}. \quad (4.144)$$

Therefore the linear current very quickly goes from zero to

$$I_{R \rightarrow L}(t) = \frac{e}{2\hbar} n N g^2 eV \left(\pi + \hbar \int_0^t d\tau \frac{R(t, t - \tau)}{\tau} \right). \quad (4.145)$$

The dependence on the history of the two-time correlation function has disappeared and the second term in eq. (4.145) goes to zero due to the rapid decay of the response function. Finally the current quickly takes an asymptotic value

$$I_{R \rightarrow L}^{\infty} = \frac{e}{2\hbar} \pi n N g^2 eV . \quad (4.146)$$

From this computation, it appears that the current only probes the very fast dynamics of the system it passes through and does not give information on the long-time dynamics. Since the short-time dynamics of the system are equilibrium ones even in the coarsening regime, the current cannot be used to tell in which regime the system is. An exact numerical integration of eq. (4.140) supports these findings for other types of DOS, for finite values of ϵ_F and far from the linear regime.

4.6 Conclusions

In this chapter we presented a detailed study of the quantum fully-connected rotor model driven out of equilibrium by a fermionic drive. We determined analytically the phase diagram of the model and we showed that a critical manifold, controlled by the value of the disorder strength, separates a QNESS with zero order parameter from an ordering phase with non-zero order parameter. We solved the equations that describe the dynamics in the different phases with a numerical integration and analytically by using various approximation schemes that give valuable physical insights. In particular, we showed that this (quasi) quadratic model maps to a set of Langevin equations with additive colored noise that describes the dynamics of the rotors. The nature of the noise is determined by the type of electron baths used and, in the driven case, the friction kernel and noise-noise correlation are not linked by any fluctuation-dissipation relation. By using this effective Langevin description we established the connection with the $3d$ coarsening dynamics of the $O(n)$ model and we showed that the long-time ordering dynamics are in the class of the classical limit of our model without a drive, *i.e.* with the typical length growing as $t^{1/2}$.

Finally, we derived a generic expression for the current flowing through the system that involves a time-convolution between the characteristics of the system (through its correlation and linear response) and the ones the leads (through their retarded and Keldysh kernels). Interestingly enough, for the type of density of states used in the large ϵ_F limit the current depends only on the short-time difference (stationary) regime in which coarsening is not relevant.

Appendices

4.A Conventions

Θ is the Heaviside step function. We choose $\Theta(0) = 1/2$, so that $\Theta(x) + \Theta(-x) = 1 \forall x \in \mathbb{R}$. We recall the identities

$$\int_{-\infty}^{\infty} \frac{dx}{2\pi} e^{ixy} = \delta(y) \quad \text{and} \quad \int_{-\infty}^y dx \delta(x) = \Theta(y), \quad (4.147)$$

where δ is the Dirac delta function. In particular $\int_{-\infty}^0 dx \delta(x) = 1/2$.

4.A.1 Fourier transform

The convention for the Fourier transform \mathcal{F} that we use is

$$\begin{aligned} \mathcal{F}[f(\tau)](\omega) \equiv f(\omega) &\equiv \int_{-\infty}^{\infty} d\tau e^{+i\omega\tau} f(\tau), \\ \mathcal{F}^{-1}[f(\omega)](\tau) \equiv f(\tau) &= \int_{-\infty}^{\infty} \frac{d\omega}{2\pi} e^{-i\omega\tau} f(\omega), \end{aligned} \quad (4.148)$$

The Fourier transform of the step function is

$$\mathcal{F}[\Theta(\tau)](\omega) = i \text{pv} \frac{1}{\omega} + \pi \delta(\omega), \quad (4.149)$$

where ‘pv’ denotes the principal value. Convolutions in real and Fourier space are defined by

$$\begin{aligned} (f \circ g)(\tau) &\equiv \int d\tau' f(\tau') g(\tau - \tau') = \mathcal{F}^{-1}[(f g)(\omega)](\tau), \\ (f \circ g)(\omega) &\equiv \int \frac{d\omega'}{2\pi} f(\omega') g(\omega - \omega') = \mathcal{F}[(f g)(\tau)](\omega). \end{aligned} \quad (4.150)$$

4.A.2 Heisenberg representation

In the Heisenberg representation the operators evolve as

$$A_H(t) = U^\dagger(t) A(t) U(t). \quad (4.151)$$

with the unitary operator

$$U(t) \equiv T e^{-\frac{i}{\hbar} \int_0^t dt' H(t')}, \quad (4.152)$$

and thus $U^\dagger(t) = \tilde{T} e^{-\frac{i}{\hbar} \int_t^0 dt' H(t')}$. T and \tilde{T} are respectively the time and anti-time-ordering operators (see App. 4.A.3). For Hamiltonians H that do not explicitly depend on time we get

$$A_H(t) = e^{iHt/\hbar} A(t) e^{-iHt/\hbar}. \quad (4.153)$$

4.A.3 Time-ordering operator

On the real time axis, the time-ordering operator T rearranges operators with ascending times to the left:

$$T A_H(t) B_H(t') = A_H(t) B_H(t') \Theta(t - t') + \zeta B_H(t') A_H(t) \Theta(t' - t) , \quad (4.154)$$

with $\zeta = -1$ if both A and B are fermionic operators, $\zeta = 1$ otherwise. The anti-time-ordering operator \tilde{T} rearranges operators the other way round:

$$\tilde{T} A_H(t) B_H(t') = A_H(t) B_H(t') \Theta(t' - t) + \zeta B_H(t') A_H(t) \Theta(t - t') , \quad (4.155)$$

On the Keldysh contour \mathcal{C} , the position of an operator is specified by both the time and the branch index. By the notation $A_H(t, a)$, we denote the operator A in the Heisenberg representation at time t ($t \in [0, +\infty[$) on the branch a ($a = \pm$). One can similarly define a time-ordering operator $T_{\mathcal{C}}$ that rearranges operators along the contour \mathcal{C} represented in Fig. 4.5. The rules are

$$\begin{aligned} T_{\mathcal{C}} A_H(t, -) B_H(t', +) &= A_H(t) B_H(t') , \\ T_{\mathcal{C}} A_H(t, +) B_H(t', -) &= \zeta B_H(t') A_H(t) , \\ T_{\mathcal{C}} A_H(t, +) B_H(t', +) &= A_H(t) B_H(t') \Theta(t - t') + \zeta B_H(t') A_H(t) \Theta(t' - t) , \\ T_{\mathcal{C}} A_H(t, -) B_H(t', -) &= A_H(t) B_H(t') \Theta(t' - t) + \zeta B_H(t') A_H(t) \Theta(t - t') . \end{aligned} \quad (4.156)$$

4.A.4 Green's functions

Let ϕ and ϕ^\dagger be respectively annihilation and creation operator (bosonic or fermionic). In the field theory formalism of the Keldysh approach, we define the Green's functions as

$$i\hbar G^{ab}(t, t') \equiv \langle \phi^a(t) \bar{\phi}^b(t') \rangle . \quad (4.157)$$

$a, b = \pm$, $\bar{\phi}$ is either the complex conjugate (for bosons) or the Grassmannian conjugate (for fermions) of ϕ and the average is understood as

$$\langle \dots \rangle \equiv \int \mathcal{D}[\phi^\pm, \bar{\phi}^\pm] \dots \exp \left(\frac{i}{\hbar} S[\phi^\pm, \bar{\phi}^\pm] \right) . \quad (4.158)$$

In the operator formalism the Green's function read

$$i\hbar G^{ab}(t, t') \equiv \text{Tr} \left[T_{\mathcal{C}} \phi_H(t, a) \phi_H^\dagger(t', b) \varrho_H(0, \pm) \right] , \quad (4.159)$$

where $\phi_H(t, a)$ denotes the Heisenberg representation of the operator ϕ at time t on the a -branch of the Keldysh contour. $\varrho_H(0, \pm) = \varrho(0)$ is the initial density matrix (normalized to be of unit trace) and its location on the $+$ or $-$ -branch does not matter thanks to the cyclicity

of the trace. T_C is the time-ordering operator acting with respect to the relative position of (t, a) and (t', b) on the Keldysh contour (see App. 4.A.3).

One has, independently of the bosonicity or fermionicity of the field

$$G^{ab}(t', t) = -G^{\bar{b}\bar{a}}(t, t')^* , \quad (4.160)$$

where the star indicates complex conjugate and $\bar{a} \equiv -a$.

4.B Fermionic reservoir

We define the fermionic Keldysh Green's functions

$$i\hbar G^{ab}(t, t') \equiv \langle \psi^a(t) \bar{\psi}^b(t') \rangle , \quad (4.161)$$

where $a, b = \pm$. Like for bosons [see eqs. (4.29)], one has

$$\begin{aligned} G^{++}(t, t') &= G^{-+}(t, t')\Theta(t - t') + G^{+-}(t, t')\Theta(t' - t) , \\ G^{--}(t, t') &= G^{+-}(t, t')\Theta(t - t') + G^{-+}(t, t')\Theta(t' - t) , \end{aligned} \quad (4.162)$$

leading to the relation between Keldysh Green's functions

$$G^{++} + G^{--} = G^{+-} + G^{-+} . \quad (4.163)$$

4.B.1 Keldysh rotation

We introduce the new fermionic fields

$$\begin{cases} 2\psi^{(1)} &\equiv \psi^+ + \psi^- , & 2\bar{\psi}^{(1)} &\equiv \bar{\psi}^+ + \bar{\psi}^- , \\ \hbar\psi^{(2)} &\equiv \psi^+ - \psi^- , & \hbar\bar{\psi}^{(2)} &\equiv \bar{\psi}^+ - \bar{\psi}^- . \end{cases} \quad (4.164)$$

These definitions leads to

$$\begin{aligned} i\hbar G^{(11)}(t, t') &\equiv \langle \psi^{(1)}(t) \bar{\psi}^{(1)}(t') \rangle = i\hbar/4 [G^{++} + G^{--} + G^{-+} + G^{+-}] \equiv G^K , \\ i\hbar G^{(12)}(t, t') &\equiv \langle \psi^{(1)}(t) \bar{\psi}^{(2)}(t') \rangle = i/2 [G^{++} - G^{--} + G^{-+} - G^{+-}] \equiv -iG^R , \\ i\hbar G^{(21)}(t, t') &\equiv \langle \psi^{(2)}(t) \bar{\psi}^{(1)}(t') \rangle = i/2 [G^{++} - G^{--} - G^{-+} + G^{+-}] \equiv iG^A , \\ i\hbar G^{(22)}(t, t') &\equiv \langle \psi^{(2)}(t) \bar{\psi}^{(2)}(t') \rangle = i/\hbar [G^{++} + G^{--} - G^{-+} - G^{+-}] = 0 . \end{aligned}$$

Where we defined, *en passant*, the Keldysh G^K , the retarded G^R and the advanced G^A Green's functions in the same manner that we did for C and R in Sec. 4.2.3. Using relation (4.163) we get

$$G^K = i\hbar/2 [G^{++} + G^{--}] = i\hbar/2 [G^{+-} + G^{-+}] , \quad (4.165)$$

$$G^R = -[G^{++} - G^{+-}] = [G^{+-} - G^{-+}] \Theta(\tau) , \quad (4.166)$$

$$G^A = [G^{++} - G^{-+}] = [G^{+-} - G^{-+}] \Theta(-\tau) , \quad (4.167)$$

which are inverted as

$$i\hbar G^{ab} = G^K + \frac{i\hbar}{2} (a G^A - b G^R) . \quad (4.168)$$

4.B.2 Symmetry properties under $t \leftrightarrow t'$

Using eq. (4.160), one establishes

$$G^R(\tau) = -G^A(-\tau)^* , \quad G^K(\tau) = G^K(-\tau)^* . \quad (4.169)$$

And hence in Fourier space

$$G^R(\omega) = -G^A(\omega)^* , \quad G^K(\omega) \in \mathbb{R} . \quad (4.170)$$

4.B.3 Free fermions

Single free fermion

The free fermion Hamiltonian is

$$H = \epsilon \psi^\dagger \psi . \quad (4.171)$$

Starting from the expression in terms of operators of the Keldysh Green's functions,

$$i\hbar G^{ab}(t, t') = \text{Tr} \left[T_{\mathcal{C}} \psi_H(t, a) \psi_H^\dagger(t', b) \varrho(0) \right] , \quad (4.172)$$

with $a, b = \pm$ and the grand-canonical density matrix $\varrho(0) \propto e^{-\beta(H-\mu N)}$, one computes

$$\begin{aligned} i\hbar G^{+-}(\epsilon; \tau) &= -n_F e^{-\frac{i}{\hbar}\epsilon\tau} , \\ i\hbar G^{-+}(\epsilon; \tau) &= (1 - n_F) e^{-\frac{i}{\hbar}\epsilon\tau} . \end{aligned} \quad (4.173)$$

n_F is the Fermi factor given by $n_F(\epsilon) \equiv (1 + e^{\beta(\epsilon-\mu)})^{-1}$. After the Keldysh rotation we get

$$\begin{aligned} G^K(\epsilon; \tau) &= \frac{1}{2} \tanh \left(\beta \frac{\epsilon - \mu}{2} \right) e^{-\frac{i}{\hbar}\epsilon\tau} , \\ G^R(\epsilon; \tau) &= \frac{i}{\hbar} e^{-\frac{i}{\hbar}\epsilon\tau} \Theta(\tau) , \\ G^A(\epsilon; \tau) &= \frac{i}{\hbar} e^{-\frac{i}{\hbar}\epsilon\tau} \Theta(-\tau) . \end{aligned} \quad (4.174)$$

Collection of free fermions

For our left and right reservoirs, we consider continuous distribution (density of states) $\rho_L(\epsilon)$ and $\rho_R(\epsilon)$ of these free fermions. This yields to the Keldysh Green's functions

$$G_\alpha^{ab}(\tau) = \int d\epsilon \rho_\alpha(\epsilon) G_\alpha^{ab}(\epsilon; \tau) , \quad (4.175)$$

with $\alpha = L, R$. After a Keldysh rotation it yields

$$\begin{aligned} G^K(\tau) &= \int d\epsilon \rho(\epsilon) \frac{1}{2} \tanh[\beta(\epsilon - \mu)/2] e^{-\frac{i}{\hbar}\epsilon\tau} = \frac{1}{2} \langle \tanh[\beta(\epsilon - \mu)/2] e^{-\frac{i}{\hbar}\epsilon\tau} \rangle_\epsilon, \\ G^R(\tau) &= \int d\epsilon \rho(\epsilon) \frac{i}{\hbar} e^{-\frac{i}{\hbar}\epsilon\tau} \Theta(\tau) = \frac{i}{\hbar} \langle e^{-\frac{i}{\hbar}\epsilon\tau} \rangle_\epsilon \Theta(\tau), \\ G^A(\tau) &= \int d\epsilon \rho(\epsilon) \frac{i}{\hbar} e^{-\frac{i}{\hbar}\epsilon\tau} \Theta(-\tau) = \frac{i}{\hbar} \langle e^{-\frac{i}{\hbar}\epsilon\tau} \rangle_\epsilon \Theta(-\tau), \end{aligned} \quad (4.176)$$

where we introduced a short-hand notation for the integration over energy levels. In terms of the Fourier transforms of $\rho(\epsilon)$ it reads

$$G^R(\tau) = \frac{i}{\hbar} 2\pi\rho(\tau/\hbar)\Theta(\tau), \quad G^A(\tau) = \frac{i}{\hbar} 2\pi\rho(\tau/\hbar)\Theta(-\tau). \quad (4.177)$$

Fourier transforms

$$\begin{aligned} G^K(\omega) &= \pi\hbar \tanh\left(\beta \frac{\hbar\omega - \mu}{2}\right) \rho(\hbar\omega) \in \mathbb{R}, \\ G^R(\omega) + G^A(\omega) &= 2i\pi\rho(\hbar\omega) \in i\mathbb{R}. \end{aligned} \quad (4.178)$$

Since $\rho(\epsilon)$ is real, one computes

$$\text{Im} G^R(\omega) = \pi\rho(\hbar\omega). \quad (4.179)$$

Thus we get, as a check, the grand-canonical fermionic fluctuation-dissipation theorem that is established generally in Sec. 4.C:

$$G^K(\omega) = \hbar \tanh\left(\beta \frac{\hbar\omega - \mu}{2}\right) \text{Im} G^R(\omega). \quad (4.180)$$

4.C Fluctuation-Dissipation Theorem

In this Section we give a proof of the fluctuation-dissipation theorem both in its bosonic and fermionic versions. This theorem only holds in equilibrium and gives a relation between the Green's functions. In the grand-canonical ensemble, the initial density operator reads $\varrho(0) \propto \exp(-\beta(H - \mu N))$, where N is the number operator commuting with H (in non-relativistic quantum mechanics), μ is the chemical potential fixing the average number of particles. One can obtain the theorem for the canonical ensemble by formally setting $\mu = 0$. Let us consider a pair of either bosonic or fermionic operators, for instance creation and annihilation operators ϕ^\dagger and ϕ . Let us write the following Keldysh Green's function

$$i\hbar G^{+-}(t, t') = \text{Tr} \left[T_C \phi_H(t, +) \phi_H^\dagger(t', -) \varrho(0) \right]. \quad (4.181)$$

By resolving the time-ordering we get

$$i\hbar G^{+-}(t, t') = \zeta \operatorname{Tr} \left[\phi_H^\dagger(t') \phi_H(t) \varrho(0) \right] , \quad (4.182)$$

with $\zeta = +1$ in the bosonic case and $\zeta = -1$ in the fermionic case. Using the *analyticity* of the Green's functions and then expanding $\phi_H(t + i\beta\hbar) = \exp(-\beta H) \phi_H(t) \exp(+\beta H)$, we get

$$i\hbar G^{+-}(t + i\beta\hbar, t') = \zeta \operatorname{Tr} \left[\phi_H^\dagger(t') \phi_H(t + i\beta\hbar) \varrho(0) \right] \quad (4.183)$$

$$\propto \zeta \operatorname{Tr} \left[\phi_H^\dagger(t') \exp(-\beta H) \phi_H(t) \exp(\beta\mu N) \right] . \quad (4.184)$$

Since H and N commute and since for any operator $f(N)$, one has $\phi f(N) = f(N+1)\phi$, we have

$$\phi_H(t) \exp(\beta\mu N) = \exp(\beta\mu(N+1)) \phi_H(t) , \quad (4.185)$$

and so

$$i\hbar G^{+-}(t + i\beta\hbar, t') = \zeta \exp(\beta\mu) \operatorname{Tr} \left[\phi_H^\dagger(t') \varrho(0) \phi_H(t) \right] . \quad (4.186)$$

Using the *cyclicity* of the trace, we come to

$$i\hbar G^{+-}(t + i\beta\hbar, t') = \zeta \exp(\beta\mu) \operatorname{Tr} \left[\phi_H(t) \phi_H^\dagger(t') \varrho(0) \right] \quad (4.187)$$

$$= \zeta \exp(\beta\mu) i\hbar G^{-+}(t, t') . \quad (4.188)$$

If the system is in equilibrium, the *time translational invariance* of the previous equation gives the KMS relation:

$$G^{+-}(\omega) \exp(\beta\hbar\omega) = \zeta \exp(\beta\mu) G^{-+}(\omega) . \quad (4.189)$$

Using eqs. (4.166) and (4.167), we have on the one hand

$$G^R(\omega) + G^A(\omega) = G^{+-}(\omega)(1 - \zeta \exp(\beta(\hbar\omega - \mu))) . \quad (4.190)$$

On the other hand eq. (4.165) implies

$$G^K(\omega) = \frac{i\hbar}{2} G^{+-}(\omega) [1 + \zeta \exp(\beta(\hbar\omega - \mu))] . \quad (4.191)$$

These two last relations yield the grand-canonical quantum FDT:

$$G^K(\omega) = \hbar \tanh \left(\beta \frac{\hbar\omega - \mu}{2} \right)^{-\zeta} \operatorname{Im} G^R(\omega) . \quad (4.192)$$

4.D Computing the self-energy

4.D.1 Derivation within the Schwinger-Keldysh formalism

In the Schwinger-Keldysh path-integral representation we had (see eq. (4.20)) for the whole system (rotors and environment)

$$\mathcal{Z}[\mathbf{h}^\pm] \equiv \int_{\mathcal{C}} \mathcal{D}[\mathbf{s}^\pm, \boldsymbol{\psi}^\pm, \bar{\boldsymbol{\psi}}^\pm] e^{\frac{i}{\hbar} S_{\text{tot}}[\mathbf{s}^\pm, \boldsymbol{\psi}^\pm, \bar{\boldsymbol{\psi}}^\pm]} \langle \mathbf{s}^+(0), \bar{\boldsymbol{\psi}}^+(0) | \varrho_{\text{tot}}(0) | \mathbf{s}^-(0), \boldsymbol{\psi}^-(0) \rangle ,$$

At time $t = 0$, just after the quench, the initial density is assumed to be factorized: $\varrho_{\text{tot}}(0) = I \otimes \varrho_L^{\text{free}}(0) \otimes \varrho_R^{\text{free}}(0)$ (see Sec. 4.2.1) yielding

$$\begin{aligned} & \langle \mathbf{s}^+(0), \bar{\boldsymbol{\psi}}^+(0) | \varrho_{\text{tot}}(0) | \mathbf{s}^-(0), \bar{\boldsymbol{\psi}}^-(0) \rangle \\ &= \delta(\mathbf{s}^+(0) - \mathbf{s}^-(0)) \langle \bar{\boldsymbol{\psi}}_L^+(0) | \varrho_L^{\text{free}}(0) | \boldsymbol{\psi}_L^-(0) \rangle \langle \bar{\boldsymbol{\psi}}_R^+(0) | \varrho_R^{\text{free}}(0) | \boldsymbol{\psi}_R^-(0) \rangle . \end{aligned}$$

The generating functional reads

$$\mathcal{Z}[\mathbf{h}^\pm] = \int_{\mathcal{C}'} \mathcal{D}[\mathbf{s}^+, \mathbf{s}^-] e^{\frac{i}{\hbar} S_{\text{tot}}[\mathbf{s}^+, \mathbf{s}^-, \mathbf{h}]} \langle \langle e^{\frac{i}{\hbar} S_{\text{int}}[\mathbf{s}^+, \boldsymbol{\psi}^+, \bar{\boldsymbol{\psi}}^+, \mathbf{s}^-, \boldsymbol{\psi}^-, \bar{\boldsymbol{\psi}}^-]} \rangle_L \rangle_R . \quad (4.193)$$

The index c' at the bottom of the integral is here to remind the constraints on the field integration, namely $\mathbf{s}_i^+(t)^2 = \mathbf{s}_i^-(t)^2 = 1$ and $\mathbf{s}_i^+(0) = \mathbf{s}_i^-(0) \forall i$. We introduced the average over the free environment composed of the two reservoirs:

$$\begin{aligned} \langle \langle \cdots \rangle_L \rangle_R &\equiv \int \mathcal{D}[\boldsymbol{\psi}^\pm, \bar{\boldsymbol{\psi}}^\pm] \cdots e^{\frac{i}{\hbar} S_L^L} e^{\frac{i}{\hbar} S_R^R} \\ &\quad \times \langle \bar{\boldsymbol{\psi}}_L^+(0) | \varrho_L^{\text{free}}(0) | \boldsymbol{\psi}_L^-(0) \rangle \langle \bar{\boldsymbol{\psi}}_R^+(0) | \varrho_R^{\text{free}}(0) | \boldsymbol{\psi}_R^-(0) \rangle . \end{aligned} \quad (4.194)$$

We now develop the coupling $e^{\frac{i}{\hbar} S_{\text{int}}}$ up to the second order,

$$\langle \langle e^{\frac{i}{\hbar} S_{\text{int}}} \rangle_L \rangle_R \simeq 1 + \frac{i}{\hbar} \langle \langle S_{\text{int}} \rangle_L \rangle_R - \frac{1}{2\hbar^2} \langle \langle S_{\text{int}}^2 \rangle_L \rangle_R . \quad (4.195)$$

The first order term is zero. The second order term reads

$$\begin{aligned} \langle \langle S_{\text{int}}^2 \rangle_L \rangle_R &= n \left(\frac{\hbar\omega_c}{N_s} \right)^2 \sum_{ab=\pm} ab \int \int_0^\infty dt dt' \sum_{ij=1}^N \sum_{kk'qq'=1}^{N_s} \sum_{\mu\nu=1}^n \sum_{ll'mm'=1}^M \\ &\quad \times s_i^{\mu a}(t) s_j^{\nu b}(t') \sigma_{ll'}^\mu \sigma_{mm'}^\nu \\ &\quad \times \langle \langle [\bar{\psi}_{Likl}^a(t) \psi_{Rik'l'}^a(t) + L \leftrightarrow R] [\bar{\psi}_{Ljqm}^b(t') \psi_{Rjq'm'}^b(t') + L \leftrightarrow R] \rangle_L \rangle_R . \end{aligned} \quad (4.196)$$

Developing the term on the second line, we obtain

$$\begin{aligned} & \langle \langle [\bar{\psi}_{Likl}^a(t) \psi_{Rik'l'}^a(t) + L \leftrightarrow R] [\bar{\psi}_{Ljqm}^b(t') \psi_{Rjq'm'}^b(t') + L \leftrightarrow R] \rangle_L \rangle_R \\ &= \langle \langle \bar{\psi}_{Rikl}^a(t) \psi_{Lik'l'}^a(t) \bar{\psi}_{Ljqm}^b(t') \psi_{Rjq'm'}^b(t') + L \leftrightarrow R \rangle_L \rangle_R \\ &= -\langle \psi_{Lik'l'}^a(t) \bar{\psi}_{Ljqm}^b(t') \rangle_L \langle \psi_{Rjq'm'}^b(t') \bar{\psi}_{Rikl}^a(t) \rangle_R + L \leftrightarrow R \\ &= \delta_{ij} \delta_{k'q} \delta_{kq'} \delta_{l'm} \delta_{lm'} \hbar^2 \left[G_{Lk'}^{ab}(t, t') G_{Rk}^{ba}(t', t) + L \leftrightarrow R \right] . \end{aligned} \quad (4.197)$$

With the free fermionic Green's functions defined on the Keldysh contour as $i\hbar G_{\alpha k}^{ab}(t, t') = \langle \psi_k^a(t) \bar{\psi}_k^b(t') \rangle_\alpha$ for $\alpha = L, R$, $a, b = \pm$ and where k labels the electron's energy. Expression (4.196) now reads

$$\begin{aligned} \langle S_{\text{int}}^2 \rangle_{LR} = & \hbar^2 n \left(\frac{\hbar \omega_c}{N_s} \right)^2 \sum_{ab=\pm} ab \iint_0^\infty dt dt' \sum_{i=1}^N \sum_{kk'=1}^{N_s} \sum_{\mu\nu=1}^n \sum_{ll'=1}^M s_i^{\mu a}(t) s_i^{\nu b}(t') \sigma_{ll'}^\mu \sigma_{ll'}^\nu \\ & \times \left[G_{Lk'}^{ab}(t, t') G_{Rk}^{ba}(t', t) + L \leftrightarrow R \right]. \end{aligned} \quad (4.198)$$

By using the property $\text{Tr } \sigma^\mu \sigma^\nu = \delta_{\mu\nu}$, we get

$$\begin{aligned} \langle S_{\text{int}}^2 \rangle_{LR} = & n \hbar^2 \left(\frac{\hbar \omega_c}{N_s} \right)^2 \sum_{ab=\pm} ab \iint_0^\infty dt dt' \sum_{i=1}^N \mathbf{s}_i^a(t) \cdot \mathbf{s}_i^b(t') \\ & \times \sum_{kk'} \left[G_{Lk'}^{ab}(t, t') G_{Rk}^{ba}(t', t) + L \leftrightarrow R \right]. \end{aligned} \quad (4.199)$$

Finally expression (4.195) can be recast into

$$\langle \langle e^{\frac{i}{\hbar} S_{\text{int}}} \rangle_L \rangle_R \simeq e^{\frac{i}{\hbar} S_{\text{int}}^{(2)}}, \quad (4.200)$$

with

$$S_{\text{int}}^{(2)}[\mathbf{s}^+, \mathbf{s}^-] \equiv -\frac{1}{2} n \sum_{ab=\pm} \iint_0^{+\infty} dt dt' \Sigma_{\text{env}}^{ab}(t, t') \sum_{i=1}^N \mathbf{s}_i^a(t) \cdot \mathbf{s}_i^b(t'), \quad (4.201)$$

where the exponent (2) is here to recall that we developed until second order and with the self-energy

$$\Sigma_{\text{env}}^{ab}(t, t') \equiv -abi\hbar (\hbar \omega_c)^2 \left[G_L^{ab}(t, t') G_R^{ba}(t', t) + G_R^{ab}(t, t') G_L^{ba}(t', t) \right], \quad (4.202)$$

where the Keldysh Green's functions of the fermions in the α -reservoir ($\alpha = L, R$) are given by

$$G_\alpha^{ab}(t, t') \equiv \int d\epsilon_\alpha \rho_\alpha(\epsilon_\alpha) G_\alpha^{ab}(\epsilon_\alpha; t - t') = G_\alpha^{ab}(t - t'). \quad (4.203)$$

$\rho_\alpha(\epsilon)$ is the density of states in α -reservoir and $G_\alpha^{ab}(\epsilon; \tau)$ are the Keldysh Green's functions of a free fermion with energy ϵ in equilibrium in the α -reservoir (see App. 4.B.3):

$$\begin{aligned} i\hbar G_\alpha^{+-}(\epsilon; \tau) &= -n_\alpha(\epsilon) e^{-\frac{i}{\hbar} \epsilon \tau}, \\ i\hbar G_\alpha^{-+}(\epsilon; \tau) &= [1 - n_\alpha(\epsilon)] e^{-\frac{i}{\hbar} \epsilon \tau}, \\ i\hbar G_\alpha^{++}(\epsilon; \tau) &= i\hbar G_\alpha^{-+}(\epsilon; \tau) \Theta(\tau) + i\hbar G_\alpha^{+-}(\epsilon; \tau) \Theta(-\tau), \\ i\hbar G_\alpha^{--}(\epsilon; \tau) &= i\hbar G_\alpha^{+-}(\epsilon; \tau) \Theta(\tau) + i\hbar G_\alpha^{-+}(\epsilon; \tau) \Theta(-\tau), \end{aligned} \quad (4.204)$$

with the Fermi factor $n_\alpha(\epsilon) \equiv (1 + e^{\beta_\alpha(\epsilon - \mu_\alpha)})^{-1}$. It is clear then that the self-energy is time translational invariant: $\Sigma_{\text{env}}^{ab}(t, t') \equiv \Sigma_{\text{env}}^{ab}(\tau)$ with $\tau \equiv t - t'$. Moreover $\Sigma_{\text{env}}^{ab}(\tau)$ is a symmetric matrix with respect to time and Keldysh indices:

$$\Sigma_{\text{env}}^{ab}(\tau) = \Sigma_{\text{env}}^{ba}(-\tau), \quad (4.205)$$

Using the time reversal property eq. (4.160) of the Keldysh Green's functions one also establishes

$$\Sigma_{\text{env}}^{ab}(\tau)^* = -\Sigma_{\text{env}}^{\bar{a}\bar{b}}(\tau), \quad (4.206)$$

where we note $\bar{a} \equiv -a$.

After a Keldysh rotation of the rotors coordinates, it yields

$$\frac{i}{\hbar} S_{\text{int}}^{(2)}[\mathbf{s}^{(1)}, \mathbf{s}^{(2)}] = \frac{1}{2} n \sum_{rs=(1),(2)} \int \int_0^\infty dt dt' \Sigma_{\text{env}}^{rs}(t, t') \sum_{i=1}^N \mathbf{s}_i^r(t) \mathbf{s}_i^s(t'), \quad (4.207)$$

with

$$\begin{aligned} \Sigma_{\text{env}}^{(22)} &= -i\hbar/2 [\Sigma_{\text{env}}^{++} + \Sigma_{\text{env}}^{--}] , \\ \Sigma_{\text{env}}^{(21)} &= -i [\Sigma_{\text{env}}^{++} + \Sigma_{\text{env}}^{+-}] , \\ \Sigma_{\text{env}}^{(12)} &= -i [\Sigma_{\text{env}}^{++} + \Sigma_{\text{env}}^{-+}] , \\ \Sigma_{\text{env}}^{(11)} &= -i/\hbar [\Sigma_{\text{env}}^{++} + \Sigma_{\text{env}}^{+-} + \Sigma_{\text{env}}^{-+} + \Sigma_{\text{env}}^{--}] = 0 . \end{aligned} \quad (4.208)$$

which is inverted as

$$i\hbar \Sigma_{\text{env}}^{ab} = -ab \Sigma_{\text{env}}^{(22)} - \frac{\hbar}{2} \left(a \Sigma_{\text{env}}^{(21)} + b \Sigma_{\text{env}}^{(12)} \right) . \quad (4.209)$$

4.D.2 FDT check

We checked that the fermion-reservoir self-energy satisfies the bosonic FDT. This is only valid when the reservoirs constitute an equilibrium bath, *i.e.* $\beta_L = \beta_R = \beta$ and $\mu_L = \mu_R = \mu_0$ ($V = 0$). Note that distribution functions $\rho_L(\omega)$ and $\rho_R(\omega)$ can be different although the proof given below uses $\rho_L(\omega) = \rho_R(\omega) = \rho(\epsilon)$ for simplicity reasons. The goal is to check

$$\Sigma_{\text{env}}^K(\omega) = \hbar \coth\left(\beta \frac{\hbar\omega}{2}\right) \text{Im} \Sigma_{\text{env}}^R(\omega) = \hbar \coth\left(\beta \frac{\hbar\omega}{2}\right) \frac{[\Sigma_{\text{env}}^R + \Sigma_{\text{env}}^A](\omega)}{2i} . \quad (4.210)$$

We first develop the term in the LHS, then we do the same with the RHS to prove their equality.

$$\begin{aligned} \Sigma_{\text{env}}^K(\omega) &= \text{TF} \Sigma_{\text{env}}^K(\tau) \\ &= -2(\hbar\omega_c)^2 \text{TF} \{G^K G^{K*} - \hbar^2/4 [G^A G^{A*} + G^R G^{R*}]\} \\ &= -2(\hbar\omega_c)^2 \text{TF} \{G^K G^{K*} - \hbar^2/4 [G^R + G^A] [G^{R*} + G^{A*}]\} , \end{aligned}$$

where we used the nullity of cross terms of the type $G^R G^A$ since $G^R \propto \Theta(\tau)$ and $G^A \propto \Theta(-\tau)$.

$$\Sigma_{\text{env}}^K(\omega) = -2(\hbar\omega_c)^2 \{G^K \circ G^{K*} - \hbar^2/4 [G^R + G^A] \circ [G^{R*} + G^{A*}]\}, \quad (4.211)$$

where \circ is the symbol for the convolution (see App. 4.A) and $G^{R*}(\omega)$ stands for the Fourier transform of $G^R(\tau)^*$. Since we easily obtain

$$\begin{aligned} G^R(\omega) + G^A(\omega) &= 2i\pi\rho(\hbar\omega), \\ G^{R*}(\omega) + G^{A*}(\omega) &= -2i\pi\rho(-\hbar\omega), \end{aligned} \quad (4.212)$$

and

$$\begin{aligned} G^K(\omega) &= \pi\hbar\rho(\hbar\omega) \tanh\left(\beta\frac{\hbar\omega-\mu_0}{2}\right), \\ G^{K*}(\omega) &= \pi\hbar\rho(-\hbar\omega) \tanh\left(\beta\frac{-\hbar\omega-\mu_0}{2}\right), \end{aligned} \quad (4.213)$$

we get by replacing in (4.211)

$$\begin{aligned} \Sigma_{\text{env}}^K(\omega) &= -2(\hbar\omega_c)^2(\pi\hbar)^2 \\ &\times \left\{ \left[\rho(\hbar\omega) \tanh\left(\beta\frac{\hbar\omega-\mu_0}{2}\right) \right] \circ \left[\rho(-\hbar\omega) \tanh\left(\beta\frac{-\hbar\omega-\mu_0}{2}\right) \right] - [\rho(\hbar\omega)] \circ [\rho(-\hbar\omega)] \right\} \\ &= -2(\hbar\omega_c)^2(\pi\hbar) \int \frac{d\epsilon'}{2\pi} \rho(\epsilon') \rho(\epsilon' - \hbar\omega) \left\{ \tanh\left(\beta\frac{\epsilon'-\mu_0}{2}\right) \tanh\left(\beta\frac{\epsilon'-\hbar\omega-\mu_0}{2}\right) - 1 \right\} \\ &= -\pi\hbar(\hbar\omega_c)^2 \coth\left(\beta\frac{\hbar\omega}{2}\right) \int d\epsilon' \rho(\epsilon') \rho(\epsilon' - \hbar\omega) \left\{ \tanh\left(\beta\frac{\epsilon'-\hbar\omega-\mu_0}{2}\right) - \tanh\left(\beta\frac{\epsilon'-\mu_0}{2}\right) \right\}, \end{aligned} \quad (4.214)$$

where we used the trigonometry relation

$$\tanh(x - y) = \frac{\tanh x - \tanh y}{1 - \tanh x \tanh y}.$$

Let's now calculate the Rhs of (4.210).

$$\begin{aligned} \frac{[\Sigma_{\text{env}}^R + \Sigma_{\text{env}}^A](\omega)}{2i} &= i(\hbar\omega_c)^2 \text{TF} \{G^R G^{K*} + G^A G^{K*} + G^K G^{R*} + G^K G^{A*}\} \\ &= i(\hbar\omega_c)^2 \text{TF} \{(G^R + G^A)G^{K*} + G^K(G^{R*} + G^{A*})\} \\ &= i(\hbar\omega_c)^2 \{[G^R + G^A] \circ [G^{K*}] + [G^K] \circ [G^{R*} + G^{A*}]\}, \end{aligned}$$

giving

$$\begin{aligned} &\hbar \coth\left(\beta\frac{\hbar\omega}{2}\right) \frac{[\Sigma_{\text{env}}^R + \Sigma_{\text{env}}^A](\omega)}{2i} \\ &= -2(\pi\hbar)^2(\hbar\omega_c)^2 \coth\left(\beta\frac{\hbar\omega}{2}\right) \\ &\times \left\{ [\rho(\hbar\omega)] \circ \left[\rho(-\hbar\omega) \tanh\left(\beta\frac{-\hbar\omega-\mu_0}{2}\right) \right] - \left[\rho(\hbar\omega) \tanh\left(\beta\frac{\hbar\omega-\mu_0}{2}\right) \right] \circ [\rho(-\hbar\omega)] \right\} \\ &= -\pi\hbar(\hbar\omega_c)^2(2\pi\hbar) \coth\left(\beta\frac{\hbar\omega}{2}\right) \int d\epsilon' \rho(\epsilon') \rho(\epsilon' - \hbar\omega) \\ &\times \left\{ \tanh\left(\beta\frac{\epsilon'-\hbar\omega-\mu_0}{2}\right) - \tanh\left(\beta\frac{\epsilon'-\mu_0}{2}\right) \right\}. \end{aligned}$$

We recognize here the development (4.214) of Σ_{env}^K . We just proved that the bosonic FDT is satisfied provided that the two fermionic reservoirs have the same temperature and chemical potential. They can have a different density of states.

4.E Dynamics

4.E.1 Quadratic effective action

One can render the effective action quadratic at the price of introducing new fields. For a given i and a given pair of (r, μ, t) and (s, ν, t') , the identity

$$1 = \int dQ_{i\mu\nu}^{rs}(t, t') \delta(s_i^{\mu r}(t) s_i^{\nu s}(t') - Q_{i\mu\nu}^{rs}(t, t')) , \quad (4.215)$$

becomes, after using the integral representation of the delta distribution (see App. 4.A),

$$1 \propto \int dQ_{i\mu\nu}^{rs}(t, t') d\lambda_{i\mu\nu}^{rs}(t, t') \exp\left(-i\frac{n}{2}\lambda_{i\mu\nu}^{rs}(t, t') (s_i^{\mu r}(t) s_i^{\nu s}(t') - Q_{i\mu\nu}^{rs}(t, t'))\right) .$$

Introducing similar identities for all possible pairs of (r, μ, t) and (s, ν, t') , we obtain a path integral over two³ fields $Q_{i\mu\nu}^{rs}(t, t')$ and $\lambda_{i\mu\nu}^{rs}(t, t')$ that are symmetric in the Keldysh indices, times and rotor components: $Q_{i\nu\mu}^{sr}(t', t) = Q_{i\mu\nu}^{rs}(t, t')$ and $\lambda_{i\nu\mu}^{sr}(t', t) = \lambda_{i\mu\nu}^{rs}(t, t')$. The effective action is now also a functional of Q and λ and reads

$$\begin{aligned} \frac{i}{\hbar} S_{\text{eff}} = & -\frac{n}{2} \sum_{r,s=(1),(2)} \iint dt dt' \sum_i \sum_{\mu\nu} s_i^{\mu r}(t) [Op_{i\mu\nu}^{rs}(t, t') + i\lambda_{i\mu\nu}^{rs}(t, t')] s_i^{\nu s}(t') \\ & + \frac{J^2 n^2}{2N} \sum_{i,j} \iint dt dt' \sum_{\mu,\nu} Q_{i\mu\nu}^{(11)}(t, t') Q_{j\mu\nu}^{(22)}(t, t') + Q_{i\mu\nu}^{(12)}(t, t') Q_{j\mu\nu}^{(21)}(t, t') \\ & + \frac{i}{\hbar} \frac{n}{2} \sum_a \int dt \sum_i z_i^a(t) + i\frac{n}{2} \sum_{rs} \iint dt dt' \sum_i \sum_{\mu\nu} \lambda_{i\mu\nu}^{rs}(t, t') Q_{i\mu\nu}^{rs}(t, t') \\ & + \text{boundary terms} , \end{aligned}$$

where we introduced the operator $Op_{i\mu\nu}^{rs}(t, t')$ defined as

$$\begin{aligned} Op_{i\mu\nu}^{(12)}(t, t') & \equiv i\delta_{\mu\nu}\delta(t-t') \left[\frac{1}{\Gamma} \partial_{t'}^2 + \frac{1}{2} \sum_{a=\pm} z_i^a(t) \right] - i\delta_{\mu\nu} \Sigma_{\text{env}}^R(t', t) , \\ Op_{i\mu\nu}^{(21)}(t, t') & \equiv Op_{i\nu\mu}^{(12)}(t', t) , \\ Op_{i\mu\nu}^{(22)}(t, t') & \equiv \frac{i\hbar}{4} \delta_{\mu\nu} \delta(t-t') \sum_{a=\pm} a z_i^a(t) + \delta_{\mu\nu} \Sigma_{\text{env}}^K(t, t') , \\ Op_{i\mu\nu}^{(11)}(t, t') & \equiv \frac{i}{2\hbar} \delta_{\mu\nu} \delta(t-t') \sum_{a=\pm} a z_i^a(t) . \end{aligned} \quad (4.216)$$

$Op_{i\mu\nu}^{rs}(t, t')$ is symmetric in the Keldysh indices, times and rotor components: $Op_{i\nu\mu}^{sr}(t', t) = Op_{i\mu\nu}^{rs}(t, t')$. The functional integration over $s_i^{\mu r}$ is now quadratic and can be performed,

3. There are $N(n^2 K^2 + nK)/2$ of each of these fields, where $K = 2$ is the number of possible Keldysh indices.

leading to

$$\begin{aligned} \frac{i}{\hbar} S_{\text{eff}} = & -\frac{1}{2} \text{Tr} \ln n (Op + i\lambda) \\ & -\frac{J^2 n^2}{2N} \sum_{i,j} \iint dt dt' \sum_{\mu,\nu} Q_{i\mu\nu}^{(11)}(t,t') Q_{j\mu\nu}^{(22)}(t,t') + Q_{i\mu\nu}^{(12)}(t,t') Q_{j\mu\nu}^{(21)}(t,t') \\ & + \frac{i}{\hbar} \frac{n}{2} \sum_a \int dt \sum_i z_i^a(t) + i \frac{n}{2} \sum_{rs} \iint dt dt' \sum_i \sum_{\mu\nu} \lambda_{i\mu\nu}^{rs}(t,t') Q_{i\mu\nu}^{rs}(t,t') \end{aligned} \quad (4.217)$$

where the trace in the first term is spanning the whole space of indices, namely rotor sites, Keldysh indices, times and rotor components.

4.E.2 Saddle-point evaluation

In this subsection, we evaluate in the limit $nN \rightarrow \infty$ the saddle-point equations with respect to the dummy fields we introduced previously, namely $\lambda_{i\mu\nu}^{rs}(t,t')$, $Q_{i\mu\nu}^{rs}(t,t')$ and $z_i^a(t)$. The fluctuations around the saddle are neglected. In particular, using eq. (4.215) we have the identity (see the definition of Green's functions in Sec. 4.2.3)

$$Q_{i\mu\nu}^{rs}(t,t') = i\hbar G_{i\mu\nu}^{rs}(t,t') . \quad (4.218)$$

Along the lines we prove that the solution in the saddle is $O(N)$ and $O(n)$, like the starting Hamiltonian.

The saddle-point with respect to $\lambda_{i\mu\nu}^{rs}(t,t')$ yields

$$\frac{\delta S_{\text{eff}}}{\delta \lambda_{i\mu\nu}^{rs}(t,t')} = -\frac{1}{2} \text{Tr} \frac{\delta}{\delta \lambda_{i\mu\nu}^{rs}(t,t')} \ln n (Op + i\lambda) + i \frac{n}{2} Q_{i\mu\nu}^{rs}(t,t') = 0 , \quad (4.219)$$

giving in matrix notations

$${}^t(Op + i\lambda)^{-1} = nQ , \quad (4.220)$$

where the symbol t represents the transposition. Since all operators in the last equation are symmetric by definition, we get

$$Op + i\lambda = \frac{1}{n} Q^{-1} . \quad (4.221)$$

The saddle-point equation with respect to $Q_{i\mu\nu}^{rs}(t,t')$ yields

$$i\lambda_{i\mu\nu}^{rs}(t,t') = \frac{J^2 n}{N} \sum_j Q_{j\mu\nu}^{\bar{r}\bar{s}}(t,t') \quad \forall i , \quad (4.222)$$

where $\overline{(2)} \equiv (1)$ and $\overline{(1)} \equiv (2)$. The Rhs of this last equation being site-independent, $\lambda_{i\mu\nu}^{rs}(t, t')$ does not depend on i : $\lambda_{i\mu\nu}^{rs}(t, t') = \lambda_{\mu\nu}^{rs}(t, t')$. Equations (4.221) and (4.222) imply

$$Op_i^{rs} + \frac{J^2 n}{N} \sum_j Q_j^{\bar{r}\bar{s}} - \frac{1}{n} Q^{-1} i^{rs} = 0. \quad (4.223)$$

The saddle-point equation with respect to $z_i^a(t)$ yields to the two equations:

$$\begin{aligned} \sum_{\mu} \left([Op + i\lambda]^{-1} \right)_{i\mu\mu}^{(12)}(t, t) + \left([Op + i\lambda]^{-1} \right)_{i\mu\mu}^{(21)}(t, t) &= 0, \\ \sum_{\mu} \left([Op + i\lambda]^{-1} \right)_{i\mu\mu}^{(11)}(t, t) + \frac{\hbar^2}{4} \left([Op + i\lambda]^{-1} \right)_{i\mu\mu}^{(22)}(t, t) &= n. \end{aligned} \quad (4.224)$$

This is nothing more than the constraint that rotors should have a unit length. However, λ being site-independent, it is clear from these equations that it has to be the same for Op . Finally at the saddle, Op , Q and z are site-independent (homogeneous) so we can get rid of the sites indices: $Op_{i\mu\nu}^{rs}(t, t') = Op_{\mu\nu}^{rs}(t, t')$, $Q_{i\mu\nu}^{rs}(t, t') = Q_{\mu\nu}^{rs}(t, t')$ and $z_i^a(t) = z^a(t)$. Equation (4.223) becomes

$$Op^{rs} + J^2 n Q^{\bar{r}\bar{s}} - \frac{1}{n} Q^{-1}{}^{rs} = 0. \quad (4.225)$$

Since from its definition (4.216) $Op_{\mu\nu}^{rs}(t, t') \propto \delta_{\mu\nu}$, the previous equation tells us that it has to be the same for $Q_{\mu\nu}^{rs}(t, t')$ so we can get rid of all the rotor component indices. Multiplying by $Q^{sv}(t', t'')$, and summing over s and t' , we get

$$\int dt' \sum_s Op^{rs}(t, t') Q^{sv}(t', t'') + J^2 n Q^{\bar{r}\bar{s}}(t, t') Q^{sv}(t', t'') - \frac{1}{n} \delta_{rv} \delta(t - t'') = 0. \quad (4.226)$$

The macroscopic Green's function reading $i\hbar G^{rs}(t, t') = n Q^{rs}(t, t')$ we obtain

$$\epsilon_v \int dt' \sum_s Op^{rs}(t, t') i\hbar G^{sv}(t', t'') + J^2 i\hbar G^{\bar{r}\bar{s}}(t, t') i\hbar G^{sv}(t', t'') - \delta_{rv} \delta(t - t'') = 0. \quad (4.227)$$

4.E.3 Schwinger-Dyson equations

The $(r = (2), v = (1))$ component of eq. (4.227) gives a complex equation the real part of which yields

$$z^+(t) = z^-(t) \equiv z(t) \forall t, \quad (4.228)$$

and the imaginary part of which is the dynamic equation for the self-correlation:

$$\left[\frac{1}{\Gamma} \frac{\partial^2}{\partial t^2} + z(t) \right] C(t, t') = \int_0^{t'} dt'' \Sigma^K(t, t'') R(t', t'') + \int_0^t dt'' \Sigma^R(t, t'') C(t'', t'), \quad (4.229)$$

where we introduced

$$\Sigma^K \equiv J^2 C + \Sigma_{\text{env}}^K, \quad \Sigma^R \equiv J^2 R + \Sigma_{\text{env}}^R. \quad (4.230)$$

Similarly, the $(r = (2), v = (2))$ component of eq. (4.227) yields the equation of motion for the self-response:

$$\left[\frac{1}{\Gamma} \frac{\partial^2}{\partial t^2} + z(t) \right] R(t, t') = \delta(t - t') + \int_{t'}^t dt'' \Sigma^R(t, t'') R(t'', t'). \quad (4.231)$$

The $(r = (1), v = (1))$ component of eq. (4.227) leads to the same equation and the $(r = (1), v = (2))$ component expresses $0 = 0$. Setting $t' = t$ in eq. (4.229) we obtain the expression for the Lagrange multiplier

$$z(t) = \int_0^t dt'' \Sigma^K(t, t'') R(t, t'') + \Sigma^R(t, t'') C(t, t'') - \frac{1}{\Gamma} \frac{\partial^2 C}{\partial t^2}(t, t' \rightarrow t^-). \quad (4.232)$$

Equations (4.229) and (4.231) together with eq. (4.232) constitute the Schwinger-Dyson equations that fully determine the dynamics of the interacting system.

CONCLUSIONS AND OUTLOOK

IN this manuscript, we studied some aspects of the dynamics of systems coupled to an environment. We first had some formal considerations on the classical equilibrium dynamics. We started from the Langevin equation which gives a heuristic modeling of the interactions between a system and its thermal environment. We did not restrict ourselves to the Markovian case and to additive noise, but we coped with inertial systems coupled to a generic multiplicative and colored bath. By considering the associated MSRJD path-integral formalism, we showed that equilibrium dynamics can be seen as a symmetry at the level of the MSRJD action and more generally as a symmetry of the corresponding generating functional. At the level of observables, the corresponding Ward-Takahashi identities yield all the equilibrium theorems.

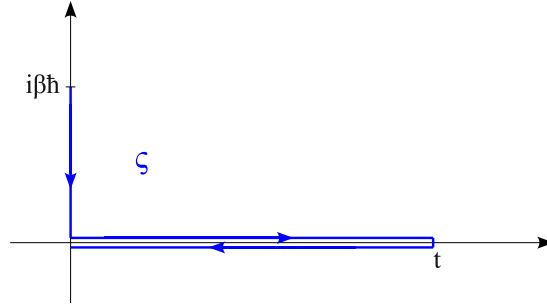
We then turned to out-of-equilibrium situations where we showed how the broken symmetry naturally gives rise to all the fluctuation theorems at the level of observables. Furthermore, we exhibited another symmetry of the MSRJD generating functional, valid out of equilibrium, that yields Schwinger-Dyson-type equations which correlations and responses. They are of particular interest for numerical simulations where the possibility to compute responses without applying any extra-field – but *via* correlations – is often of great help.

From the third chapter and on, we left these formal and system-independent considerations to focus on some of the aspects of out-of-equilibrium dynamics. We looked at the scaling relations in the dynamics that take place after a quench that drives the system through a phase transition. We placed the emphasis on scaling relations in the long-time dynamics, and more specifically, on the super-universality conjecture. By means of numer-

ical simulations, we compared the aging dynamics of a $3d$ Ising ferromagnet with random fields (RFIM) to the ones of a $3d$ Ising spin glass (EA). The former is an archetypal model of coarsening phenomena with weak disorder whereas the latter is probably the simplest model for a $3d$ glass. In both cases we showed that global observables obey some scaling relations once lengths and times are measured in units of a growing length we exhibited for each case. We also proved that the distribution of a local observable – namely the coarse-grained two-time correlation function – exhibits the same kind of scaling property. However, as far as super-universality is concerned, both models differs since the spin glass does not show super-universal scalings contrary to the ferromagnet.

In the fourth chapter, we analytically studied the impact of both quantum fluctuations and a non-equilibrium environment – a fermionic drive – on the dynamics of a disordered system of rotors that shows aspects of a ferromagnet in many regards. We gave a detailed description of the influence of the two-lead environment that creates the fermionic current tunneling through the system. In particular, we showed that the fermionic drive behaves like an equilibrium thermal bath on the long-time dynamics of the rotors. By solving the mean-field dynamics, we determined the full dynamical phase diagram of the rotors. In the ordering phase, we gave an expression for the long-time limit of two-time correlation, and showed its scaling function does not depend on the temperature, the strength of disorder, the strength of quantum fluctuations nor the strength of the drive. This super-universality feature of the long-time dynamics allowed us to extend the well-know mapping between the classical $p = 2$ spherical model and the clean $3d$ coarsening ferromagnet to this driven out-of-equilibrium quantum case.

In models of quantum coupled rotors, there are visible effects when the angular momentum states are restricted to even or odd symmetry. This is the case for instance in the models used for Josephson junctions [288, 289] or systems like solid hydrogen where homonuclear molecules (H_2 and D_2) can assume only even or odd values of the rotational quantum number j , depending on the parity of the nuclear spin. At low pressure or high temperature, even- j species are found in a paramagnetic state. Increasing the pressure causes an increase of the molecular coupling and eventually leads to a orientationally ordered state. Odd- j species on the other hand are orientationally ordered at low temperatures and ambient pressure and remain ordered as pressure is increased. The stronger tendency for odd- j species to order can be traced back to the fact that their $j = 1$ lowest rotational state allows for a spherically asymmetric ground state unlike the $j = 0$ ground state of even- j species [290]. Noteworthy enough, when all the rotational states are allowed, and when the gap between the ground state $j = 0$ and $j = 1$ is not too large, small thermal excitations can induce the ordering by populating the $j = 1$ level. The order is lost when the thermal fluctuations become too large. This phenomenon is responsible for a reentrant phase diagram. In our language this means that the critical point \bar{T}_c is rejected to infinity in the case of odd- j species. By implementing such restrictions on the angular momenta, it would be interesting

Figure 5.1: The complex-time contour ζ .

to study their effects on the phase diagram of our disordered model and see if they yield similar effects in equilibrium and predict out-of-equilibrium features.

In order to complete the work presented here, we intended to generalize the discussion around the equilibrium symmetry of the Langevin generating functionals to the case of quantum interacting systems. Unfortunately, we were not able to finish the work and make in presentable in time, but we give here some of the main ingredients. The MSRJD path-integral has a natural quantum extension in the Schwinger-Keldysh formalism. For systems described by a time-dependent Hamiltonian $H(t)$ and prepared at time $t_0 = 0$ in thermal equilibrium with respect to $H(0)$, the expectation value of an operator O a time t is given by

$$\langle O(t) \rangle \equiv \text{Tr} \left[\tilde{T} \left\{ e^{-\frac{i}{\hbar} \int_t^0 du H(u)} \right\} O(t) T \left\{ e^{-\frac{i}{\hbar} \int_0^t du H(u)} \right\} e^{-\beta H(0)} \right] / \mathcal{Z}, \quad (5.1)$$

where β is the inverse temperature of the initial preparation and $\mathcal{Z} \equiv \text{Tr} [e^{-\beta H(0)}]$. T and \tilde{T} are respectively the time and anti-time-ordering operators (see Appendix 4.A.3). Reading the arguments in the above trace from the right to the left, one sees that we can design an complex-time contour ζ with a branch going from $i\beta\hbar$ to 0 along the imaginary axis then a forward branch from 0 to t along the real axis and then coming backward to 0. This contour is illustrated in Fig. 5.1. Letting the variable u run along this same contour, eq. (5.1) can be formally recast as

$$\langle O(t) \rangle = \text{Tr} \left[T_\zeta \left\{ e^{-\frac{i}{\hbar} \int_\zeta du H(u)} O(t) \right\} \right] / \mathcal{Z}, \quad (5.2)$$

where T_ζ is time-ordering operator that rearranges operators along the contour ζ . The trace over the operators can be recast into a path integral using the standard techniques (Suzuki-Trotter decomposition). Let us consider the simple case of a time-dependent Hamiltonian of the form $H = \frac{\pi^2}{2m} + V(\phi, t)$ where π is the momentum conjugated to the coordinate ϕ . This yields a path-integral whose action reads $S[\phi] = \int_\zeta du \mathcal{L}([\phi(u)], u)$ where \mathcal{L} is the time-dependent Lagrangian. The field $\phi(u)$ has support on the complex-time contour ζ . Thanks to the unitary evolution, we are free to deform this contour in the complex plane as long as

it passes through t , where the operator O has to be evaluated. Under the condition of a time-independent Lagrangian (*i.e.* equilibrium dynamics), and for particular contours, we were able to exhibit some field transformations that leave the corresponding action invariant. At the level of observables, the corresponding Ward-Takahashi identities yield relations such as reciprocity relations or the quantum fluctuation-dissipation theorem. We hope to report soon on these.

The out of equilibrium quantum fluctuations theorems have not reached the same level of understanding obtained for the classical systems. We believe our approach based on symmetries in a field theory description is a powerful tool not only to derive relations in a systematic manner but also to better understand the underlying physics. Moreover, the identification of these symmetries is fundamental to construct a theory of dynamical fluctuations in and out of equilibrium. It should serve as guide to select self-consistent approximations which do not violate important physical symmetries, to construct approximation schemes for interacting problems such as mode-coupling methods.

SYNOPSIS

Sommaire

6.1	Symétries autour des équations de Langevin	152
6.1.1	Équation de Langevin	152
6.1.2	Fonctionnelle génératrice	153
6.1.3	Équilibre	154
6.1.4	Hors d'équilibre	156
6.2	Lois d'échelle dynamiques et super-universalité	157
6.2.1	Modèles	157
6.2.2	Croissance d'une échelle de longueur	158
6.2.3	Lois d'échelle dynamique	158
6.2.4	Super-universalité	159
6.3	Dynamique forcée de rotateurs quantiques désordonnés	159
6.3.1	Modèle	160
6.3.2	Influence de l'environnement	161
6.3.3	Diagramme de phase	161
6.3.4	Dynamique	161

CETTE thèse traite principalement de la dynamique de systèmes statistiques hors d'équilibre. Dans la nature, les systèmes physiques ne sont jamais isolés. Si à l'équilibre thermodynamique, l'influence de l'environnement peut être caractérisée par un tout petit nombre de paramètres (comme la température), il est en revanche *a priori* nécessaire d'être

renseigné sur les détails de l'environnement et de son couplage avec le système pour décrire les situations hors de l'équilibre thermodynamique.

Nous distinguons deux types d'environnements. Les premiers sont les environnements à l'équilibre, comme par exemple un bain thermique à une température β^{-1} . Les variables internes qui les décrivent obéissent, entre autres, au théorème de fluctuation-dissipation. Les seconds sont les environnements intrinsèquement hors d'équilibre qui déstabilisent le système en injectant (ou en pompant) de l'énergie. Ils sont, par exemple, l'ensemble constitué par deux bains thermiques à des températures différentes. Nous considérerons aussi le cas de deux réservoirs d'électrons qui, sous l'effet d'une différence de potentiel, peuvent passer de l'un à l'autre par effet tunnel à travers le système. Par extension, nous incluons dans les environnements hors d'équilibre le cas des forces extérieures appliquées sur le système.

6.1 Symétries autour des équations de Langevin

6.1.1 Équation de Langevin

Dans le chapitre 2, nous nous arrêtons sur le cas des systèmes classiques en interaction avec un environnement à l'équilibre à la température β^{-1} . La dynamique du système peut être très généralement décrite par une équation de Langevin. Dans nombre d'applications, l'inertie peut être négligée et l'effet du bain peut être capturé par un bruit blanc. Toutefois, motivés par une généralisation aux systèmes quantiques (où les effets de mémoire du bain sont incontournables, typiquement sur des temps de l'ordre de $\beta\hbar$), nous conservons le terme de masse et considérons le cas générique d'un bruit coloré et multiplicatif. En toute généralité, l'équation de Langevin pour une masse m repérée par la coordonnée ψ est donnée par

$$m\ddot{\psi}(t) - F([\psi], t) + M'(\psi(t)) \int du \eta(t-u) M'(\psi(u)) \dot{\psi}(u) = M'(\psi(t)) \xi(t) . \quad (6.1)$$

où la force $F([\psi], t) = -V'(\psi, \lambda(t)) + f^{\text{nc}}([\psi], t)$ rassemble les contributions conservatives et non-conservatives. V est un potentiel dont la dépendance temporelle est contrôlée, s'il y a lieu, par le protocole $\lambda(t)$. M est une fonction bien comportée qui caractérise le couplage non linéaire à l'environnement ($M(0) = 0$ et $M'(0) = 1$). Le cas du bruit additif est retrouvé en prenant un couplage linéaire, $M(\psi) = \psi$. Le dernier terme du membre de gauche de l'éq. (6.1) ainsi que le membre de droite modélisent les interactions avec le bain. La friction visqueuse est donnée par une intégrale temporelle sur le noyau de friction, $\eta(t, t')$. Celui-ci, causalité oblige, est nul pour $t < t'$. Le cas du bruit blanc est retrouvé en prenant $\eta(t, t') = \gamma_0 \delta(t - t')$. ξ est une force aléatoire, issue d'un processus stochastique gaussien, qui modélise l'agitation thermique. Puisque le bain est supposé à l'équilibre à la

température β^{-1} , le noyau $\eta(t, t')$ est une fonction de $t - t'$ et il est relié à la statistique du bruit ξ par un théorème de fluctuation-dissipation :

$$\langle \xi(t) \xi(t') \rangle_\xi = \beta^{-1} \aleph(t - t') , \quad (6.2)$$

où nous avons introduit la notation $\aleph(t - t') \equiv \eta(t - t') + \eta(t' - t)$.

6.1.2 Fonctionnelle génératrice

Nous construisons la fonctionnelle génératrice associée à cette l'équation de Langevin (6.1) dans le formalisme de Martin-Siggia-Rose-Jassen-deDominicis (MSRJD) [81, 82, 85]. Nous travaillons dans un intervalle de temps symétrique $t \in [-T, T]$. Nous prêtons une attention particulière aux conditions initiales dont la distribution statistique est encodée dans la mesure $P_i(\psi, \dot{\psi})$. Si au temps initial ($t = -T$) le système est préparé à l'équilibre thermodynamique, P_i est donnée par la mesure de Gibbs-Boltzmann.

Action de MSRJD

L'action de MSRJD s'écrit avec l'aide d'un champ auxiliaire $\hat{\psi}$ (souvent qualifié de champ de réponse) comme la somme de trois termes : $S[\psi, \hat{\psi}] \equiv S^{\text{det}}[\psi, \hat{\psi}] + S^{\text{diss}}[\psi, \hat{\psi}] + S^{\mathcal{J}}[\psi]$, avec

$$\begin{aligned} S^{\text{det}}[\psi, \hat{\psi}] &\equiv \ln P_i(\psi(-T), \dot{\psi}(-T)) - \int du \, i\hat{\psi}(u) \left[m\ddot{\psi}(u) - F([\psi], u) \right] , \quad (6.3) \\ S^{\text{diss}}[\psi, \hat{\psi}] &\equiv \int du \, i\hat{\psi}(u) \int dv \, M'(\psi(u)) \eta(u - v) M'(\psi(v)) \left[\beta^{-1} i\hat{\psi}(v) - \dot{\psi}(v) \right] . \end{aligned}$$

S^{diss} provient de l'interaction avec le bain tandis que S^{det} regroupe toutes les autres forces appliquées au système ainsi que la mesure initiale P_i . $S^{\mathcal{J}}$ est issu du jacobien résultant du changement du champ d'intégration ξ au champ ψ . Dans le cas général, on montre que le jacobien est une constante positive dont on peut se débarrasser dans une redéfinition de la mesure de l'intégrale fonctionnelle. On peut aussi choisir de l'exprimer *via* une intégrale gaussienne sur deux champs de Grassmann c et c^* . En étendant l'intégrale fonctionnelle de MSRJD à ces deux nouveaux champs, la contribution jacobienne à l'action s'écrit alors :

$$\begin{aligned} S^{\mathcal{J}}[c, c^*, \psi] &= \iint du \, dv \, c^*(u) \left[m\partial_u^2 \delta(u - v) - \frac{\delta F([\psi], u)}{\delta \psi(v)} \right. \\ &\quad \left. + M'(\psi(u)) \partial_u \eta(u - v) M'(\psi(v)) \right] c(v) \\ &\quad - \int du \, c^*(u) \frac{M''(\psi(u))}{M'(\psi(u))} \left[m\partial_u^2 \psi(u) - F([\psi], u) \right] c(u) . \quad (6.4) \end{aligned}$$

Observables

Dans le formalisme de MSRJD, la moyenne prise sur les conditions initiales et les histoires thermiques d'une observable $A[\psi]$ au temps t s'exprime de manière transparente comme

$$\langle A[\psi(t)] \rangle_S \equiv \int \mathcal{D}[\psi, \hat{\psi}, c, c^*] A[\psi(t)] e^{S[\psi, \hat{\psi}, c, c^*]} . \quad (6.5)$$

Entre autres, la fonction d'auto-corrélation à deux temps et la fonction d'auto-réponse linéaire s'expriment comme

$$C(t, t') = \langle \psi(t) \psi(t') \rangle_S \quad \text{et} \quad R(t, t') = \langle \psi(t) i\hat{\psi}(t') \rangle_S . \quad (6.6)$$

6.1.3 Équilibre

Symétrie de l'équilibre

Il y a deux conditions pour qu'un système soit assuré d'évoluer avec une dynamique d'équilibre : il doit être préparé dans un état d'équilibre et son évolution doit se faire avec les mêmes forces (autres que celles provenant du bain d'équilibre) qui ont participé à sa préparation. Plus précisément, il doit évoluer avec les mêmes forces conservatives (et indépendantes du temps) que celles qui ont servi à sa préparation et les seules forces non-conservatives autorisées sont celles de l'interaction avec l'environnement. Celui-ci doit être à l'équilibre et sa température doit correspondre à la température de préparation du système.

Nous montrons que sous ces conditions d'équilibre, la fonctionnelle génératrice de MSRJD est invariante sous la transformation des champs suivante :

$$\mathcal{T}_{\text{eq}} \equiv \begin{cases} \psi(u) \mapsto \psi(-u) , & c(u) \mapsto c^*(-u) , \\ i\hat{\psi}(u) \mapsto i\hat{\psi}(-u) + \beta \partial(u) \psi(-u) , & c^*(u) \mapsto -c(-u) . \end{cases} \quad (6.7)$$

Cette transformation comporte un renversement du temps et ne dépend pas de η ce qui, en particulier, la rend valable dans la limite newtonienne $\eta = 0$, c'est à dire pour les évolutions isolées.

Les identités de Ward-Takahashi qui correspondent à cette transformation s'écrivent

$$\begin{aligned} \langle A[\psi(t)] \rangle_S &= \langle A[\psi(-t)] \rangle_S \\ \langle \psi(t) \psi(t') \rangle_S &= \langle \psi(-t) \psi(-t') \rangle_S \\ \langle \psi(t) i\hat{\psi}(t') \rangle_S &= \langle \psi(-t) i\hat{\psi}(-t') \rangle_S + \beta \partial_{t'} \langle \psi(-t) \psi(-t') \rangle_S \\ &\dots \end{aligned} \quad (6.8)$$

Nous montrons que ces identités donnent lieu à tous les théorèmes généraux de l'équilibre tels que la stationnarité, le théorème d'équipartition de l'énergie, les relations de réciprocité d'Onsager, le théorème de fluctuation-dissipation, etc.

Super-symétrie

Dans le cas de forces conservatives ($f^{\text{nc}} = 0$) et indépendantes du temps ($\dot{\lambda} = 0$), la fonctionnelle génératrice associée aux équations de Langevin admet une représentation super-symétrique. Cela a été démontré et discuté pour le cas du bruit additif dans nombre de publications [98–101]. Nous étendons le champ d’application de ce formalisme au cas du bruit multiplicatif et coloré. L’action correspondante s’écrit $S = S_{\text{susy}}^{\text{det}} + S_{\text{susy}}^{\text{diss}}$ avec

$$S_{\text{susy}}^{\text{det}}[\Psi] \equiv -\beta \int d\theta d\theta^* \theta^* \theta \mathcal{H}[\Psi(-T, \theta, \theta^*)] - \ln \mathcal{Z} + \int d\Upsilon \mathcal{L}[\Psi(\Upsilon)] , \quad (6.9)$$

$$S_{\text{susy}}^{\text{diss}}[\Psi] \equiv \frac{1}{2} \iint d\Upsilon' d\Upsilon M(\Psi(\Upsilon')) \mathbf{D}^{(2)}(\Upsilon', \Upsilon) M(\Psi(\Upsilon)) , \quad (6.10)$$

où Ψ est le champ composite (super-champ) formé à partir des champs ψ , $\hat{\psi}$, c et c^* selon

$$\Psi(\Upsilon) \equiv \psi(t) + c^*(t) \theta + \theta^* c(t) + \theta^* \theta \left(i\hat{\psi}(t) + c^*(t) c(t) \frac{M''(\psi(t))}{M'(\psi(t))} \right) .$$

θ et θ^* sont deux coordonnées de Grassmann supplémentaires regroupées dans les notations $\Upsilon \equiv (t, \theta, \theta^*)$ et $d\Upsilon \equiv dt d\theta d\theta^*$. \mathcal{Z} est la fonction de partition. $\mathcal{H}[\Psi] \equiv \frac{1}{2} m \dot{\Psi}^2 + V(\Psi)$ et $\mathcal{L}[\Psi] \equiv \frac{1}{2} m \dot{\Psi}^2 - V(\Psi)$. L’opérateur différentiel correspondant à l’interaction avec le bain est donné par

$$\mathbf{D}^{(2)}(\Upsilon', \Upsilon) = \eta(t' - t) \delta(\theta'^* - \theta^*) \delta(\theta' - \theta) (\bar{\mathbf{D}} \mathbf{D} - \mathbf{D} \bar{\mathbf{D}}) , \quad (6.11)$$

où les opérateurs

$$\bar{\mathbf{D}} \equiv \frac{\partial}{\partial \theta} \quad \text{et} \quad \mathbf{D} \equiv \beta^{-1} \frac{\partial}{\partial \theta^*} - \theta \frac{\partial}{\partial t} , \quad (6.12)$$

obéissent aux relations d’anticommutation suivantes : $\{\bar{\mathbf{D}}, \mathbf{D}\} = -\frac{\partial}{\partial t}$ et $\{\mathbf{D}, \mathbf{D}\} = \{\bar{\mathbf{D}}, \bar{\mathbf{D}}\} = 0$.

Sous couvert d’avoir une mesure initiale donnée par la distribution d’équilibre de Gibbs-Boltzmann [*c.f.* le premier terme de l’éq. (6.9)], l’action est invariante sous les transformations engendrées par

$$\mathbf{Q} \equiv \frac{\partial}{\partial \theta^*} \quad \text{et} \quad \bar{\mathbf{Q}} \equiv \beta^{-1} \frac{\partial}{\partial \theta} + \theta^* \frac{\partial}{\partial t} ,$$

qui obéissent aux relations d’anticommutation suivantes : $\{\bar{\mathbf{Q}}, \mathbf{Q}\} = \frac{\partial}{\partial t}$ et $\{\mathbf{Q}, \mathbf{Q}\} = \{\bar{\mathbf{Q}}, \bar{\mathbf{Q}}\} = \{\mathbf{D}, \mathbf{Q}\} = \{\mathbf{D}, \bar{\mathbf{Q}}\} = \{\bar{\mathbf{D}}, \mathbf{Q}\} = \{\bar{\mathbf{D}}, \bar{\mathbf{Q}}\} = 0$.

Cette super-symétrie de l’action donne lieu, *via* les identités de Ward-Takahashi correspondantes, à certains théorèmes d’équilibre comme la stationnarité ou le théorème de fluctuation-dissipation mais elle ne permet pas de montrer les relations comportant explicitement un renversement du temps comme, par exemple, les relations de réciprocity d’Onsager. Nous explicitons le lien entre la symétrie discutée précédemment et cette super-symétrie.

6.1.4 Hors d'équilibre

Nous abordons ensuite le cas des dynamiques hors d'équilibre. Le système peut être maintenant préparé de manière arbitraire et évoluer avec des forces non-conservatives et dépendantes du temps. Nous n'envisageons pas le cas d'un bain hors d'équilibre mais la généralisation des résultats à ce cas est immédiate.

Théorèmes de fluctuation

La symétrie d'équilibre discutée précédemment est bien sûr brisée. La transformation des champs \mathcal{T}_{eq} appliquée à l'action $S[\psi, \hat{\psi}, c, c^*]$ génère des termes qui brisent explicitement la symétrie. Nous montrons que ces termes donnent lieu de manière très naturelle aux diverses relations de fluctuations (théorème de fluctuation de Crooks [27, 29, 192], égalité de Jarzynski [191, 150], identité de Kawasaki [193, 194], théorème de fluctuation [27, 29, 192]). Le cas des systèmes isolés peut être facilement retrouvé en prenant la limite $\eta = 0$.

Symétrie hors d'équilibre

Nous exhibons ensuite une nouvelle symétrie valable cette fois hors d'équilibre. Nous montrons que la fonctionnelle génératrice de MSRJD est invariante sous la transformation des champs suivante :

$$\mathcal{T}_{\text{eom}} \equiv \begin{cases} \psi(u) & \mapsto \psi(u) , \\ i\hat{\psi}(u) & \mapsto -i\hat{\psi}(u) + \frac{2\beta}{M'(\psi(u))} \int dv \mathbb{N}^{-1}(u-v) \frac{\text{EQ}([\psi], v)}{M'(\psi(v))} . \end{cases} \quad (6.13)$$

où $\text{EQ}([\psi], t)$ désigne l'intégralité du membre de gauche de l'éq. (6.1). Cette fois-ci, la limite newtonienne ($\eta = 0$) n'est pas bien définie. Les identités de Ward-Takahashi correspondant à cette transformation donnent lieu à des équations dynamiques du type Schwinger-Dyson couplant les corrélations et les réponses. Ces relations permettent en particulier d'exprimer la réponse $R(t, t')$ en fonction de corrélations ce qui a une application directe dans les simulations numériques hors d'équilibre, où le théorème de fluctuation-dissipation ne peut être utilisé, et où le calcul direct de la réponse est souvent problématique car il nécessite une moyenne sur un grand nombre d'histoires thermiques.

Dans les chapîtres 3 et 4, nous laissons ces considérations formelles pour se pencher sur quelques aspects plus concrets de la dynamique hors d'équilibre. Nous portons principalement notre intérêt sur lois d'échelles dynamiques qui se développent après une trempe brutale d'un système à travers une transition de phase du second ordre. Plus particulièrement nous étudions leurs caractères super-universels, c'est à dire leur dépendance aux paramètres

de contrôles tels que la température, le désordre, les fluctuations quantiques ou même les forçages extérieurs.

6.2 Lois d'échelle dynamiques et super-universalité

Dans le chapitre 3, nous effectuons une étude comparative des lois d'échelles dynamiques et des propriétés de super-universalité en dimension 3 en confrontant le cas de la croissance de domaines ferromagnétiques en présence de désordre gelé faible et celui de la dynamique vitreuse d'un verre de spin (avec du désordre gelé fort).

6.2.1 Modèles

Pour le cas de la croissance de domaines, nous choisissons de suivre la relaxation lente du modèle d'Ising 3d soumis à un champ magnétique aléatoire – le 3d Random Field Ising Model (RFIM) – après une trempe en température. Le hamiltonien du modèle est donné par

$$H = -J \sum_{\langle i,j \rangle} s_i s_j - \sum_i H_i s_i. \quad (6.14)$$

Les $s_i = \pm 1$ sont des spins d'Ising placés sur les nœuds d'un réseau cubique de volume L^3 . Le premier terme décrit des interactions ferromagnétiques ($J > 0$) à courte portée entre plus proches voisins. H_i représente un champ magnétique localisé sur le site i . Nous choisissons une distribution bi-modale pour ces variables aléatoires, $H_i = \pm H$ avec la même probabilité. H quantifie l'intensité du désordre gelé. Dans le cas $H = 0$, le RFIM se ramène au modèle d'Ising 3d avec une transition de phase d'une phase paramagnétique à une phase ferromagnétique à la température critique $T_c \simeq 4.415J$. En présence de désordre ($H > 0$), la phase ordonnée est réduite mais survit jusqu'à $H_c \simeq 2.215(35)J$ [61, 62].

Pour le cas de la dynamique vitreuse, nous choisissons le modèle d'Edwards-Anderson (EA) 3d défini par le hamiltonien

$$H = - \sum_{\langle i,j \rangle} J_{ij} s_i s_j. \quad (6.15)$$

Les $s_i = \pm 1$ sont encore des spins d'Ising placés sur les nœuds d'un réseau cubique de taille L^3 . Les couplages entre plus proches voisins sont tirés selon une distribution bi-modale, $J_{ij} = \pm J$ avec la même probabilité. Dans ce modèle, c'est J qui quantifie l'intensité du désordre gelé. À la température $T_g \simeq 1.14(1)J$ [69], le modèle passe d'une phase paramagnétique à une phase vitreuse. La nature exacte de la phase de basse température est encore soumise à interprétation et l'on distingue deux écoles quant à la relaxation hors d'équilibre. La vision en termes de gouttelettes (*droplet picture*) repose sur une compétition

entre deux états fondamentaux [70, 71], alors que l'autre interprétation repose sur les solutions du modèle de Sherrington-Kirkpatrick qui est la version en champ-moyen du modèle d'EA [72].

Nous suivons la relaxation de ces deux modèles au moyen de simulations de Monte Carlo. La trempe depuis une température initiale infinie est réalisée en prenant des conditions initiales aléatoires $s_i = \pm 1$ avec la même probabilité. Pour le cas du ferromagnétique, nous utilisons une version revisitée de l'algorithme de Metropolis [97], le *continuous time Monte Carlo*, qui permet d'avoir un taux de rejet nul [219–221]. Les paramètres de contrôles pertinents sont H/J et T/J pour le 3d RFIM, T/J pour le 3d EA.

6.2.2 Croissance d'une échelle de longueur

Dans le 3d RFIM, nous extrayons une longueur typique $R(t)$ de l'analyse de la décroissance spatiale de la fonction de corrélation à un temps $C_2(r; t) \equiv \langle s_i(t) s_j(t) \rangle_{|\vec{r}_i - \vec{r}_j| = r}$. Le comportement de R dépend des paramètres H/J et T/J . En particulier, pour $H = 0$ R croît comme $t^{1/2}$ alors qu'en présence de désordre sa croissance est logarithmique (activée).

Pour le 3d EA, il est impossible d'extraire une quelconque longueur à partir de la fonction $C_2(r; t)$ car celle-ci est strictement nulle pour $r > 0$. Toutefois, l'analyse d'une fonction de corrélation plus complexe, $C_4(r; t, t') \equiv \langle s_i(t) s_i(t') s_j(t) s_j(t') \rangle_{|\vec{r}_i - \vec{r}_j| = r}$, permet la détermination d'une échelle de longueur à deux temps $\xi(t, t')$. Celle-ci dépend de T/J et est très lentement croissante en ses deux temps (elle ne dépasse pas 2 fois le pas du réseau sur des simulations de 10^8 pas de Monte Carlo).

6.2.3 Lois d'échelle dynamique

Nous suivons le comportements de quelques observables pendant la relaxation des deux modèles. Nous en distinguons les contributions thermiques des contributions vieillissantes. Lorsque cette distinction est difficilement réalisable, nous travaillons à basse température où les effets thermiques sont moindres. Nous montrons que les contributions vieillissantes sont invariantes dans le temps une fois que les temps et les longueurs sont mesurés en unités de R ou de ξ .

Observables globales

Dans le cas du RFIM, nous vérifions que les parties vieillissantes de la fonction de corrélation à deux temps, $C(t, t') \equiv \langle s_i(t) s_i(t') \rangle = C_{\text{th}}(t - t') + C_{\text{ag}}(t, t')$, obéit à la loi d'échelle dynamique $C_{\text{ag}}(t, t') = C_{\text{ag}}(R(t)/R(t'))$. En extrayant dans ce modèle, comme dans le 3d EA, une longueur à deux temps $\xi(t, t')$ à partir de la fonction de corrélation $C_4(r; t, t')$,

nous montrons qu'elle obéit à $\xi(t, t') = R(t')g(C(t, t'))$ où g est une fonction décroissante. Nous montrons plus généralement que $C_4(r; t, t') = C_4(r/R(t'), R(t)/R(t'))$.

Dans le cas du modèle d'EA, la corrélation à deux temps est connue pour écheler selon la loi du « vieillissement simple » : $C_{\text{ag}}(t, t') = C_{\text{ag}}(t/t')$ [202] ; ce qui incite à penser que s'il y a une longueur typique $R(t)$ qui se développe, elle doit croître selon une loi de puissance, $R(t) \sim t^{1/z}$, où l'exposant dynamique z dépend *a priori* de T/T_g . En faisant cette hypothèse et en ajustant z à la main, nous obtenons la même loi d'échelle que dans le cas de la croissance de domaines ferromagnétiques : $\xi(t, t') = R(t')g(C(t, t'))$. Cela peut être également vu comme une nouvelle méthode pour déterminer l'exposant dynamique z dans le cas des verres de spin.

Observables locales

Pour les deux modèles, nous étudions les dynamiques locales par le biais d'observables qui ne sont plus moyennées sur tout l'échantillon (de volume L^3) mais seulement sur un petit volume l^3 . Leurs fluctuations spatiales peuvent être décrites par des densités de probabilité.

En particulier, nous nous concentrons sur la moyenne dans un volume de taille l^3 de la fonction de corrélation à deux temps, $C_r(t, t')$, et nous mesurons sa densité de probabilité $\rho(C_r; t, t', l)$. Pour les deux modèles considérés, nous montrons que celle-ci obéit à la loi d'échelle $\rho(C_r; C(t, t'), l/\xi(t, t'))$.

6.2.4 Super-universalité

La longueur typique R ou ξ dépend des paramètres de contrôles que sont la température T et l'intensité du désordre H . Nous testons l'hypothèse de super-universalité selon laquelle les lois d'échelle sont indépendantes de T et H [70] en faisant varier ces derniers. Dans le cas du modèle de croissance de domaines, nous montrons que toutes les lois d'échelles mentionnées précédemment, y compris celles sur les fluctuations des observables locales, sont super-universelles au sens qu'elles sont identiques au cas $T = H = 0$. En revanche, dans le cas du verre de spin, aucune des lois d'échelles discutées précédemment ne présente de caractère super-universel.

6.3 Dynamique forcée de rotateurs quantiques désordonnés

Dans le chapitre 4, nous étudions l'impact des fluctuations quantiques et d'un forçage extérieur sur la dynamique d'un système de rotateurs en présence d'interactions désordonnées. Plus précisément, la dynamique hors d'équilibre est créée en préparant le système à très haute température puis en le couplant brutalement à un environnement constitué de deux

réservoirs de fermions – un à gauche et un à droite du système. La différence de potentiel chimique V entre les deux réservoirs génère un courant qui s'établit à travers le système et le maintient hors de l'équilibre.

6.3.1 Modèle

En ce qui concerne les rotateurs, nous considérons le hamiltonien complètement connecté suivant :

$$H = \frac{\Gamma}{2n} \sum_{i=1}^N \mathbf{L}_i^2 - \frac{n}{\sqrt{N}} \sum_{i,j < i} J_{ij} \mathbf{s}_i \cdot \mathbf{s}_j . \quad (6.16)$$

Les \mathbf{s}_i sont des rotateurs à n composantes dont la longueur est fixée à l'unité ($\mathbf{s}_i \cdot \mathbf{s}_i = 1$). Les couplages entre les rotateurs sont tirés selon une distribution gaussienne de valeur moyenne 0 et d'écart type J . J quantifie l'intensité du désordre. Les \mathbf{L}_i sont les opérateurs de moment angulaires généralisés à n dimensions. Les composantes s_i^μ obéissent aux relations de commutation standards avec les moments conjugués p_i^μ qui interviennent dans l'expression des \mathbf{L}_i . Γ joue le rôle d'un moment d'inertie et quantifie l'intensité des fluctuations quantiques ; lorsque $\hbar^2 \Gamma / J \rightarrow 0$, le modèle tend vers la version classique du verre de spin d'Heisenberg complètement connecté. Dans la limite où n est grand, le modèle est équivalent à la version quantique du verre de spin $p = 2$ sphérique [257, 258] dont la température critique classique ($\Gamma = 0$) est $T_c = J$. La connection avec la croissance de domaines ferromagnétiques du modèle $O(n \rightarrow \infty)$ en $3d$ [52] se généralise à notre cas quantique et hors d'équilibre.

Ce modèle a déjà été étudié dans le cadre d'un couplage à un bain d'équilibre [258]. Pour des fortes fluctuation thermiques (T) et quantiques (Γ), les rotateurs sont dans une phase paramagnétique. En revanche pour des valeurs plus faibles de T et Γ , il y a une transition de phase du second ordre vers une phase ordonnée (l'ordre met d'ailleurs un temps infini pour s'établir).

Notre environnement hors d'équilibre est composé de deux réservoirs d'électrons libres. La différence de potentiel V entre les deux quantifie l'intensité du forçage. Pour simplifier la discussion, nous choisissons de travailler avec les mêmes températures et les mêmes densités d'états pour le réservoir de droite que pour celui de gauche. De plus, nous considérons des densités d'états contrôlées par une unique énergie typique ϵ_F comme, par exemple, une distribution semi-circulaire de rayon ϵ_F . La limite $\epsilon_F \rightarrow \infty$ correspond au cas où les électrons qui participent à la dynamique (ceux qui sont près du niveau de Fermi) voient une densité d'états constante. Nous choisissons une interaction très simple entre les fermions et les rotateurs en couplant linéairement chaque composante s_i^μ au processus qu'un fermion passe d'un réservoir à l'autre. Les constantes de couplages sont prises toutes identiques et égales à $\hbar \omega_c$. $g \equiv \hbar \omega_c / \epsilon_F$ quantifie l'intensité du couplage à l'environnement.

6.3.2 Influence de l'environnement

L'influence de cet environnement intrinsèquement hors d'équilibre est étudié en perturbations à l'ordre g^2 . Nous réalisons une étude détaillée de la self énergie selon la forme des densités d'états et les valeurs des paramètres de contrôle. En particulier, nous montrons que l'environnement se comporte sur les modes lents des rotateurs comme un bain ohmique à l'équilibre à la température $T^* \equiv \frac{eV}{2} \coth(\beta eV/2)$.

6.3.3 Diagramme de phase

Nous utilisons le formalisme de Schwinger-Keldysh, particulièrement adapté pour traiter la dynamique après une trempe des systèmes quantiques avec du désordre gelé. Dans la limite $nN \rightarrow \infty$, nous établissons les équations de Schwinger-Dyson qui couplent la corrélation à deux temps et la réponse linéaire. Pour $g \rightarrow 0$, nous calculons le diagramme de phase dans l'espace des paramètres de contrôle que sont T, Γ, V . Nous prouvons l'existence d'une transition de phase dynamique entre une phase stationnaire de non-équilibre et une phase ordonnée à basse température, faibles fluctuations quantiques et faible différence de potentiel. Pour des valeurs de g finies, la phase ordonnée gagne du terrain en déplaçant le point critique quantique $\Gamma_c(T = V = 0)$ vers le haut. Nous démontrons l'existence d'un nouveau point critique sur l'axe V (le forçage) et la ligne critique à $\Gamma \rightarrow 0$ obéit à la simple équation $T_c^* = J$ ce qui corrobore l'idée que l'environnement agit comme un bain ohmique à l'équilibre à la température T^* sur les modes lents des rotateurs.

6.3.4 Dynamique

En exploitant une similitude entre l'action de Keldysh et celle de MSRJD, nous écrivons la dynamique sous la forme d'une équation de Langevin avec inertie et bruit coloré. Nous étudions la relaxation lente dans la phase ordonnée. Dans la limite des temps longs, la couleur du bruit est négligeable et T^* apparaît alors naturellement comme la température d'un bain d'équilibre. Lorsque par ailleurs, l'inertie (contrôlée par Γ) est négligeable, l'équation de Langevin devient intégrable analytiquement et nous montrons que tout se passe comme dans la version classique (et sans inertie) du modèle $p = 2$ sphérique couplé à un bain d'équilibre à la température T^* . En particulier, la fonction de corrélation $C_{ag}(t, t')$ est une fonction super-universelle de t/t' au sens où elle ne dépend de T, J et V que par l'intermédiaire d'un préfacteur numérique (qui se trouve être le paramètre d'ordre de Edwards-Anderson). La fonction de réponse elle aussi se comporte comme dans le cas avec $T = \Gamma = V = 0$. Le théorème de fluctuation-dissipation est brisé de la même façon, avec une température effective du système infinie. Dans le cas où Γ est fini, nous résolvons la dynamique numériquement et montrons que le scénario précédent est encore valable : l'inertie

n'intervient que par une renormalisation des préfacteurs des lois d'échelle dynamiques.

Finalement, nous calculons le courant fermionique qui s'établit à travers le système. Nous montrons qu'il converge rapidement vers une constante qui ne donne pas d'information sur l'état dynamique des rotateurs.

Le travail présenté dans cette thèse a donné lieu aux publications suivantes :

- C. Aron, G. Biroli et L. F. Cugliandolo, “Symmetries of generating functionals of Langevin processes with colored multiplicative noise”, J. Stat. Mech. P11018 (2010), arXiv :1007.5059 ;
- C. Aron, G. Biroli et L. F. Cugliandolo, “Coarsening of disordered quantum rotors under a bias Voltage”, Phys. Rev. B **82**, 174203 (2010), arXiv :1005.2414 ;
- C. Aron, G. Biroli et L. F. Cugliandolo, “Driven Quantum Coarsening”, Phys. Rev. Lett. **102**, 050404 (2009), arXiv :0809.0590 ;
- C. Aron, C. Chamon, L. F. Cugliandolo et M. Picco, “Scaling and Super-Universality in the Coarsening Dynamics of the 3D Random Field Ising Model”, J. Stat. Mech, P05016 (2008), arXiv :0803.0664.

BIBLIOGRAPHY

- [1] D. Laërtius, *Lives and Opinions of Eminent Philosophers* (3rd century B.C.). Engl. transl. by Robert Drew Hicks, Loeb Classical Library, (1925).
- [2] J. Dalton, *A New System of Chemical Philosophy*, vol. I, II and III (Manchester, London, 1808, 1810 and 1827).
- [3] A. Avogadro, "Essay on a manner of determining the relative masses of the elementary molecules of bodies, and the proportions in which they enter into these compounds," *Journal de Physique* **73**, 58 (1811).
- [4] J. C. Maxwell, "Illustrations of the dynamical theory of gases, Part 1, On the motions and collisions of perfectly elastic spheres," *Philos. Mag.* **19**, 19 (1860).
- [5] J. C. Maxwell, "Illustrations of the dynamical theory of gases, Part 2, On the process of diffusion of two or more kinds of moving particles among one another," *Philos. Mag.* **20**, 21 (1860).
- [6] L. Boltzmann, "Weitere Studien über das Wärmegleichgewicht unter Gasmolekülen," *Wien. Ber.* **66**, 275 (1872).
- [7] J. W. Gibbs, *Elementary principles in statistical mechanics* (Charles Scribner's Sons, New York, 1902).
- [8] A. Einstein, "Über die von der molekularkinetischen Theorie der Wärme geforderte Bewegung von in Flüssigkeiten suspendierten Teilchen," *Ann. Phys. (Leipzig)* **17**, 549 (1905).
- [9] R. Brown, "A brief account of microscopical observations made on the particles contained in the pollen of plants," *Philos. Mag.* **4**, 161 (1828).
- [10] J. B. Perrin, *Les atomes* (Éditions F. Alcan, Paris, 1913–1936), 1st ed. Reed. Flammarion, Paris, 1993.
- [11] L. Onsager, "Reciprocal relations in irreversible processes I," *Phys. Rev.* **37**, 405 (1931).

- [12] L. Onsager, “Reciprocal relations in irreversible processes II,” Phys. Rev. **38**, 2265 (1931).
- [13] H. B. Callen and T. A. Welton, “Irreversibility and generalized noise,” Phys. Rev. **83**, 34 (1951).
- [14] L. D. Landau, Phys. Z. Sowjetunion **11**, 545 (1937).
- [15] P. W. Anderson, “Absence of diffusion in certain random lattices,” Phys. Rev. **109**, 1492 (1958).
- [16] S. F. Edwards and P. W. Anderson, “Theory of spin glasses,” J. Phys. F: Met. Phys. **5**, 965 (1975).
- [17] D. Sherrington and S. Kirkpatrick, “Solvable model of a spin-glass,” Phys. Rev. Lett. **35**, 1792 (1975).
- [18] G. Parisi, “Infinite number of order parameters for spin-glasses,” Phys. Rev. Lett. **43**, 1754 (1979).
- [19] L. F. Cugliandolo and J. Kurchan, “On the out-of-equilibrium relaxation of the Sherrington-Kirkpatrick model,” J. Phys. A: Math. Gen. **27**, 5749 (1994).
- [20] M. Talagrand, *Spin Glasses: A Challenge for Mathematicians* (Springer, Berlin, 2003).
- [21] A. Bovier, *Statistical mechanics of disordered systems. A mathematical perspective*, no. 18 in Cambridge Series in Statistical and Probabilistic Mathematics (Cambridge University Press, Cambridge, 2006).
- [22] M. Mézard, G. Parisi, and M. A. Virasoro, *Spin Glass Theory and Beyond*, vol. 9 of *Lecture Notes in Physics* (World Scientific, Singapore, 1987).
- [23] H. Nishimori, *Statistical Physics of Spin Glasses and Information Processing* (Oxford University Press, Oxford, 2001).
- [24] M. Mézard and A. Montanari, *Information, Physics, and Computation* (Oxford University Press, Oxford, 2009).
- [25] D. Evans, E. D. G. Cohen, and G. P. Morriss, “Probability of second law violations in shearing steady states,” Phys. Rev. Lett. **71**, 2401 (1993).
- [26] D. Evans and D. J. Searles, “Equilibrium microstates which generate second law violating steady states,” Phys. Rev. E **50**, 1645 (1994).

-
- [27] G. Gallavotti and E. D. G. Cohen, “Dynamical ensembles in nonequilibrium statistical mechanics,” *Phys. Rev. Lett.* **74**, 2694 (1995).
 - [28] G. Crooks, “Nonequilibrium measurements of free energy differences for microscopically reversible Markovian systems,” *J. Stat. Phys.* **90**, 1481 (1998).
 - [29] J. Kurchan, “Fluctuation theorem for stochastic dynamics,” *J. Phys. A: Math. Gen.* **31**, 3719 (1998).
 - [30] M. Esposito, U. Harbola, and S. Mukamel, “Nonequilibrium fluctuations, fluctuation theorems, and counting statistics in quantum systems,” *Rev. Mod. Phys.* **81**, 1665 (2009).
 - [31] A. Hosoya and M. aki Sakagam, “Time development of Higgs field at finite temperature,” *Phys. Rev. D* **29**, 2228 (1984).
 - [32] M. Morikawa, “Classical fluctuations in dissipative quantum systems,” *Phys. Rev. D* **33**, 3607 (1986).
 - [33] B. L. Hu, J. P. Paz, and Y. Zhang, *The Origin of Structure in the Universe* (Kluwer, Dordrecht, 1993).
 - [34] D. Lee and D. Boyanovsky, “Dynamics of phase transitions induced by a heat bath,” *Nucl. Phys. B* **406**, 631 (1993).
 - [35] M. Gleiser, “Microphysical approach to nonequilibrium dynamics of quantum fields,” *Phys. Rev. D* **50**, 2441 (1994).
 - [36] J. Imbrie, “Lower critical dimension of the random-field Ising model,” *Phys. Rev. Lett.* **53**, 1747 (1984).
 - [37] J. Bricmont and A. Kupiainen, “Lower critical dimension for the random-field Ising model,” *Phys. Rev. Lett.* **59**, 1829 (1987).
 - [38] J.-P. Bouchaud, L. F. Cugliandolo, J. Kurchan, and M. Mezard, “Out of equilibrium dynamics in spin-glasses and other glassy systems,” *arXiv:cond-mat/9702070* (1997).
 - [39] A. Cavagna, “Supercooled liquids for pedestrians,” *Phys. Rep.* **476**, 51 – 124 (2009).
 - [40] N. Kawashima and A. P. Young, “Phase transition in the three-dimensional $\pm j$ Ising spin glass,” *Phys. Rev. B* **53**, R484 (1996).
 - [41] M. Palassini and S. Caracciolo, “Universal finite-size scaling functions in the 3D Ising spin glass,” *Phys. Rev. Lett.* **82**, 5128 (1999).

-
- [42] E. Marinari, G. Parisi, and J. J. Ruiz-Lorenzo, “Phase structure of the three-dimensional edwards-anderson spin glass,” *Phys. Rev. B* **58**, 14852 (1998).
 - [43] A. K. Hartmann, “Scaling of stiffness energy for three-dimensional $\pm j$ Ising spin glasses,” *Phys. Rev. E* **59**, 84 (1999).
 - [44] H. G. Ballesteros, A. Cruz, L. A. Fernández, V. Martín-Mayor, J. Pech, J. J. Ruiz-Lorenzo, A. Tarancón, P. Téllez, C. L. Ullod, and C. Ungil, “Critical behavior of the three-dimensional Ising spin glass,” *Phys. Rev. B* **62**, 14237 (2000).
 - [45] J. Ye, S. Sachdev, and N. Read, “Solvable spin glass of quantum rotors,” *Phys. Rev. Lett.* **70**, 4011 (1993).
 - [46] M. P. Kennett, C. Chamon, and J. Ye, “Aging dynamics of quantum spin glasses of rotors,” *Phys. Rev. B* **64**, 224408 (2001).
 - [47] G. Biroli and O. Parcollet, “Out-of-equilibrium dynamics of a quantum Heisenberg spin glass,” *Phys. Rev. B* **65**, 094414 (2002).
 - [48] N. Linden, S. Popescu, A. J. Short, and A. Winter, “Quantum mechanical evolution towards thermal equilibrium,” *Phys. Rev. E* **79**, 061103 (2009).
 - [49] V. Spirin, P. Krapivsky, and S. Redner, “Freezing in Ising ferromagnets,” *Phys. Rev. E* **65**, 016119 (2001).
 - [50] A. J. Bray, “Theory of phase-ordering kinetics,” *Adv. Phys.* **43**, 357 (1994).
 - [51] E. Vincent, “Ageing, rejuvenation and memory: The example of spin-glasses,” in “Ageing and the Glass Transition,” , vol. 716 of *Lecture Notes in Physics* (Springer, Berlin, Heidelberg, 2007), p. 7.
 - [52] L. F. Cugliandolo, “Course 7: Dynamics of glassy systems,” in “Slow Relaxations and nonequilibrium dynamics in condensed matter,” , vol. 77 of *Les Houches*, J.-L. B. et al. et al., ed. (Springer - EDP Sciences, Berlin, Heidelberg, 2003), p. 367.
 - [53] F. Corberi, C. Castellano, E. Lippiello, and M. Zannetti, “Generic features of the fluctuation dissipation relation in coarsening systems,” *Phys. Rev. E* **70**, 017103 (2004).
 - [54] M. Henkel, M. Paessens, and M. Pleimling, “Scaling of the linear response in simple aging systems without disorder,” *Phys. Rev. E* **69**, 056109 (2004).
 - [55] T. Nattermann and J. Villain, “Random-field Ising systems - a survey of current theoretical views,” *Phase Transitions* **11**, 5 (1988).
 - [56] T. Nattermann and P. Rujan, “Random fields and other systems dominated by disorder fluctuations,” *Int. J. Mod. Phys. B* **3**, 1597 (1989).

-
- [57] T. Nattermann, “Theory of the random field Ising model,” in “Spin Glasses and Random Fields,” , vol. 12 of *Directions in Condensed Matter Physics*, A. P. Young, ed. (World Scientific, Singapore, 1998), p. 277.
 - [58] D. P. Belanger, “Experiments on the random field Ising model,” in “Spin Glasses and Random Fields,” , vol. 12 of *Directions in Condensed Matter Physics*, A. P. Young, ed. (World Scientific, Singapore, 1997), p. 251.
 - [59] F. Alberici-Kious, J. Bouchaud, L. Cugliandolo, P. Doussineau, and A. Levelut, “Aging in $K_{1-x}Li_xTaO_3$: A domain growth interpretation,” *Phys. Rev. Lett.* **81**, 4987 (1998).
 - [60] F. Alberici-Kious, J.-P. Bouchaud, L. Cugliandolo, P. Doussineau, and A. Levelut, “Aging and domain growth in $K_{1-x}Li_xTaO_3$ ($x \lesssim 0.05$),” *Phys. Rev. B* **62**, 14766 (2000).
 - [61] M. R. Swift, A. J. Bray, A. Maritan, M. Cieplak, and J. R. Banavar, “Scaling of the random-field Ising model at zero temperature,” *Europhys. Lett.* **38**, 273 (1997).
 - [62] N. G. Fytas and A. Malakis, “Phase diagram of the 3D bimodal random-field Ising model,” *Eur. Phys. J. B* **61**, 111 (2008).
 - [63] A. Young and M. Nauenberg, “Quasicritical behavior and first-order transition in the $d = 3$ random-field Ising model,” *Phys. Rev. Lett.* **54**, 2429 (1985).
 - [64] H. Rieger, “Critical behavior of the three-dimensional random-field Ising model: Two-exponent scaling and discontinuous transition,” *Phys. Rev. B* **52**, 6659 (1995).
 - [65] A. Middleton and D. Fisher, “Three-dimensional random-field Ising magnet: Interfaces, scaling, and the nature of states,” *Phys. Rev. B* **65**, 134411 (2002).
 - [66] M. Mézard and R. Monasson, “Glassy transition in the three-dimensional random-field Ising model,” *Phys. Rev. B* **50**, 7199 (1994).
 - [67] F. Krzakala, F. Ricci-Tersenghi, and L. Zdeborová, “Elusive spin-glass phase in the random field Ising model,” *Phys. Rev. Lett.* **104**, 207208 (2010).
 - [68] D. Mouhanna and G. Tarjus, “Spontaneous versus explicit replica symmetry breaking in the theory of disordered systems,” *Phys. Rev. E* **81**, 051101 (2010).
 - [69] H. Ballesteros, A. Cruz, L. Fernández, V. Martín-or, J. Pech, J. Ruiz-Lorenzo, A. Tarancón, P. Téllez, C. Ullod, and C. Ungil, “Critical behavior of the three-dimensional Ising spin glass,” *Phys. Rev. B* **62**, 14237 (2000).

- [70] D. Fisher and D. A. Huse, “Nonequilibrium dynamics of spin glasses,” *Phys. Rev. B* **38**, 373 (1988).
- [71] A. J. Bray and M. A. Moore, “Nonanalytic magnetic field dependence of the magnetisation in spin glasses,” *Journal of Physics C: Solid State Physics* **17**, L613 (1984).
- [72] K. H. Fischer and J. A. Hertz, *Spin Glasses*, Cambridge Studies in Magnetism (Cambridge University Press, Cambridge, 1991).
- [73] H. E. Stanley, “Spherical model as the limit of infinite spin dimensionality,” *Phys. Rev.* **176**, 718 (1968).
- [74] J. R. L. de Almeida, R. C. Jones, J. M. Kosterlitz, and D. J. Thouless, “The infinite-ranged spin glass with m -component spins,” *J. Phys. C: Solid State Phys.* **11**, L871 (1978).
- [75] A. J. Leggett, S. Chakravarty, A. T. Dorsey, M. P. A. Fisher, A. Garg, and W. Zwerger, “Dynamics of the dissipative two-state system,” *Rev. Mod. Phys.* **59**, 1 (1987).
- [76] I. Tupitsyn and B. Barbara, “Quantum tunneling of magnetization in molecular complexes with large spins - effect of the environment,” in “Magnetism: Molecules to Materials III,” (Wiley-VCH Verlag GmbH, Weinheim, 2002).
- [77] W. Wu, B. Ellman, T. F. Rosenbaum, G. Aeppli, and D. H. Reich, “From classical to quantum glass,” *Phys. Rev. Lett.* **67**, 2076 (1991).
- [78] S. Sachdev, *Quantum Phase Transitions* (Cambridge University Press, Cambridge, 2001).
- [79] B. Diu, C. Guthmann, D. Lederer, and B. Roulet, *Physique Statistique* (Hermann, Paris, 2001), chap. IV Évolution vers l’équilibre et irréversibilité, p. 595.
- [80] P. Langevin, “Sur la théorie du mouvement brownien,” *C. R. Acad. Sci.* **146**, 530 (1908). Engl. transl. in *Am. J. Phys.* **65**, 1079 (1997).
- [81] P. Martin, E. Siggia, and H. Rose, “Statistical dynamics of classical systems,” *Phys. Rev. A* **8**, 423 (1973).
- [82] H.-K. Janssen, “On a Lagrangean for classical field dynamics and renormalization group calculations of dynamical critical properties,” *Z. Phys. B: Condens. Matter Quanta* **23**, 377 (1976).
- [83] H. Janssen, “Field-theoretic method applied to critical dynamics,” in “Dynamical Critical Phenomena and Related Topics,” , vol. 104 of *Lecture Notes in Physics*, C. P. Enz, ed. (Springer, Berlin, Heidelberg, 1979), p. 25.

-
- [84] H.-K. Janssen, *From Phase Transition to Chaos: topics in modern statistical physics* (World Scientific, Singapore, 1992), chap. On the renormalized field theory of non-linear critical relaxation, p. 68.
 - [85] C. De Dominicis, “Dynamics as a substitute for replicas in systems with quenched random impurities,” *Phys. Rev. B* **18**, 4913 (1978).
 - [86] C. D. Dominicis, “Techniques de renormalisation de la théorie des champs et dynamique des phénomènes critiques,” *J. Phys., Colloq.* **37**, 247 (1976).
 - [87] M. Månson and A. Sjölander, “Spin correlations in a Heisenberg system within the paramagnetic region,” *Phys. Rev. B* **11**, 4639 (1975).
 - [88] A. Volkov and S. Kogan, *JETP* **38**, 1018 (1974).
 - [89] A. Larkin and Y. Ovchinnikov, *JETP* **41**, 960 (1976).
 - [90] Y. N. Ovchinnikov, “Penetration of an electrical field into a superconductor,” *J. Low Temp. Phys.* **28**, 43 (1977).
 - [91] C.-R. Hu, “New set of time-dependent ginzburg-landau equations for dirty superconductors near T_c ,” *Phys. Rev. B* **21**, 2775 (1980).
 - [92] V. Korenman, “Nonequilibrium quantum statistics; application to the laser,” *Annals of Physics* **39**, 72 – 126 (1966).
 - [93] P. Nozières and E. Abrahams, “Threshold singularities of the X-ray raman scattering in metals,” *Phys. Rev. B* **10**, 3099 (1974).
 - [94] C. Caroli, B. Roulet, and D. Saint-James, “Evaporation from superfluid helium,” *Phys. Rev. B* **13**, 3875 (1976).
 - [95] B. Bezzerides and D. F. DuBois, “Quantum electrodynamics of nonthermal relativistic plasmas: Kinetic theory,” *Annals of Physics* **70**, 10 – 66 (1972).
 - [96] D. Langreth, *Linear and nonlinear electron transport in solids*, NATO advanced study institutes series. Series B, Physics ; v. 17 (Plenum Press, New York, 1976).
 - [97] N. Metropolis, A. W. Rosenbluth, M. N. Rosenbluth, A. H. Teller, and E. Teller, “Equation of state calculations by fast computing machines,” *J. Chem. Phys.* **21**, 1087 (1953).
 - [98] J. Zinn-Justin, *Quantum Field Theory and Critical Phenomena*, no. 113 in International Series of Monographs on Physics (Oxford University Press, Oxford, 2002), 4th ed.

- [99] E. Gozzi, “Functional-integral approach to Parisi-Wu stochastic quantization: Scalar theory,” *Phys. Rev. D* **28**, 1922 (1983).
- [100] J. Kurchan, “Supersymmetry in spin glass dynamics,” *J. Phys. I (France)* **2**, 1333 (1992).
- [101] J. Bouchaud, L. Cugliandolo, J. Kurchan, and M. Mézard, “Mode-coupling approximations, glass theory and disordered systems,” *Physica A* **226**, 243 (1996).
- [102] A. Coniglio and M. Zannetti, “Multiscaling in growth kinetics,” *Europhys. Lett.* **10**, 575 (1989).
- [103] J. G. Amar and F. Family, “Diffusion annihilation in one dimension and kinetics of the Ising model at zero temperature,” *Phys. Rev. A* **41**, 3258 (1990).
- [104] B. Derrida, C. Godrèche, and I. Yekutieli, “Scale-invariant regimes in one-dimensional models of growing and coalescing droplets,” *Phys. Rev. A* **44**, 6241 (1991).
- [105] T. J. Newman, A. J. Bray, and M. A. Moore, “Growth of order in vector spin systems and self-organized criticality,” *Phys. Rev. B* **42**, 4514 (1990).
- [106] J. Arenzon, A. J. Bray, L. F. Cugliandolo, and A. Sicilia, “Exact results for curvature-driven coarsening in two dimensions,” *Phys. Rev. Lett.* **98** (2007).
- [107] A. Sicilia, J. J. Arenzon, A. J. Bray, and L. F. Cugliandolo, “Domain growth morphology in curvature-driven two-dimensional coarsening,” *Phys. Rev. E* **76** (2007).
- [108] E. Lippiello, A. Mukherjee, S. Puri, and M. Zannetti, “Scaling behavior of response functions in the coarsening dynamics of disordered ferromagnets,” *Europhys. Lett.* **90**, 46006 (2010).
- [109] M. Rao and A. Chakrabarti, “Kinetics of domain growth in a random-field model in three dimensions,” *Phys. Rev. Lett.* **71**, 3501 (1993).
- [110] S. Puri and N. Parekh, “Non-algebraic domain growth for phase ordering dynamics in a random field,” *J. Phys. A: Math. Gen.* **26**, 2777 (1993).
- [111] A. J. Bray and K. Huun, “Universality class for domain growth in random magnets,” *J. Phys. A: Math. Gen.* **24**, L1185 (1991).
- [112] A. Sicilia, J. J. Arenzon, A. J. Bray, and L. F. Cugliandolo, “Geometric properties of two-dimensional coarsening with weak disorder,” *Europhys. Lett.* **82**, 10001 (2008).
- [113] M. Henkel and M. Pleimling, “Superuniversality in phase-ordering disordered ferromagnets,” *Phys. Rev. B* **78**, 224419 (2008).

-
- [114] C. M. Newman and D. L. Stein, "Simplicity of state and overlap structure in finite-volume realistic spin glasses," *Phys. Rev. E* **57**, 1356 (1998).
 - [115] C. M. Newman and D. L. Stein, "The state(s) of replica symmetry breaking: Mean field theories vs. short-ranged spin glasses," *J. Stat. Phys.* **106**, 213 (2002).
 - [116] T. Komori, H. Yoshino, and H. Takayama, "Numerical study on aging dynamics in the 3D Ising spin-glass model. i. energy relaxation and domain coarsening," *J. Phys. Soc. Jpn.* **68**, 3387 (1999).
 - [117] T. Komori, H. Yoshino, and H. Takayama, "Numerical study on aging dynamics in Ising spin-glass models: Ii. quasi-equilibrium regime of spin auto-correlation function," *J. Phys. Soc. Jpn.* **69**, 1192 (1999).
 - [118] T. Komori, H. Yoshino, and H. Takayama, "Numerical study on aging dynamics in Ising spin-glass models: Temperature-change protocols," *J. Phys. Soc. Jpn.* **69**, 228 (2000).
 - [119] F. Belletti, M. Cotallo, A. Cruz, L. A. Fernandez, A. Gordillo-Guerrero, M. Guidetti, A. Maiorano, F. Mantovani, E. Marinari, V. Martin-Mayor, A. M. n. Sudupe, D. Navarro, G. Parisi, S. Perez-Gaviro, J. J. Ruiz-Lorenzo, S. F. Schifano, D. Sciretti, A. Tarancon, R. Tripiccion, J. L. Velasco, and D. Yllanes, "Nonequilibrium spin-glass dynamics from picoseconds to a tenth of a second," *Phys. Rev. Lett.* **101**, 157201 (2008).
 - [120] C. Chamon and L. F. Cugliandolo, "Fluctuations in glassy systems," *Journal of Statistical Mechanics: Theory and Experiment* **2007**, P07022 (2007).
 - [121] D. Dalidovich and P. Phillips, "Nonlinear transport near a quantum phase transition in two dimensions," *Phys. Rev. Lett.* **93**, 027004 (2004).
 - [122] A. G. Green and S. L. Sondhi, "Nonlinear quantum critical transport and the Schwinger mechanism for a superfluid-Mott-insulator transition of bosons," *Phys. Rev. Lett.* **95**, 267001 (2005).
 - [123] P. M. Hogan and A. G. Green, "Universal nonlinear conductivity close to an itinerant-electron quantum critical point," *Phys. Rev. B* **78**, 195104 (2008).
 - [124] A. Mitra, S. Takei, Y. B. Kim, and A. J. Millis, "Nonequilibrium quantum criticality in open electronic systems," *Phys. Rev. Lett.* **97**, 236808 (2006).
 - [125] D. E. Feldman, "Nonequilibrium quantum phase transition in itinerant electron systems," *Phys. Rev. Lett.* **95**, 177201 (2005).

- [126] A. Mitra and A. J. Millis, “Current-driven quantum criticality in itinerant electron ferromagnets,” *Phys. Rev. B* **77**, 220404 (2008).
- [127] H. Risken and T. Frank, *The Fokker-Planck Equation*, vol. 18 of *Springer Series in Synergetics* (Springer, Berlin, 1989), 2nd ed.
- [128] N. G. V. Kampen, *Stochastic Processes in Physics and Chemistry*, North-Holland Personal Library (Elsevier, Amsterdam, 2004).
- [129] C. Gardiner, *Stochastic Methods: A Handbook for the Natural and Social Sciences*, vol. 13 of *Springer Series in Synergetics* (Springer, Berlin, 2009), 3rd ed.
- [130] W. Brown, “Thermal fluctuations of a single-domain particle,” *Phys. Rev.* **130**, 1677 (1963).
- [131] R. Kubo and N. Hashitume, “Brownian motion of spins,” *Prog. Theor. Phys. Suppl.* **46**, 210 (1970).
- [132] A. Lau and T. Lubensky, “State-dependent diffusion: Thermodynamic consistency and its path integral formulation,” *Phys. Rev. E* **76**, 011123 (2007).
- [133] K. Kawasaki, “Stochastic model of slow dynamics in supercooled liquids and dense colloidal suspensions,” *Physica A* **208**, 35 (1994).
- [134] D. S. Dean, “Langevin equation for the density of a system of interacting Langevin processes,” *J. Phys. A: Math. Gen.* **29**, L613 (1996).
- [135] A. Hosoya and M. aki Sakagami, “Time development of Higgs field at finite temperature,” *Phys. Rev. D* **29**, 2228 (1984).
- [136] M. Gleiser and R. Ramos, “Microphysical approach to nonequilibrium dynamics of quantum fields,” *Phys. Rev. D* **50**, 2441 (1994).
- [137] W. Horsthemke and R. Lefever, “Phase transition induced by external noise,” *Phys. Lett. A* **64**, 19 (1977).
- [138] C. Van den Broeck, J. Parrondo, and R. Toral, “Noise-induced nonequilibrium phase transition,” *Phys. Rev. Lett.* **73**, 3395 (1994).
- [139] C. Van den Broeck, J. M. R. Parrondo, R. Toral, and R. Kawai, “Nonequilibrium phase transitions induced by multiplicative noise,” *Phys. Rev. E* **55**, 4084 (1997).
- [140] G. Grinstein, M. Muñoz, and Y. Tu, “Phase structure of systems with multiplicative noise,” *Phys. Rev. Lett.* **76**, 4376 (1996).

-
- [141] Y. Tu, G. Grinstein, and M. Muñoz, “Systems with multiplicative noise: Critical behavior from KPZ equation and numerics,” *Phys. Rev. Lett.* **78**, 274 (1997).
 - [142] N. G. van Kampen, “Itô versus Stratonovich,” *J. Stat. Phys.* **24**, 175 (1981).
 - [143] R. Kupferman, G. Pavliotis, and A. Stuart, “Itô versus Stratonovich white-noise limits for systems with inertia and colored multiplicative noise,” *Phys. Rev. E* **70**, 036120 (2004).
 - [144] H. Callen and T. Welton, “Irreversibility and generalized noise,” *Phys. Rev.* **83**, 34 (1951).
 - [145] R. Kubo, “Statistical-mechanical theory of irreversible processes. i. general theory and simple applications to magnetic and conduction problems,” *J. Phys. Soc. Jpn.* **12**, 570 (1957).
 - [146] S. R. D. Groot and P. Mazur, *Non-Equilibrium Thermodynamics* (Dover, 1984).
 - [147] R. L. Stratonovich, *Nonlinear Nonequilibrium Thermodynamics I: Linear and Non-linear Fluctuation-Dissipation Theorems* (Springer-Verlag, Berlin, 1992).
 - [148] R. Kubo, M. Toda, and N. Hashitsume, *Statistical Physics II: Nonequilibrium Statistical Mechanics* (Springer-Verlag, Berlin, Heidelberg, New York, 1985), 2nd ed.
 - [149] R. Kubo, “The fluctuation-dissipation theorem,” *Rep. Prog. Phys.* **29**, 255 (1966).
 - [150] C. Jarzynski, “Nonequilibrium work theorem for a system strongly coupled to a thermal environment,” *J. Stat. Mech.: Theory Exp.* **2004**, P09005 (2004).
 - [151] G. Crooks, “Entropy production fluctuation theorem and the nonequilibrium work relation for free energy differences,” *Phys. Rev. E* **60**, 2721 (1999).
 - [152] G. E. Crooks, “Path-ensemble averages in systems driven far from equilibrium,” *Phys. Rev. E* **61**, 2361 (2000).
 - [153] T. Harada and S. ichi Sasa, “Equality connecting energy dissipation with a violation of the fluctuation-response relation,” *Phys. Rev. Lett.* **95**, 130602 (2005).
 - [154] F. Zamponi, F. Bonetto, L. F. Cugliandolo, and J. Kurchan, “A fluctuation theorem for non-equilibrium relaxational systems driven by external forces,” *J. Stat. Mech.: Theory Exp.* **2005**, P09013 (2005).
 - [155] T. Mai and A. Dhar, “Nonequilibrium work fluctuations for oscillators in non-Markovian baths,” *Phys. Rev. E* **75**, 061101 (2007).

- [156] T. Speck and U. Seifert, “The Jarzynski relation, fluctuation theorems, and stochastic thermodynamics for non-Markovian processes,” *J. Stat. Mech.: Theory Exp.* **2007**, L09002 (2007).
- [157] T. Ohkuma and T. Ohta, “Fluctuation theorems for non-linear generalized Langevin systems,” *J. Stat. Mech.: Theory Exp.* **2007**, P10010 (2007).
- [158] R. García-García, D. Domínguez, V. Lecomte, and A. B. Kolton, “Unifying approach for fluctuation theorems from joint probability distributions,” *Phys. Rev. E* **82**, 030104.
- [159] J. Kurchan, *Six out of equilibrium lectures* (Oxford University Press, Oxford, 2009), Les Houches Session XC.
- [160] F. Ritort, *Nonequilibrium fluctuations in small systems: From physics to biology* (John Wiley & Sons, Hoboken, 2008), vol. 137, p. 31.
- [161] P. Gaspard, *Hamiltonian dynamics, nanosystems, and nonequilibrium statistical mechanics* (Leuven, 2005).
- [162] L. F. Cugliandolo, J. Kurchan, and G. Parisi, “Off equilibrium dynamics and aging in unfrustrated systems,” *J. Phys. I (France)* **4**, 1641 (1994).
- [163] C. Chatelain, “A far-from-equilibrium fluctuation–dissipation relation for an Ising–Glauber-like model,” *J. Phys. A: Math. Gen.* **36**, 10739 (2003).
- [164] F. Ricci-Tersenghi, “Measuring the fluctuation-dissipation ratio in glassy systems with no perturbing field,” *Phys. Rev. E* **68** (2003).
- [165] E. Lippiello, F. Corberi, and M. Zannetti, “Off-equilibrium generalization of the fluctuation dissipation theorem for Ising spins and measurement of the linear response function,” *Phys. Rev. E* **71**, 036104 (2005).
- [166] G. Diezemann, “Fluctuation-dissipation relations for a general class of master equations,” arXiv:cond-mat/0309105 (2003).
- [167] A. Crisanti and F. Ritort, “Violation of the fluctuation–dissipation theorem in glassy systems: basic notions and the numerical evidence,” *J. Phys. A: Math. Gen.* **36**, R181 (2003).
- [168] L. Berthier, “Efficient measurement of linear susceptibilities in molecular simulations: Application to aging supercooled liquids,” *Phys. Rev. Lett.* **98** (2007).
- [169] F. Corberi, A. Sarracino, and M. Zannetti, “Fluctuation-dissipation relations and field-free algorithms for the computation of response functions,” *Phys. Rev. E* **81**, 011124 (2010).

-
- [170] M. Baiesi, C. Maes, and B. Wynants, “Nonequilibrium linear response for Markov dynamics, I: Jump processes and overdamped diffusions,” *J. Stat. Phys.* **137**, 1094 (2009).
 - [171] M. Baiesi, E. Boksenbojm, C. Maes, and B. Wynants, “Nonequilibrium linear response for Markov dynamics, II: Inertial dynamics,” *J. Stat. Phys.* **139**, 492 (2010).
 - [172] U. Seifert and T. Speck, “Fluctuation-dissipation theorem in nonequilibrium steady states,” *Europhys. Lett.* **89**, 10007 (2010).
 - [173] D. Villamaina, A. Baldassarri, A. Puglisi, and A. Vulpiani, “The fluctuation-dissipation relation: how does one compare correlation functions and responses?” *J. Stat. Mech.: Theory Exp.* **2009**, P07024 (2009).
 - [174] R. Ch  trite, G. Falkovich, and K. Gaw  dzki, “Fluctuation relations in simple examples of non-equilibrium steady states,” *J. Stat. Mech.: Theory Exp.* **2008**, P08005 (2008).
 - [175] R. Zwanzig, *Nonequilibrium Statistical Mechanics* (Oxford University Press, Oxford, 2004).
 - [176] U. Weiss, *Quantum Dissipative Systems*, vol. 13 of *Series in Modern Condensed Matter Physics* (World Scientific, Singapore, 2008), 3rd ed.
 - [177] R. L. Stratonovich, “A new representation for stochastic integrals and equations,” *SIAM J. Control* **4**, 362 (1966).
 - [178] R. L. Stratonovich, *Topics in the Theory of Random Noise* (Gordon and Breach, New York, 1963).
 - [179] K. It  , “Stochastic integral,” *Proc. Imp. Acad. (Tokyo)* **20**, 519 (1944).
 - [180] K. It  , “On a stochastic integral equation,” *Proc. Imp. Acad. (Tokyo)* **22**, 32 (1946).
 - [181] F. Langouche, D. Roekaerts, and E. Tirapegui, *Functional Integration and Semiclassical Expansions* (Reidel, Dordrecht, 1982).
 - [182] H. Casimir, “On Onsager’s principle of microscopic reversibility,” *Rev. Mod. Phys.* **17**, 343 (1945).
 - [183] L. Onsager and S. Machlup, “Fluctuations and irreversible processes,” *Phys. Rev.* **91**, 1505 (1953).
 - [184] S. Machlup and L. Onsager, “Fluctuations and irreversible process. II. systems with kinetic energy,” *Phys. Rev.* **91**, 1512 (1953).

- [185] A. Kamenev and A. Levchenko, “Keldysh technique and non-linear σ -model: basic principles and applications,” *Adv. Phys.* **58**, 197 (2009).
- [186] C. Aron, G. Biroli, and L. F. Cugliandolo, “Symmetries of quantum dissipative system’s generating functionals,” in preparation .
- [187] A. Velenich, C. Chamon, L. F. Cugliandolo, and D. Kreimer, “On the Brownian gas: a field theory with a Poissonian ground state,” *J. Phys. A: Math. Theor.* **41**, 235002 (2008).
- [188] G. Semerjian, L. F. Cugliandolo, and A. Montanari, “On the stochastic dynamics of disordered spin models,” *J. Stat. Phys.* **115**, 493 (2004).
- [189] G. Parisi and N. Sourlas, “Supersymmetric field theories and stochastic differential equations,” *Nuclear Physics B* **206**, 321 (1982).
- [190] Z. G. Arenas and D. G. Barci, “Functional integral approach for multiplicative stochastic processes,” *Phys. Rev. E* **81**, 051113 (2010).
- [191] C. Jarzynski, “Nonequilibrium equality for free energy differences,” *Phys. Rev. Lett.* **78**, 2690 (1997).
- [192] J. L. Lebowitz and H. Spohn, “A Gallavotti–Cohen-type symmetry in the large deviation functional for stochastic dynamics,” *J. Stat. Phys.* **95**, 333 (1999).
- [193] T. Yamada and K. Kawasaki, “Nonlinear effects in the shear viscosity of critical mixtures,” *Progress of Theoretical Physics* **38**, 1031–1051 (1967).
- [194] K. Kawasaki and J. D. Gunton, “Theory of nonlinear transport processes: Nonlinear shear viscosity and normal stress effects,” *Phys. Rev. A* **8**, 2048 (1973).
- [195] S. Puri, “Kinetics of phase transitions,” *Phase Transitions* **77**, 407 (2004).
- [196] R. Paul, G. Schehr, and H. Rieger, “Superaging in two-dimensional random ferromagnets,” *Phys. Rev. E* **75**, 030104 (2007).
- [197] R. Paul, S. Puri, and H. Rieger, “Domain growth in Ising systems with quenched disorder,” *Phys. Rev. E* **71**, 061109 (2005).
- [198] F. Baumann, M. Henkel, and M. Pleimling, “Phase-ordering kinetics of two-dimensional disordered Ising models,” *arXiv:0709.3228* (2007).
- [199] H. Hinrichsen, “Dynamical response function of the disordered kinetic Ising model,” *arXiv:0711.2421* (2007).

-
- [200] A. Baldassarri, L. F. Cugliandolo, J. Kurchan, and G. Parisi, “On the out-of-equilibrium order parameter in long-range spin-glasses,” *J. Phys. A: Math. Gen.* **28**, 1831 (1995).
- [201] H. Rieger, “Nonequilibrium dynamics and aging in the three-dimensional Ising spin-glass model,” *J. Phys. A: Math. Gen.* **26**, L615 (1993).
- [202] M. Picco, F. Ricci-Tersenghi, and F. Ritort, “Aging effects and dynamic scaling in the 3D Edwards-Anderson spin glasses: a comparison with experiments,” *Eur. Phys. J. B* **21**, 211 (2001).
- [203] J. Kisker, L. Santen, M. Schreckenberg, and H. Rieger, “Off-equilibrium dynamics in finite-dimensional spin-glass models,” *Phys. Rev. B* **53**, 6418 (1996).
- [204] E. Marinari, G. Parisi, F. Ricci-Tersenghi, and J. J. Ruiz-Lorenzo, “Off-equilibrium dynamics at very low temperatures in three-dimensional spin glasses,” *J. Phys. A: Math. Gen.* **33**, 2373 (2000).
- [205] L. D. C. Jaubert, C. Chamon, L. F. Cugliandolo, and M. Picco, “Growing dynamical length, scaling, and heterogeneities in the 3D Edwards–Anderson model,” *J. Stat. Mech.: Theory Exp.* **2007**, P05001 (2007).
- [206] F. Belletti, M. Cotallo, A. Cruz, L. Fernandez, A. Gordillo-Guerrero, M. Guidetti, A. Maiorano, F. Mantovani, E. Marinari, V. Martin-or, A. Sudupe, D. Navarro, G. Parisi, S. Perez-Gaviro, J. Ruiz-Lorenzo, S. Schifano, D. Sciretti, A. Tarancon, R. Tripiccone, J. Velasco, and D. Yllanes, “Nonequilibrium spin-glass dynamics from picoseconds to a tenth of a second,” *Phys. Rev. Lett.* **101**, 157201 (2008).
- [207] H. Castillo, C. Chamon, L. Cugliandolo, and M. Kennett, “Heterogeneous aging in spin glasses,” *Phys. Rev. Lett.* **88**, 237201 (2002).
- [208] H. Castillo, C. Chamon, L. Cugliandolo, J. Iguain, and M. Kennett, “Spatially heterogeneous ages in glassy systems,” *Phys. Rev. B* **68**, 134442 (2003).
- [209] A. Parsaeian and H. Castillo, “Growth of spatial correlations in the aging of a simple structural glass,” *Phys. Rev. E* **78**, 060105 (2008).
- [210] C. Chamon, L. F. Cugliandolo, G. Fabricius, J. L. Iguain, and E. R. Weeks, “From particles to spins: Eulerian formulation of supercooled liquids and glasses,” *Proc. Natl. Acad. Sci. U. S. A.* **105**, 15263 (2008).
- [211] C. Chamon and L. F. Cugliandolo, “Fluctuations in glassy systems,” *J. Stat. Mech.: Theory Exp.* **2007**, P07022 (2007).

- [212] C. Chamon, L. F. Cugliandolo, and H. Yoshino, “Fluctuations in the coarsening dynamics of the $O(N)$ model with $N \rightarrow \infty$ are they similar to those in glassy systems?” *J. Stat. Mech.: Theory Exp.* **2006**, P01006 (2006).
- [213] P. Mayer, H. Bissig, L. Berthier, L. Cipelletti, J. Garrahan, P. Sollich, and V. Trappe, “Heterogeneous dynamics of coarsening systems,” *Phys. Rev. Lett.* **93**, 115701 (2004).
- [214] P. Mayer, P. Sollich, L. Berthier, and J. P. Garrahan, “Dynamic heterogeneity in the Glauber–Ising chain,” *J. Stat. Mech.: Theory Exp.* **2005**, P05002 (2005).
- [215] C. Chamon, P. Charbonneau, L. F. Cugliandolo, D. R. Reichman, and M. Sellitto, “Out-of-equilibrium dynamical fluctuations in glassy systems,” *J. Chem. Phys.* **121**, 10120 (2004).
- [216] H. E. Castillo and A. Parsaeian, “Local fluctuations in the ageing of a simple structural glass,” *Nat. Phys.* **3**, 26 (2006).
- [217] Y. Imry and S. keng Ma, “Random-field instability of the ordered state of continuous symmetry,” *Phys. Rev. Lett.* **35**, 1399 (1975).
- [218] É. Brézin and C. D. Dominicis, “Dynamics versus replicas in the random field Ising model,” *C. R. Acad. Sci., Ser. Iib: Mec.* **327**, 383 (1999).
- [219] A. Bortz, M. Kalos, and J. Lebowitz, “A new algorithm for Monte Carlo simulation of Ising spin systems,” *J. Comput. Phys.* **17**, 10 (1975).
- [220] J. Dall and P. Sibani, “Faster Monte Carlo simulations at low temperatures. the waiting time method,” *Comput. Phys. Commun.* **141**, 260 (2001).
- [221] M. A. Novotny, *A Tutorial on Advanced Dynamic Monte Carlo Methods for Systems with Discrete State Spaces* (World Scientific, Singapore, 2001), p. 153.
- [222] N. Mackenzie and A. Young, “Lack of ergodicity in the infinite-range Ising spin-glass,” *Phys. Rev. Lett.* **49**, 301 (1982).
- [223] K. Binder, “Spin glasses: Experimental facts, theoretical concepts, and open questions,” *Rev. Mod. Phys.* **58**, 801 (1986).
- [224] J. Villain, “Nonequilibrium ”critical” exponents in the random-field Ising model,” *Phys. Rev. Lett.* **52**, 1543 (1984).
- [225] J. Villain, “Commensurate-incommensurate transition with frozen impurities,” *J. Phys., Lett.* **43**, 551 (1982).

-
- [226] G. Grinstein and S. keng Ma, “Roughening and lower critical dimension in the random-field Ising model,” *Phys. Rev. Lett.* **49**, 685 (1982).
- [227] G. Grinstein and J. Fernandez, “Equilibration of random-field Ising systems,” *Phys. Rev. B* **29**, 6389 (1984).
- [228] J. F. Fernandez, “Random fields generated by dilution in zero external field,” *Europhys. Lett.* **5**, 129 (1988).
- [229] V. S. Dotsenko and V. S. Dotsenko, “Phase transition in the 2d Ising model with impurity bonds,” *Sov. Phys. JETP Lett.* **33**, 37 (1981).
- [230] B. Shalaev, *Sov. Phys. Solid State* **26**, 1811 (1984).
- [231] R. Shankar, “Exact critical behavior of a random bond two-dimensional ising model,” *Phys. Rev. Lett.* **58**, 2466 (1987).
- [232] A. W. W. Ludwig, “Comment on ”exact critical behavior of a random-bond two-dimensional ising model”,” *Phys. Rev. Lett.* **61**, 2388 (1988).
- [233] M. Picco (2010). Private discussion.
- [234] E. Oguz, “Domain growth in the three-dimensional random-field Ising model,” *J. Phys. A: Math. Gen.* **27**, 2985 (1994).
- [235] S. Anderson, “Growth and equilibration in the two-dimensional random-field Ising model,” *Phys. Rev. B* **36**, 8435 (1987).
- [236] N. Lačević, F. Starr, T. Schröder, V. Novikov, and S. Glotzer, “Growing correlation length on cooling below the onset of caging in a simulated glass-forming liquid,” *Phys. Rev. E* **66**, 030101 (R) (2002).
- [237] P. Calabrese and J. Cardy, “Entanglement entropy in extended quantum systems,” *J. Phys. A: Math. Theor.* **42**, 500301 (2009).
- [238] D. Segal, D. R. Reichman, and A. J. Millis, “Nonequilibrium quantum dissipation in spin-fermion systems,” *Phys. Rev. B* **76**, 195316 (2007).
- [239] S. Miyashita, S. Tanaka, H. D. Raedt, and B. Barbara, “Quantum response to time-dependent external fields,” *J. Phys.: Conf. Ser.* **143**, 012005 (2009).
- [240] T. Kadowaki and H. Nishimori, “Quantum annealing in the transverse Ising model,” *Phys. Rev. E* **58**, 5355 (1998).

- [241] E. Farhi, J. Goldstone, S. Gutmann, J. Lapan, A. Lundgren, and D. Preda, “A quantum adiabatic evolution algorithm applied to random instances of an NP-Complete problem,” *Science* **292**, 472 (2001).
- [242] W. H. Zurek, U. Dorner, and P. Zoller, “Dynamics of a quantum phase transition,” *Phys. Rev. Lett.* **95**, 105701 (2005).
- [243] L. F. Cugliandolo, G. S. Lozano, and H. Lozza, “Static properties of the dissipative random quantum Ising ferromagnetic chain,” *Phys. Rev. B* **71**, 224421 (2005).
- [244] G. Schehr and H. Rieger, “Strong-disorder fixed point in the dissipative random transverse-field Ising model,” *Phys. Rev. Lett.* **96**, 227201 (2006).
- [245] L. Arrachea, “DC response of a dissipative driven mesoscopic ring,” *Phys. Rev. B* **70**, 155407 (2004).
- [246] A. Caso, L. Arrachea, and G. S. Lozano, “Local and effective temperatures of quantum driven systems,” *Phys. Rev. B* **81**, 041301 (2010).
- [247] L. Arrachea and L. F. Cugliandolo, “Study of a fluctuation-dissipation relation of a dissipative driven mesoscopic system,” *Europhys. Lett.* **70**, 642 (2005).
- [248] A. Onuki and K. Kawasaki, “Nonequilibrium steady state of critical fluids under shear flow: A renormalization group approach,” *Ann. Phys.* **121**, 456 (1979).
- [249] H. Hinrichsen, “Non-equilibrium critical phenomena and phase transitions into absorbing states,” *Adv. Phys.* **49**, 815 (2000).
- [250] B. Schmittmann and R. K. P. Zia, *Statistical Mechanics of Driven Diffusive Systems*, vol. 17 of *Phase Transitions and Critical Phenomena* (London Academic Press, London, 1995).
- [251] U. C. Täuber, “Field-theory approaches to nonequilibrium dynamics,” in “Ageing and the Glass Transition,” , vol. 716 of *Lecture Notes in Physics* (Springer, Berlin, Heidelberg, 2007), p. 295.
- [252] L. C. E. Struick, *Physical Aging in Amorphous Polymers and Other Materials* (Elsevier, Amsterdam New York, 1978).
- [253] A. Kamenev, “Many-body theory of non-equilibrium systems,” arXiv:cond-mat/0412296 (2004).
- [254] A. Kamenev, “Keldysh and Doi-Peliti techniques for out-of-equilibrium systems,” arXiv:cond-mat/0109316 (2001).

-
- [255] C. Aron, G. Biroli, and L. F. Cugliandolo, “Driven quantum coarsening,” *Phys. Rev. Lett.* **102**, 050404 (2009).
 - [256] T. K. Kopec, “Infinite-range-interaction M -component quantum spin glasses: Statics and dynamics in the large- M limit,” *Phys. Rev. B* **50**, 9963 (1994).
 - [257] P. Shukla and S. Singh, “A quantum spherical model of spin glass,” *Phys. Lett. A* **81**, 477 (1981).
 - [258] M. Rokni and P. Chandra, “Dynamical study of the disordered quantum $p = 2$ spherical model,” *Phys. Rev. B* **69**, 094403 (2004).
 - [259] L. F. Cugliandolo and G. Lozano, “Real-time nonequilibrium dynamics of quantum glassy systems,” *Phys. Rev. B* **59**, 915 (1999).
 - [260] L. F. Cugliandolo and G. Lozano, “Quantum aging in mean-field models,” *Phys. Rev. Lett.* **80**, 4979 (1998).
 - [261] A. Núñez and R. Duine, “Effective temperature and Gilbert damping of a current-driven localized spin,” *Phys. Rev. B* **77**, 054401 (2008).
 - [262] D. M. Basko and M. G. Vavilov, “Stochastic dynamics of magnetization in a ferromagnetic nanoparticle out of equilibrium,” *Phys. Rev. B* **79**, 064418 (2009).
 - [263] L. F. Cugliandolo, D. R. Grempel, G. Lozano, H. Lozza, and C. A. da Silva Santos, “Dissipative effects on quantum glassy systems,” *Phys. Rev. B* **66**, 014444 (2002).
 - [264] L. F. Cugliandolo, D. R. Grempel, G. Lozano, and H. Lozza, “Effects of dissipation on disordered quantum spin models,” *Phys. Rev. B* **70**, 024422 (2004).
 - [265] M. P. Kennett and C. Chamon, “Time reparametrization group and the long time behavior in quantum glassy systems,” *Phys. Rev. Lett.* **86**, 1622 (2001).
 - [266] H. Westfahl, J. Schmalian, and P. G. Wolynes, “Dynamical mean-field theory of quantum stripe glasses,” *Phys. Rev. B* **68**, 134203 (2003).
 - [267] G. Busiello, E. V. Gazeeva, R. V. Saburova, I. R. Khaibutdinova, and G. P. Chugunova, *Phys. Met. Metallogr.* **97**, 552 (2004).
 - [268] G. Buziello, E. Gazeeva, R. Saburova, I. Khaibutdinova, and G. Chugunova, “Temperature shifts in the quantum spherical p -spin model of glass,” *Phys. Met. Metallogr.* **101**, 109 (2006).
 - [269] G. Buziello, E. Gazeeva, R. Saburova, I. Khaibutdinova, and G. Chugunova, “Aging effects in the nonequilibrium quantum spin glass in weak magnetic fields,” *Phys. Met. Metallogr.* **102**, 244 (2006).

- [270] L. F. Cugliandolo, T. Gai, and P. L. Doussal, “Dynamic compressibility and aging in Wigner crystals and quantum glasses,” *Phys. Rev. Lett.* **96**, 217203 (2006).
- [271] G. Biroli and L. F. Cugliandolo, “Quantum Thouless-Anderson-Palmer equations for glassy systems,” *Phys. Rev. B* **64**, 014206 (2001).
- [272] L. F. Cugliandolo and D. S. Dean, “Full dynamical solution for a spherical spin-glass model,” *J. Phys. A: Math. Gen.* **28**, 4213 (1995).
- [273] L. F. Cugliandolo and D. S. Dean, “On the dynamics of a spherical spin-glass in a magnetic field,” *J. Phys. A: Math. Gen.* **28**, L453 (1995).
- [274] A. Schmid, “On a quasiclassical Langevin equation,” *J. Low Temp. Phys.* **49**, 609 (1982).
- [275] A. O. Caldeira and A. J. Leggett, “Path integral approach to quantum Brownian motion,” *Physica A* **121**, 587 (1983).
- [276] H. Grabert, P. Schramm, and G. Ingold, “Quantum Brownian motion: The functional integral approach,” *Phys. Rep.* **168**, 115 (1988).
- [277] C. Greiner and S. Leupold, “Stochastic interpretation of Kadanoff-Baym equations and their relation to Langevin processes,” *Ann. Phys.* **270**, 328 (1998).
- [278] L. F. Cugliandolo, J. Kurchan, and L. Peliti, “Energy flow, partial equilibration, and effective temperatures in systems with slow dynamics,” *Phys. Rev. E* **55**, 3898 (1997).
- [279] D. Goldhaber-Gordon, H. Shtrikman, D. Mahalu, D. Abusch-Magder, U. Meirav, and M. A. Kastner, “Kondo effect in a single-electron transistor,” *Nature* **391**, 156 (1998).
- [280] D. Goldhaber-Gordon, J. Göres, M. A. Kastner, H. Shtrikman, D. Mahalu, and U. Meirav, “From the Kondo regime to the mixed-valence regime in a single-electron transistor,” *Phys. Rev. Lett.* **81**, 5225 (1998).
- [281] W. Liang, M. P. Shores, M. Bockrath, J. R. Long, and H. Park, “Kondo resonance in a single-molecule transistor,” *Nature* **417**, 725 (2002).
- [282] P. Mehta and N. Andrei, “Nonequilibrium transport in quantum impurity models: The Bethe ansatz for open systems,” *Phys. Rev. Lett.* **96**, 216802 (2006).
- [283] S. Kehrein, “Scaling and decoherence in the nonequilibrium Kondo model,” *Phys. Rev. Lett.* **95**, 056602 (2005).
- [284] E. Boulat, H. Saleur, and P. Schmitteckert, “Twofold advance in the theoretical understanding of far-from-equilibrium properties of interacting nanostructures,” *Phys. Rev. Lett.* **101**, 140601 (2008).

-
- [285] B. Doyon, “Universal aspects of nonequilibrium currents in a quantum dot,” *Phys. Rev. B* **73** (2006).
- [286] R. Landauer, “Spatial variation of currents and fields due to localized scatterers in metallic conduction,” *IBM J. Res. Dev.* **1**, 223 (1957).
- [287] M. Büttiker, “Four-terminal phase-coherent conductance,” *Phys. Rev. Lett.* **57**, 1761 (1986).
- [288] E. Šimánek, “Reentrant phase diagram for granular superconductors,” *Phys. Rev. B* **32**, 500 (1985).
- [289] M. V. Simkin, “Josephson-oscillator spectrum and the reentrant phase transition in granular superconductors,” *Phys. Rev. B* **44**, 7074 (1991).
- [290] B. Hetényi, S. Scandolo, and E. Tosatti, “Theoretical evidence for a reentrant phase diagram in ortho-para mixtures of solid h_2 at high pressure,” *Phys. Rev. Lett.* **94**, 125503 (2005).

Titre Dynamique hors d'équilibre classique et quantique. Formalisme et applications.

Résumé Cette thèse traite de la dynamique de systèmes couplés à un environnement. Nous recensons les symétries du formalisme Martin-Siggia-Rose-Janssen-deDominicis associé aux équations de Langevin. À l'équilibre, nous étendons le formalisme super-symétrique aux cas d'un bruit coloré et multiplicatif et exhibons une symétrie qui génère tous les théorèmes d'équilibre. Brisée, elle donne lieu aux différents théorèmes de fluctuations. Une autre symétrie, valable aussi hors d'équilibre, fournit des équations dynamiques couplant corrélations et réponses. Par ailleurs nous étendons le formalisme super-symétrique au cas du bruit coloré et multiplicatif.

Nous suivons, par des simulations de Monte Carlo, la croissance de domaines dans le modèle d'Ising $3d$ soumis à un champ magnétique aléatoire après une trempe en température. En étudiant les lois d'échelle dynamiques, nous confirmons la conjecture de super-universalité. En revanche, nous montrons qu'elle est absente dans la dynamique vitreuse du modèle d'Edwards-Anderson $3d$ malgré l'existence d'une échelle de longueur permettant d'écheler des observables globales et locales.

Nous étudions analytiquement la dynamique de rotateurs quantiques désordonnés couplés brutalement à un environnement qui impose un courant électrique à travers le système. Nous prouvons l'existence d'une transition de phase dynamique entre une phase stationnaire de non-équilibre et une phase ordonnée à basse température, faibles fluctuations quantiques et faible courant. Nous montrons que celui-ci joue le rôle d'un bain d'équilibre sur la dynamique vieillissante qui est décrite par des lois d'échelle super-universelles.

Mots-clefs physique statistique hors-équilibre ; fluctuations ; croissance de domaine ; désordre ; verre de spin ; loi d'échelle dynamique ; super-universalité.

Laboratoire Laboratoire de Physique Théorique et Hautes Énergies, LPTHE, Université Pierre et Marie Curie — UMR 7589 du CNRS, 4 Place Jussieu, 75005 Paris, France.

Title Classical and quantum out-of-equilibrium dynamics. Formalism and applications.

Abstract This thesis deals with the dynamics of systems coupled to an environment. We review the symmetries of the Martin-Siggia-Rose-Janssen-deDominicis formalism associated to Langevin equations. In equilibrium, we generalize the supersymmetric formalism to the case of a colored multiplicative noise and we exhibit a symmetry yielding all the equilibrium theorems. If broken, it naturally gives rise to all sorts of fluctuation theorems. Another symmetry, valid also out of equilibrium, yields dynamical equations coupling correlations and responses.

We follow, by means of Monte Carlo simulations, the coarsening dynamics of the $3d$ Random Field Ising Model after a temperature quench. By studying the dynamical scalings, we confirm the super-universality conjecture. On the contrary, it fails in the case of the glassy dynamics of the $3d$ Edwards-Anderson model despite the existence of a growing length that is shown to scale both global and local observables.

We analytically study the dynamics of disordered quantum rotors after an instantaneous coupling to an environment which creates an electronic current tunneling through the system. We show the existence of a dynamical phase transition between a non-equilibrium stationary phase and an ordering phase at low temperature, weak quantum fluctuations and weak current. The latter is shown to act as an equilibrium bath on the aging dynamics which have super-universal scaling properties.

Keywords out-of-equilibrium statistical physics; fluctuations; coarsening; disorder; spin glass; dynamical scaling; super-universality.

Laboratory Laboratoire de Physique Théorique et Hautes Énergies, LPTHE, Université Pierre et Marie Curie — UMR 7589 du CNRS, 4 Place Jussieu, 75005 Paris, France.